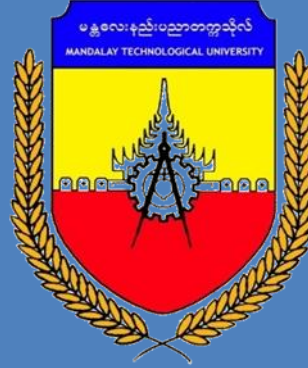


# MANDALAY TECHNOLOGICAL UNIVERSITY DEPARTMENT OF MECHATRONIC ENGINEERING



## CONTROL ENGINEERING II

McE 42077

**Motto: Creative, Innovative, Mechatronics**

## CHAPTER

# 5

# *The Performance of Feedback Control Systems*

---

5.1	Introduction	305
5.2	Test Input Signals	305
5.3	Performance of Second-Order Systems	308
5.4	Effects of a Third Pole and a Zero on the Second-Order System Response	314
5.5	The s-Plane Root Location and the Transient Response	320
5.6	The Steady-State Error of Feedback Control Systems	322
5.7	Performance Indices	330
5.8	The Simplification of Linear Systems	339
5.9	Design Examples	342
5.10	System Performance Using Control Design Software	356
5.11	Sequential Design Example: Disk Drive Read System	360
5.12	Summary	364

### *P R E V I E W*

The ability to adjust the transient and steady-state response of a control system is a beneficial outcome of the design of control systems. In this chapter, we introduce the time-domain performance specifications and we use key input signals to test the response of the control system. The correlation between the system performance and the location of the transfer function poles and zeros is discussed. We will develop relationships between the performance specifications and the natural frequency and damping ratio for second-order systems. Relying on the notion of dominant poles, we can extrapolate the ideas associated with second-order systems to those of higher order. The concept of a performance index will be considered. We will present a set of popular quantitative performance indices that adequately represent the performance of the control system. The chapter concludes with a performance analysis of the Sequential Design Example: Disk Drive Read System.

### *DESIRED OUTCOMES*

Upon completion of Chapter 5, students should:

- Be aware of key test signals used in controls and of the resulting transient response characteristics of second-order systems to test signal inputs.
- Recognize the direct relationship between the pole locations of second-order systems and the transient response.
- Be familiar with the design formulas that relate the second-order pole locations to percent overshoot, settling time, rise time, and time to peak.
- Be aware of the impact of a zero and a third pole on the second-order system response.
- Gain a sense of optimal control as measured with performance indices.

## 5.1 INTRODUCTION

The ability to adjust the transient and steady-state performance is a distinct advantage of feedback control systems. To analyze and design a control system, we must define and measure its performance. Based on the desired performance of the control system, the system parameters may be adjusted to provide the desired response. Because control systems are inherently dynamic, their performance is usually specified in terms of both the transient response and the steady-state response. The **transient response** is the response that disappears with time. The **steady-state response** is the response that exists for a long time following an input signal initiation.

The **design specifications** for control systems normally include several time-response indices for a specified input command, as well as a desired steady-state accuracy. In the course of any design, the specifications are often revised to effect a compromise. Therefore, specifications are seldom a rigid set of requirements, but rather a first attempt at listing a desired performance. The effective compromise and adjustment of specifications are graphically illustrated in Figure 5.1. The parameter  $p$  may minimize the performance measure  $M_2$  if we select  $p$  as a very small value. However, this results in large measure  $M_1$ , an undesirable situation. If the performance measures are equally important, the crossover point at  $p_{\min}$  provides the best compromise. This type of compromise is normally encountered in control system design. It is clear that if the original specifications called for both  $M_1$  and  $M_2$  to be zero, the specifications could not be simultaneously met; they would then have to be altered to allow for the compromise resulting with  $p_{\min}$  [1, 10, 15, 20].

The specifications, which are stated in terms of the measures of performance, indicate the quality of the system to the designer. In other words, the performance measures help to answer the question, How well does the system perform the task for which it was designed?

## 5.2 TEST INPUT SIGNALS

The time-domain performance specifications are important indices because control systems are inherently time-domain systems. That is, the system transient or time performance is the response of prime interest for control systems. It is necessary to

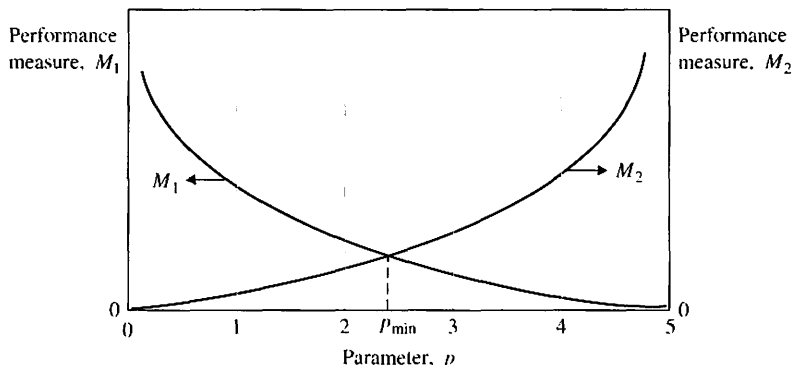


**FIGURE 5.1**  
Two performance measures versus parameter  $p$ .

determine initially whether the system is stable; we can achieve this goal by using the techniques of ensuing chapters. If the system is stable, the response to a specific input signal will provide several measures of the performance. However, because the actual input signal of the system is usually unknown, a standard **test input signal** is normally chosen. This approach is quite useful because there is a reasonable correlation between the response of a system to a standard test input and the system's ability to perform under normal operating conditions. Furthermore, using a standard input allows the designer to compare several competing designs. Many control systems experience input signals that are very similar to the standard test signals.

The standard test input signals commonly used are the step input, the ramp input, and the parabolic input. These inputs are shown in Figure 5.2. The equations representing these test signals are given in Table 5.1, where the Laplace transform can be obtained by using Table 2.3 and a more complete list of Laplace transform pairs can be found at the MCS website. The ramp signal is the integral of the step input, and the parabola is simply the integral of the ramp input. A **unit impulse** function is also useful for test signal purposes. The unit impulse is based on a rectangular function

$$f_\epsilon(t) = \begin{cases} 1/\epsilon, & -\frac{\epsilon}{2} \leq t \leq \frac{\epsilon}{2}; \\ 0, & \text{otherwise,} \end{cases}$$

where  $\epsilon > 0$ . As  $\epsilon$  approaches zero, the function  $f_\epsilon(t)$  approaches the unit impulse function  $\delta(t)$ , which has the following properties:

$$\int_{-\infty}^{\infty} \delta(t) dt = 1 \quad \text{and} \quad \int_{-\infty}^{\infty} \delta(t-a)g(t) dt = g(a). \quad (5.1)$$

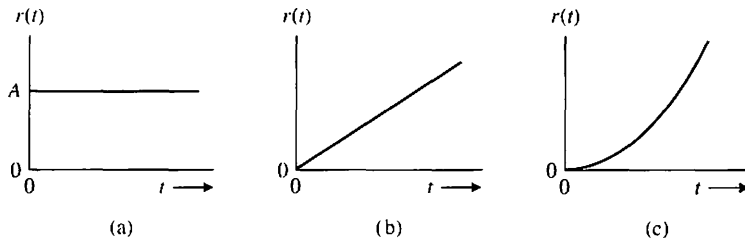
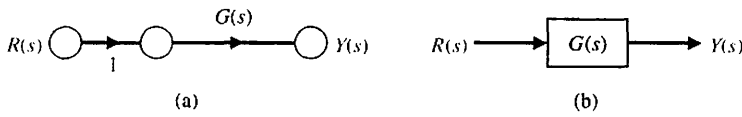


**FIGURE 5.2**  
Test input signals:  
(a) step, (b) ramp,  
and (c) parabolic.

**Table 5.1 Test Signal Inputs**

Test Signal	$r(t)$	$R(s)$
Step	$r(t) = A, t > 0$ $= 0, t < 0$	$R(s) = A/s$
Ramp	$r(t) = At, t > 0$ $= 0, t < 0$	$R(s) = A/s^2$
Parabolic	$r(t) = At^2, t > 0$ $= 0, t < 0$	$R(s) = 2A/s^3$

**FIGURE 5.3**  
Open-loop control system.



The impulse input is useful when we consider the convolution integral for the output  $y(t)$  in terms of an input  $r(t)$ , which is written as

$$y(t) = \int_{-\infty}^t g(t - \tau)r(\tau) d\tau = \mathcal{L}^{-1}\{G(s)R(s)\}. \quad (5.2)$$

This relationship is shown in block diagram form in Figure 5.3. If the input is a unit impulse function, we have

$$y(t) = \int_{-\infty}^t g(t - \tau)\delta(\tau) d\tau. \quad (5.3)$$

The integral has a value only at  $\tau = 0$ ; therefore,

$$y(t) = g(t),$$

the impulse response of the system  $G(s)$ . The impulse response test signal can often be used for a dynamic system by subjecting the system to a large-amplitude, narrow-width pulse of area  $A$ .

The standard test signals are of the general form

$$r(t) = t^n, \quad (5.4)$$

and the Laplace transform is

$$R(s) = \frac{n!}{s^{n+1}}. \quad (5.5)$$

Hence, the response to one test signal may be related to the response of another test signal of the form of Equation (5.4). The step input signal is the easiest to generate and evaluate and is usually chosen for performance tests.

Consider the response of the system shown in Figure 5.3 for a unit step input when

$$G(s) = \frac{9}{s + 10}.$$

Then the output is

$$Y(s) = \frac{9}{s(s + 10)},$$

the response during the transient period is

$$y(t) = 0.9(1 - e^{-10t}),$$

and the steady-state response is

$$y(\infty) = 0.9.$$

If the error is  $E(s) = R(s) - Y(s)$ , then the steady-state error is

$$e_{ss} = \lim_{s \rightarrow 0} sE(s) = 0.1.$$

### 5.3 PERFORMANCE OF SECOND-ORDER SYSTEMS

Let us consider a single-loop second-order system and determine its response to a unit step input. A closed-loop feedback control system is shown in Figure 5.4. The closed-loop system is

$$Y(s) = \frac{G(s)}{1 + G(s)} R(s). \quad (5.6)$$

We may rewrite Equation (5.6) as

$$Y(s) = \frac{\omega_n^2}{s^2 + 2\zeta\omega_n s + \omega_n^2} R(s).$$

(5.7)

With a unit step input, we obtain

$$Y(s) = \frac{\omega_n^2}{s(s^2 + 2\zeta\omega_n s + \omega_n^2)}, \quad (5.8)$$

for which the transient output, as obtained from the Laplace transform table in Table 2.3, is

$$y(t) = 1 - \frac{1}{\beta} e^{-\zeta\omega_n t} \sin(\omega_n \beta t + \theta), \quad (5.9)$$

where  $\beta = \sqrt{1 - \zeta^2}$ ,  $\theta = \cos^{-1} \zeta$ , and  $0 < \zeta < 1$ . The transient response of this second-order system for various values of the damping ratio  $\zeta$  is shown in Figure 5.5.

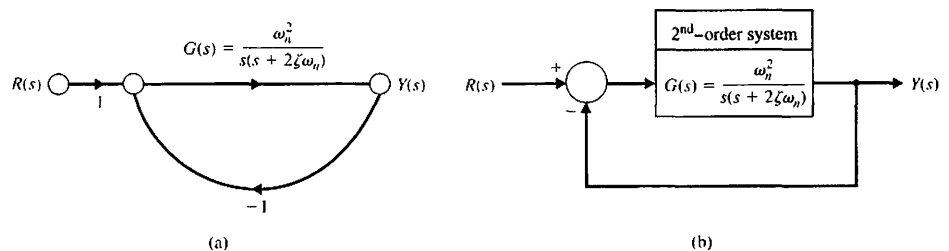
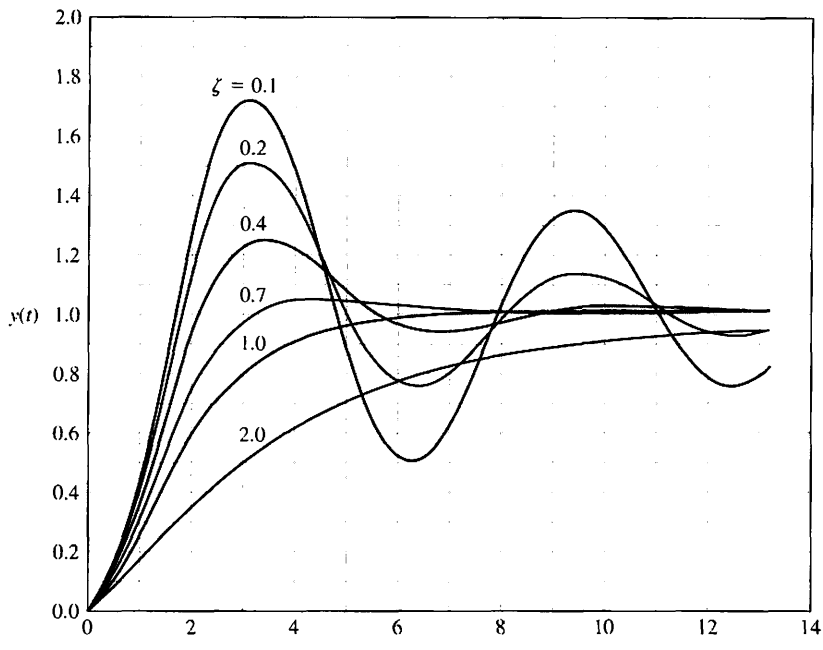


**FIGURE 5.4**  
Second-order  
closed-loop control  
system.



(a)

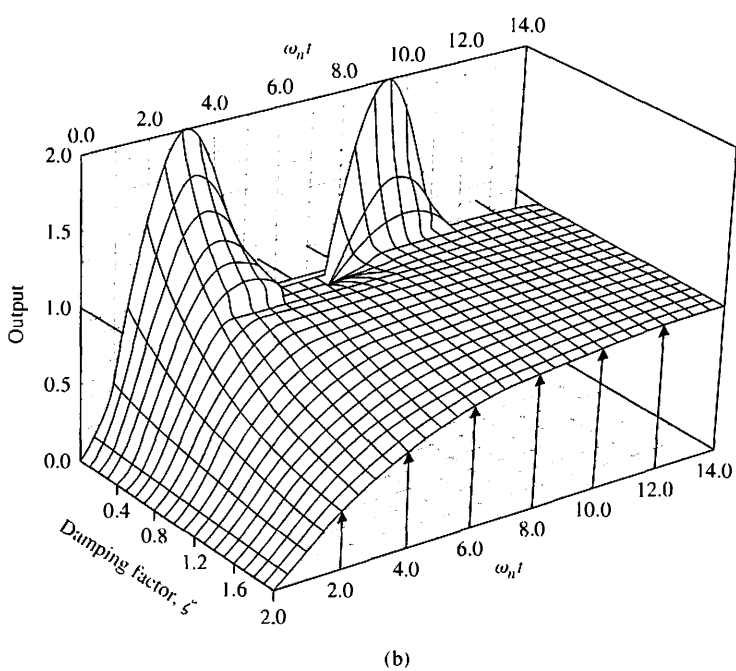


**FIGURE 5.5**  
 (a) Transient response of a second-order system (Equation 5.9) for a step input.  
 (b) The transient response of a second-order system (Equation 5.9) for a step input as a function of  $\zeta$  and  $\omega_n t$ . (Courtesy of Professor R. Jacquot, University of Wyoming.)

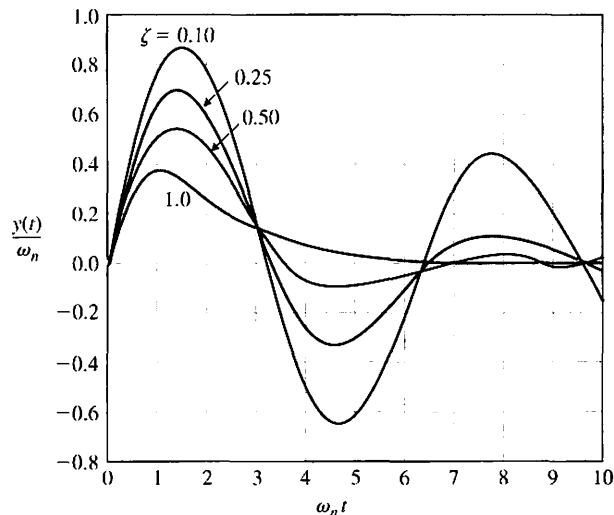


**FIGURE 5.6**  
Response of a second-order system for an impulse function input.

As  $\zeta$  decreases, the closed-loop roots approach the imaginary axis, and the response becomes increasingly oscillatory. The response as a function of  $\zeta$  and time is also shown in Figure 5.5(b) for a step input.

The Laplace transform of the unit impulse is  $R(s) = 1$ , and therefore the output for an impulse is

$$Y(s) = \frac{\omega_n^2}{s^2 + 2\zeta\omega_n s + \omega_n^2}, \quad (5.10)$$

which is  $T(s) = Y(s)/R(s)$ , the transfer function of the closed-loop system. The transient response for an impulse function input is then

$$y(t) = \frac{\omega_n}{\beta} e^{-\zeta\omega_n t} \sin(\omega_n \beta t), \quad (5.11)$$

which is the derivative of the response to a step input. The impulse response of the second-order system is shown in Figure 5.6 for several values of the damping ratio  $\zeta$ . The designer is able to select several alternative performance measures from the transient response of the system for either a step or impulse input.

Standard performance measures are usually defined in terms of the step response of a system as shown in Figure 5.7. The swiftness of the response is measured by the **rise time**  $T_r$  and the **peak time**  $T_p$ . For underdamped systems with an overshoot, the 0–100% rise time is a useful index. If the system is overdamped, then the peak time is not defined, and the 10–90% rise time  $T_{r_1}$  is normally used. The similarity with which the actual response matches the step input is measured by the percent overshoot and settling time  $T_s$ . The **percent overshoot** is defined as

$$P.O. = \frac{M_{p_t} - f_v}{f_v} \times 100\% \quad (5.12)$$

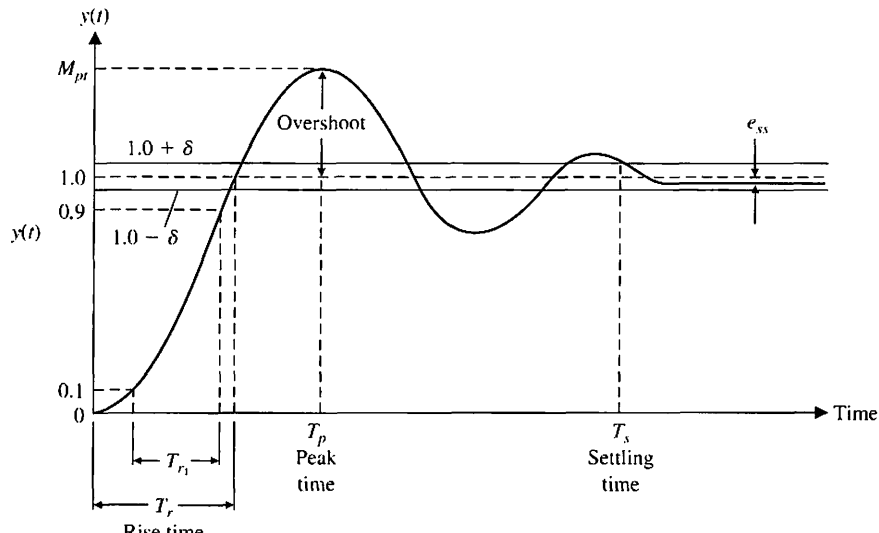


**FIGURE 5.7**  
Step response of a control system (Equation 5.9).

for a unit step input, where  $M_{pt}$  is the peak value of the time response, and  $fv$  is the final value of the response. Normally,  $fv$  is the magnitude of the input, but many systems have a final value significantly different from the desired input magnitude. For the system with a unit step represented by Equation (5.8), we have  $fv = 1$ .

The **settling time**,  $T_s$ , is defined as the time required for the system to settle within a certain percentage  $\delta$  of the input amplitude. This band of  $\pm\delta$  is shown in Figure 5.7. For the second-order system with closed-loop damping constant  $\zeta\omega_n$  and a response described by Equation (5.9), we seek to determine the time  $T_s$  for which the response remains within 2% of the final value. This occurs approximately when

$$e^{-\zeta\omega_n T_s} < 0.02,$$

or

$$\zeta\omega_n T_s \approx 4.$$

Therefore, we have

$$T_s = 4\tau = \frac{4}{\zeta\omega_n}. \quad (5.13)$$

Hence, we will define the settling time as four time constants (that is,  $\tau = 1/\zeta\omega_n$ ) of the dominant roots of the characteristic equation. The steady-state error of the system may be measured on the step response of the system as shown in Figure 5.7.

The transient response of the system may be described in terms of two factors:

1. The swiftness of response, as represented by the rise time and the peak time.
2. The closeness of the response to the desired response, as represented by the overshoot and settling time.

As nature would have it, these are contradictory requirements; thus, a compromise must be obtained. To obtain an explicit relation for  $M_{pt}$  and  $T_p$  as a function of  $\zeta$ , one can differentiate Equation (5.9) and set it equal to zero. Alternatively, one can utilize the differentiation property of the Laplace transform, which may be written as

$$\mathcal{L}\left\{\frac{dy(t)}{dt}\right\} = sY(s)$$

when the initial value of  $y(t)$  is zero. Therefore, we may acquire the derivative of  $y(t)$  by multiplying Equation (5.8) by  $s$  and thus obtaining the right side of Equation (5.10). Taking the inverse transform of the right side of Equation (5.10), we obtain Equation (5.11), which is equal to zero when  $\omega_n \beta t = \pi$ . Thus, we find that the peak time relationship for this second-order system is

$$T_p = \frac{\pi}{\omega_n \sqrt{1 - \zeta^2}}, \quad (5.14)$$

and the peak response is

$$M_{pt} = 1 + e^{-\zeta \pi / \sqrt{1 - \zeta^2}}. \quad (5.15)$$

Therefore, the percent overshoot is

$$P.O. = 100e^{-\zeta \pi / \sqrt{1 - \zeta^2}}. \quad (5.16)$$

The percent overshoot versus the damping ratio,  $\zeta$ , is shown in Figure 5.8. Also, the normalized peak time,  $\omega_n T_p$ , is shown versus the damping ratio,  $\zeta$ , in Figure 5.8. The percent overshoot versus the damping ratio is listed in Table 5.2 for selected values of

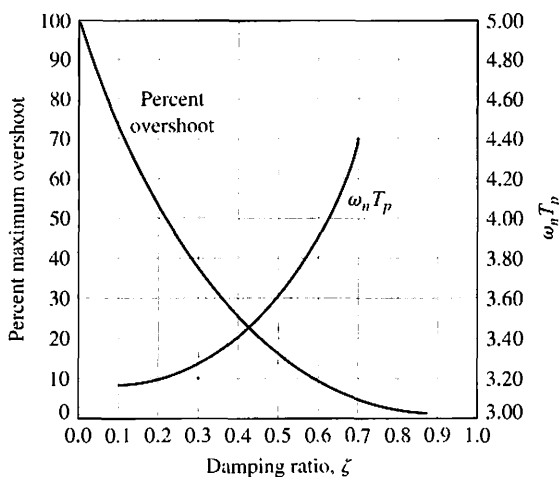


**FIGURE 5.8**  
Percent overshoot  
and normalized  
peak time versus  
damping ratio  $\zeta$   
for a second-order  
system (Equation  
5.8).

**Table 5.2 Percent Peak Overshoot Versus Damping Ratio for a Second-Order System**

Damping ratio	0.9	0.8	0.7	0.6	0.5	0.4	0.3
Percent overshoot	0.2	1.5	4.6	9.5	16.3	25.4	37.2

the damping ratio. Again, we are confronted with a necessary compromise between the swiftness of response and the allowable overshoot.

The swiftness of step response can be measured as the time it takes to rise from 10% to 90% of the magnitude of the step input. This is the definition of the rise time,  $T_{r1}$ , shown in Figure 5.7. The normalized rise time,  $\omega_n T_{r1}$ , versus  $\zeta$  ( $0.05 \leq \zeta \leq 0.95$ ) is shown in Figure 5.9. Although it is difficult to obtain exact analytic expressions for  $T_{r1}$ , we can utilize the linear approximation

$$\boxed{T_{r1} = \frac{2.16\zeta + 0.60}{\omega_n}}, \quad (5.17)$$

which is accurate for  $0.3 \leq \zeta \leq 0.8$ . This linear approximation is shown in Figure 5.9.

The swiftness of a response to a step input as described by Equation (5.17) is dependent on  $\zeta$  and  $\omega_n$ . For a given  $\zeta$ , the response is faster for larger  $\omega_n$ , as shown in Figure 5.10. Note that the overshoot is independent of  $\omega_n$ .

For a given  $\omega_n$ , the response is faster for lower  $\zeta$ , as shown in Figure 5.11. The swiftness of the response, however, will be limited by the overshoot that can be accepted.

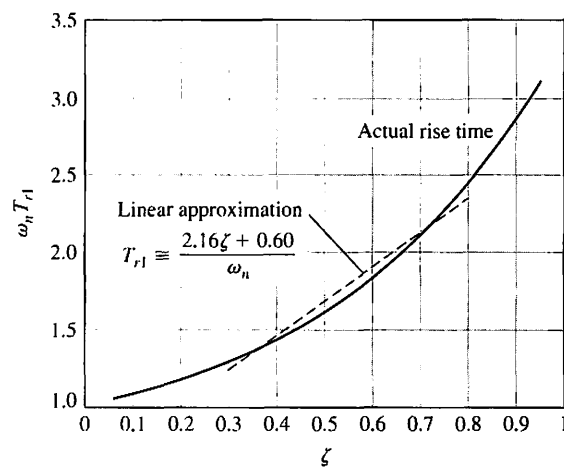


**FIGURE 5.9**  
Normalized rise time,  $\omega_n T_{r1}$ , versus  $\zeta$  for a second-order system.

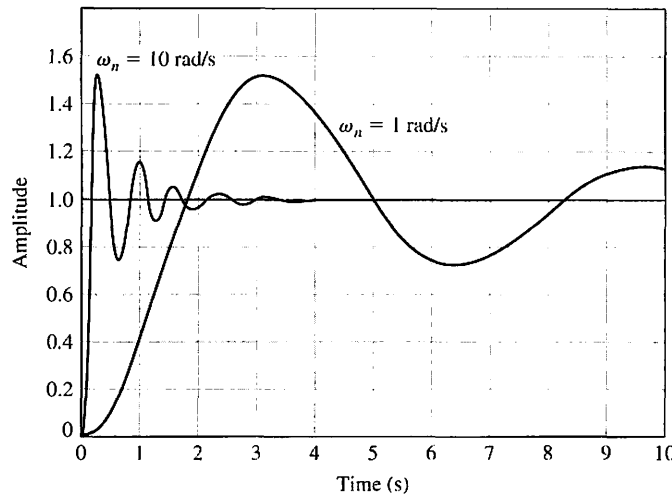


**FIGURE 5.10**  
The step response  
for  $\zeta = 0.2$  for  
 $\omega_n = 1$  and  
 $\omega_n = 10$ .

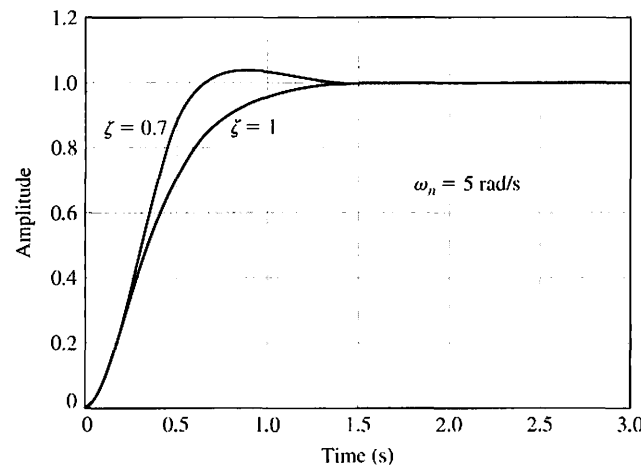


**FIGURE 5.11**  
The step response  
for  $\omega_n = 5$  with  
 $\zeta = 0.7$  and  $\zeta = 1$ .

#### 5.4 EFFECTS OF A THIRD POLE AND A ZERO ON THE SECOND-ORDER SYSTEM RESPONSE

The curves presented in Figure 5.8 are exact only for the second-order system of Equation (5.8). However, they provide a remarkably good source of data because many systems possess a dominant pair of roots, and the step response can be estimated by utilizing Figure 5.8. This approach, although an approximation, avoids the evaluation of the inverse Laplace transformation in order to determine the percent overshoot and other performance measures. For example, for a third-order system with a closed-loop transfer function

$$T(s) = \frac{1}{(s^2 + 2\zeta s + 1)(\gamma s + 1)}, \quad (5.18)$$

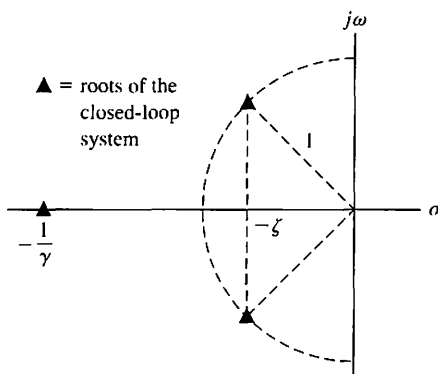


**FIGURE 5.12**  
An  $s$ -plane diagram  
of a third-order  
system.

the  $s$ -plane diagram is shown in Figure 5.12. This third-order system is normalized with  $\omega_n = 1$ . It was ascertained experimentally that the performance (as indicated by the percent overshoot,  $P.O.$ , and the settling time,  $T_s$ ), was adequately represented by the second-order system curves when [4]

$$|1/\gamma| \geq 10|\zeta\omega_n|.$$

In other words, the response of a third-order system can be approximated by the **dominant roots** of the second-order system as long as the real part of the dominant roots is less than one tenth of the real part of the third root [15, 20].

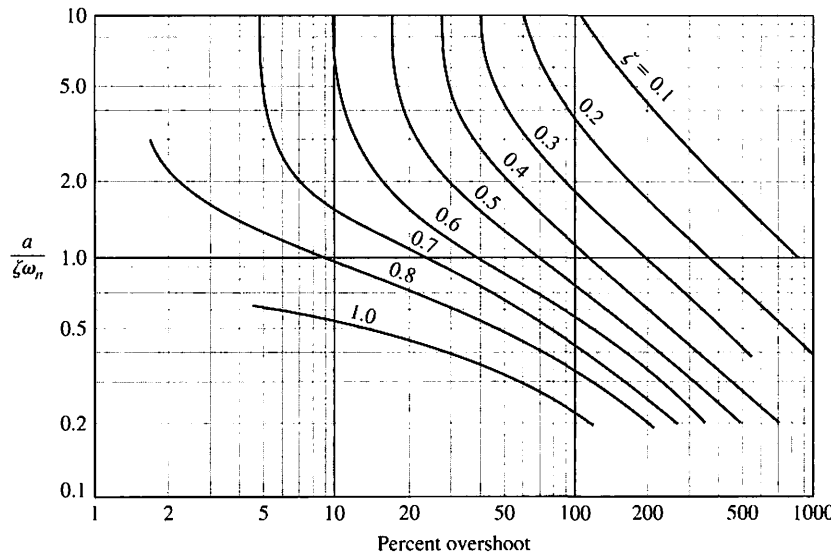
Using a computer simulation, we can determine the response of a system to a unit step input when  $\zeta = 0.45$ . When  $\gamma = 2.25$ , we find that the response is over-damped because the real part of the complex poles is  $-0.45$ , whereas the real pole is equal to  $-0.444$ . The settling time (to within 2% of the final value) is found via the simulation to be 9.6 seconds. If  $\gamma = 0.90$  or  $1/\gamma = 1.11$  is compared with  $\zeta\omega_n = 0.45$  of the complex poles, the overshoot is 12% and the settling time is 8.8 seconds. If the complex roots were dominant, we would expect the overshoot to be 20% and the settling time to be  $4/\zeta\omega_n = 8.9$  seconds. The results are summarized in Table 5.3.

The performance measures of Figure 5.8 are correct only for a transfer function without finite zeros. If the transfer function of a system possesses finite zeros and they are located relatively near the dominant complex poles, then the zeros will materially affect the transient response of the system [5].

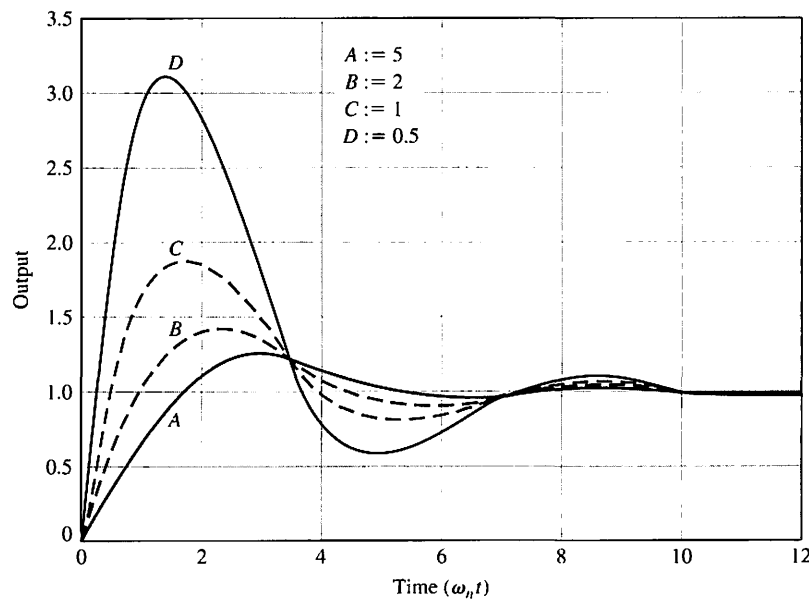
**Table 5.3 Effect of a Third Pole (Equation 5.18) for  $\zeta = 0.45$**

$\gamma$	$\frac{1}{\gamma}$	Percent Overshoot	Settling Time*
2.25	0.444	0	9.63
1.5	0.666	3.9	6.3
0.9	1.111	12.3	8.81
0.4	2.50	18.6	8.67
0.05	20.0	20.5	8.37
$0\infty$	20.5	8.24	

\*Note: Settling time is normalized time,  $\omega_n T_s$ , and uses a 2% criterion.



(a)



(b)

**FIGURE 5.13** (a) Percent overshoot as a function of  $\zeta$  and  $\omega_n$  when a second-order transfer function contains a zero. Redrawn with permission from R. N. Clark, *Introduction to Automatic Control Systems* (New York: Wiley, 1962). (b) The response for the second-order transfer function with a zero for four values of the ratio  $a/\zeta \omega_n$ ;  $A = 5$ ,  $B = 2$ ,  $C = 1$ , and  $D = 0.5$  when  $\zeta = 0.45$ .

**Table 5.4 The Response of a Second-Order System with a Zero and  $\zeta = 0.45$**

$a/\zeta\omega_n$	Percent Overshoot	Settling Time	Peak Time
5	23.1	8.0	3.0
2	39.7	7.6	2.2
1	89.9	10.1	1.8
0.5	210.0	10.3	1.5

Note: Time is normalized as  $\omega_n t$ , and settling time is based on a 2% criterion.

The transient response of a system with one zero and two poles may be affected by the location of the zero [5]. The percent overshoot for a step input as a function of  $a/\zeta\omega_n$ , when  $\zeta \leq 1$ , is given in Figure 5.13(a) for the system transfer function

$$T(s) = \frac{(\omega_n^2/a)(s + a)}{s^2 + 2\zeta\omega_n s + \omega_n^2}$$

The actual transient response for a step input is shown in Figure 5.13(b) for selected values of  $a/\zeta\omega_n$ . The actual response for these selected values is summarized in Table 5.4 when  $\zeta = 0.45$ .

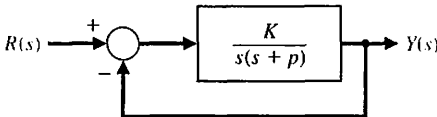
The correlation of the time-domain response of a system with the  $s$ -plane location of the poles of the closed-loop transfer function is very useful for selecting the specifications of a system. To illustrate clearly the utility of the  $s$ -plane, let us consider a simple example.

#### EXAMPLE 5.1 Parameter selection

A single-loop feedback control system is shown in Figure 5.14. We select the gain  $K$  and the parameter  $p$  so that the time-domain specifications will be satisfied. The transient response to a step should be as fast as is attainable while retaining an overshoot of less than 5%. Furthermore, the settling time to within 2% of the final value should be less than 4 seconds. The damping ratio,  $\zeta$ , for an overshoot of 4.3% is 0.707. This damping ratio is shown graphically as a line in Figure 5.15. Because the settling time is

$$T_s = \frac{4}{\zeta\omega_n} \leq 4 \text{ s},$$

**FIGURE 5.14**  
Single-loop feedback control system.



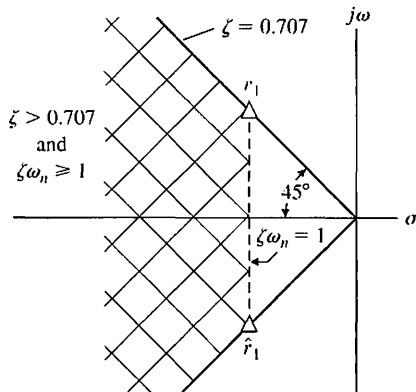


**FIGURE 5.15**  
Specifications and root locations on the  $s$ -plane.

we require that the real part of the complex poles of  $T(s)$  be

$$\zeta\omega_n \geq 1.$$

This region is also shown in Figure 5.15. The region that will satisfy both time-domain requirements is shown cross-hatched on the  $s$ -plane of Figure 5.15.

When the closed-loop roots are  $r_1 = -1 + j1$  and  $\hat{r}_1 = -1 - j1$ , we have  $T_s = 4$  s and an overshoot of 4.3%. Therefore,  $\zeta = 1/\sqrt{2}$  and  $\omega_n = 1/\zeta = \sqrt{2}$ . The closed-loop transfer function is

$$T(s) = \frac{G(s)}{1 + G(s)} = \frac{K}{s^2 + ps + K} = \frac{\omega_n^2}{s^2 + 2\zeta\omega_n s + \omega_n^2}.$$

Hence, we require that  $K = \omega_n^2 = 2$  and  $p = 2\zeta\omega_n = 2$ . A full comprehension of the correlation between the closed-loop root location and the system transient response is important to the system analyst and designer. Therefore, we shall consider the matter more completely in the following sections. ■

### EXAMPLE 5.2 Dominant poles of $T(s)$

Consider a system with a closed-loop transfer function

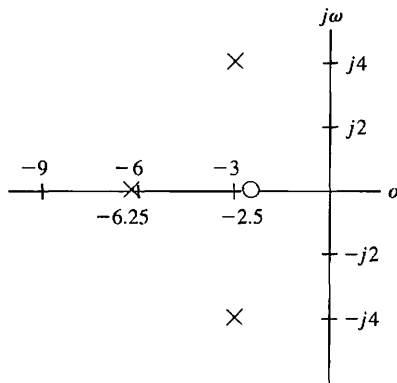
$$\frac{Y(s)}{R(s)} = T(s) = \frac{\frac{\omega_n^2}{a}(s + a)}{(s^2 + 2\zeta\omega_n s + \omega_n^2)(1 + \tau s)}.$$

Both the zero and the real pole may affect the transient response. If  $a \gg \zeta\omega_n$  and  $\tau \ll 1/\zeta\omega_n$ , then the pole and zero will have little effect on the step response.

Assume that we have

$$T(s) = \frac{62.5(s + 2.5)}{(s^2 + 6s + 25)(s + 6.25)}.$$

Note that the DC gain is equal to 1 ( $T(0) = 1$ ), and we expect a zero steady-state error for a step input. We have  $\zeta\omega_n = 3$ ,  $\tau = 0.16$ , and  $a = 2.5$ . The poles and the

**FIGURE 5.16**

The poles and zeros on the s-plane for a third-order system.

zero are shown on the s-plane in Figure 5.16. As a first approximation, we neglect the real pole and obtain

$$T(s) \approx \frac{10(s + 2.5)}{s^2 + 6s + 25}.$$

We now have  $\zeta = 0.6$  and  $\omega_n = 5$  for dominant poles with one accompanying zero for which  $a/(\zeta\omega_n) = 0.833$ . Using Figure 5.13(a), we find that the percent overshoot is 55%. We expect the settling time to within 2% of the final value to be

$$T_s = \frac{4}{\zeta\omega_n} = \frac{4}{0.6(5)} = 1.33 \text{ s.}$$

Using a computer simulation for the actual third-order system, we find that the percent overshoot is equal to 38% and the settling time is 1.6 seconds. Thus, the effect of the third pole of  $T(s)$  is to dampen the overshoot and increase the settling time (hence the real pole cannot be neglected). ■

The damping ratio plays a fundamental role in closed-loop system performance. As seen in the design formulas for settling time, percent overshoot, peak time, and rise time, the damping ratio is a key factor in determining the overall performance. In fact, for second-order systems, the damping ratio is the only factor determining the value of the percent overshoot to a step input. As it turns out, the damping ratio can be estimated from the response of a system to a step input [12]. The step response of a second-order system for a unit step input is given in Equation (5.9), which is

$$y(t) = 1 - \frac{1}{\beta} e^{-\zeta\omega_n t} \sin(\omega_n\beta t + \theta),$$

where  $\beta = \sqrt{1 - \zeta^2}$ , and  $\theta = \cos^{-1} \zeta$ . Hence, the frequency of the damped sinusoidal term for  $\zeta < 1$  is

$$\omega = \omega_n(1 - \zeta^2)^{1/2} = \omega_n\beta,$$

and the number of cycles in 1 second is  $\omega/(2\pi)$ .

The time constant for the exponential decay is  $\tau = 1/(\zeta\omega_n)$  in seconds. The number of cycles of the damped sinusoid during one time constant is

$$(\text{cycles/time}) \times \tau = \frac{\omega}{2\pi\zeta\omega_n} = \frac{\omega_n\beta}{2\pi\zeta\omega_n} = \frac{\beta}{2\pi\zeta}.$$

Assuming that the response decays in  $n$  visible time constants, we have

$$\text{cycles visible} = \frac{n\beta}{2\pi\zeta}. \quad (5.19)$$

For the second-order system, the response remains within 2% of the steady-state value after four time constants ( $4\tau$ ). Hence,  $n = 4$ , and

$$\text{cycles visible} = \frac{4\beta}{2\pi\zeta} = \frac{4(1 - \zeta^2)^{1/2}}{2\pi\zeta} \approx \frac{0.55}{\zeta} \quad (5.20)$$

for  $0.2 \leq \zeta \leq 0.6$ .

As an example, examine the response shown in Figure 5.5(a) for  $\zeta = 0.4$ . Use  $y(t) = 0$  as the first minimum point and count 1.4 cycles visible (until the response settles with 2% of the final value). Then we estimate

$$\zeta = \frac{0.55}{\text{cycles}} = \frac{0.55}{1.4} = 0.39.$$

We can use this approximation for systems with dominant complex poles so that

$$T(s) \approx \frac{\omega_n^2}{s^2 + 2\zeta\omega_n s + \omega_n^2}.$$

Then we are able to estimate the damping ratio  $\zeta$  from the actual system response of a physical system.

An alternative method of estimating  $\zeta$  is to determine the percent overshoot for the step response and use Figure 5.8 to estimate  $\zeta$ . For example, we determine an overshoot of 25% for  $\zeta = 0.4$  from the response of Figure 5.5(a). Using Figure 5.8, we estimate that  $\zeta = 0.4$ , as expected.

## 5.5 THE s-PLANE ROOT LOCATION AND THE TRANSIENT RESPONSE

The transient response of a closed-loop feedback control system can be described in terms of the location of the poles of the transfer function. The closed-loop transfer function is written in general as

$$T(s) = \frac{Y(s)}{R(s)} = \frac{\sum P_i(s) \Delta_i(s)}{\Delta(s)},$$

where  $\Delta(s) = 0$  is the characteristic equation of the system. For the single-loop system of Figure 5.4, the characteristic equation reduces to  $1 + G(s) = 0$ . It is the

poles and zeros of  $T(s)$  that determine the transient response. However, for a closed-loop system, the poles of  $T(s)$  are the roots of the characteristic equation  $\Delta(s) = 0$  and the poles of  $\Sigma P_i(s) \Delta_i(s)$ . The output of a system (with gain = 1) without repeated roots and a unit step input can be formulated as a partial fraction expansion as

$$Y(s) = \frac{1}{s} + \sum_{i=1}^M \frac{A_i}{s + \sigma_i} + \sum_{k=1}^N \frac{B_k s + C_k}{s^2 + 2\alpha_k s + (\alpha_k^2 + \omega_k^2)}, \quad (5.21)$$

where the  $A_i$ ,  $B_k$ , and  $C_k$  are constants. The roots of the system must be either  $s = -\sigma_i$  or complex conjugate pairs such as  $s = -\alpha_k \pm j\omega_k$ . Then the inverse transform results in the transient response as the sum of terms

$$y(t) = 1 + \sum_{i=1}^M A_i e^{-\sigma_i t} + \sum_{k=1}^N D_k e^{-\alpha_k t} \sin(\omega_k t + \theta_k), \quad (5.22)$$

where  $D_k$  is a constant and depends on  $B_k$ ,  $C_k$ ,  $\alpha_k$ , and  $\omega_k$ . The transient response is composed of the steady-state output, exponential terms, and damped sinusoidal terms. For the response to be stable—that is, bounded for a step input—the real part of the roots,  $-\sigma_i$  and  $-\alpha_k$ , must be in the left-hand portion of the  $s$ -plane. The impulse response for various root locations is shown in Figure 5.17. The information imparted by the location of the roots is graphic indeed, and usually well worth the effort of determining the location of the roots in the  $s$ -plane.

It is important for the control system analyst to understand the complete relationship of the complex-frequency representation of a linear system, the poles and zeros of its transfer function, and its time-domain response to step and other inputs. In such areas as signal processing and control, many of the analysis and design calculations are done in the complex-frequency plane, where a system model is

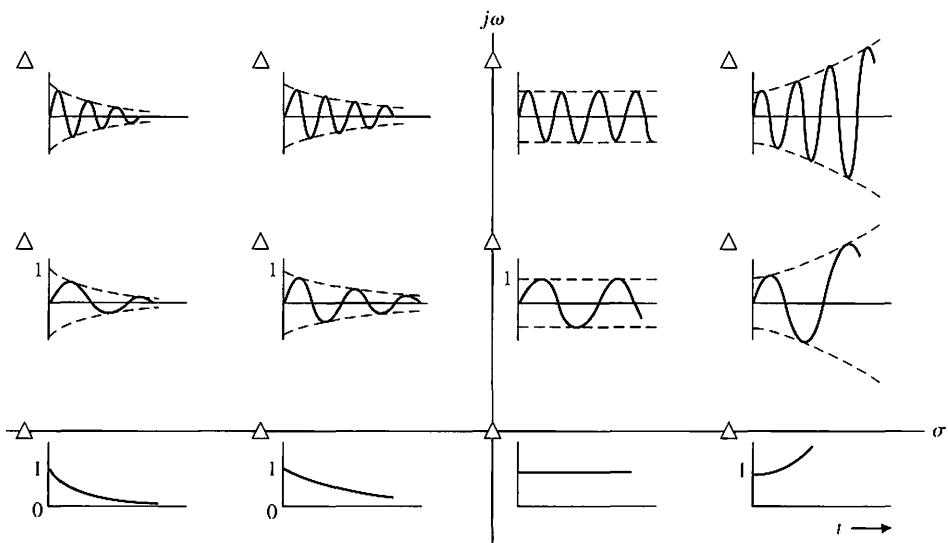


**FIGURE 5.17**  
Impulse response  
for various root  
locations in the  
 $s$ -plane. (The  
conjugate root is  
not shown.)

represented in terms of the poles and zeros of its transfer function  $T(s)$ . On the other hand, system performance is often analyzed by examining time-domain responses, particularly when dealing with control systems.

The capable system designer will envision the effects on the step and impulse responses of adding, deleting, or moving poles and zeros of  $T(s)$  in the  $s$ -plane. Likewise, the designer should visualize the necessary changes for the poles and zeros of  $T(s)$ , in order to effect desired changes in the model's step and impulse responses.

An experienced designer is aware of the effects of zero locations on system response. The poles of  $T(s)$  determine the particular response modes that will be present, and the zeros of  $T(s)$  establish the relative weightings of the individual mode functions. For example, moving a zero closer to a specific pole will reduce the relative contribution of the mode function corresponding to the pole.

A computer program can be developed to allow a user to specify arbitrary sets of poles and zeros for the transfer function of a linear system. Then the computer will evaluate and plot the system's impulse and step responses individually. It will also display them in reduced form along with the pole-zero plot.

Once the program has been run for a set of poles and zeros, the user can modify the locations of one or more of them. Plots may then be presented showing the old and new poles and zeros in the complex plane and the old and new impulse and step responses.

## 5.6 THE STEADY-STATE ERROR OF FEEDBACK CONTROL SYSTEMS

One of the fundamental reasons for using feedback, despite its cost and increased complexity, is the attendant improvement in the reduction of the steady-state error of the system. As illustrated in Section 4.6, the steady-state error of a stable closed-loop system is usually several orders of magnitude smaller than the error of an open-loop system. The system actuating signal, which is a measure of the system error, is denoted as  $E_a(s)$ . Consider the closed-loop feedback system shown in Figure 5.18. According to the discussions in Chapter 4, we know from Equation (4.3) that with  $N(s) = 0$ ,  $T_d(s) = 0$ , the tracking error is

$$E(s) = \frac{1}{1 + G_c(s)G(s)} R(s).$$

Using the final value theorem and computing the steady-state tracking error yields

$$\lim_{t \rightarrow \infty} e(t) = e_{ss} = \lim_{s \rightarrow 0} s \frac{1}{1 + G_c(s)G(s)} R(s). \quad (5.23)$$

It is useful to determine the steady-state error of the system for the three standard test inputs for the unity feedback system. Later in this section we will consider steady-state tracking errors for non-unity feedback systems.

**Step Input.** The steady-state error for a step input of magnitude  $A$  is therefore

$$e_{ss} = \lim_{s \rightarrow 0} \frac{s(A/s)}{1 + G_c(s)G(s)} = \frac{A}{1 + \lim_{s \rightarrow 0} G_c(s)G(s)}.$$

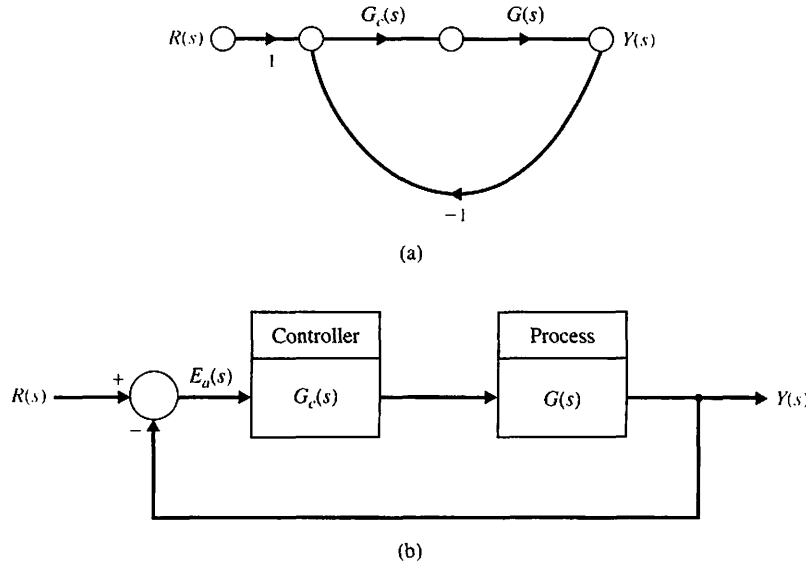


**FIGURE 5.18**  
Closed-loop control  
system with unity  
feedback.

It is the form of the loop transfer function  $G_c(s)G(s)$  that determines the steady-state error. The loop transfer function is written in general form as

$$G_c(s)G(s) = \frac{K \prod_{i=1}^M (s + z_i)}{s^N \prod_{k=1}^Q (s + p_k)}, \quad (5.24)$$

where  $\prod$  denotes the product of the factors and  $z_i \neq 0, p_k \neq 0$  for any  $1 \leq i \leq M$  and  $i \leq k \leq Q$ . Therefore, the loop transfer function as  $s$  approaches zero depends on the number of integrations,  $N$ . If  $N$  is greater than zero, then  $\lim_{s \rightarrow 0} G_c(s)G(s)$  approaches infinity, and the steady-state error approaches zero. The number of integrations is often indicated by labeling a system with a **type number** that simply is equal to  $N$ .

Consequently, for a type-zero system,  $N = 0$ , the steady-state error is

$$e_{ss} = \frac{A}{1 + G_c(0)G(0)} = \frac{A}{1 + K \prod_{i=1}^M z_i / \prod_{k=1}^Q p_k}. \quad (5.25)$$

The constant  $G_c(0)G(0)$  is denoted by  $K_p$ , the **position error constant**, and is given by

$$K_p = \lim_{s \rightarrow 0} G_c(s)G(s).$$

The steady-state tracking error for a step input of magnitude  $A$  is thus given by

$$e_{ss} = \frac{A}{1 + K_p}. \quad (5.26)$$

Hence, the steady-state error for a unit step input with one integration or more,  $N \geq 1$ , is zero because

$$\begin{aligned} e_{ss} &= \lim_{s \rightarrow 0} \frac{A}{1 + K \prod z_i / (s^N \prod p_k)} \\ &= \lim_{s \rightarrow 0} \frac{As^N}{s^N + K \prod z_i / \prod p_k} = 0. \end{aligned} \quad (5.27)$$

**Ramp Input.** The steady-state error for a ramp (velocity) input with a slope  $A$  is

$$e_{ss} = \lim_{s \rightarrow 0} \frac{s(A/s^2)}{1 + G_c(s)G(s)} = \lim_{s \rightarrow 0} \frac{A}{s + sG_c(s)G(s)} = \lim_{s \rightarrow 0} \frac{A}{sG_c(s)G(s)}. \quad (5.28)$$

Again, the steady-state error depends upon the number of integrations,  $N$ . For a type-zero system,  $N = 0$ , the steady-state error is infinite. For a type-one system,  $N = 1$ , the error is

$$e_{ss} = \lim_{s \rightarrow 0} \frac{A}{sK \prod (s + z_i) / [s \prod (s + p_k)]},$$

or

$$e_{ss} = \frac{A}{K \prod z_i / \prod p_k} = \frac{A}{K_v}, \quad (5.29)$$

where  $K_v$  is designated the **velocity error constant**. The velocity error constant is computed as

$$K_v = \lim_{s \rightarrow 0} sG_c(s)G(s).$$

When the transfer function possesses two or more integrations,  $N \geq 2$ , we obtain a steady-state error of zero. When  $N = 1$ , a steady-state error exists. However, the steady-state velocity of the output is equal to the velocity of input, as we shall see shortly.

**Acceleration Input.** When the system input is  $r(t) = At^2/2$ , the steady-state error is

$$e_{ss} = \lim_{s \rightarrow 0} \frac{s(A/s^3)}{1 + G_c(s)G(s)} = \lim_{s \rightarrow 0} \frac{A}{s^2 G_c(s)G(s)}. \quad (5.30)$$

**Table 5.5 Summary of Steady-State Errors**

Number of Integrations in $G_c(s)G(s)$ , Type Number	Step, $r(t) = A$ , $R(s) = A/s$	Input
	$e_{ss} = \frac{A}{1 + K_p}$	Ramp, $At$ , $A/s^2$
	$e_{ss} = 0$	Parabola, $At^2/2$ , $A/s^3$
0	$e_{ss} = \frac{A}{1 + K_p}$	Infinite
1	$e_{ss} = 0$	$\frac{A}{K_v}$
2	$e_{ss} = 0$	0
		$\frac{A}{K_a}$

The steady-state error is infinite for one integration. For two integrations,  $N = 2$ , and we obtain

$$e_{ss} = \frac{A}{K \prod z_i / \prod p_k} = \frac{A}{K_a}, \quad (5.31)$$

where  $K_a$  is designated the **acceleration error constant**. The acceleration error constant is

$$K_a = \lim_{s \rightarrow 0} s^2 G_c(s)G(s).$$

When the number of integrations equals or exceeds three, then the steady-state error of the system is zero.

Control systems are often described in terms of their type number and the error constants,  $K_p$ ,  $K_v$ , and  $K_a$ . Definitions for the error constants and the steady-state error for the three inputs are summarized in Table 5.5. The usefulness of the error constants can be illustrated by considering a simple example.

### EXAMPLE 5.3 Mobile robot steering control

A mobile robot may be designed as an assisting device or servant for a severely disabled person [7]. The steering control system for such a robot can be represented by the block diagram shown in Figure 5.19. The steering controller is

$$G_c(s) = K_1 + K_2/s. \quad (5.32)$$

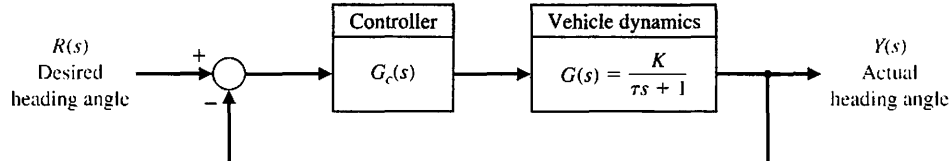


**FIGURE 5.19**  
Block diagram of steering control system for a mobile robot.

Therefore, the steady-state error of the system for a step input when  $K_2 = 0$  and  $G_c(s) = K_1$  is

$$e_{ss} = \frac{A}{1 + K_p}, \quad (5.33)$$

where  $K_p = KK_1$ . When  $K_2$  is greater than zero, we have a type-1 system,

$$G_c(s) = \frac{K_1 s + K_2}{s},$$

and the steady-state error is zero for a step input.

If the steering command is a ramp input, the steady-state error is

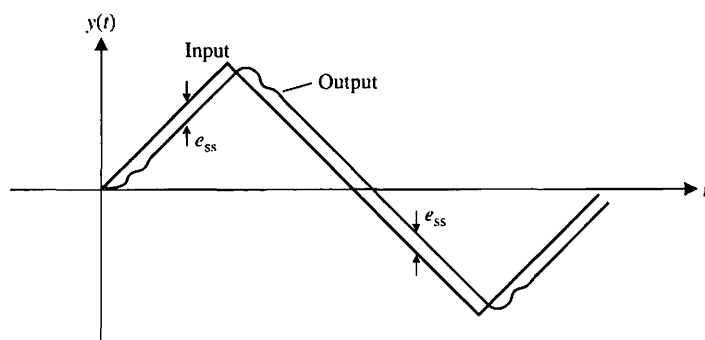
$$e_{ss} = \frac{A}{K_v}, \quad (5.34)$$

where

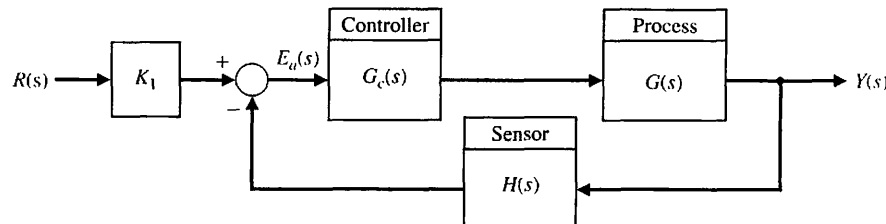
$$K_v = \lim_{s \rightarrow 0} sG_c(s)G(s) = K_2 K.$$

The transient response of the vehicle to a triangular wave input when  $G_c(s) = (K_1 s + K_2)/s$  is shown in Figure 5.20. The transient response clearly shows the effect of the steady-state error, which may not be objectionable if  $K_v$  is sufficiently large. Note that the output attains the desired velocity as required by the input, but it exhibits a steady-state error. ■

The control system's error constants,  $K_p$ ,  $K_v$ , and  $K_a$ , describe the ability of a system to reduce or eliminate the steady-state error. Therefore, they are utilized as numerical measures of the steady-state performance. The designer determines the error constants for a given system and attempts to determine methods of increasing the error constants while maintaining an acceptable transient response. In the case of the steering control system, we want to increase the gain factor  $KK_2$  in order to increase  $K_v$  and reduce the steady-state error. However, an increase in  $KK_2$  results in an attendant decrease in the system's damping ratio  $\zeta$  and therefore a



**FIGURE 5.20**  
Triangular wave response.

**FIGURE 5.21**

A nonunity feedback system.

more oscillatory response to a step input. Thus, we want a compromise that provides the largest  $K_v$  based on the smallest  $\zeta$  allowable.

In the preceding discussions, we assumed that we had a unity feedback system where  $H(s) = 1$ . Now we consider nonunity feedback systems. A general feedback system with nonunity feedback is shown in Figure 5.21. For a system in which the feedback is not unity, the units of the output  $Y(s)$  are usually different from the output of the sensor. For example, a speed control system is shown in Figure 5.22, where  $H(s) = K_2$ . The constants  $K_1$  and  $K_2$  account for the conversion of one set of units to another set of units (here we convert rad/s to volts). We can select  $K_1$ , and thus we set  $K_1 = K_2$  and move the block for  $K_1$  and  $K_2$  past the summing node. Then we obtain the equivalent block diagram shown in Figure 5.23. Thus, we obtain a unity feedback system as desired.

Let us return to the system of Figure 5.21 with  $H(s)$ . In this case, suppose

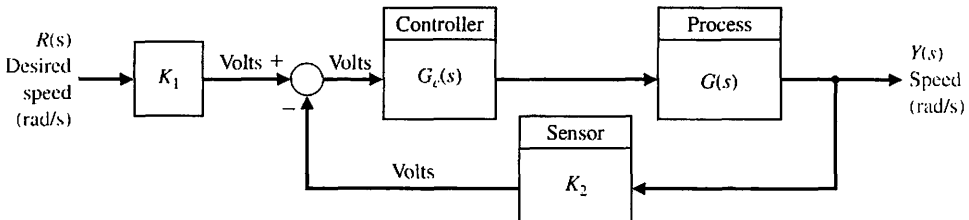
$$H(s) = \frac{K_2}{\tau s + 1}$$

which has a DC gain of

$$\lim_{s \rightarrow 0} H(s) = K_2.$$

The factor  $K_2$  is a conversion-of-units factor. If we set  $K_2 = K_1$ , then the system is transformed to that of Figure 5.23 for the steady-state calculation. To see this, consider error of the system  $E(s)$ , where

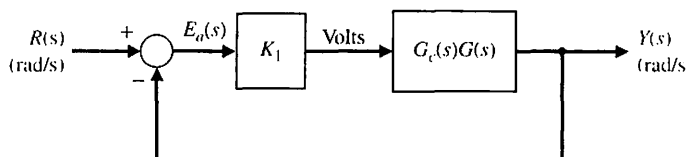
$$E(s) = R(s) - Y(s) = [1 - T(s)]R(s), \quad (5.35)$$

**FIGURE 5.22**

A speed control system.

**FIGURE 5.23**

The speed control system of Figure 5.22 with  $K_1 = K_2$ .



since  $Y(s) = T(s)R(s)$ . Note that

$$T(s) = \frac{K_1 G_c(s)G(s)}{1 + H(s)G_c(s)G(s)} = \frac{(\tau s + 1)K_1 G_c(s)G(s)}{\tau s + 1 + K_1 G_c(s)G(s)},$$

and therefore,

$$E(s) = \frac{1 + \tau s(1 - K_1 G_c(s)G(s))}{\tau s + 1 + K_1 G_c(s)G(s)} R(s).$$

Then the steady-state error for a unit step input is

$$e_{ss} = \lim_{s \rightarrow 0} s E(s) = \frac{1}{1 + K_1 \lim_{s \rightarrow 0} G_c(s)G(s)}. \quad (5.36)$$

We assume here that

$$\lim_{s \rightarrow 0} s G_c(s)G(s) = 0.$$

#### EXAMPLE 5.4 Steady-state error

Let us determine the appropriate value of  $K_1$  and calculate the steady-state error for a unit step input for the system shown in Figure 5.21 when

$$G_c(s) = 40 \quad \text{and} \quad G(s) = \frac{1}{s + 5}$$

and

$$H(s) = \frac{20}{s + 10}.$$

We can rewrite  $H(s)$  as

$$H(s) = \frac{2}{0.1s + 1}.$$

Selecting  $K_1 = K_2 = 2$ , we can use Equation (5.36) to determine

$$e_{ss} = \frac{1}{1 + K_1 \lim_{s \rightarrow 0} G_c(s)G(s)} = \frac{1}{1 + 2(40)(1/5)} = \frac{1}{17},$$

or 5.9% of the magnitude of the step input. ■

#### EXAMPLE 5.5 Feedback system

Let us consider the system of Figure 5.24, where we assume we cannot insert a gain  $K_1$  following  $R(s)$  as we did for the system of Figure 5.21. Then the actual error is given by Equation (5.35), which is

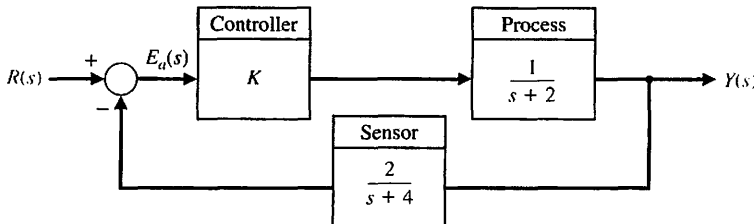


**FIGURE 5.24**  
A system with a feedback  $H(s)$ .

$$E(s) = [1 - T(s)]R(s).$$

Let us determine an appropriate gain  $K$  so that the steady-state error to a step input is minimized. The steady-state error is

$$e_{ss} = \lim_{s \rightarrow 0} s[1 - T(s)]\frac{1}{s},$$

where

$$T(s) = \frac{G_c(s)G(s)}{1 + G_c(s)G(s)H(s)} = \frac{K(s+4)}{(s+2)(s+4) + 2K}.$$

Then we have

$$T(0) = \frac{4K}{8 + 2K}.$$

The steady-state error for a unit step input is

$$e_{ss} = 1 - T(0).$$

Thus, to achieve a zero steady-state error, we require that

$$T(0) = \frac{4K}{8 + 2K} = 1,$$

or  $8 + 2K = 4K$ . Thus,  $K = 4$  will yield a zero steady-state error. ■

The determination of the steady-state error is simpler for unity feedback systems. However, it is possible to extend the notion of error constants to nonunity feedback systems by first appropriately rearranging the block diagram to obtain an equivalent unity feedback system. Remember that the underlying system must be stable, otherwise our use of the final value theorem will be compromised. Consider the nonunity feedback system in Figure 5.21 and assume that  $K_1 = 1$ . The closed-loop transfer function is

$$\frac{Y(s)}{R(s)} = T(s) = \frac{G_c(s)G(s)}{1 + H(s)G_c(s)G(s)}.$$

By manipulating the block diagram appropriately we can obtain the equivalent unity feedback system with

$$\frac{Y(s)}{R(s)} = T(s) = \frac{Z(s)}{1 + Z(s)} \text{ where } Z(s) = \frac{G_c(s)G(s)}{1 + G_c(s)G(s)(H(s) - 1)}.$$

The loop transfer function of the equivalent unity feedback system is  $Z(s)$ . It follows that the error constants for nonunity feedback systems are given as:

$$K_p = \lim_{s \rightarrow 0} Z(s), K_v = \lim_{s \rightarrow 0} sZ(s), \text{ and } K_a = \lim_{s \rightarrow 0} s^2 Z(s).$$

Note that when  $H(s) = 1$ , then  $Z(s) = G_c(s)G(s)$  and we maintain the unity feedback error constants. For example, when  $H(s) = 1$ , then  $K_p = \lim_{s \rightarrow 0} Z(s) = \lim_{s \rightarrow 0} G_c(s)G(s)$ , as expected.

## 5.7 PERFORMANCE INDICES

Increasing emphasis on the mathematical formulation and measurement of control system performance can be found in the recent literature on automatic control. Modern control theory assumes that the systems engineer can specify quantitatively the required system performance. Then a performance index can be calculated or measured and used to evaluate the system's performance. A quantitative measure of the performance of a system is necessary for the operation of modern adaptive control systems, for automatic parameter optimization of a control system, and for the design of optimum systems.

Whether the aim is to improve the design of a system or to design a control system, a performance index must be chosen and measured.

**A performance index is a quantitative measure of the performance of a system and is chosen so that emphasis is given to the important system specifications.**

A system is considered an **optimum control system** when the system parameters are adjusted so that the index reaches an extremum, commonly a minimum value. To be useful, a performance index must be a number that is always positive or zero. Then the best system is defined as the system that minimizes this index.

A suitable performance index is the integral of the square of the error, ISE, which is defined as

$$\text{ISE} = \int_0^T e^2(t) dt. \quad (5.37)$$

The upper limit  $T$  is a finite time chosen somewhat arbitrarily so that the integral approaches a steady-state value. It is usually convenient to choose  $T$  as the settling time  $T_s$ . The step response for a specific feedback control system is shown in Figure 5.25(b), and the error in Figure 5.25(c). The error squared is shown in Figure 5.25(d), and the integral of the error squared in Figure 5.25(e). This criterion will discriminate between excessively overdamped and excessively underdamped systems. The minimum value of the integral occurs for a compromise value of the damping. The performance index of Equation (5.37) is easily adapted for practical measurements because a squaring circuit is readily obtained. Furthermore, the squared error is mathematically convenient for analytical and computational purposes.

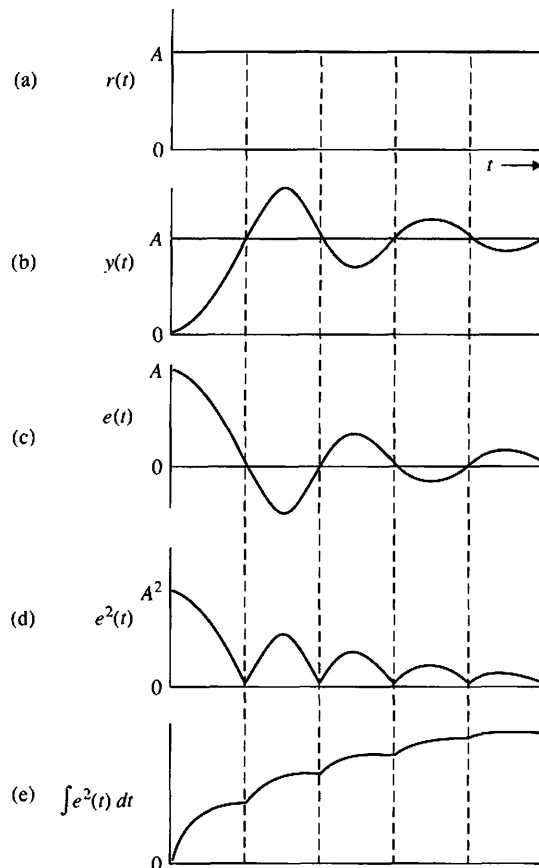


**FIGURE 5.25**  
 The calculation of the integral squared error.

Another readily instrumented performance criterion is the integral of the absolute magnitude of the error, IAE, which is written as

$$\text{IAE} = \int_0^T |e(t)| dt. \quad (5.38)$$

This index is particularly useful for computer simulation studies.

To reduce the contribution of the large initial error to the value of the performance integral, as well as to emphasize errors occurring later in the response, the following index has been proposed [6]:

$$\text{ITAE} = \int_0^T t|e(t)| dt. \quad (5.39)$$

This performance index is designated the integral of time multiplied by absolute error, ITAE. Another similar index is the integral of time multiplied by the squared error, or

$$\text{ITSE} = \int_0^T t e^2(t) dt. \quad (5.40)$$

The performance index ITAE provides the best selectivity of the performance indices; that is, the minimum value of the integral is readily discernible as the system parameters are varied. The general form of the performance integral is

$$I = \int_0^T f(e(t), r(t), y(t), t) dt, \quad (5.41)$$

where  $f$  is a function of the error, input, output, and time. We can obtain numerous indices based on various combinations of the system variables and time. Note that the minimization of IAE or ISE is often of practical significance. For example, the minimization of a performance index can be directly related to the minimization of fuel consumption for aircraft and space vehicles.

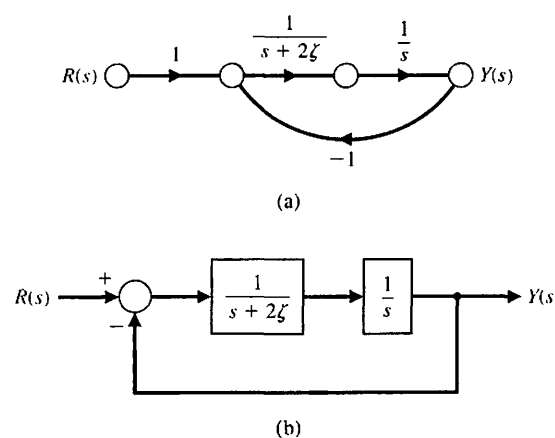
Performance indices are useful for the analysis and design of control systems. Two examples will illustrate the utility of this approach.

#### EXAMPLE 5.6 Performance criteria

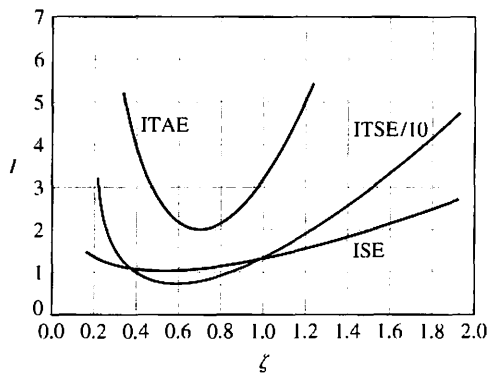
A single-loop feedback control system is shown in Figure 5.26, where the natural frequency is the normalized value,  $\omega_n = 1$ . The closed-loop transfer function is then

$$T(s) = \frac{1}{s^2 + 2\zeta s + 1}. \quad (5.42)$$

Three performance indices—ISE, ITAE, and ITSE—calculated for various values of the damping ratio  $\zeta$  and for a step input are shown in Figure 5.27. These curves show the selectivity of the ITAE index in comparison with the ISE index. The value of the damping ratio  $\zeta$  selected on the basis of ITAE is 0.7. For a second-order system, this results in a swift response to a step with a 4.6% overshoot. ■



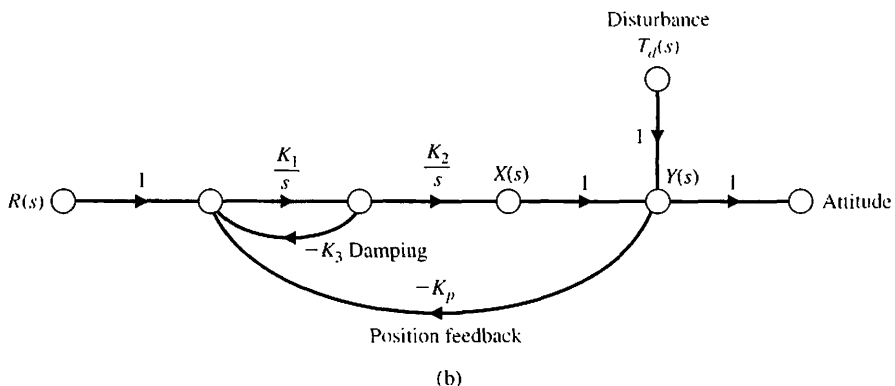
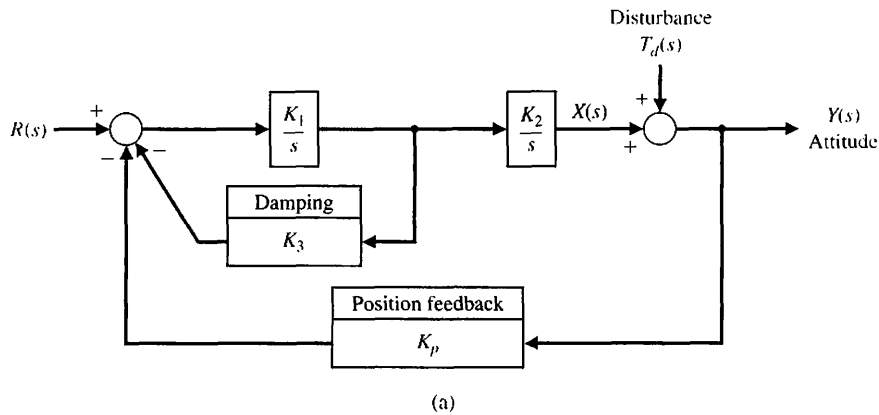
**FIGURE 5.26**  
Single-loop  
feedback control  
system. (a) Signal-  
flow graph.  
(b) Block diagram  
model.

**FIGURE 5.27**

Three performance criteria for a second-order system.

### EXAMPLE 5.7 Space telescope control system

The signal-flow graph and block diagram of a space telescope pointing control system are shown in Figure 5.28 [9]. We desire to select the magnitude of the gain,  $K_3$ , to minimize the effect of the disturbance,  $T_d(s)$ . In this case, the disturbance is equivalent to an initial attitude error. The closed-loop transfer function

**FIGURE 5.28**

A space telescope pointing control system. (a) Block diagram. (b) Signal-flow graph.

for the disturbance is obtained by using Mason's signal-flow gain formula as follows:

$$\begin{aligned}\frac{Y(s)}{T_d(s)} &= \frac{P_1(s) \Delta_1(s)}{\Delta(s)} \\ &= \frac{1 \cdot (1 + K_1 K_3 s^{-1})}{1 + K_1 K_3 s^{-1} + K_1 K_2 K_p s^{-2}} \\ &= \frac{s(s + K_1 K_3)}{s^2 + K_1 K_3 s + K_1 K_2 K_p}.\end{aligned}\quad (5.43)$$

Typical values for the constants are  $K_1 = 0.5$  and  $K_1 K_2 K_p = 2.5$ . Then the natural frequency of the vehicle is  $f_n = \sqrt{2.5}/(2\pi) = 0.25$  cycles/s. For a unit step disturbance, the minimum ISE can be analytically calculated. The attitude is

$$y(t) = \frac{\sqrt{10}}{\beta} \left[ e^{-0.25K_3 t} \sin\left(\frac{\beta}{2}t + \psi\right) \right], \quad (5.44)$$

where  $\beta = \sqrt{10 - K_3^2/4}$ . Squaring  $y(t)$  and integrating the result, we have

$$\begin{aligned}I &= \int_0^\infty \frac{10}{\beta^2} e^{-0.5K_3 t} \sin^2\left(\frac{\beta}{2}t + \psi\right) dt \\ &= \int_0^\infty \frac{10}{\beta^2} e^{-0.5K_3 t} \left( \frac{1}{2} - \frac{1}{2} \cos(\beta t + 2\psi) \right) dt \\ &= \frac{1}{K_3} + 0.1 K_3.\end{aligned}\quad (5.45)$$

Differentiating  $I$  and equating the result to zero, we obtain

$$\frac{dI}{dK_3} = -K_3^{-2} + 0.1 = 0. \quad (5.46)$$

Therefore, the minimum ISE is obtained when  $K_3 = \sqrt{10} = 3.2$ . This value of  $K_3$  corresponds to a damping ratio  $\zeta$  of 0.50. The values of ISE and IAE for this system are plotted in Figure 5.29. The minimum for the IAE performance index is obtained when  $K_3 = 4.2$  and  $\zeta = 0.665$ . While the ISE criterion is not as selective as the IAE criterion, it is clear that it is possible to solve analytically for the minimum value of ISE. The minimum of IAE is obtained by measuring the actual value of IAE for several values of the parameter of interest. ■

A control system is optimum when the selected performance index is minimized. However, the optimum value of the parameters depends directly on the definition of optimum, that is, the performance index. Therefore, in Examples 5.6

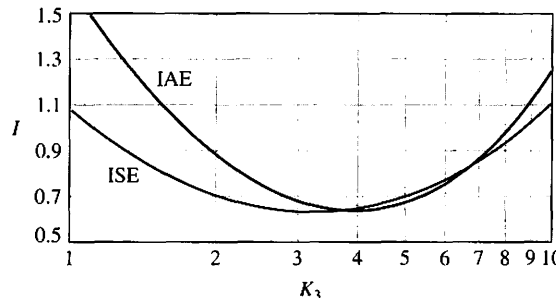


**FIGURE 5.29**  
The performance indices of the telescope control system versus  $K_3$ .

and 5.7, we found that the optimum setting varied for different performance indices.

The coefficients that will minimize the ITAE performance criterion for a step input have been determined for the general closed-loop transfer function [6]

$$T(s) = \frac{Y(s)}{R(s)} = \frac{b_0}{s^n + b_{n-1}s^{n-1} + \dots + b_1s + b_0}. \quad (5.47)$$

This transfer function has a steady-state error equal to zero for a step input. Note that the transfer function has  $n$  poles and no zeros. The optimum coefficients for the ITAE criterion are given in Table 5.6. The responses using optimum coefficients for a step input are given in Figure 5.30 for ISE, IAE, and ITAE. The responses are provided for normalized time  $\omega_n t$ . Other standard forms based on different performance indices are available and can be useful in aiding the designer to determine the range of coefficients for a specific problem. A final example will illustrate the utility of the standard forms for ITAE.

#### EXAMPLE 5.8 Two-camera control

A very accurate and rapidly responding control system is required for a system that allows live actors to appear as if they are performing inside of complex miniature sets. The two-camera system is shown in Figure 5.31(a), where one camera is trained on the actor and the other on the miniature set. The challenge is to obtain rapid and accurate coordination of the two cameras by using sensor information from the

**Table 5.6 The Optimum Coefficients of  $T(s)$  Based on the ITAE Criterion for a Step Input**

$$\begin{aligned} & s + \omega_n \\ & s^2 + 1.4\omega_n s + \omega_n^2 \\ & s^3 + 1.75\omega_n s^2 + 2.15\omega_n^2 s + \omega_n^3 \\ & s^4 + 2.1\omega_n s^3 + 3.4\omega_n^2 s^2 + 2.7\omega_n^3 s + \omega_n^4 \\ & s^5 + 2.8\omega_n s^4 + 5.0\omega_n^2 s^3 + 5.5\omega_n^3 s^2 + 3.4\omega_n^4 s + \omega_n^5 \\ & s^6 + 3.25\omega_n s^5 + 6.60\omega_n^2 s^4 + 8.60\omega_n^3 s^3 + 7.45\omega_n^4 s^2 + 3.95\omega_n^5 s + \omega_n^6 \end{aligned}$$

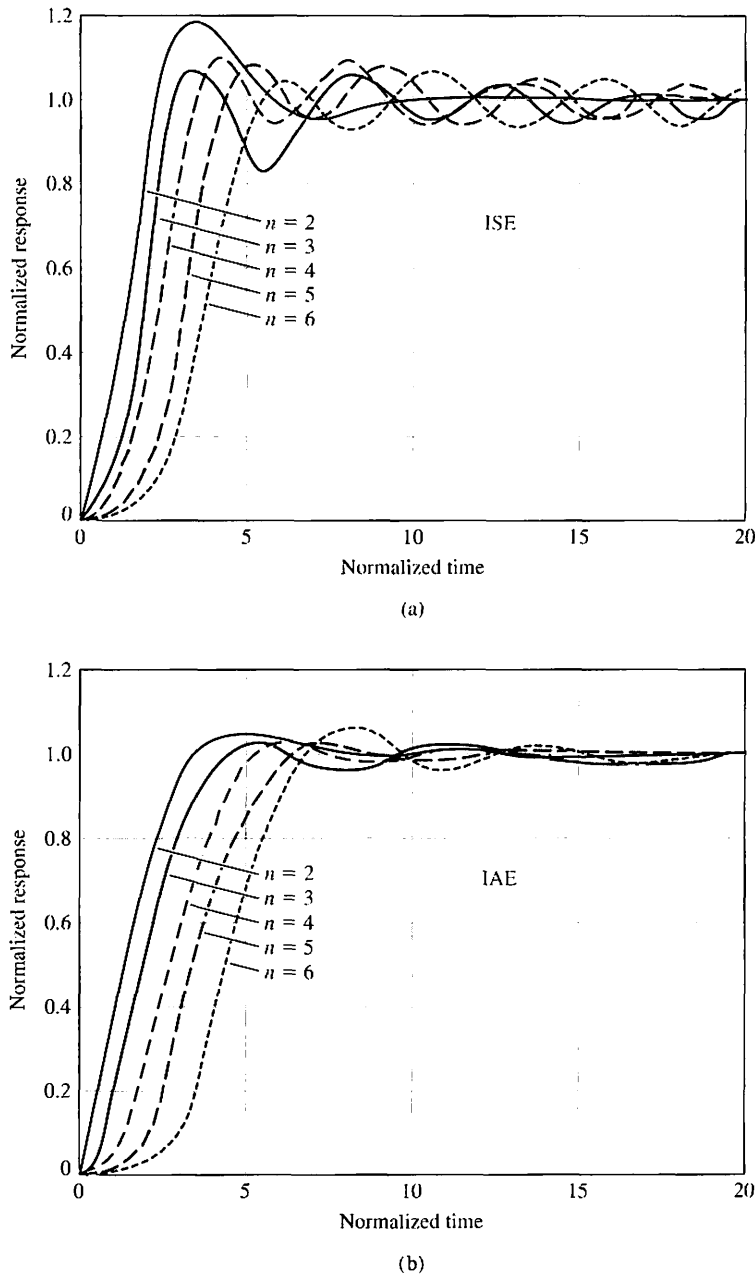
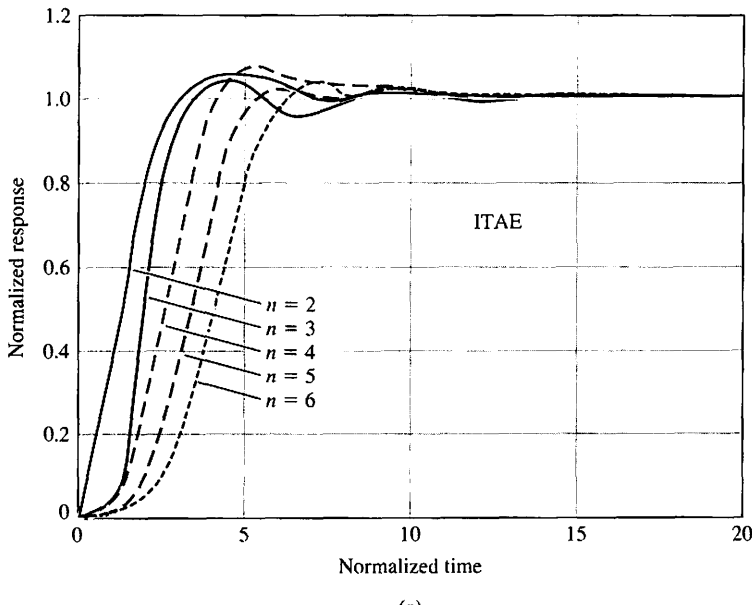


**FIGURE 5.30**  
Step responses of a normalized transfer function using optimum coefficients for (a) ISE, (b) IAE, and (c) ITAE. The response is for normalized time,  $\omega_n t$ .

foreground camera to control the movement of the background camera. The block diagram of the background camera system is shown in Figure 5.31(b) for one axis of movement of the background camera. The closed-loop transfer function is

$$T(s) = \frac{K_a K_m \omega_0^2}{s^3 + 2\zeta\omega_0 s^2 + \omega_0^2 s + K_a K_m \omega_0^2}. \quad (5.48)$$



(c)

**FIGURE 5.30**  
(Continued)

The standard form for a third-order system given in Table 5.6 requires that

$$2\zeta\omega_0 = 1.75\omega_n, \quad \omega_0^2 = 2.15\omega_n^2, \quad \text{and} \quad K_a K_m \omega_0^2 = \omega_n^3.$$

Examining Figure 5.30(c) for  $n = 3$ , we estimate that the settling time is approximately 8 seconds (normalized time). Therefore, we estimate that

$$\omega_n T_s = 8.$$

Because a rapid response is required, a large  $\omega_n$  will be selected so that the settling time will be less than 1 second. Thus,  $\omega_n$  will be set equal to 10 rad/s. Then, for an ITAE system, it is necessary that the parameters of the camera dynamics be

$$\omega_0 = 14.67 \text{ rad/s}$$

and

$$\zeta = 0.597.$$

The amplifier and motor gain are required to be

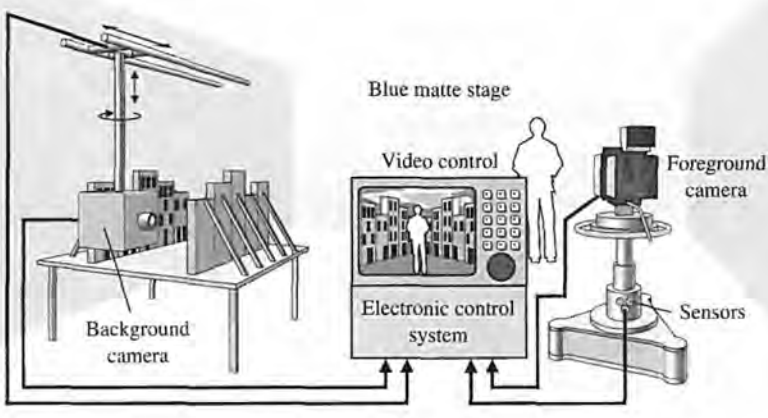
$$K_a K_m = \frac{\omega_n^3}{\omega_0^2} = \frac{\omega_n^3}{2.15\omega_n^2} = \frac{\omega_n}{2.15} = 4.65.$$

Then the closed-loop transfer function is

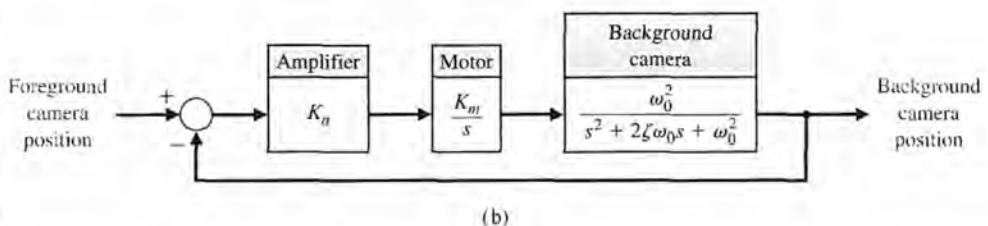
$$\begin{aligned} T(s) &= \frac{1000}{s^3 + 17.5s^2 + 215s + 1000} \\ &= \frac{1000}{(s + 7.08)(s + 5.21 + j10.68)(s + 5.21 - j10.68)}. \end{aligned} \quad (5.49)$$

**FIGURE 5.31**

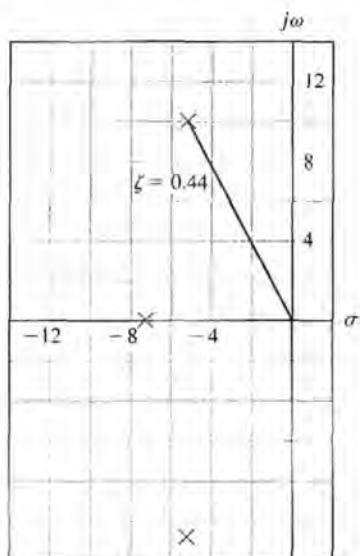
The foreground camera, which may be either a film or video camera, is trained on the blue cyclorama stage. The electronic servocontrol installation permits the slaving, by means of electronic servodevices, of the two cameras. The background camera reaches into the miniature set with a periscope lens and instantaneously reproduces all movements of the foreground camera in the scale of the miniature. The video control installation allows the composite image to be monitored and recorded live. (Part (a) reprinted with permission from *Electronic Design* 24, 11, May 24, 1976. Copyright © Hayden Publishing Co., Inc., 1976.)



(a)



(b)

**FIGURE 5.32**

The closed-loop roots of a minimum ITAE system.

**Table 5.7 The Optimum Coefficients of  $T(s)$  Based on the ITAE Criterion for a Ramp Input**

$$\begin{aligned} & s^2 + 3.2\omega_n s + \omega_n^2 \\ & s^3 + 1.75\omega_n s^2 + 3.25\omega_n^2 s + \omega_n^3 \\ & s^4 + 2.41\omega_n s^3 + 4.93\omega_n^2 s^2 + 5.14\omega_n^3 s + \omega_n^4 \\ & s^5 + 2.19\omega_n s^4 + 6.50\omega_n^2 s^3 + 6.30\omega_n^3 s^2 + 5.24\omega_n^4 s + \omega_n^5 \end{aligned}$$


---

The locations of the closed-loop roots dictated by the ITAE system are shown in Figure 5.32. The damping ratio of the complex roots is  $\zeta = 0.44$ . However, the complex roots do not dominate. The actual response to a step input using a computer simulation showed the overshoot to be only 2% and the settling time (to within 2% of the final value) to be equal to 0.75 second.

For a ramp input, the coefficients have been determined that minimize the ITAE criterion for the general closed-loop transfer function [6]

$$T(s) = \frac{b_1 s + b_0}{s^n + b_{n-1}s^{n-1} + \dots + b_1 s + b_0}. \quad (5.50)$$

This transfer function has a steady-state error equal to zero for a ramp input. The optimum coefficients for this transfer function are given in Table 5.7. The transfer function, Equation (5.50), implies that the process  $G(s)$  has two or more pure integrations, as required to provide zero steady-state error. ■

## 5.8 THE SIMPLIFICATION OF LINEAR SYSTEMS

It is quite useful to study complex systems with high-order transfer functions by using lower-order approximate models. For example, a fourth-order system could be approximated by a second-order system leading to a use of the performance indices in Figure 5.8. Several methods are available for reducing the order of a systems transfer function.

One relatively simple way to delete a certain insignificant pole of a transfer function is to note a pole that has a negative real part that is much more negative than the other poles. Thus, that pole is expected to affect the transient response insignificantly.

For example, if we have a system with transfer function

$$G(s) = \frac{K}{s(s+2)(s+30)},$$

we can safely neglect the impact of the pole at  $s = -30$ . However, we must retain the steady-state response of the system, so we reduce the system to

$$G(s) = \frac{(K/30)}{s(s+2)}.$$

A more sophisticated approach attempts to match the frequency response of the reduced-order transfer function with the original transfer function frequency response as closely as possible. Although frequency response methods are covered in Chapter 8, the associated approximation method strictly relies on algebraic manipulation and is presented here. We will let the high-order system be described by the transfer function

$$G_H(s) = K \frac{a_m s^m + a_{m-1} s^{m-1} + \cdots + a_1 s + 1}{b_n s^n + b_{n-1} s^{n-1} + \cdots + b_1 s + 1}, \quad (5.51)$$

in which the poles are in the left-hand  $s$ -plane and  $m \leq n$ . The lower-order approximate transfer function is

$$G_L(s) = K \frac{c_p s^p + \cdots + c_1 s + 1}{d_g s^g + \cdots + d_1 s + 1}, \quad (5.52)$$

where  $p \leq g < n$ . Notice that the gain constant,  $K$ , is the same for the original and approximate system; this ensures the same steady-state response. The method outlined in Example 5.9 is based on selecting  $c_i$  and  $d_i$  in such a way that  $G_L(s)$  has a frequency response (see Chapter 8) very close to that of  $G_H(s)$ . This is equivalent to stating that  $G_H(j\omega)/G_L(j\omega)$  is required to deviate the least amount from unity for various frequencies. The  $c$  and  $d$  coefficients are obtained by using the equations

$$M^{(k)}(s) = \frac{d^k}{ds^k} M(s) \quad (5.53)$$

and

$$\Delta^{(k)}(s) = \frac{d^k}{ds^k} \Delta(s), \quad (5.54)$$

where  $M(s)$  and  $\Delta(s)$  are the numerator and denominator polynomials of  $G_H(s)/G_L(s)$ , respectively. We also define

$$M_{2q} = \sum_{k=0}^{2q} \frac{(-1)^{k+q} M^{(k)}(0) M^{(2q-k)}(0)}{k!(2q-k)!}, \quad q = 0, 1, 2 \dots \quad (5.55)$$

and an analogous equation for  $\Delta_{2q}$ . The solutions for the  $c$  and  $d$  coefficients are obtained by equating

$$M_{2q} = \Delta_{2q} \quad (5.56)$$

for  $q = 1, 2, \dots$  up to the number required to solve for the unknown coefficients.

Let us consider an example to clarify the use of these equations.

**EXAMPLE 5.9 A simplified model**

Consider the third-order system

$$G_H(s) = \frac{6}{s^3 + 6s^2 + 11s + 6} = \frac{1}{1 + \frac{11}{6}s + s^2 + \frac{1}{6}s^3}. \quad (5.57)$$

Using the second-order model

$$G_L(s) = \frac{1}{1 + d_1s + d_2s^2}, \quad (5.58)$$

we determine that

$$M(s) = 1 + d_1s + d_2s^2, \quad \text{and} \quad \Delta(s) = 1 + \frac{11}{6}s + s^2 + \frac{1}{6}s^3.$$

Then we know that

$$M^{(0)}(s) = 1 + d_1s + d_2s^2, \quad (5.59)$$

and  $M^{(0)}(0) = 1$ . Similarly, we have

$$M^{(1)} = \frac{d}{ds}(1 + d_1s + d_2s^2) = d_1 + 2d_2s. \quad (5.60)$$

Therefore,  $M^{(1)}(0) = d_1$ . Continuing this process, we find that

$$\begin{aligned} M^{(0)}(0) &= 1 & \Delta^{(0)}(0) &= 1, \\ M^{(1)}(0) &= d_1 & \Delta^{(1)}(0) &= \frac{11}{6}, \\ M^{(2)}(0) &= 2d_2 & \Delta^{(2)}(0) &= 2, \end{aligned} \quad (5.61)$$

and

$$M^{(3)}(0) = 0 \quad \Delta^{(3)}(0) = 1.$$

We now equate  $M_{2q} = \Delta_{2q}$  for  $q = 1$  and 2. We find that, for  $q = 1$ ,

$$\begin{aligned} M_2 &= (-1) \frac{M^{(0)}(0)M^{(2)}(0)}{2} + \frac{M^{(1)}(0)M^{(1)}(0)}{1} + (-1) \frac{M^{(2)}(0)M^{(0)}(0)}{2} \\ &= -d_2 + d_1^2 - d_2 = -2d_2 + d_1^2. \end{aligned} \quad (5.62)$$

Since the equation for  $\Delta_2$  is similar, we have

$$\begin{aligned} \Delta_2 &= (-1) \frac{\Delta^{(0)}(0)\Delta^{(2)}(0)}{2} + \frac{\Delta^{(1)}(0)\Delta^{(1)}(0)}{1} + (-1) \frac{\Delta^{(2)}(0)\Delta^{(0)}(0)}{2} \\ &= -1 + \frac{121}{36} - 1 = \frac{49}{36}. \end{aligned} \quad (5.63)$$

Equation (5.56) with  $q = 1$  requires that  $M_2 = \Delta_2$ ; therefore,

$$-2d_2 + d_1^2 = \frac{49}{36}. \quad (5.64)$$

Completing the process for  $M_4 = \Delta_4$ , we obtain

$$d_2^2 = \frac{7}{18}. \quad (5.65)$$

Solving Equations (5.64) and (5.65) yields  $d_1 = 1.615$  and  $d_2 = 0.624$ . (The other sets of solutions are rejected because they lead to unstable poles.) The lower-order system transfer function is

$$G_L(s) = \frac{1}{1 + 1.615s + 0.624s^2} = \frac{1.60}{s^2 + 2.590s + 1.60}. \quad (5.66)$$

It is interesting to see that the poles of  $G_H(s)$  are  $s = -1, -2, -3$ , whereas the poles of  $G_L(s)$  are  $s = -1.024$  and  $-1.565$ . Because the lower-order model has two poles, we estimate that we would obtain a slightly overdamped step response with a settling time to within 2% of the final value in approximately 3 seconds. ■

It is sometimes desirable to retain the dominant poles of the original system,  $G_H(s)$ , in the low-order model. This can be accomplished by specifying the denominator of  $G_L(s)$  to be the dominant poles of  $G_H(s)$  and allowing the numerator of  $G_L(s)$  to be subject to approximation.

Another novel and useful method for reducing the order is the Routh approximation method based on the idea of truncating the Routh table used to determine stability. The Routh approximants can be computed by a finite recursive algorithm that is suited for programming on a digital computer [19].

A robot named Domo was developed to investigate robot manipulation in unstructured environments [22–23]. The robot shown in Figure 5.33 has 29 degrees of freedom, making it a very complex system. Domo employs two six-degree-of-freedom arms and hands with compliant and force-sensitive actuators coupled with a behavior-based system architecture to achieve robotic manipulation tasks in human environments. Designing a controller to control the motion of the arm and hands would require significant model reduction and approximation before the methods of design discussed in the subsequent chapters (e.g., root locus design methods) could be successfully applied.

## 5.9 DESIGN EXAMPLES

In this section we present two illustrative examples. The first example is a simplified view of the Hubble space telescope pointing control problem. The Hubble space telescope problem highlights the process of computing controller gains to achieve desired percent overshoot specifications, as well as meeting steady-state error specifications. The second example considers the control of the bank angle of an airplane. The airplane attitude motion control example represents a more in-depth look

**FIGURE 5.33**

An upper-torso humanoid robot named Domo helps researchers investigate robot manipulation in unstructured environments.  
(Photo courtesy of Aaron Edsinger, MIT Humanoid Robotics Group.)

at the control design problem. Here we consider a complex fourth-order model of the lateral dynamics of the aircraft motion that is approximated by a second-order model using the approximation methods of Section 5.8. The simplified model can be used to gain insight into the controller design and the impact of key controller parameters on the transient performance.

#### **EXAMPLE 5.10 Hubble space telescope control**

The orbiting Hubble space telescope is the most complex and expensive scientific instrument that has ever been built. Launched to 380 miles above the earth on April 24, 1990, the telescope has pushed technology to new limits. The telescope's 2.4 meter (94.5-inch) mirror has the smoothest surface of any mirror made, and its pointing system can center it on a dime 400 miles away [18]. The telescope had a spherical aberration that was largely corrected during space missions in 1993 and 1997 [21]. Consider the model of the telescope-pointing system shown in Figure 5.34.

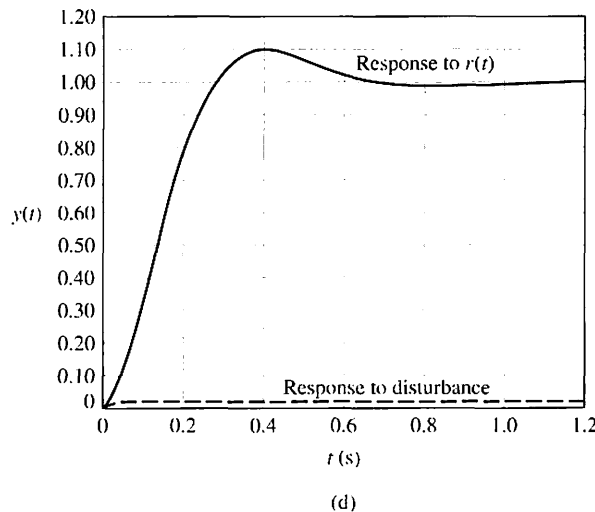
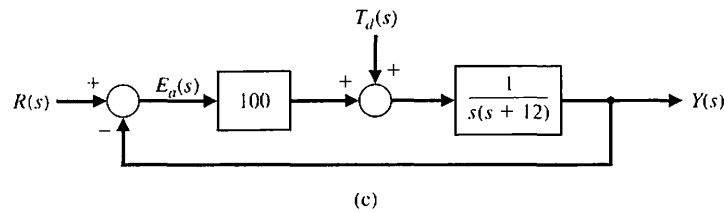
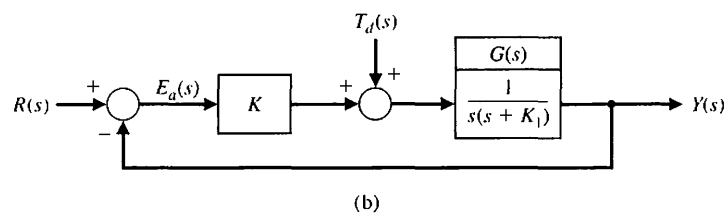
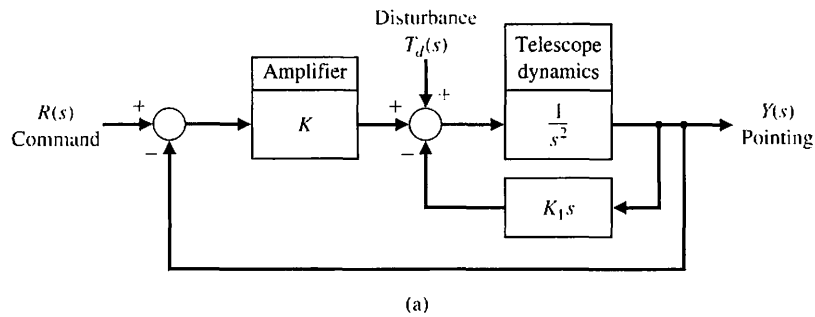


**FIGURE 5.34**  
 (a) The Hubble telescope pointing system, (b) reduced block diagram, (c) system design, and (d) system response to a unit step input command and a unit step disturbance input.

The goal of the design is to choose  $K_1$  and  $K$  so that (1) the percent overshoot of the output to a step command,  $r(t)$ , is less than or equal to 10%, (2) the steady-state error to a ramp command is minimized, and (3) the effect of a step disturbance is reduced. Since the system has an inner loop, block diagram reduction can be used to obtain the simplified system of Figure 5.34(b).

The output due to the two inputs of the system of Figure 5.34(b) is given by

$$Y(s) = T(s)R(s) + [T(s)/K]T_d(s), \quad (5.67)$$

where

$$T(s) = \frac{KG(s)}{1 + KG(s)} = \frac{L(s)}{1 + L(s)}.$$

The error is

$$E(s) = \frac{1}{1 + L(s)}R(s) - \frac{G(s)}{1 + L(s)}T_d(s). \quad (5.68)$$

First, let us select  $K$  and  $K_1$  to meet the percent overshoot requirement for a step input,  $R(s) = A/s$ . Setting  $T_d(s) = 0$ , we have

$$\begin{aligned} Y(s) &= \frac{KG(s)}{1 + KG(s)}R(s) \\ &= \frac{K}{s(s + K_1) + K} \left( \frac{A}{s} \right) = \frac{K}{s^2 + K_1s + K} \left( \frac{A}{s} \right). \end{aligned} \quad (5.69)$$

To set the overshoot less than 10%, we select  $\zeta = 0.6$  by examining Figure 5.8 or using Equation (5.16) to determine that the overshoot will be 9.5% for  $\zeta = 0.6$ . We next examine the steady-state error for a ramp,  $r(t) = Bt$ ,  $t \geq 0$ , using (Equation 5.28):

$$e_{ss} = \lim_{s \rightarrow 0} \left\{ \frac{B}{sKG(s)} \right\} = \frac{B}{K/K_1}. \quad (5.70)$$

The steady-state error due to a unit step disturbance is equal to  $-1/K$ . (The student should show this.) The transient response of the error due to the step disturbance input can be reduced by increasing  $K$  (see Equation 5.68). In summary, we seek a large  $K$  and a large value of  $K/K_1$  to obtain a low steady-state error for the ramp input (see Equation 5.70). However, we also require  $\zeta = 0.6$  to limit the overshoot.

For our design, we need to select  $K$ . With  $\zeta = 0.6$ , the characteristic equation of the system is

$$s^2 + 2\zeta\omega_n s + \omega_n^2 = s^2 + 2(0.6)\omega_n s + K. \quad (5.71)$$

Therefore,  $\omega_n = \sqrt{K}$ , and the second term of the denominator of Equation (5.69) requires  $K_1 = 2(0.6)\omega_n$ . Then  $K_1 = 1.2\sqrt{K}$ , so the ratio  $K/K_1$  becomes

$$\frac{K}{K_1} = \frac{K}{1.2\sqrt{K}} = \frac{\sqrt{K}}{1.2}.$$

Selecting  $K = 25$ , we have  $K_1 = 6$  and  $K/K_1 = 4.17$ . If we select  $K = 100$ , we have  $K_1 = 12$  and  $K/K_1 = 8.33$ . Realistically, we must limit  $K$  so that the system's operation remains linear. Using  $K = 100$ , we obtain the system shown in Figure 5.34(c). The responses of the system to a unit step input command and a unit step disturbance input are shown in Figure 5.34(d). Note how the effect of the disturbance is relatively insignificant.

Finally, we note that the steady-state error for a ramp input (see Equation 5.70) is

$$e_{ss} = \frac{B}{8.33} = 0.12B.$$

This design, using  $K = 100$ , is an excellent system. ■

#### **EXAMPLE 5.11 Attitude control of an airplane**

Each time we fly on a commercial airliner, we experience first-hand the benefits of automatic control systems. These systems assist pilots by improving the handling qualities of the aircraft over a wide range of flight conditions and by providing pilot relief (for such emergencies as going to the restroom) during extended flights. The special relationship between flight and controls began in the early work of the Wright brothers. Using wind tunnels, the Wright brothers applied systematic design techniques to make their dream of powered flight a reality. This systematic approach to design contributed to their success.

Another significant aspect of their approach was their emphasis on flight controls; the brothers insisted that their aircraft be pilot-controlled. Observing birds control their rolling motion by twisting their wings, the Wright brothers built aircraft with mechanical mechanisms that twisted their airplane wings. Today we no longer use wing warping as a mechanism for performing a roll maneuver; instead we control rolling motion by using ailerons, as shown in Figure 5.35. The Wright brothers also used elevators (located forward) for longitudinal

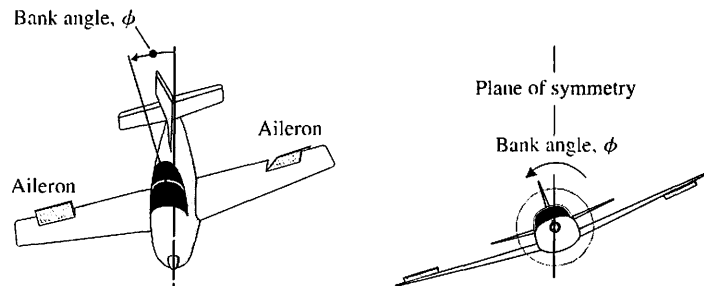


**FIGURE 5.35**  
Control of the bank angle of an airplane using differential deflections of the ailerons.

control (pitch motion) and rudders for lateral control (yaw motion). Today's aircraft still use both elevators and rudders, although the elevators are generally located on the tail (rearward).

The first controlled, powered, unassisted take-off flight occurred in 1903 with the *Wright Flyer I* (a.k.a. *Kitty Hawk*). The first practical airplane, the *Flyer III*, could fly figure eights and stay aloft for half an hour. Three-axis flight control was a major (and often overlooked) contribution of the Wright brothers. A concise historical perspective is presented in Stevens and Lewis [24]. The continuing desire to fly faster, lighter, and longer fostered further developments in automatic flight control. Today's challenge is to develop a single-stage-to-orbit aircraft/spacecraft that can take off and land on a standard runway.

The main topic of this chapter is control of the automatic rolling motion of an airplane. The elements of the design process emphasized in this chapter are illustrated in Figure 5.36.

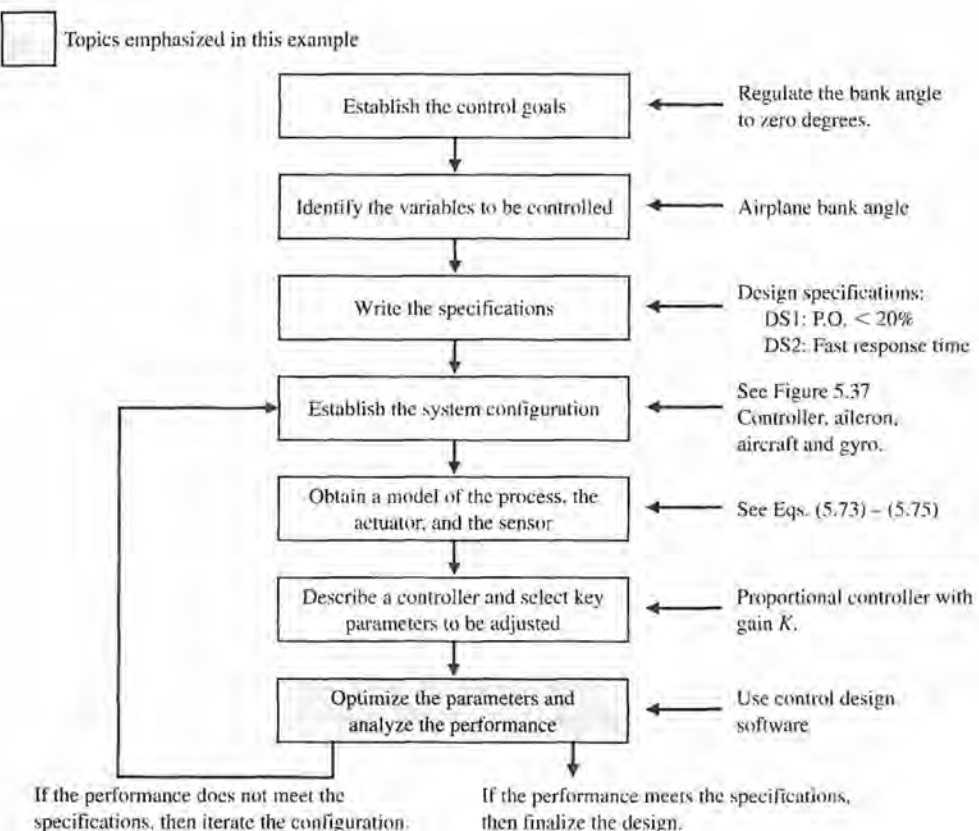


**FIGURE 5.36** Elements of the control system design process emphasized in the airplane attitude control example.

We begin by considering the model of the lateral dynamics of an airplane moving along a steady, wings-level flight path. By lateral dynamics, we mean the attitude motion of the aircraft about the forward velocity. An accurate mathematical model describing the motion (translational and rotational) of an aircraft is a complicated set of highly nonlinear, time-varying, coupled differential equations. A good description of the process of developing such a mathematical model appears in Etkin and Reid [25].

For our purposes a simplified dynamic model is required for the autopilot design process. A simplified model might consist of a transfer function describing the input/output relationship between the aileron deflection and the aircraft bank angle. Obtaining such a transfer function would require many prudent simplifications to the original high-fidelity, nonlinear mathematical model.

Suppose we have a rigid aircraft with a plane of symmetry. The airplane is assumed to be cruising at subsonic or low supersonic ( $\text{Mach} < 3$ ) speeds. This allows us to make a flat-earth approximation. We ignore any rotor gyroscopic effects due to spinning masses on the aircraft (such as propellers or turbines). These assumptions allow us to decouple the longitudinal rotational (pitching) motion from the lateral rotational (rolling and yawing) motion.

Of course, we also need to consider a linearization of the nonlinear equations of motion. To accomplish this, we consider only steady-state flight conditions such as

- Steady, wings-level flight
- Steady, level turning flight
- Steady, symmetric pull-up
- Steady roll.

For this example we assume that the airplane is flying at low speed in a steady, wings-level attitude, and we want to design an autopilot to control the rolling motion. We can state the control goal as follows:

### Control Goal

Regulate the airplane bank angle to zero degrees (steady, wings level) and maintain the wings-level orientation in the presence of unpredictable external disturbances.

We identify the variable to be controlled as

### Variable to Be Controlled

Airplane bank angle (denoted by  $\phi$ ).

Defining system specifications for aircraft control is complicated, so we do not attempt it here. It is a subject in and of itself, and many engineers have spent significant efforts developing good, practical design specifications. The goal is to design a control system such that the dominant closed-loop system poles have satisfactory natural frequency and damping [24]. We must define satisfactory and choose test input signals on which to base our analysis.

The Cooper-Harper pilot opinion ratings provide a way to correlate the feel of the airplane with control design specifications [26]. These ratings address the handling qualities issues. Many flying qualities requirements are specified by government agencies, such as the United States Air Force [27]. The USAF MIL-F-8785C is a source of time-domain control system design specifications.

For example we might design an autopilot control system for an aircraft in steady, wings-level flight to achieve a 20% overshoot to a step input with minimal oscillatory motion and rapid response time (that is, a short time-to-peak). Subsequently we implement the controller in the aircraft control system and conduct flight tests or high-fidelity computer simulations, after which the pilots tell us whether they liked the performance of the aircraft. If the overall performance was not satisfactory, we change the time-domain specification (in this case a percent overshoot specification) and redesign until we achieve a feel and performance that pilots (and ultimately passengers) will accept. Despite the simplicity of this approach and many years of research, precise-control system design specifications that provide acceptable airplane flying characteristics in all cases are still not available [24].

The control design specifications given in this example may seem somewhat contrived. In reality the specifications would be much more involved and, in many ways, less precisely known. But recall in Chapter 1 we discussed the fact that we must begin the design process somewhere. With that approach in mind, we select simple design specifications and begin the iterative design process. The design specifications are

### Control Design Specifications

**DS1** Percent overshoot less than 20% for a unit step input.

**DS2** Fast response time as measured by time-to-peak.

By making the simplifying assumptions discussed above and linearizing about the steady, wings-level flight condition, we can obtain a transfer function model describing the bank angle output,  $\phi(s)$ , to the aileron deflection input,  $\delta_a(s)$ . The transfer function has the form

$$\frac{\phi(s)}{\delta_a(s)} = \frac{k(s - c_0)(s^2 + b_1s + b_0)}{s(s + d_0)(s + e_0)(s^2 + f_1s + f_0)}. \quad (5.72)$$

The lateral (roll/yaw) motion has three main modes: Dutch roll mode, spiral mode, and roll subsidence mode. The Dutch roll mode, which gets its name from its similarities to the motion of an ice speed skater, is characterized by a rolling and yawing motion. The airplane center of mass follows nearly a straightline path, and a rudder impulse can excite this mode. The spiral mode is characterized by a mainly yawing motion with some roll motion. This is a weak mode, but it can cause an airplane to enter a steep spiral dive. The roll subsidence motion is almost a pure roll motion. This is the motion we are concerned with for our autopilot design. The denominator of the transfer function in Equation (5.72) shows two first-order modes (spiral and roll subsidence modes) and a second-order mode (Dutch roll mode).

In general the coefficients  $c_0, b_0, b_1, d_0, e_0, f_0, f_1$  and the gain  $k$  are complicated functions of stability derivatives. The stability derivatives are functions of the flight conditions and the aircraft configuration; they differ for different aircraft types. The coupling between the roll and yaw is included in Equation (5.72).

In the transfer function in Equation (5.72), the pole at  $s = -d_0$  is associated with the spiral mode. The pole at  $s = -e_0$  is associated with the roll subsidence mode. Generally,  $e_0 \gg d_0$ . For an F-16 flying at 500 ft/s in steady, wings-level flight,

we have  $e_0 = 3.57$  and  $d_0 = 0.0128$  [24]. The complex conjugate poles given by the term  $s^2 + f_1 s + f_0$  represent the Dutch roll motion.

For low angles of attack (such as with steady, wings-level flight), the Dutch roll mode generally cancels out of the transfer function with the  $s^2 + b_1 s + b_0$  term. This is an approximation, but it is consistent with our other simplifying assumptions. Also, we can ignore the spiral mode since it is essentially a yaw motion only weakly coupled to the roll motion. The zero at  $s = c_0$  represents a gravity effect that causes the aircraft to sideslip as it rolls. We assume that this effect is negligible, since it is most pronounced in a slow roll maneuver in which the sideslip is allowed to build up, and we assume that the aircraft sideslip is small or zero. Therefore we can simplify the transfer function in Eq. (5.72) to obtain a single-degree-of-freedom approximation:

$$\frac{\phi(s)}{\delta_a(s)} = \frac{k}{s(s + e_0)}. \quad (5.73)$$

For our aircraft we select  $e_0 = 1.4$  and  $k = 11.4$ . The associated time-constant of the roll subsidence is  $\tau = 1/e_0 = 0.7$  s. These values represent a fairly fast rolling motion response.

For the aileron actuator model, we typically use a simple first-order system model,

$$\frac{\delta_a(s)}{e(s)} = \frac{p}{s + p}, \quad (5.74)$$

where  $e(s) = \phi_d(s) - \phi(s)$ . In this case we select  $p = 10$ . This corresponds to a time constant of  $\tau = 1/p = 0.1$  s. This is a typical value consistent with a fast response. We need to have an actuator with a fast response so that the dynamics of the actively controlled airplane will be the dominant component of the system response. A slow actuator is akin to a time delay that can cause performance and stability problems.

For a high-fidelity simulation, we would need to develop an accurate model of the gyro dynamics. The gyro, typically an integrating gyro, is usually characterized by a very fast response. To remain consistent with our other simplifying assumptions, we ignore the gyro dynamics in the design process. This means we assume that the sensor measures the bank angle precisely. The gyro model is given by a unity transfer function,

$$K_g = 1. \quad (5.75)$$

Thus our physical system model is given by Equations (5.73), (5.74), and (5.75).

The controller we select for this design is a proportional controller,

$$G_c(s) = K.$$

The system configuration is shown in Figure 5.37. The select key parameter is as follows:

### Select Key Tuning Parameter

Controller gain  $K$ .

The closed-loop transfer function is

$$T(s) = \frac{\phi(s)}{\phi_d(s)} = \frac{114K}{s^3 + 11.4s^2 + 14s + 114K}. \quad (5.76)$$

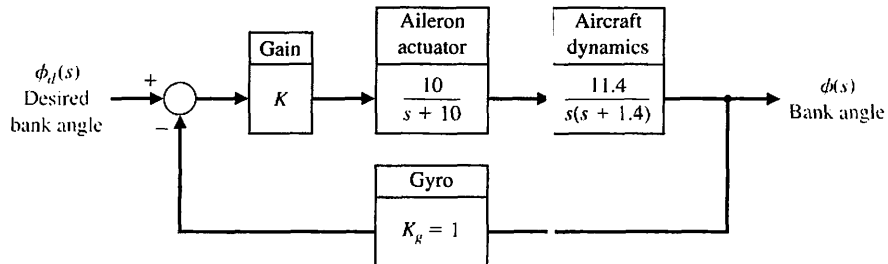


**FIGURE 5.37**  
Bank angle control autopilot.

We want to determine analytically the values of  $K$  that will give us the desired response, namely, a percent overshoot less than 20% and a fast time-to-peak. The analytic analysis would be simpler if our closed-loop system were a second-order system (since we have valuable relationships between settling time, percent overshoot, natural frequency and damping ratio); however we have a third-order system, given by  $T(s)$  in Equation (5.76). We could consider approximating the third-order transfer function by a second-order transfer function—this is sometimes a very good engineering approach to analysis. There are many methods available to obtain approximate transfer functions. Here we use the algebraic method described in Section 5.8 that attempts to match the frequency response of the approximate system as closely as possible to the actual system.

Our transfer function can be rewritten as

$$T(s) = \frac{1}{1 + \frac{14}{114K}s + \frac{11.4}{114K}s^2 + \frac{1}{114K}s^3},$$

by factoring the constant term out of the numerator and denominator. Suppose our approximate transfer function is given by the second-order system

$$G_L(s) = \frac{1}{1 + d_1s + d_2s^2}.$$

The objective is to find appropriate values of  $d_1$  and  $d_2$ . As in Section 5.8, we define  $M(s)$  and  $\Delta(s)$  as the numerator and denominator of  $T(s)/G_L(s)$ . We also define

$$M_{2q} = \sum_{k=0}^{2q} \frac{(-1)^{k+q} M^{(k)}(0) M^{(2q-k)}(0)}{k!(2q-k)!}, \quad q = 1, 2, \dots, \quad (5.77)$$

and

$$\Delta_{2q} = \sum_{k=0}^{2q} \frac{(-1)^{k+q} \Delta^{(k)}(0) \Delta^{(2q-k)}(0)}{k!(2q-k)!}, \quad q = 1, 2, \dots. \quad (5.78)$$

Then, forming the set of algebraic equations

$$M_{2q} = \Delta_{2q}, \quad q = 1, 2, \dots, \quad (5.79)$$

we can solve for the unknown parameters of the approximate function. The index  $q$  is incremented until sufficient equations are obtained to solve for the unknown coefficients of the approximate function. In this case,  $q = 1, 2$  since we have two parameters  $d_1$  and  $d_2$  to compute.

We have

$$\begin{aligned} M(s) &= 1 + d_1 s + d_2 s^2 \\ M^{(1)}(s) &= \frac{dM}{ds} = d_1 + 2d_2 s \\ M^{(2)}(s) &= \frac{d^2M}{ds^2} = 2d_2 \\ M^{(3)}(s) &= M^{(4)}(s) = \cdots = 0. \end{aligned}$$

Thus evaluating at  $s = 0$  yields

$$\begin{aligned} M^{(1)}(0) &= d_1 \\ M^{(2)}(0) &= 2d_2 \\ M^{(3)}(0) &= M^{(4)}(0) = \cdots = 0. \end{aligned}$$

Similarly,

$$\begin{aligned} \Delta(s) &= 1 + \frac{14}{114K}s + \frac{11.4}{114K}s^2 + \frac{s^3}{114K} \\ \Delta^{(1)}(s) &= \frac{d\Delta}{ds} = \frac{14}{114K} + \frac{22.8}{114K}s + \frac{3}{114K}s^2 \\ \Delta^{(2)}(s) &= \frac{d^2\Delta}{ds^2} = \frac{22.8}{114K} + \frac{6}{114K}s \\ \Delta^{(3)}(s) &= \frac{d^3\Delta}{ds^3} = \frac{6}{114K} \\ \Delta^{(4)}(s) &= \Delta^{(5)}(s) = \cdots = 0. \end{aligned}$$

Evaluating at  $s = 0$ , it follows that

$$\begin{aligned} \Delta^{(1)}(0) &= \frac{14}{114K}, \\ \Delta^{(2)}(0) &= \frac{22.8}{114K}, \\ \Delta^{(3)}(0) &= \frac{6}{114K}, \\ \Delta^{(4)}(0) &= \Delta^{(5)}(0) = \cdots = 0. \end{aligned}$$

Using Equation (5.77) for  $q = 1$  and  $q = 2$  yields

$$M_2 = -\frac{M(0)M^{(2)}(0)}{2} + \frac{M^{(1)}(0)M^{(1)}(0)}{1} - \frac{M^{(2)}(0)M(0)}{2} = -2d_2 + d_1^2,$$

and

$$\begin{aligned} M_4 &= \frac{M(0)M^{(4)}(0)}{0! 4!} - \frac{M^{(1)}(0)M^{(3)}(0)}{1! 3!} + \frac{M^{(2)}(0)M^{(2)}(0)}{2! 2!} \\ &\quad - \frac{M^{(3)}(0)M^{(1)}(0)}{3! 1!} + \frac{M^{(4)}(0)M(0)}{4! 0!} = d_2^2. \end{aligned}$$

Similarly using Equation (5.78), we find that

$$\Delta_2 = \frac{-22.8}{114K} + \frac{196}{(114K)^2} \quad \text{and} \quad \Delta_4 = \frac{101.96}{(114K)^2}.$$

Thus forming the set of algebraic equations in Equation (5.79),

$$M_2 = \Delta_2 \quad \text{and} \quad M_4 = \Delta_4,$$

we obtain

$$-2d_2 + d_1^2 = \frac{-22.8}{114K} + \frac{196}{(114K)^2} \quad \text{and} \quad d_2^2 = \frac{101.96}{(114K)^2}.$$

Solving for  $d_1$  and  $d_2$  yields

$$d_1 = \frac{\sqrt{196 - 296.96K}}{114K}, \tag{5.80}$$

$$d_2 = \frac{10.097}{114K}, \tag{5.81}$$

where we always choose the positive values of  $d_1$  and  $d_2$  so that  $G_L(s)$  has poles in the left half-plane. Thus (after some manipulation) the approximate transfer function is

$$G_L(s) = \frac{11.29K}{s^2 + \sqrt{1.92 - 2.91K}s + 11.29K}. \tag{5.82}$$

We require that  $K < 0.65$  so that the coefficient of the  $s$  term remains a real number (we do not want to have a transfer function with complex valued parameters).

Our desired second-order transfer function can be written as

$$G_L(s) = \frac{\omega_n^2}{s^2 + 2\zeta\omega_n s + \omega_n^2} \tag{5.83}$$

Comparing coefficients in Equations (5.82) and (5.83) yields

$$\omega_n^2 = 11.29K \quad \text{and} \quad \zeta^2 = \frac{0.043}{K} - 0.065. \quad (5.84)$$

The design specification that the percent overshoot  $P.O.$  is to be less than 20% implies that we want  $\zeta \geq 0.45$ . This follows from solving Equation (5.16)

$$P.O. = 100 e^{-\pi\zeta/\sqrt{1-\zeta^2}}$$

for  $\zeta$ . Setting  $\zeta = 0.45$  in Equation (5.84) and solving for  $K$  yields

$$K = 0.16.$$

With  $K = 0.16$  we compute

$$\omega_n = \sqrt{11.29K} = 1.34.$$

Then we can estimate the time-to-peak  $T_p$  from Equation (5.14) to be

$$T_p = \frac{\pi}{\omega_n \sqrt{1 - \zeta^2}} = 2.62\text{s}.$$

We might be tempted at this point to select  $\zeta > 0.45$  so that we reduce the percent overshoot even further than 20%. What happens if we decide to try this approach? From Equation (5.84) we see that  $K$  decreases as  $\zeta$  increases. Then, since

$$\omega_n = \sqrt{11.29K},$$

as  $K$  decreases, then  $\omega_n$  also decreases. But the time-to-peak, given by

$$T_p = \frac{\pi}{\omega_n \sqrt{1 - \zeta^2}},$$

increases as  $\omega_n$  decreases. Since our goal is to meet the specification of percent overshoot less than 20% while minimizing the time-to-peak, we use the initial selection of  $\zeta = 0.45$  so that we do not increase  $T_p$  unnecessarily.

The second-order system approximation has allowed us to gain insight into the relationship between the parameter  $K$  and the system response, as measured by percent overshoot and time-to-peak. Of course, the gain  $K = 0.16$  is only a starting point in the design because we in fact have a third-order system and must consider the effect of the third pole (which we have ignored so far).

A comparison of the third-order aircraft model in Equation (5.76) with the second-order approximation in Equation (5.82) for a unit step input is shown in Figure 5.38. The step response of the second-order system is a good approximation of the original system step response, so we would expect that the analytic analysis using the simpler second-order system to provide accurate indications of the relationship between  $K$  and the percent overshoot and time-to-peak.

With the second-order approximation, we estimate that with  $K = 0.16$  the percent overshoot  $P.O. = 20\%$  and the time-to-peak  $T_p = 2.62$  seconds. As shown in

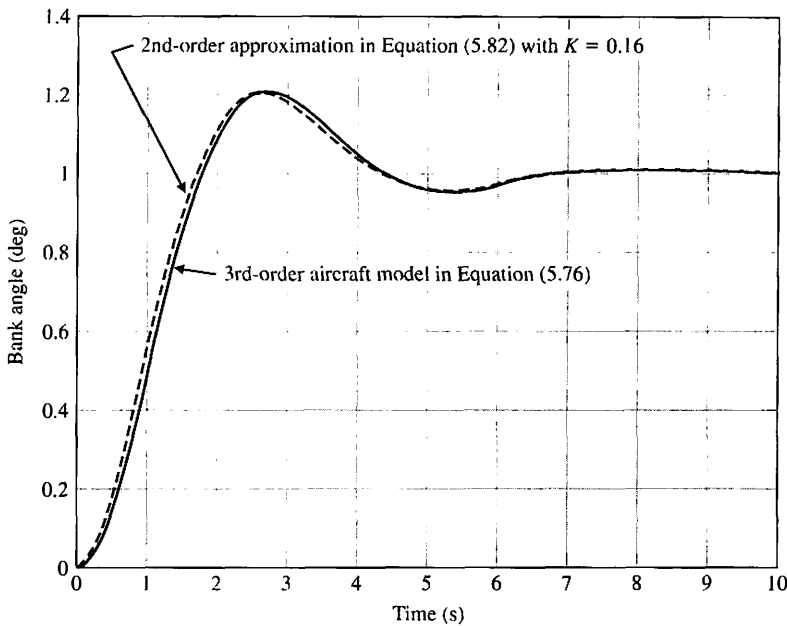


**FIGURE 5.38**  
Step response comparison of third-order aircraft model versus second-order approximation.

Figure 5.39 the percent overshoot of the original third-order system is  $P.O. = 20.5\%$  and the time-to-peak  $T_p = 2.73$  s. Thus, we see that that analytic analysis using the approximate system is an excellent predictor of the actual response. For comparison purposes, we select two variations in the gain and observe the response. For  $K = 0.1$ , the percent overshoot is  $9.5\%$  and the time-to-peak  $T_p = 3.74$  s. For  $K = 0.2$ , the percent overshoot is  $26.5\%$  and the time-to-peak  $T_p = 2.38$  s. So as predicted, as  $K$  decreases the damping ratio increases, leading to a reduction in the percent overshoot. Also as

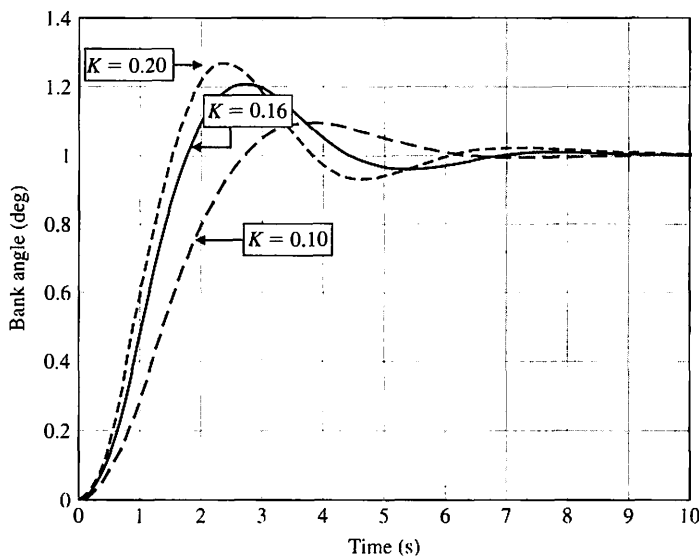


**FIGURE 5.39**  
Step response of the 3<sup>rd</sup>-order aircraft model with  $K = 0.10, 0.16$ , and  $0.20$  showing that, as predicted, as  $K$  decreases percent overshoot decreases while the time-to-peak increases.

**Table 5.8 Performance Comparison for  $K = 0.10$ ,  $0.16$ , and  $0.20$ .**

$K$	P.O. (%)	$T_p$ (s)
0.10	9.5	3.74
0.16	20.5	2.73
0.20	26.5	2.38

predicted, as the percent overshoot decreases the time-to-peak increases. The results are summarized in Table 5.8. ■

## 5.10 SYSTEM PERFORMANCE USING CONTROL DESIGN SOFTWARE

In this section, we will investigate time-domain performance specifications given in terms of transient response to a given input signal and the resulting steady-state tracking errors. We conclude with a discussion of the simplification of linear systems. The function introduced in this section is `impulse`. We will revisit the `lsim` function (introduced in Chapter 3) and see how these functions are used to simulate a linear system.

**Time-Domain Specifications.** Time-domain performance specifications are generally given in terms of the transient response of a system to a given input signal. Because the actual input signals are generally unknown, a standard test input signal is used. Consider the second-order system shown in Figure 5.4. The closed-loop output is

$$Y(s) = \frac{\omega_n^2}{s^2 + 2\zeta\omega_n s + \omega_n^2} R(s). \quad (5.85)$$

We have already discussed the use of the `step` function to compute the step response of a system. Now we address another important test signal: the impulse. The impulse response is the time derivative of the step response. We compute the impulse response with the `impulse` function shown in Figure 5.40.

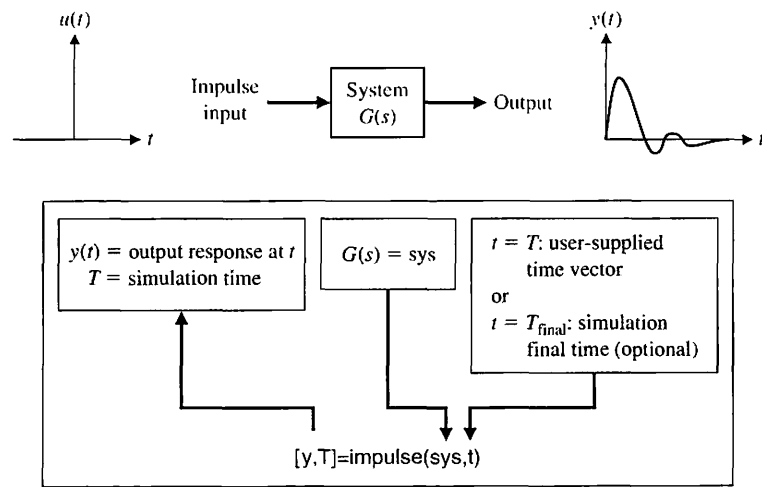
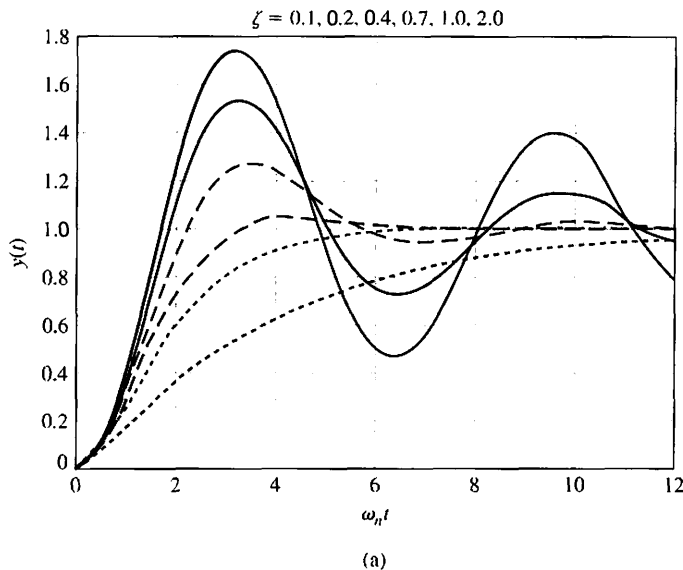
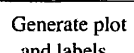
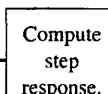


**FIGURE 5.40**  
The `impulse` function.



```
%Compute step response for a second-order system
%Duplicate Figure 5.5 (a)
%
t=[0:0.1:12]; num=[1];
zeta1=0.1; den1=[1 2*zeta1 1]; sys1=tf(num,den1);
zeta2=0.2; den2=[1 2*zeta2 1]; sys2=tf(num,den2);
zeta3=0.4; den3=[1 2*zeta3 1]; sys3=tf(num,den3);
zeta4=0.7; den4=[1 2*zeta4 1]; sys4=tf(num,den4);
zeta5=1.0; den5=[1 2*zeta5 1]; sys5=tf(num,den5);
zeta6=2.0; den6=[1 2*zeta6 1]; sys6=tf(num,den6);
%
[y1,T1]=step(sys1,t); [y2,T2]=step(sys2,t);
[y3,T3]=step(sys3,t); [y4,T4]=step(sys4,t);
[y5,T5]=step(sys5,t); [y6,T6]=step(sys6,t);
%
plot(T1,y1,T2,y2,T3,y3,T4,y4,T5,y5,T6,y6)
xlabel(' \omega_n t'), ylabel('y(t)')
title(' \zeta = 0.1, 0.2, 0.4, 0.7, 1.0, 2.0'), grid
```

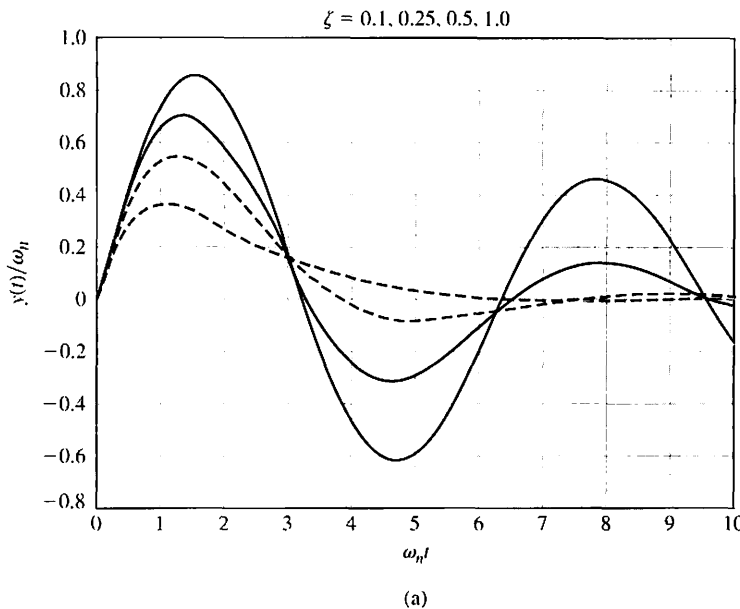


(b)

**FIGURE 5.41**  
(a) Response of a second-order system to a step input. (b) m-file script.

We can obtain a plot similar to that of Figure 5.5(a) with the `step` function, as shown in Figure 5.41. Using the `impulse` function, we can obtain a plot similar to that of Figure 5.6. The response of a second-order system for an impulse function input is shown in Figure 5.42. In the script, we set  $\omega_n = 1$ , which is equivalent to computing the step response versus  $\omega_n t$ . This gives us a more general plot valid for any  $\omega_n > 0$ .

In many cases, it may be necessary to simulate the system response to an arbitrary but known input. In these cases, we use the `lsim` function. The `lsim` function is



```
%Compute impulse response for a second-order system
%Duplicate Figure 5.6
%
t=[0:0.1:10]; num=[1];
zeta1=0.1; den1=[1 2*zeta1 1]; sys1=tf(num,den1);
zeta2=0.25; den2=[1 2*zeta2 1]; sys2=tf(num,den2);
zeta3=0.5; den3=[1 2*zeta3 1]; sys3=tf(num,den3);
zeta4=1.0; den4=[1 2*zeta4 1]; sys4=tf(num,den4);
%
[y1,T1]=impulse(sys1,t);
[y2,T2]=impulse(sys2,t);
[y3,T3]=impulse(sys3,t);
[y4,T4]=impulse(sys4,t);
%
plot(t,y1,t,y2,t,y3,t,y4) ← Compute impulse response.
xlabel(' \omega_n t'), ylabel('y(t)/\omega_n')
title(' \zeta = 0.1, 0.25, 0.5, 1.0'), grid
% Generate plot and labels.
```

**FIGURE 5.42**  
 (a) Response of a second-order system to an impulse function input. (b) m-file script.

(b)

shown in Figure 5.43. We studied the `lsim` function in Chapter 3 for use with state-variable models; however, now we consider the use of `lsim` with transfer function models. An example of the use of `lsim` is given in Example 5.12.

#### EXAMPLE 5.12 Mobile robot steering control

The block diagram for a steering control system for a mobile robot is shown in Figure 5.19. Suppose the transfer function of the steering controller is

$$G_c(s) = K_1 + \frac{K_2}{s}.$$

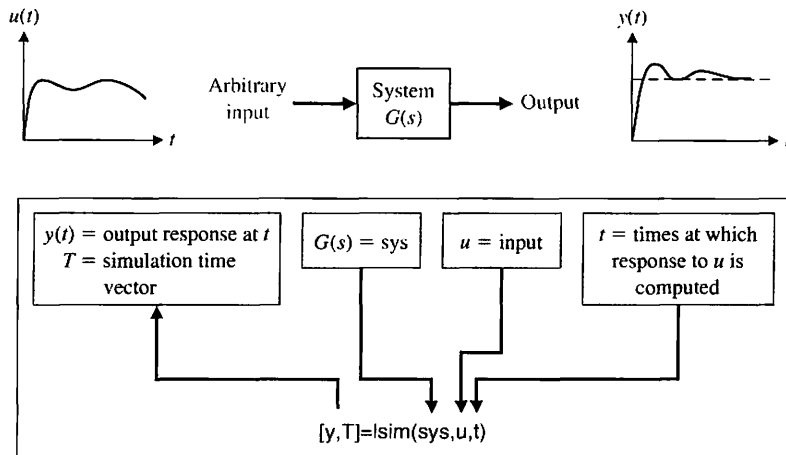


**FIGURE 5.43**  
The **lsim** function.

When the input is a ramp, the steady-state error is

$$e_{ss} = \frac{A}{K_v}, \quad (5.86)$$

where

$$K_v = K_2 K.$$

The effect of the controller constant,  $K_2$ , on the steady-state error is evident from Equation (5.86). Whenever  $K_2$  is large, the steady-state error is small.

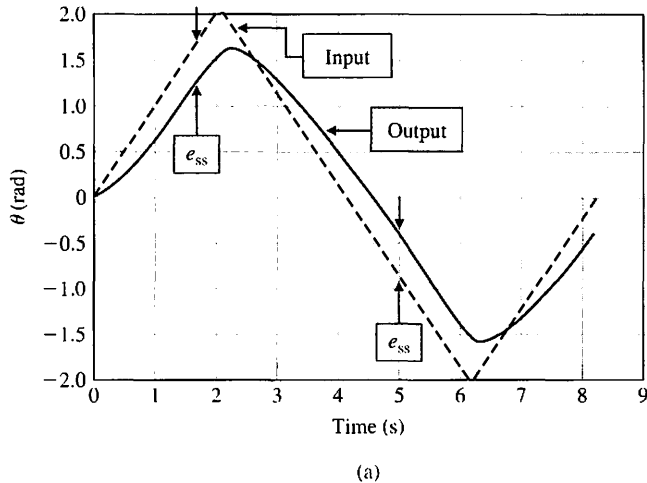
We can simulate the closed-loop system response to a ramp input using the **lsim** function. The controller gains,  $K_1$  and  $K_2$ , and the system gain  $K$  can be represented symbolically in the script so that various values can be selected and simulated. The results are shown in Figure 5.44 for  $K_1 = K = 1$ ,  $K_2 = 2$ , and  $\tau = 1/10$ . ■

**Simplification of Linear Systems.** It may be possible to develop a lower-order approximate model that closely matches the input–output response of a high-order model. A procedure for approximating transfer functions is given in Section 5.8. We can use computer simulation to compare the approximate model to the actual model, as illustrated in the following example.

#### EXAMPLE 5.13 A simplified model

Consider the third-order system

$$G_H(s) = \frac{6}{s^3 + 6s^2 + 11s + 6}.$$



```
%Compute the response of the Mobile Robot Control
%System to a triangular wave input
%
numg=[10 20]; deng=[1 10 0]; sysg=tf(numg,deng); ← G(s)G_c(s)
[sys]=feedback(sysg, [1]);
t=[0:0.1:8.2]';
v1=[0:0.1:2]'; v2=[2:-0.1:-2]'; v3=[-2:0.1:0]';
u=[v1;v2;v3];
[y,T]=lsim(sys,u,t); ← Linear simulation.
plot(T,y,t,u,'--'),
xlabel('Time (s)'), ylabel('\theta (rad)'), grid
```

(b)

**FIGURE 5.44**  
(a) Transient response of the mobile robot steering control system to a ramp input. (b) m-file script.

A second-order approximation (see Example 5.9) is

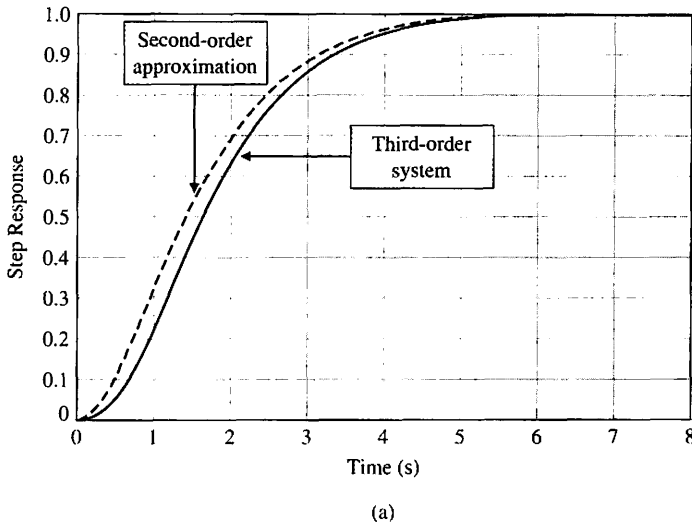
$$G_L(s) = \frac{1.60}{s^2 + 2.590s + 1.60}.$$

A comparison of their respective step responses is given in Figure 5.45. ■

## 5.11 SEQUENTIAL DESIGN EXAMPLE: DISK DRIVE READ SYSTEM



In Section 4.10, we considered the response of the closed-loop reader head control system. Let us further consider the system shown in Figure 4.35. In this section, we further consider the design process. We will specify the desired performance for the system. Then we will attempt to adjust the amplifier gain  $K_a$  in order to obtain the best performance possible.



```
% Compare step response for second-order approximation
%
```

```
num1=[6]; den1=[1 6 11 6]; sys1=tf(num1,den1);
num2=[1.6]; den2=[1 2.594 1.6]; sys2=(tf(num2,den2));
t=[0:0.1:8];
```

```
[y1,T1]=step(sys1,t);

```

```
[y2,T2]=step(sys2,t);

```

```
plot(T1,y1,T2,y2,'--'), grid
xlabel('Time (s)'), ylabel('Step Response')
```

$$G_H(s) = \frac{6}{s^3 + 6s^2 + 11s + 6}$$

$$G_L(s) = \frac{1.6}{s^2 + 2.59s + 1.6}$$

(b)

**FIGURE 5.45**  
 (a) Step response comparison for an approximate transfer function versus the actual transfer function.  
 (b) m-file script.

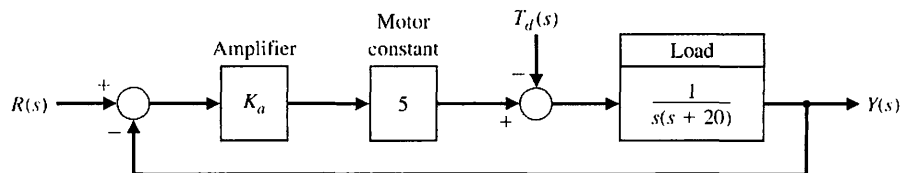
**Table 5.9 Specifications for the Transient Response**

Performance Measure	Desired Value
Percent overshoot	Less than 5%
Settling time	Less than 250 ms
Maximum value of response to a unit step disturbance	Less than $5 \times 10^{-3}$

Our goal is to achieve the fastest response to a step input  $r(t)$  while (1) limiting the overshoot and oscillatory nature of the response and (2) reducing the effect of a disturbance on the output position of the read head. The specifications are summarized in Table 5.9.

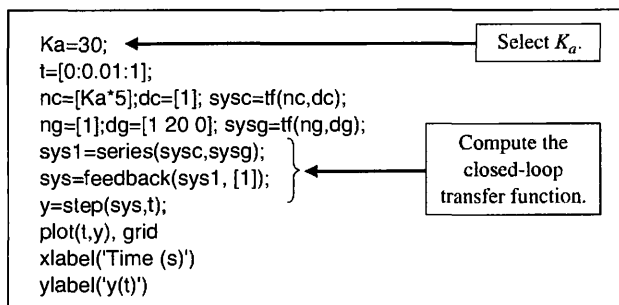
Let us consider the second-order model of the motor and arm, which neglects the effect of the coil inductance. We then have the closed-loop system shown in Figure 5.46. Then the output when  $T_d(s) = 0$  is

**FIGURE 5.46**  
Control system model with a second-order model of the motor and load.



$$\begin{aligned}
 Y(s) &= \frac{5K_a}{s(s+20) + 5K_a} R(s) \\
 &= \frac{5K_a}{s^2 + 20s + 5K_a} R(s) \\
 &= \frac{\omega_n^2}{s^2 + 2\zeta\omega_n s + \omega_n^2} R(s).
 \end{aligned} \tag{5.87}$$

Therefore,  $\omega_n^2 = 5K_a$ , and  $2\zeta\omega_n = 20$ . We then determine the response of the system as shown in Figure 5.47. Table 5.10 shows the performance measures for selected values of  $K_a$ .



(a)

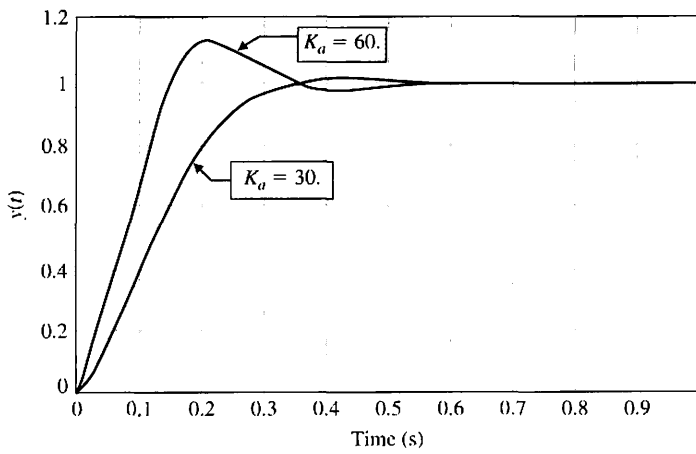


**FIGURE 5.47**  
Response of the system to a unit step input,  $r(t) = 1$ ,  $t > 0$ .  
(a) m-file script.  
(b) Response for  $K_a = 30$  and 60.

**Table 5.10 Response for the Second-Order Model for a Step Input**

$K_a$	20	30	40	60	80
Percent overshoot	0	1.2%	4.3%	10.8%	16.3%
Settling time (s)	0.55	0.40	0.40	0.40	0.40
Damping ratio	1	0.82	0.707	0.58	0.50
Maximum value of the response $y(t)$ to a unit disturbance	$-10 \times 10^{-3}$	$-6.6 \times 10^{-3}$	$-5.2 \times 10^{-3}$	$-3.7 \times 10^{-3}$	$-2.9 \times 10^{-3}$

When  $K_a$  is increased to 60, the effect of a disturbance is reduced by a factor of 2. We can show this by plotting the output,  $y(t)$ , as a result of a unit step disturbance input, as shown in Figure 5.48. Clearly, if we wish to meet our goals with this system, we need to select a compromise gain. In this case, we select  $K_a = 40$  as the best compromise. However, this compromise does not meet all the specifications. In the next chapter, we consider again the design process and change the configuration of the control system.

```

Select Ka
Ka=30;
t=0:0.01:1;
nc=[Ka*5];dc=[1]; sysc=tf(nc,dc);
ng=[1];dg=[1 20 0]; sysg=tf(ng,dg);
sys=feedback(sysg,sysc);
sys=-sys;
y=step(sys,t); plot(t,y)
xlabel('Time (s)'), ylabel('y(t)'), grid
    
```

Disturbance enters summer with a negative sign.

(a)

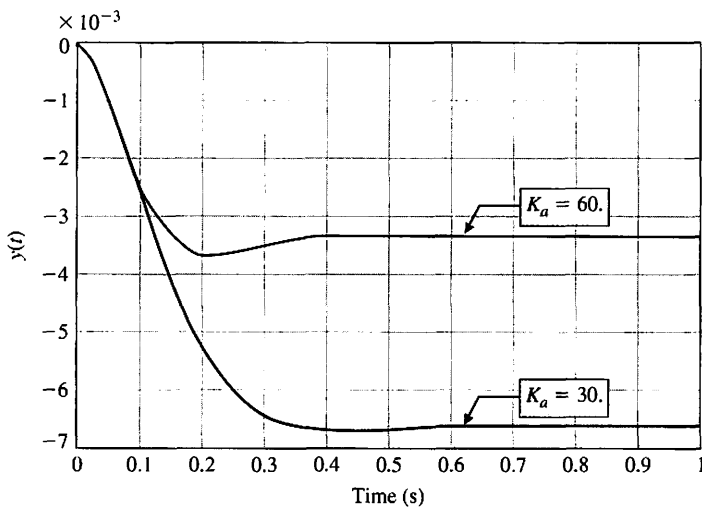


**FIGURE 5.48**  
Response of the system to a unit step disturbance,  $T_d(s) = 1/s$ .  
(a) m-file script.  
(b) Response for  $K_a = 30$  and 60.

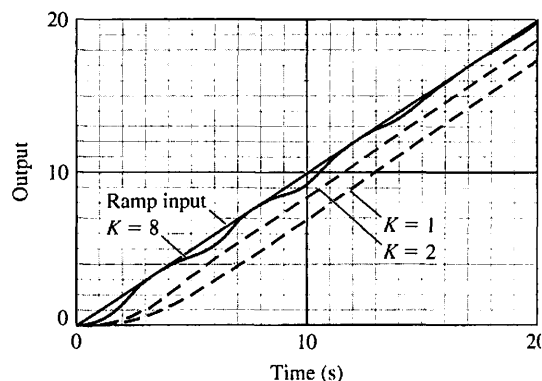


**FIGURE 5.49**  
The response of a feedback system to a ramp input with  $K = 1, 2, and } 8$  when  $G(s) = K/[s(s + 1)(s + 3)]$ . The steady-state error is reduced as  $K$  is increased, but the response becomes oscillatory at  $K = 8$ .

## 5.12 SUMMARY

In this chapter, we have considered the definition and measurement of the performance of a feedback control system. The concept of a performance measure or index was discussed, and the usefulness of standard test signals was outlined. Then, several performance measures for a standard step input test signal were delineated. For example, the overshoot, peak time, and settling time of the response of the system under test for a step input signal were considered. The fact that the specifications on the desired response are often contradictory was noted, and the concept of a design compromise was proposed. The relationship between the location of the  $s$ -plane root of the system transfer function and the system response was discussed. A most important measure of system performance is the steady-state error for specific test input signals. Thus, the relationship of the steady-state error of a system in terms of the system parameters was developed by utilizing the final-value theorem. The capability of a feedback control system is demonstrated in Figure 5.49. Finally, the utility of an integral performance index was outlined, and several design examples that minimized a system's performance index were completed. Thus, we have been concerned with the definition and usefulness of quantitative measures of the performance of feedback control systems.



## SKILLS CHECK

In this section, we provide three sets of problems to test your knowledge: True or False, Multiple Choice, and Word Match. To obtain direct feedback, check your answers with the answer key provided at the conclusion of the end-of-chapter problems. Use the block diagram in Figure 5.50 as specified in the various problem statements.

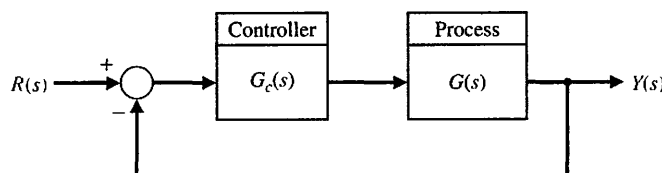


**FIGURE 5.50** Block diagram for the Skills Check.

In the following **True or False** and **Multiple Choice** problems, circle the correct answer.

1. In general, a third-order system can be approximated by a second-order system's dominant roots if the real part of the dominant roots is less than 1/10 of the real part of the third root. *True or False*
2. The number of zeros of the forward path transfer function at the origin is called the type number. *True or False*
3. The rise time is defined as the time required for the system to settle within a certain percentage of the input amplitude. *True or False*
4. For a second-order system with no zeros, the percent overshoot to a unit step is a function of the damping ratio only. *True or False*
5. A type-1 system has a zero steady-state tracking error to a ramp input. *True or False*

Consider the closed-loop control system in Figure 5.50 for Problems 6 and 7 with

$$L(s) = G_c(s)G(s) = \frac{6}{s(s + 3)}.$$

6. The steady-state error to a unit step input  $R(s) = 1/s$  is:

- a.  $e_{ss} = \lim_{t \rightarrow \infty} e(t) = 1$
- b.  $e_{ss} = \lim_{t \rightarrow \infty} e(t) = 1/2$
- c.  $e_{ss} = \lim_{t \rightarrow \infty} e(t) = 1/6$
- d.  $e_{ss} = \lim_{t \rightarrow \infty} e(t) = \infty$

7. The percent overshoot of the output to a unit step input is:

- a. P.O. = 9%
- b. P.O. = 1%
- c. P.O. = 20%
- d. No overshoot

Consider the block diagram of the control system shown in Figure 5.50 in Problems 8 and 9 with the loop transfer function

$$L(s) = G_c(s)G(s) = \frac{K}{s(s + 10)}.$$

8. Find the value of  $K$  so that the system provides an optimum ITAE response.

- a.  $K = 1.10$
- b.  $K = 12.56$
- c.  $K = 51.02$
- d.  $K = 104.7$

9. Compute the expected percent overshoot to a unit step input.

- a. P.O. = 1.4%
- b. P.O. = 4.6%
- c. P.O. = 10.8%
- d. No overshoot expected

10. A system has the closed-loop transfer function  $T(s)$  given by

$$T(s) = \frac{Y(s)}{R(s)} = \frac{2500}{(s + 20)(s^2 + 10s + 125)}.$$

Using the notion of dominant poles, estimate the expected percent overshoot.

- a.  $P.O. \approx 5\%$
- b.  $P.O. \approx 20\%$
- c.  $P.O. \approx 50\%$
- d. No overshoot expected

11. Consider the unity feedback control system in Figure 5.50 where

$$L(s) = G_c(s)G(s) = \frac{K}{s(s + 5)}.$$

The design specifications are:

- i. Peak time  $T_p \leq 1.0$
- ii. Percent overshoot  $P.O. \leq 10\%$ .

With  $K$  as the design parameter, it follows that

- a. Both specifications can be satisfied.
- b. Only the first specification  $T_p \leq 1.0$  can be satisfied.
- c. Only the second specification  $P.O. \leq 10\%$  can be satisfied.
- d. Neither specification can be satisfied.

12. Consider the feedback control system in Figure 5.51 where  $G(s) = \frac{K}{s + 10}$ .

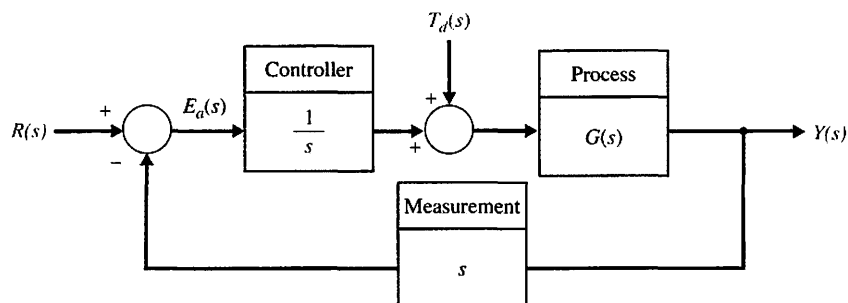


**FIGURE 5.51** Feedback system with integral controller and derivative measurement.

The nominal value of  $K = 10$ . Using a 2% criterion, compute the settling time,  $T_s$  for a unit step disturbance,  $T_d(s) = 1/s$ .

- a.  $T_s = 0.02$  s
- b.  $T_s = 0.19$  s
- c.  $T_s = 1.03$  s
- d.  $T_s = 4.83$  s

13. A plant has the transfer function given by

$$G(s) = \frac{1}{(1 + s)(1 + 0.5s)}$$

and is controlled by a proportional controller  $G_c(s) = K$ , as shown in the block diagram in Figure 5.50. The value of  $K$  that yields a steady-state error  $E(s) = Y(s) - R(s)$  with a magnitude equal to 0.01 for a unit step input is:

- a.  $K = 49$
- b.  $K = 99$

c.  $K = 169$

d. None of the above

In Problems 14 and 15, consider the control system in Figure 5.50, where

$$G(s) = \frac{6}{(s+5)(s+2)} \quad \text{and} \quad G_c(s) = \frac{K}{s+50}.$$

14. A second-order approximate model of the loop transfer function is:

a.  $\hat{G}_c(s)\hat{G}(s) = \frac{(3/25)K}{s^2 + 7s + 10}$

b.  $\hat{G}_c(s)\hat{G}(s) = \frac{(1/25)K}{s^2 + 7s + 10}$

c.  $\hat{G}_c(s)\hat{G}(s) = \frac{(3/25)K}{s^2 + 7s + 500}$

d.  $\hat{G}_c(s)\hat{G}(s) = \frac{6K}{s^2 + 7s + 10}$

15. Using the second-order system approximation (see Problem 14), estimate the gain  $K$  so that the percent overshoot is approximately  $P.O. \approx 15\%$ .

a.  $K = 10$

b.  $K = 300$

c.  $K = 1000$

d. None of the above

In the following **Word Match** problems, match the term with the definition by writing the correct letter in the space provided.

a. Unit impulse	The time for a system to respond to a step input and rise to a peak response.	_____
b. Rise time	The roots of the characteristic equation that cause the dominant transient response of the system.	_____
c. Settling time	The number $N$ of poles of the transfer function, $G(s)$ , at the origin.	_____
d. Type number	The constant evaluated as $\lim_{s \rightarrow 0} sG(s)$ .	_____
e. Percent overshoot	An input signal used as a standard test of a system's ability to respond adequately.	_____
f. Position error constant, $K_p$	The time required for the system output to settle within a certain percentage of the input amplitude.	_____
g. Velocity error constant, $K_v$	A set of prescribed performance criteria.	_____
h. Steady-state response	A system whose parameters are adjusted so that the performance index reaches an extremum value.	_____
i. Peak time	A quantitative measure of the performance of a system.	_____
j. Dominant roots	The time for a system to respond to a step input and attain a response equal to a percentage of the magnitude of the input.	_____
k. Test input signal	The amount by which the system output response proceeds beyond the desired response.	_____
l. Acceleration error constant, $K_a$	The constant evaluated as $\lim_{s \rightarrow 0} s^2 G(s)$ .	_____
m. Transient response	The constant evaluated as $\lim_{s \rightarrow 0} G(s)$ .	_____

- n. Design specifications The constituent of the system response that exists a long time following any signal initiation.
- o. Performance index The constituent of the system response that disappears with time.
- p. Optimum control system A test input consisting of an impulse of infinite amplitude and zero width, and having an area of unity.

## EXERCISES

**E5.1** A motor control system for a computer disk drive must reduce the effect of disturbances and parameter variations, as well as reduce the steady-state error. We want to have no steady-state error for the head-positioning control system, which is of the form shown in Figure 5.18. (a) What type number is required? (How many integrations?) (b) If the input is a ramp signal, and we want to achieve a zero steady-state error, what type number is required?

**E5.2** The engine, body, and tires of a racing vehicle affect the acceleration and speed attainable [9]. The speed control of the car is represented by the model shown in Figure E5.2. (a) Calculate the steady-state error of the car to a step command in speed. (b) Calculate overshoot of the speed to a step command.

*Answer:* (a)  $e_{ss} = A/11$ ; (b) P.O. = 36%

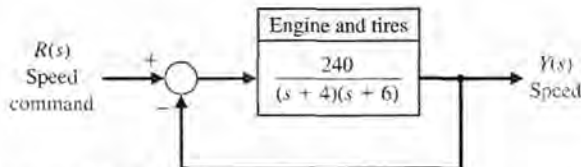


**FIGURE E5.2** Racing car speed control.

**E5.3** New passenger rail systems that could profitably compete with air travel are under development. Two of these systems, the French TGV and the Japanese Shinkansen, reach speeds of 160 mph [17]. The Transrapid, a magnetic levitation train, is shown in Figure E5.3(a).

The use of magnetic levitation and electromagnetic propulsion to provide contactless vehicle movement makes the Transrapid technology radically different. The underside of the carriage (where the wheel trucks would be on a conventional car) wraps around a guideway. Magnets on the bottom of the guideway attract electromagnets on the "wraparound," pulling it up toward the guideway. This suspends the vehicles about one centimeter above the guideway.

The levitation control is represented by Figure E5.3(b). (a) Using Table 5.6 for a step input, select  $K$  so

that the system provides an optimum ITAE response. (b) Using Figure 5.8, determine the expected overshoot to a step input of  $I(s)$ .

*Answer:*  $K = 100$ ; 4.6%

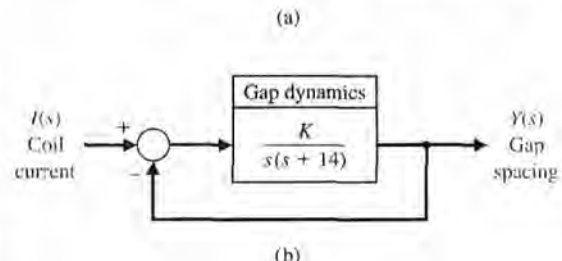


**FIGURE E5.3** Levitated train control.

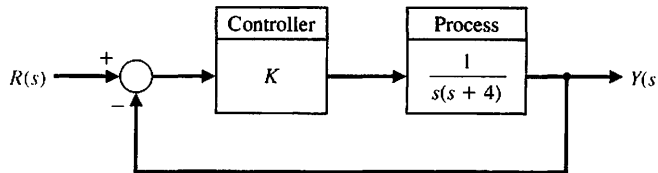
**E5.4** A feedback system with negative unity feedback has a loop transfer function

$$L(s) = G_c(s)G(s) = \frac{2(s + 8)}{s(s + 4)}$$

- (a) Determine the closed-loop transfer function  $T(s) = Y(s)/R(s)$ . (b) Find the time response,  $y(t)$ , for a step input  $r(t) = A$  for  $t > 0$ . (c) Using Figure 5.13(a), determine the overshoot of the response. (d) Using the final-value theorem, determine the steady-state value of  $y(t)$ .

*Answer:* (b)  $y(t) = 1 - 1.07e^{-3t} \sin(\sqrt{7}t + 1.2)$

**FIGURE E5.5**  
Feedback system with proportional controller  
 $G_c(s) = K$ .



**E5.5** Consider the feedback system in Figure E5.5. Find  $K$  such that the closed-loop system minimizes the ITAE performance criterion for a step input.

**E5.6** Consider the block diagram shown in Figure E5.6 [16].  
(a) Calculate the steady-state error for a ramp input.  
(b) Select a value of  $K$  that will result in zero overshoot to a step input. Provide the most rapid response that is attainable.

Plot the poles and zeros of this system and discuss the dominance of the complex poles. What overshoot for a step input do you expect?

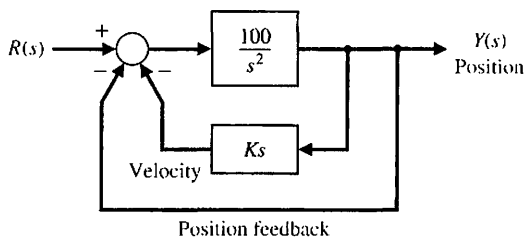


**FIGURE E5.6** Block diagram with position and velocity feedback.

**E5.7** Effective control of insulin injections can result in better lives for diabetic persons. Automatically controlled insulin injection by means of a pump and a sensor that measures blood sugar can be very effective. A pump and injection system has a feedback control as shown in Figure E5.7. Calculate the suitable gain  $K$  so that the overshoot of the step response due to the drug injection is approximately 7%.  $R(s)$  is the desired blood-sugar level and  $Y(s)$  is the actual blood-sugar level. (Hint: Use Figure 5.13a.)

*Answer:*  $K = 1.67$

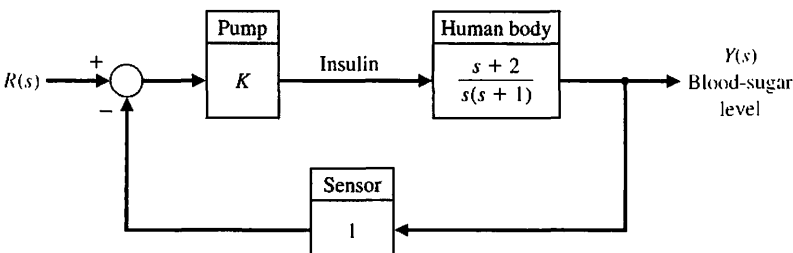


**FIGURE E5.7**  
Blood-sugar level control.

**E5.8** A control system for positioning the head of a floppy disk drive has the closed-loop transfer function

$$T(s) = \frac{11.1(s + 18)}{(s + 20)(s^2 + 4s + 10)}.$$

Plot the poles and zeros of this system and discuss the dominance of the complex poles. What overshoot for a step input do you expect?

**E5.9** A unity negative feedback control system has the loop transfer function

$$L(s) = G_c(s)G(s) = \frac{K}{s(s + \sqrt{2K})}.$$

- (a) Determine the percent overshoot and settling time (using a 2% settling criterion) due to a unit step input.
- (b) For what range of  $K$  is the settling time less than 1 second?

**E5.10** A second-order control system has the closed-loop transfer function  $T(s) = Y(s)/R(s)$ . The system specifications for a step input follow:

- (1) Percent overshoot  $P.O. \leq 5\%$ .
- (2) Settling time  $T_s < 4s$ .
- (3) Peak time  $T_p < 1s$ .

Show the permissible area for the poles of  $T(s)$  in order to achieve the desired response. Use a 2% settling criterion to determine settling time.

**E5.11** A system with unity feedback is shown in Figure E5.11. Determine the steady-state error for a step and a ramp input when

$$G(s) = \frac{5(s + 8)}{s(s + 1)(s + 4)(s + 10)}.$$

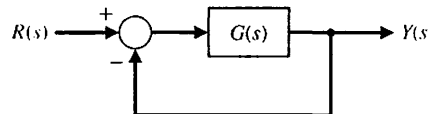


**FIGURE E5.11**  
Unity feedback  
system.

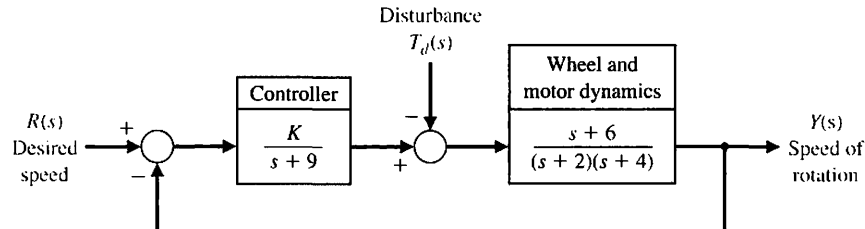


**FIGURE E5.12**  
Speed control of a  
Ferris wheel.

**E5.12** We are all familiar with the Ferris wheel featured at state fairs and carnivals. George Ferris was born in Galesburg, Illinois, in 1859; he later moved to Nevada and then graduated from Rensselaer Polytechnic Institute in 1881. By 1891, Ferris had considerable experience with iron, steel, and bridge construction. He conceived and constructed his famous wheel for the 1893 Columbian Exposition in Chicago [8]. To avoid upsetting passengers, set a requirement that the steady-state speed must be controlled to within 5% of the desired speed for the system shown in Figure E5.12.

- Determine the required gain  $K$  to achieve the steady-state requirement.
- For the gain of part (a), determine and plot the error  $e(t)$  for a disturbance  $T_d(s) = 1/s$ . Does the speed change more than 5%? (Set  $R(s) = 0$  and recall that  $E(s) = R(s) - T(s)$ .)

**E5.13** For the system with unity feedback shown in Figure E5.11, determine the steady-state error for a step and a ramp input when

$$G(s) = \frac{20}{s^2 + 14s + 50}.$$

**Answer:**  $e_{ss} = 0.71$  for a step and  $e_{ss} = \infty$  for a ramp.

**E5.14** A feedback system is shown in Figure E5.14.

- Determine the steady-state error for a unit step when  $K = 0.4$  and  $G_p(s) = 1$ .

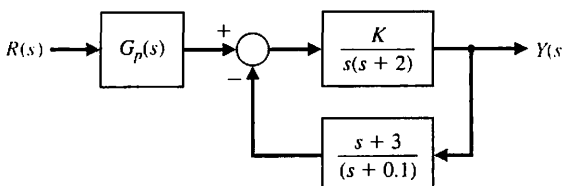


**FIGURE E5.14** Feedback system.

- Select an appropriate value for  $G_p(s)$  so that the steady-state error is equal to zero for the unit step input.

**E5.15** A closed-loop control system has a transfer function  $T(s)$  as follows:

$$\frac{Y(s)}{R(s)} = T(s) = \frac{2500}{(s+50)(s^2 + 10s + 50)}.$$

Plot  $y(t)$  for a step input  $R(s)$  when (a) the actual  $T(s)$  is used, and (b) using the relatively dominant complex poles. Compare the results.

**E5.16** A second-order system is

$$\frac{Y(s)}{R(s)} = T(s) = \frac{(10/z)(s+z)}{(s+1)(s+8)}.$$

Consider the case where  $1 < z < 8$ . Obtain the partial fraction expansion, and plot  $y(t)$  for a step input  $r(t)$  for  $z = 2, 4$ , and  $6$ .

**E5.17** A closed-loop control system transfer function  $T(s)$  has two dominant complex conjugate poles. Sketch the region in the left-hand  $s$ -plane where the complex poles should be located to meet the given specifications.

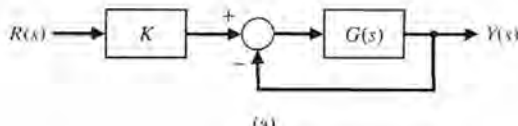
- $0.6 \leq \zeta \leq 0.8, \omega_n \leq 10$
- $0.5 \leq \zeta \leq 0.707, \omega_n \geq 10$
- $\zeta \geq 0.5, 5 \leq \omega_n \leq 10$
- $\zeta \leq 0.707, 5 \leq \omega_n \leq 10$
- $\zeta \geq 0.6, \omega_n \leq 6$

**E5.18** A system is shown in Figure E5.18(a). The response to a unit step, when  $K = 1$ , is shown in Figure E5.18(b). Determine the value of  $K$  so that the steady-state error is equal to zero.

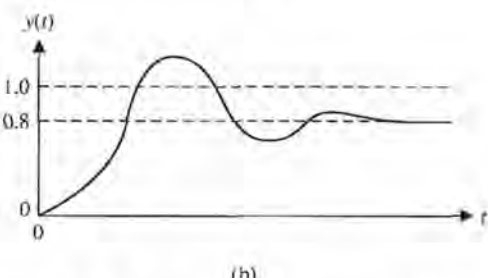
**Answer:**  $K = 1.25$ .

**E5.19** A second-order system has the closed-loop transfer function

$$T(s) = \frac{Y(s)}{R(s)} = \frac{\omega_n^2}{s^2 + 2\zeta\omega_n s + \omega_n^2} = \frac{7}{s^2 + 3.175s + 7}.$$



(a)



(b)

**FIGURE E5.18** Feedback system with prefilter.

- (a) Determine the percent overshoot  $P.O.$ , the time to peak  $T_p$ , and the settling time  $T_s$  of the unit step response,  $R(s) = 1/s$ . To compute the settling time, use a 2% criterion.  
 (b) Obtain the system response to a unit step and verify the results in part (a).

## PROBLEMS

**P5.1** An important problem for television systems is the jumping or wobbling of the picture due to the movement of the camera. This effect occurs when the camera is mounted in a moving truck or airplane. The Dynalens system has been designed to reduce the effect of rapid scanning motion; see Figure P5.1. A maximum scanning motion of  $25^\circ/s$  is expected. Let  $K_g = K_t = 1$  and assume that  $\tau_g$  is negligible. (a) Determine the error of the system  $E(s)$ . (b) Determine the necessary loop gain  $K_a K_m K_t$  when a 1% steady-state error is allowable. (c) The motor time constant is 0.40 s. Determine the necessary loop gain so that the settling time (to within 2% of the final value of  $v_b$ ) is less than or equal to 0.03 s.

**P5.2** A specific closed-loop control system is to be designed for an underdamped response to a step input. The specifications for the system are as follows:

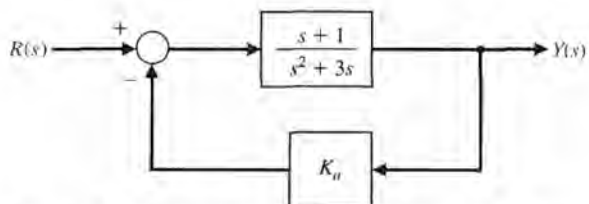
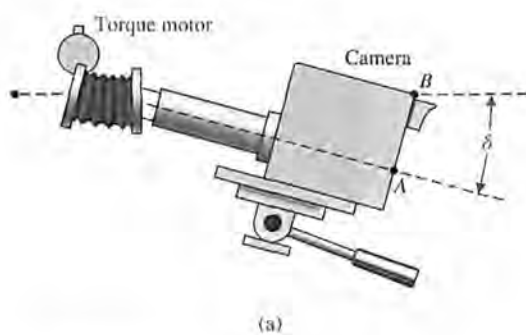
$$10\% < \text{percent overshoot} < 20\%, \\ \text{Settling time} < 0.6 \text{ s.}$$

- (a) Identify the desired area for the dominant roots of the system. (b) Determine the smallest value of a third root  $r_3$  if the complex conjugate roots are to represent the dominant response. (c) The closed-loop system transfer function  $T(s)$  is third-order, and the feedback has a unity gain. Determine the forward transfer function  $G(s) = Y(s)/E(s)$  when the settling time to within 2% of the final value is 0.6 s and the percent overshoot is 20%.

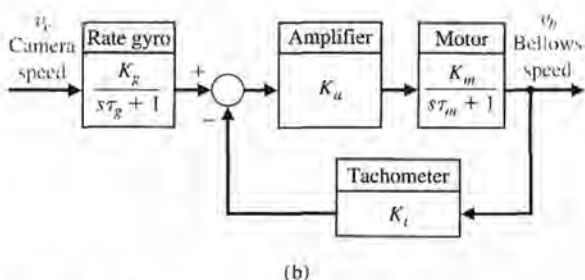
**E5.20** Consider the closed-loop system in Figure E5.19, where

$$G_e(s)G(s) = \frac{s + 1}{s^2 + 0.3s} \text{ and } H(s) = K_a$$

- (a) Determine the closed-loop transfer function  $T(s) = Y(s)/R(s)$ .  
 (b) Determine the steady-state error of the closed-loop system response to a unit ramp input,  $R(s) = 1/s^2$ .  
 (c) Select a value for  $K_a$  so that the steady-state error of the system response to a unit step input,  $R(s) = 1/s$ , is zero.

**FIGURE E5.20** Nonunity closed-loop feedback control system with parameter  $K_a$ .

(a)



(b)

**FIGURE P5.1** Camera wobble control.

**P5.3** A laser beam can be used to weld, drill, etch, cut, and mark metals, as shown in Figure P5.3(a) [14]. Assume we have a work requirement for an accurate laser to mark a parabolic path with a closed-loop control system, as shown in Figure P5.3(b). Calculate the necessary gain to result in a steady-state error of 5 mm for  $r(t) = t^2$  cm.

**P5.4** The loop transfer function of a unity negative feedback system (see Figure E5.11) is

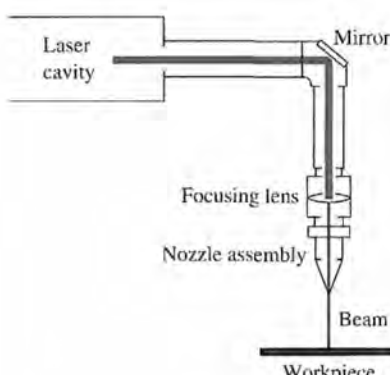
$$L(s) = G_c(s)G(s) = \frac{K}{s(s + 2)}.$$

A system response to a step input is specified as follows:

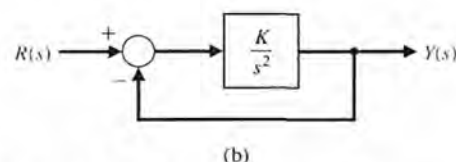
$$\begin{aligned} \text{peak time } T_p &= 1.1 \text{ s,} \\ \text{percent overshoot } P.O. &= 5\%. \end{aligned}$$

(a) Determine whether both specifications can be met simultaneously. (b) If the specifications cannot be met simultaneously, determine a compromise value for  $K$  so that the peak time and percent overshoot specifications are relaxed by the same percentage.

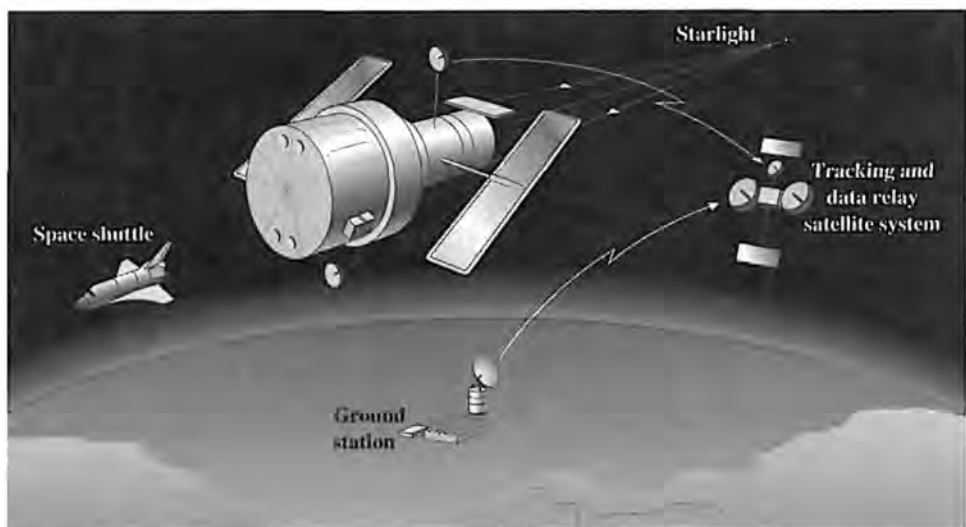
**P5.5** A space telescope is to be launched to carry out astronomical experiments [8]. The pointing control system is desired to achieve 0.01 minute of arc and track solar objects with apparent motion up to 0.21 arc minute per second. The system is illustrated in Figure P5.5(a). The control system is shown in



(a)



(b)

**FIGURE P5.3** Laser beam control.

(a)

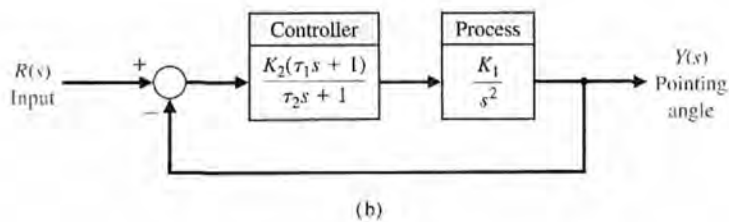


**FIGURE P5.5**  
(a) The space telescope. (b) The space telescope pointing control system.

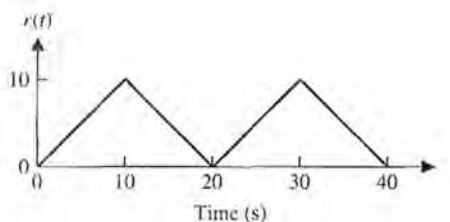
Figure P5.5(b). Assume that  $\tau_1 = 1$  second and  $\tau_2 = 0$  (an approximation). (a) Determine the gain  $K = K_1 K_2$  required so that the response to a step command is as rapid as reasonable with an overshoot of less than 5%. (b) Determine the steady-state error of the system for a step and a ramp input. (c) Determine the value of  $K_1 K_2$  for an ITAE optimal system for (1) a step input and (2) a ramp input.

- P5.6** A robot is programmed to have a tool or welding torch follow a prescribed path [7, 11]. Consider a robot tool that is to follow a sawtooth path, as shown in Figure P5.6(a). The transfer function of the plant is

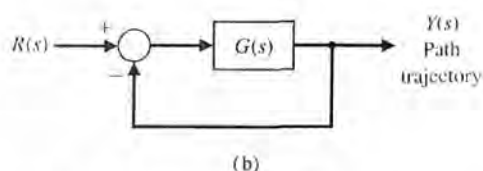
$$G(s) = \frac{75(s + 1)}{s(s + 5)(s + 25)}$$

for the closed-loop system shown in Figure 5.6(b). Calculate the steady-state error.

- P5.7** Astronaut Bruce McCandless II took the first untethered walk in space on February 7, 1984, using the gas-jet propulsion device illustrated in Figure P5.7(a).



(a)



(b)

**FIGURE P5.6** Robot path control.

The controller can be represented by a gain  $K_2$ , as shown in Figure P5.7(b). The moment of inertia of the equipment and man is  $25 \text{ kg m}^2$ . (a) Determine the

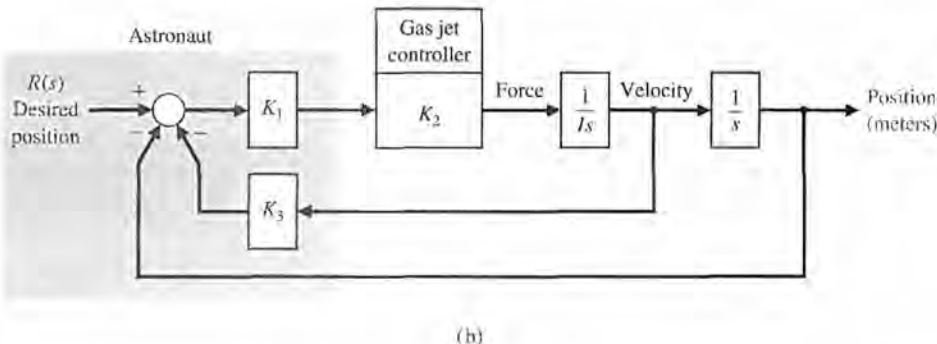


(a)

**FIGURE P5.7**

(a) Astronaut Bruce McCandless II is shown a few meters away from the earth-orbiting space shuttle. He used a nitrogen-propelled hand-controlled device called the manned maneuvering unit. (Courtesy of National Aeronautics and Space Administration.)

(b) Block diagram of controller.



(b)

necessary gain  $K_3$  to maintain a steady-state error equal to 1 cm when the input is a ramp  $r(t) = t$  (meters). (b) With this gain  $K_3$ , determine the necessary gain  $K_1K_2$  in order to restrict the percent overshoot to 10%. (c) Determine analytically the gain  $K_1K_2$  in order to minimize the ISE performance index for a step input.

- P5.8** Photovoltaic arrays (solar cells) generate a DC voltage that can be used to drive DC motors or that can be converted to AC power and added to the distribution network. It is desirable to maintain the power out of

the array at its maximum available as the solar incidence changes during the day. One such closed-loop system is shown in Figure P5.8. The transfer function for the process is

$$G(s) = \frac{K}{s + 20},$$

where  $K = 20$ . Find (a) the time constant of the closed-loop system and (b) the settling time to within 2% of the final value of the system to a unit step disturbance.

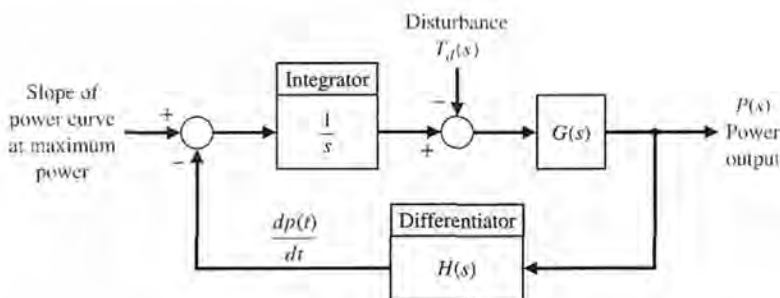


**FIGURE P5.8**  
Solar cell control.

- P5.9** The antenna that receives and transmits signals to the *Telstar* communication satellite is the largest horn antenna ever built. The microwave antenna is 177 ft long, weighs 340 tons, and rolls on a circular track. A photo of the antenna is shown in Figure P5.9. The *Telstar* satellite is 34 inches in diameter and moves about 16,000 mph at an altitude of 2500 miles. The

antenna must be positioned accurately to 1/10 of a degree, because the microwave beam is 0.2° wide and highly attenuated by the large distance. If the antenna is following the moving satellite, determine the  $K_b$  necessary for the system.

- P5.10** A speed control system of an armature-controlled DC motor uses the back emf voltage of the motor as a feedback signal. (a) Draw the block diagram of this system (see Equation (2.69)). (b) Calculate the steady-state error of this system to a step input command setting the speed to a new level. Assume that  $R_a = L_a = J = b = 1$ , the motor constant is  $K_m = 1$ , and  $K_b = 1$ . (c) Select a feedback gain for the back emf signal to yield a step response with an overshoot of 15%.

- P5.11** A simple unity feedback control system has a process transfer function

$$\frac{Y(s)}{E(s)} = G(s) = \frac{K}{s}.$$

The system input is a step function with an amplitude  $A$ . The initial condition of the system at time  $t_0$  is  $y(t_0) = Q$ , where  $y(t)$  is the output of the system. The performance index is defined as

$$J = \int_0^{\infty} e^2(t) dt.$$

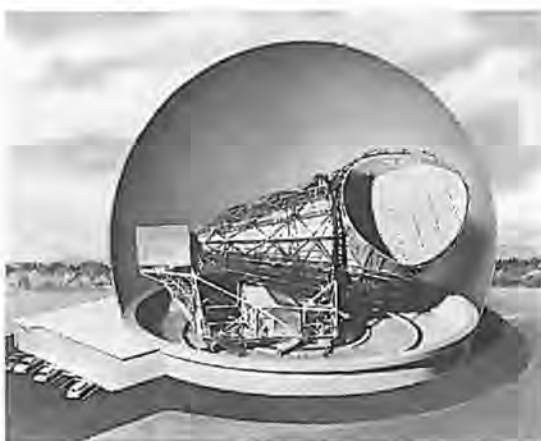


**FIGURE 5.9** A model of the antenna for the *Telstar* System at Andover, Maine. (Photo courtesy of Bell Telephone Laboratories, Inc.)

- (a) Show that  $I = (A - Q)^2/(2K)$ . (b) Determine the gain  $K$  that will minimize the performance index  $I$ . Is this gain a practical value? (c) Select a practical value of gain and determine the resulting value of the performance index.

**P5.12** Train travel between cities will increase as trains are developed that travel at high speeds, making the travel time from city center to city center equivalent to airline travel time. The Japanese National Railway has a train called the Bullet Express that travels between Tokyo and Osaka on the Tokaido line. This train travels the 320 miles in 3 hours and 10 minutes, an average speed of 101 mph [17]. This speed will be increased as new systems are used, such as magnetically levitated systems to float vehicles above an aluminum guideway. To maintain a desired speed, a speed control system is proposed that yields a zero steady-state error to a ramp input. A third-order system is sufficient. Determine the optimum system transfer function  $T(s)$  for an ITAE performance criterion. Estimate the settling time (with a 2% criterion) and overshoot for a step input when  $\omega_n = 10$ .

**P5.13** We want to approximate a fourth-order system by a lower-order model. The transfer function of the original system is

$$\begin{aligned} G_H(s) &= \frac{s^3 + 7s^2 + 24s + 24}{s^4 + 10s^3 + 35s^2 + 50s + 24} \\ &= \frac{s^3 + 7s^2 + 24s + 24}{(s+1)(s+2)(s+3)(s+4)}. \end{aligned}$$

Show that if we obtain a second-order model by the method of Section 5.8, and we do not specify the poles

and the zero of  $G_L(s)$ , we have

$$\begin{aligned} G_L(s) &= \frac{0.2917s + 1}{0.399s^2 + 1.375s + 1} \\ &= \frac{0.731(s + 3.428)}{(s + 1.043)(s + 2.4)}. \end{aligned}$$

**P5.14** For the original system of Problem P5.13, we want to find the lower-order model when the poles of the second-order model are specified as  $-1$  and  $-2$  and the model has one unspecified zero. Show that this low-order model is

$$G_L(s) = \frac{0.986s + 2}{s^2 + 3s + 2} = \frac{0.986(s + 2.028)}{(s + 1)(s + 2)}.$$

**P5.15.** Consider a unity feedback system with loop transfer function

$$L(s) = G_c(s)G(s) = \frac{K(s+1)}{(s+4)(s^2+s+10)}.$$

Determine the value of the gain  $K$  such that the percent overshoot to a unit step is minimized.

**P5.16** A magnetic amplifier with a low-output impedance is shown in Figure P5.16 in cascade with a low-pass filter and a preamplifier. The amplifier has a high-input impedance and a gain of 1 and is used for adding the signals as shown. Select a value for the capacitance  $C$  so that the transfer function  $V_0(s)/V_{in}(s)$  has a damping ratio of  $1/\sqrt{2}$ . The time constant of the magnetic amplifier is equal to 1 second, and the gain is  $K = 10$ . Calculate the settling time (with a 2% criterion) of the resulting system.

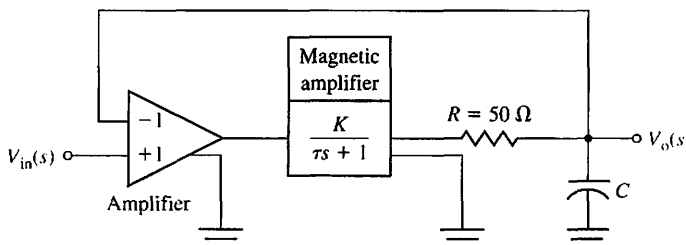


**FIGURE P5.16**  
Feedback amplifier.

**P5.17** Electronic pacemakers for human hearts regulate the speed of the heart pump. A proposed closed-loop system that includes a pacemaker and the measurement of the heart rate is shown in Figure P5.17 [2, 3]. The transfer function of the heart pump and the pacemaker is found to be

$$G(s) = \frac{K}{s(s/12 + 1)}.$$

Design the amplifier gain to yield a system with a settling time to a step disturbance of less than 1 second. The overshoot to a step in desired heart rate should be less than 10%. (a) Find a suitable range of  $K$ . (b) If the nominal value of  $K$  is  $K = 10$ , find the sensitivity of the system to small changes in  $K$ . (c) Evaluate the sensitivity of part (b) at DC (set  $s = 0$ ). (d) Evaluate the magnitude of the sensitivity at the normal heart rate of 60 beats/minute.

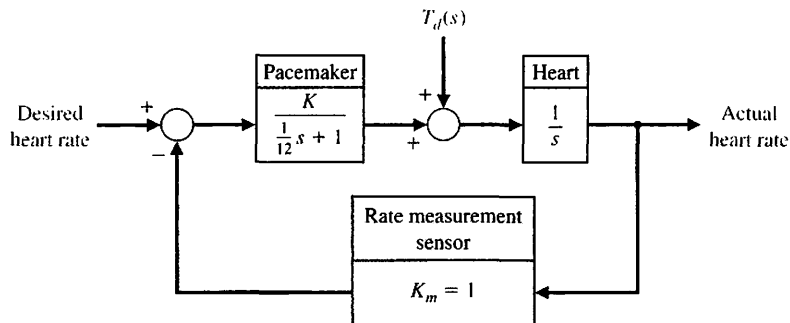


**FIGURE P5.17**  
Heart pacemaker.

**P5.18** Consider the original third-order system given in Example 5.9. Determine a first-order model with one pole unspecified and no zeros that will represent the third-order system.

**P5.19** A closed-loop control system with negative unity feedback has a loop transfer function

$$L(s) = G_c(s)G(s) = \frac{8}{s(s^2 + 6s + 12)}.$$

- (a) Determine the closed-loop transfer function  $T(s)$ .
- (b) Determine a second-order approximation for  $T(s)$ .
- (c) Plot the response of  $T(s)$  and the second-order approximation to a unit step input and compare the results.

**P5.20** A system is shown in Figure P5.20.

- (a) Determine the steady-state error for a unit step input in terms of  $K$  and  $K_1$ , where  $E(s) = R(s) - Y(s)$ .
- (b) Select  $K_1$  so that the steady-state error is zero.

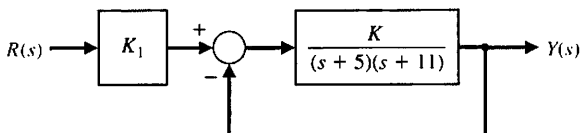


**FIGURE P5.20** System with pre-gain,  $K_1$ .

**P5.21** Consider the closed-loop system in Figure P5.21. Determine values of the parameters  $k$  and  $a$  so that the following specifications are satisfied:

- (a) The steady-state error to a unit step input is zero.

- (b) The closed-loop system has a percent overshoot of less than 5%.

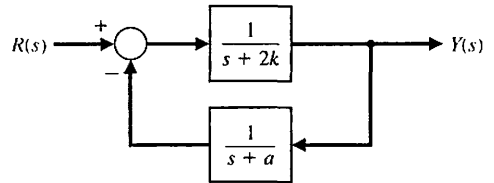


**FIGURE P5.21** Closed-loop system with parameters  $k$  and  $a$ .

**P5.22** Consider the closed-loop system in Figure P5.22, where

$$G_c(s)G(s) = \frac{2}{s + 0.2K} \quad \text{and} \quad H(s) = \frac{2}{2s + \tau}.$$

- (a) If  $\tau = 2.43$ , determine the value of  $K$  such that the steady-state error of the closed-loop system response to a unit step input,  $R(s) = 1/s$ , is zero.
- (b) Determine the percent overshoot  $P.O.$  and the time to peak  $T_p$  of the unit step response when  $K$  is as in part (a).

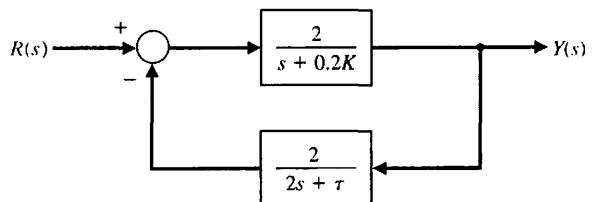


**FIGURE P5.22** Nonunity closed-loop feedback control system.

## ADVANCED PROBLEMS

**AP5.1** A closed-loop transfer function is

$$T(s) = \frac{Y(s)}{R(s)} = \frac{108(s + 3)}{(s + 9)(s^2 + 8s + 36)}.$$

- (a) Determine the steady-state error for a unit step input  $R(s) = 1/s$ .
- (b) Assume that the complex poles dominate, and determine the overshoot and settling time to within 2% of the final value.
- (c) Plot the actual system response, and compare it with the estimates of part (b).

**AP5.2** A closed-loop system is shown in Figure AP5.2.

Plot the response to a unit step input for the system for  $\tau_z = 0, 0.05, 0.1$ , and  $0.5$ . Record the percent overshoot, rise time, and settling time (with a 2% criterion) as  $\tau_z$  varies. Describe the effect of varying  $\tau_z$ . Compare the location of the zero  $-1/\tau_z$  with the location of the closed-loop poles.

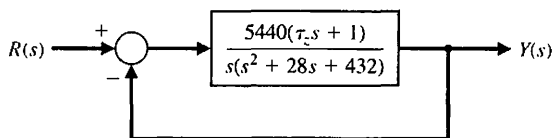


**FIGURE AP5.2** System with a variable zero.

**AP5.3** A closed-loop system is shown in Figure AP5.3.

Plot the response to a unit step input for the system with  $\tau_p = 0, 0.5, 2$ , and  $5$ . Record the percent overshoot, rise time, and settling time (with a 2% criterion) as  $\tau_p$  varies. Describe the effect of varying  $\tau_p$ . Compare the location of the open-loop pole  $-1/\tau_p$  with the location of the closed-loop poles.

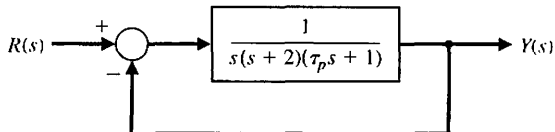


**FIGURE AP5.3** System with a variable pole in the process.

**AP5.4** The speed control of a high-speed train is represented by the system shown in Figure AP5.4 [17]. Determine the equation for steady-state error for  $K$  for a unit step input  $r(t)$ . Consider the three values for  $K$  equal to 1, 10, and 100.

- (a) Determine the steady-state error.
- (b) Determine and plot the response  $y(t)$  for (i) a unit step input  $R(s) = 1/s$  and (ii) a unit step disturbance input  $T_d(s) = 1/s$ .
- (c) Create a table showing overshoot, settling time (with a 2% criterion),  $e_{ss}$  for  $r(t)$ , and  $|y/t_d|_{max}$  for the three values of  $K$ . Select the best compromise value.

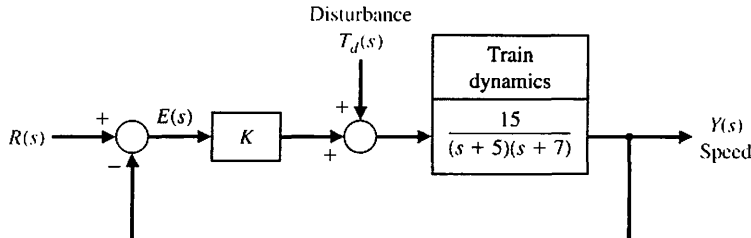


**FIGURE AP5.4** Speed control.

**AP5.5** A system with a controller is shown in Figure AP5.5. The zero of the controller may be varied. Let  $\alpha = 0, 10, 100$ .

- (a) Determine the steady-state error for a step input  $r(t)$  for  $\alpha = 0$  and  $\alpha \neq 0$ .

- (b) Plot the response of the system to a step input disturbance for the three values of  $\alpha$ . Compare the results and select the best value of the three values of  $\alpha$ .

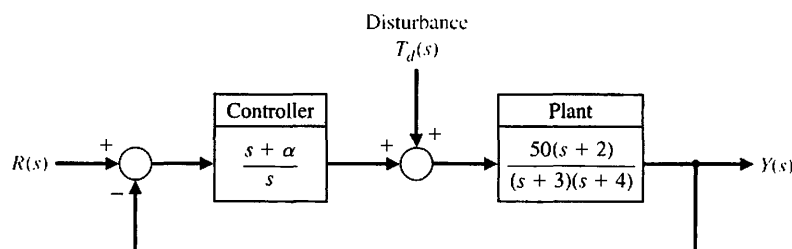


**FIGURE AP5.5** System with control parameter  $\alpha$ .

**AP5.6** The block diagram model of an armature-current-controlled DC motor is shown in Figure AP5.6.

- (a) Determine the steady-state tracking error to a ramp input  $r(t) = t$ ,  $t \geq 0$ , in terms of  $K$ ,  $K_b$ , and  $K_m$ .

(b) Let  $K_m = 10$  and  $K_b = 0.05$ , and select  $K$  so that steady-state tracking error is equal to 1.

(c) Plot the response to a unit step input and a unit ramp input for 20 seconds. Are the responses acceptable?

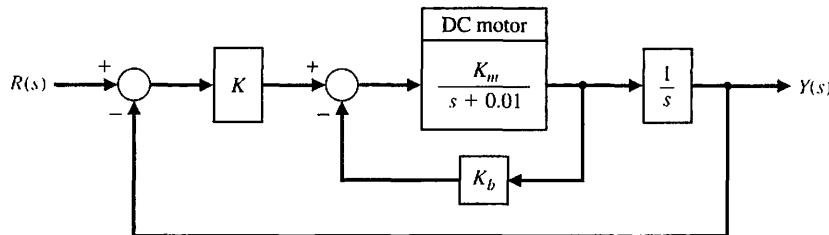


**FIGURE AP5.6**  
DC motor control.

**AP5.7** Consider the closed-loop system in Figure AP5.7 with transfer functions

$$G_c(s) = \frac{100}{s + 100} \quad \text{and} \quad G(s) = \frac{K}{s(s + 50)},$$

where

$$1000 \leq K \leq 5000.$$

- (a) Assume that the complex poles dominate and estimate the settling time and percent overshoot to a unit step input for  $K = 1000, 2000, 3000, 4000$ , and  $5000$ .

(b) Determine the actual settling time and percent overshoot to a unit step for the values of  $K$  in part (a).

(c) Co-plot the results of (a) and (b) and comment.

**AP5.8** A unity negative feedback system (as shown in Figure E5.11) has the loop transfer function

$$L(s) = G_c(s)G(s) = \frac{K(s + 2)}{s^2 + \frac{2}{3}s + \frac{1}{3}}.$$

Determine the gain  $K$  that minimizes the damping ratio  $\zeta$  of the closed-loop system poles. What is the minimum damping ratio?

**AP5.9**. The unity negative feedback system in Figure AP5.9 has the process given by

$$G(s) = \frac{1}{s(s + 15)(s + 25)}.$$

The controller is a proportional plus integral controller with gains  $K_p$  and  $K_I$ . The objective is to design the controller gains such that the dominant roots have a damping ratio  $\zeta$  equal to 0.707. Determine the resulting peak time and settling time (with a 2% criterion) of the system to a unit step input.

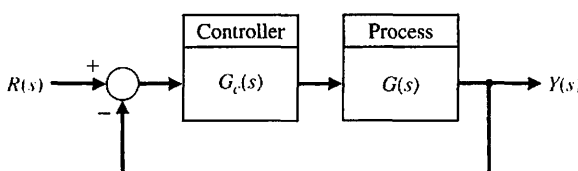


**FIGURE AP5.7** Closed-loop system with unity feedback.

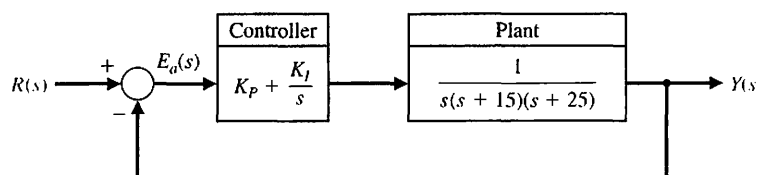


**FIGURE AP5.9**  
Feedback control system with a proportional plus integral controller.

## DESIGN PROBLEMS

**CDP5.1** The capstan drive system of the previous problems (see CDP1.1–CDP4.1) has a disturbance due to changes in the part that is being machined as material is removed. The controller is an amplifier  $G_c(s) = K_a$ . Evaluate the effect of a unit step disturbance, and determine the best value of the amplifier gain so that the overshoot to a step command  $r(t) = A, t > 0$  is less than 5%, while reducing the effect of the disturbance as much as possible.

**DP5.1** The roll control autopilot of a jet fighter is shown in Figure DP5.1. The goal is to select a suitable  $K$  so that the response to a unit step command  $\phi_d(t) = A, t \geq 0$ ,

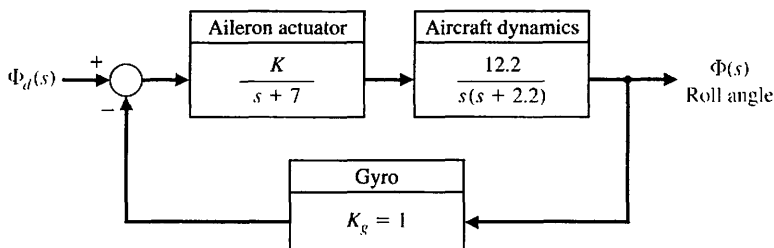


**FIGURE DP5.1**  
Roll angle control.

**DP5.2** The design of the control for a welding arm with a long reach requires the careful selection of the parameters [13]. The system is shown in Figure DP5.2, where  $\zeta = 0.6$ , and the gain  $K$  and the natural frequency  $\omega_n$  can be selected. (a) Determine  $K$  and  $\omega_n$  so that the response to a unit step input achieves a peak

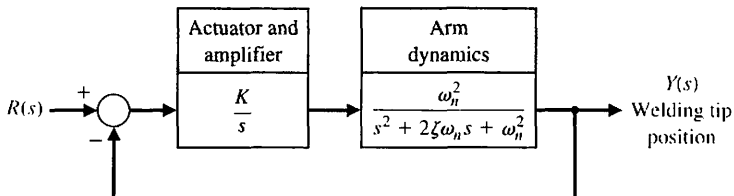


**FIGURE DP5.2**  
Welding tip position control.

**DP5.3** Active suspension systems for modern automobiles provide a comfortable firm ride. The design of an active suspension system adjusts the valves of the shock absorber so that the ride fits the conditions. A small electric motor, as shown in Figure DP5.3, changes the valve settings [13]. Select a design value

will provide a response  $\phi(t)$  that is a fast response and has an overshoot of less than 20%. (a) Determine the closed-loop transfer function  $\phi(s)/\phi_d(s)$ . (b) Determine the roots of the characteristic equation for  $K = 0.7, 3$ , and  $6$ . (c) Using the concept of dominant roots, find the expected overshoot and peak time for the approximate second-order system. (d) Plot the actual response and compare with the approximate results of part (c). (e) Select the gain  $K$  so that the percentage overshoot is equal to 16%. What is the resulting peak time?

time for the first overshoot (above the desired level of 1) that is less than or equal to 1 second and the overshoot is less than 5%. (*Hint:* Try  $0.2 < K/\omega_n < 0.4$ .) (b) Plot the response of the system designed in part (a) to a step input.

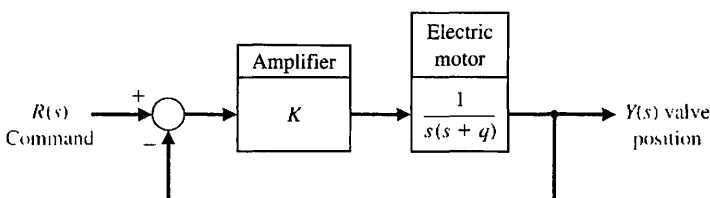
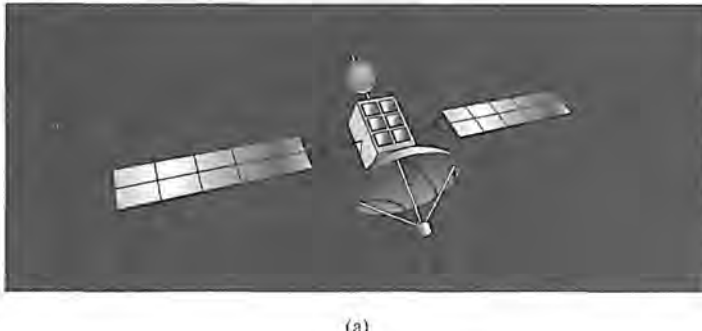


**FIGURE DP5.3**  
Active suspension system.

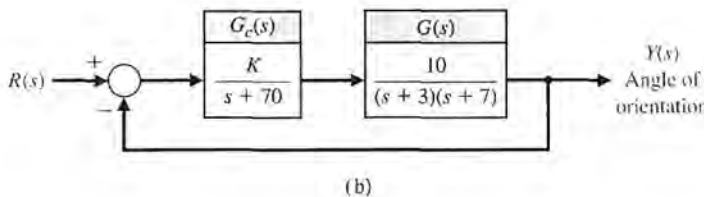
for  $K$  and the parameter  $q$  in order to satisfy the ITAE performance for a step command  $R(s)$  and a settling time (with a 2% criterion) for the step response of less than or equal to 0.5 second. Upon completion of your design, predict the resulting overshoot for a step input.

- DP5.4** The space satellite shown in Figure DP5.4(a) uses a control system to readjust its orientation, as shown in Figure DP5.4(b).
- Determine a second-order model for the closed-loop system.

- Using the second-order model, select a gain  $K$  so that the percent overshoot is less than 15% and the steady-state error to a step is less than 12%.
- Verify your design by determining the actual performance of the third-order system.



(a)



(b)

**FIGURE DP5.4**  
Control of a space satellite.

**DP5.5** A deburring robot can be used to smooth off machined parts by following a preplanned path (input command signal). In practice, errors occur due to robot inaccuracy, machining errors, large tolerances, and tool wear. These errors can be eliminated using force feedback to modify the path online [8, 11].

While force control has been able to address the problem of accuracy, it has been more difficult to solve the contact stability problem. In fact, by closing the force loop and introducing a compliant wrist force

sensor (the most common type of force control), one can add to the stability problem.

A model of a robot deburring system is shown in Figure DP5.5. Determine the region of stability for the system for  $K_1$  and  $K_2$ . Assume both adjustable gains are greater than zero.

**DP5.6** The model for a position control system using a DC motor is shown in Figure DP5.6. The goal is to select  $K_1$  and  $K_2$  so that the peak time is  $T_p \leq 0.5$

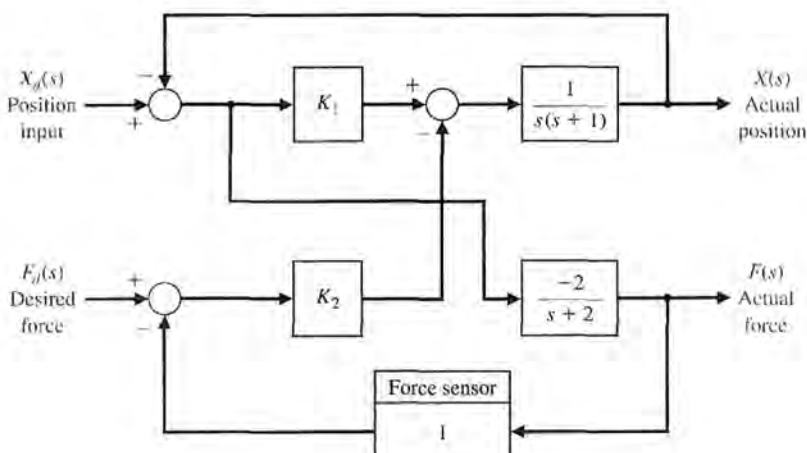


**FIGURE DP5.5**  
Deburring robot.

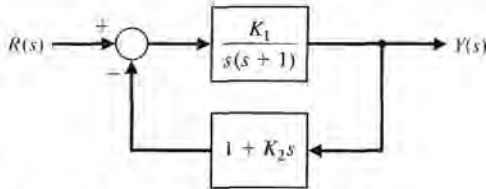


**FIGURE DP5.6** Position control robot.

second and the overshoot  $P.O.$  for a step input is  $P.O. \leq 2\%$ .

**DP5.7** A three-dimensional cam for generating a function of two variables is shown in Figure DP5.7(a). Both  $x$  and  $y$  may be controlled using a position control system

[31]. The control of  $x$  may be achieved with a DC motor and position feedback of the form shown in Figure DP5.7(b), with the DC motor and load represented by

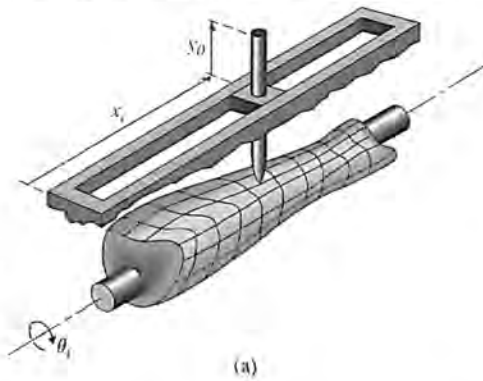
$$G(s) = \frac{K}{s(s+p)(s+4)}$$

where  $K = 2$  and  $p = 2$ . Design a proportional plus derivative controller

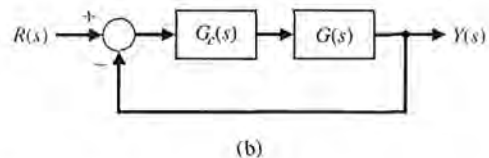
$$G_c(s) = K_p + K_D s$$

to achieve a percent overshoot  $P.O. \leq 5\%$  to a unit step input and a settling time  $T_s \leq 2$  seconds.

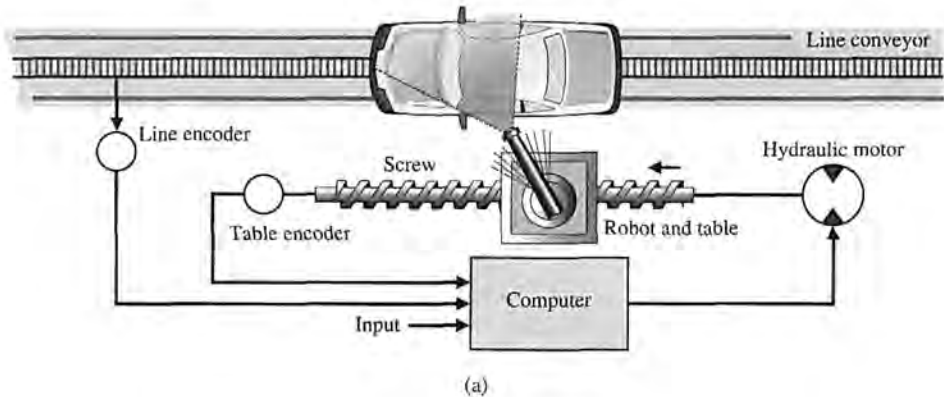
**DP5.8.** Computer control of a robot to spray-paint an automobile is accomplished by the system shown in



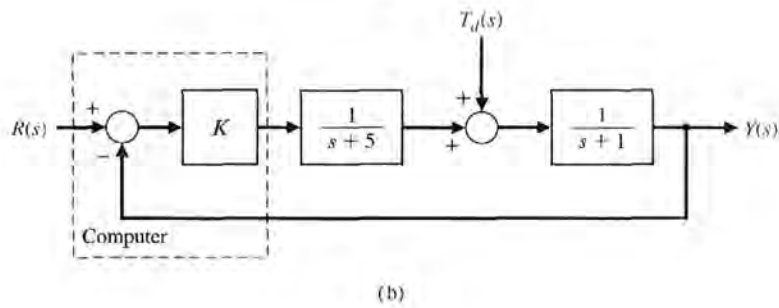
(a)



(b)



(a)



(b)

**FIGURE DP5.8** Spray-paint robot.

Figure DP5.8(a) [7]. We wish to investigate the system when  $K = 1, 10$ , and  $20$ . The feedback control block diagram is shown in Figure DP5.8(b). (a) For the three values of  $K$ , determine the percent overshoot, the settling time (with a  $2\%$  criterion), and the steady-state

error for a unit step input. Record your results in a table. (b) Choose one of the three values of  $K$  that provides acceptable performance. (c) For the value selected in part (b), determine  $y(t)$  for a disturbance  $T_d(s) = 1/s$  when  $R(s) = 0$ .



## COMPUTER PROBLEMS

**CP5.1** Consider the closed-loop transfer function

$$T(s) = \frac{15}{s^2 + 8s + 15}.$$

Obtain the impulse response analytically and compare the result to one obtained using the impulse function.

**CP5.2** A unity negative feedback system has the loop transfer function

$$L(s) = G_c(s)G(s) = \frac{s + 10}{s^2(s + 15)}.$$

Using Isim, obtain the response of the closed-loop system to a unit ramp input,

$$R(s) = 1/s^2.$$

Consider the time interval  $0 \leq t \leq 50$ . What is the steady-state error?

**CP5.3** A working knowledge of the relationship between the pole locations of the second-order system shown in Figure CP5.3 and the transient response is important in control design. With that in mind, consider the following four cases:

1.  $\omega_n = 2, \zeta = 0$ ,
2.  $\omega_n = 2, \zeta = 0.1$ ,
3.  $\omega_n = 1, \zeta = 0$ ,
4.  $\omega_n = 1, \zeta = 0.2$ .

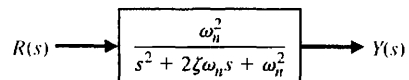


**FIGURE CP5.3** A simple second-order system.

Using the impulse and subplot functions, create a plot containing four subplots, with each subplot depicting the impulse response of one of the four cases listed. Compare the plot with Figure 5.17 in Section 5.5, and discuss the results.

**CP5.4** Consider the control system shown in Figure CP5.4.

- (a) Show analytically that the expected percent overshoot of the closed-loop system response to a unit step input is about  $50\%$ .
- (b) Develop an m-file to plot the unit step response of the closed-loop system and estimate the percent overshoot from the plot. Compare the result with (a).

**CP5.5** Consider the feedback system in Figure CP5.5. Develop an m-file to design a controller and prefilter

$$G_c(s) = K \frac{s + z}{s + p} \quad \text{and} \quad G_p(s) = \frac{K_p}{s + \tau}$$

such that the ITAE performance criterion is minimized. For  $\omega_n = 0.45$  and  $\zeta = 0.59$ , plot the unit step response and determine the percent overshoot and settling time.

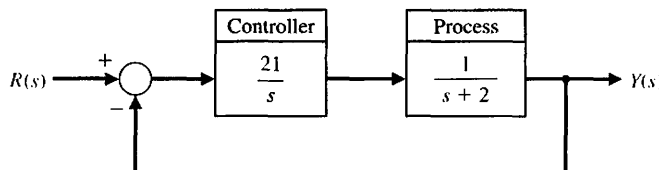


**FIGURE CP5.4**  
A negative feedback control system.

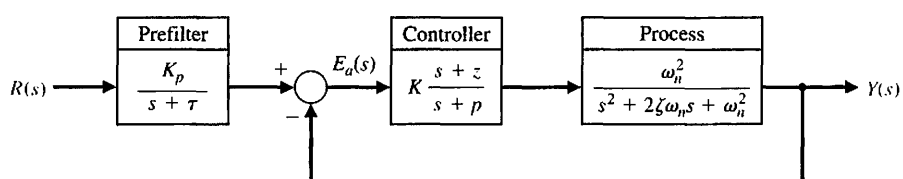


**FIGURE CP5.5**  
Feedback control system with controller and prefilter.

**CP5.6** The loop transfer function of a unity negative feedback system is

$$L(s) = G_c(s)G(s) = \frac{25}{s(s + 5)}.$$

Develop an m-file to plot the unit step response and determine the values of peak overshoot  $M_p$ , time to peak  $T_p$ , and settling time  $T_s$  (with a 2% criterion).

**CP5.7** An autopilot designed to hold an aircraft in straight and level flight is shown in Figure CP5.7.

(a) Suppose the controller is a constant gain controller given by  $G_c(s) = 2$ . Using the `lsim` function, compute and plot the ramp response for  $\theta_d(t) = at$ , where  $a = 0.5^\circ/\text{s}$ . Determine the attitude error after 10 seconds.

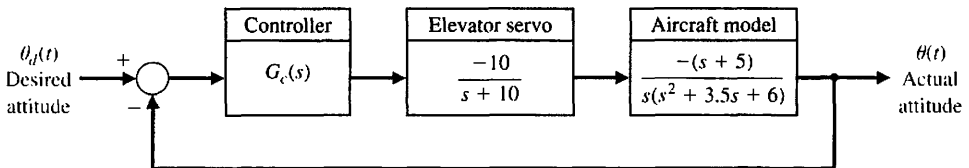


**FIGURE CP5.7**

An aircraft autopilot block diagram.

**CP5.8** The block diagram of a rate loop for a missile autopilot is shown in Figure CP5.8. Using the analytic formulas for second-order systems, predict  $M_{pt}$ ,  $T_p$ , and  $T_s$  for the closed-loop system due to a unit step input.

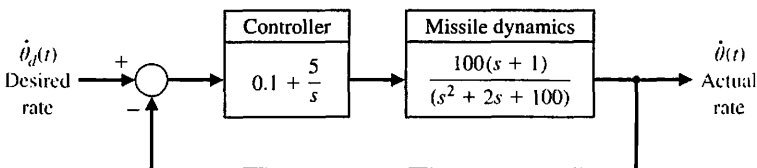


**FIGURE CP5.8**

A missile rate loop autopilot.

**CP5.9** Develop an m-file that can be used to analyze the closed-loop system in Figure CP5.9. Drive the system with a step input and display the output on a graph. What is the settling time and the percent overshoot?

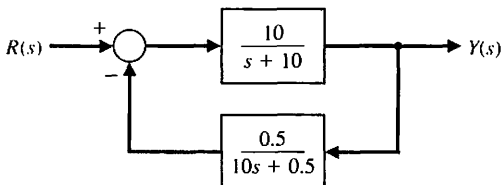


**FIGURE CP5.9** Nonunity feedback system.

**CP5.10** Develop an m-file to simulate the response of the system in Figure CP5.10 to a ramp input  $R(s) = 1/s^2$ . What is the steady-state error? Display the output on an x-y graph.

(b) If we increase the complexity of the controller, we can reduce the steady-state tracking error. With this objective in mind, suppose we replace the constant gain controller with the more sophisticated controller

$$G_c(s) = K_1 + \frac{K_2}{s} = 2 + \frac{1}{s}.$$

This type of controller is known as a proportional plus integral (PI) controller. Repeat the simulation of part (a) with the PI controller, and compare the steady-state tracking errors of the constant gain controller versus the PI controller.

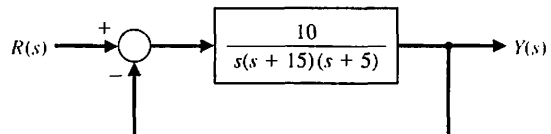


**FIGURE CP5.10** Closed-loop system for m-file.

**CP5.11** Consider the closed-loop system in Figure CP5.11. Develop an m-file to accomplish the following tasks:

- Determine the closed-loop transfer function  $T(s) = Y(s)/R(s)$ .
- Plot the closed-loop system response to an impulse input  $R(s) = 1$ , a unit step input  $R(s) = 1/s$ , and a unit ramp input  $R(s) = 1/s^2$ . Use the `subplot` function to display the three system responses.

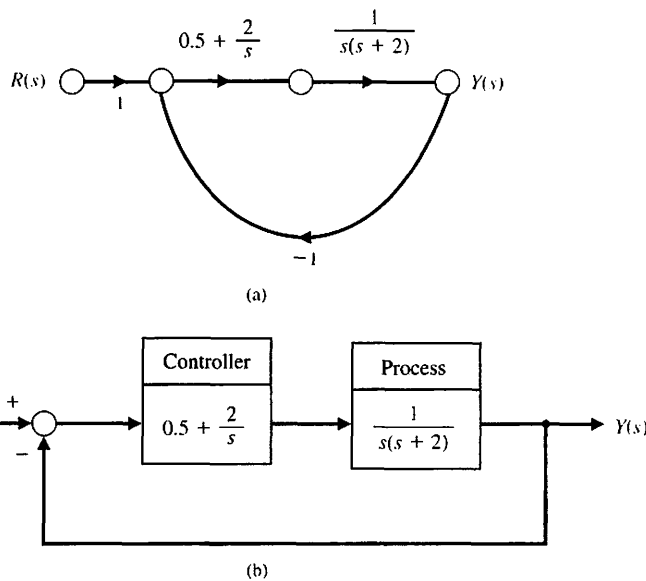


**FIGURE CP5.11**  
A single loop unity feedback system.  
(a) Signal flow graph. (b) Block diagram.

**CP5.12** A closed-loop transfer function is given by

$$T(s) = \frac{Y(s)}{R(s)} = \frac{77(s+2)}{(s+7)(s^2+4s+22)}.$$

- (a) Obtain the response of the closed-loop transfer function  $T(s) = Y(s)/R(s)$  to a unit step input.

- What is the settling time  $T_s$  (use a 2% criterion) and percent overshoot  $P.O.?$   
(b) Neglecting the real pole at  $s = -7$ , determine the settling time  $T_s$  and percent overshoot  $P.O.$ . Compare the results with the actual system response in part (a). What conclusions can be made regarding neglecting the pole?



### ANSWERS TO SKILLS CHECK

True or False: (1) True; (2) False; (3) False; (4) True;  
(5) False

Multiple Choice: (6) a; (7) a; (8) c; (9) b; (10) b; (11)  
a; (12) b; (13) b; (14) a; (15) b

Word Match (in order, top to bottom): i, j, d, g, k, c,  
n, p, o, b, e, l, f, h, m, a

### TERMS AND CONCEPTS

**Acceleration error constant,  $K_a$**  The constant evaluated as  $\lim_{s \rightarrow 0} [s^2 G_c(s)G(s)]$ . The steady-state error for a parabolic input,  $r(t) = At^2/2$ , is equal to  $A/K_a$ .

**Design specifications** A set of prescribed performance criteria.

**Dominant roots** The roots of the characteristic equation that cause the dominant transient response of the system.

**Optimum control system** A system whose parameters are adjusted so that the performance index reaches an extremum value.

**Peak time** The time for a system to respond to a step input and rise to a peak response.

**Percent overshoot** The amount by which the system output response proceeds beyond the desired response.

**Performance index** A quantitative measure of the performance of a system.

**Position error constant,  $K_p$**  The constant evaluated as  $\lim_{s \rightarrow 0} G_c(s)G(s)$ . The steady-state error for a step input (of magnitude  $A$ ) is equal to  $A/(1 + K_p)$ .

**Rise time** The time for a system to respond to a step input and attain a response equal to a percentage of the

magnitude of the input. The 0–100% rise time,  $T_r$ , measures the time to 100% of the magnitude of the input. Alternatively,  $T_{r_1}$  measures the time from 10% to 90% of the response to the step input.

**Settling time** The time required for the system output to settle within a certain percentage of the input amplitude.

**Steady-state response** The constituent of the system response that exists a long time following any signal initiation.

**Test input signal** An input signal used as a standard test of a system's ability to respond adequately.

**Transient response** The constituent of the system response that disappears with time.

**Type number** The number  $N$  of poles of the transfer function,  $G_c(s)G(s)$ , at the origin.  $G_c(s)G(s)$  is the loop transfer function.

**Unit impulse** A test input consisting of an impulse of infinite amplitude and zero width, and having an area of unity. The unit impulse is used to determine the impulse response.

**Velocity error constant,  $K_v$**  The constant evaluated as  $\lim_{s \rightarrow 0} [sG_c(s)G(s)]$ . The steady-state error for a ramp input (of slope  $A$ ) for a system is equal to  $A/K_v$ .

---

**CHAPTER****6**

# *The Stability of Linear Feedback Systems*

---

6.1	The Concept of Stability	387
6.2	The Routh-Hurwitz Stability Criterion	391
6.3	The Relative Stability of Feedback Control Systems	399
6.4	The Stability of State Variable Systems	401
6.5	Design Examples	404
6.6	System Stability Using Control Design Software	413
6.7	Sequential Design Example: Disk Drive Read System	421
6.8	Summary	424

## **P R E V I E W**

Stability of closed-loop feedback systems is central to control system design. A stable system should exhibit a bounded output if the corresponding input is bounded. This is known as bounded-input–bounded-output stability and is one of the main topics of this chapter. The stability of a feedback system is directly related to the location of the roots of the characteristic equation of the system transfer function and to the location of the eigenvalues of the system matrix for a system in state variable format. The Routh–Hurwitz method is introduced as a useful tool for assessing system stability. The technique allows us to compute the number of roots of the characteristic equation in the right half plane without actually computing the values of the roots. This gives us a design method for determining values of certain system parameters that will lead to closed-loop stability. For stable systems, we will introduce the notion of relative stability, which allows us to characterize the degree of stability. The chapter concludes with a stabilizing controller design based on the Routh–Hurwitz method for the Sequential Design Example: Disk Drive Read System.

## **DESIRED OUTCOMES**

Upon completion of Chapter 6, students should:

- Understand the concept of stability of dynamic systems.
- Be aware of the key concepts of absolute and relative stability.
- Be familiar with the notion of bounded-input, bounded-output stability.
- Understand the relationship of the  $s$ -plane pole locations (for transfer function models) and of the eigenvalue locations (for state variable models) to system stability.
- Know how to construct a Routh array and be able to employ the Routh–Hurwitz stability criterion to determine stability.

## 6.1 THE CONCEPT OF STABILITY

When considering the design and analysis of feedback control systems, **stability** is of the utmost importance. From a practical point of view, a closed-loop feedback system that is unstable is of little value. As with all such general statements, there are exceptions; but for our purposes, we will declare that all our control designs must result in a closed-loop stable system. Many physical systems are inherently open-loop unstable, and some systems are even designed to be open-loop unstable. Most modern fighter aircraft are open-loop *unstable by design*, and without active feedback control assisting the pilot, they cannot fly. Active control is introduced by engineers to stabilize the unstable system—that is, the aircraft—so that other considerations, such as transient performance, can be addressed. Using feedback, we can stabilize unstable systems and then with a judicious selection of controller parameters, we can adjust the transient performance. For open-loop stable systems, we still use feedback to adjust the closed-loop performance to meet the design specifications. These specifications take the form of steady-state tracking errors, percent overshoot, settling time, time to peak, and the other indices discussed in Chapters 4 and 5.

We can say that a closed-loop feedback system is either stable or it is not stable. This type of stable/not stable characterization is referred to as **absolute stability**. A system possessing absolute stability is called a stable system—the label of absolute is dropped. Given that a closed-loop system is stable, we can further characterize the degree of stability. This is referred to as **relative stability**. The pioneers of aircraft design were familiar with the notion of relative stability—the more stable an aircraft was, the more difficult it was to maneuver (that is, to turn). One outcome of the relative instability of modern fighter aircraft is high maneuverability. A fighter aircraft is less stable than a commercial transport, hence it can maneuver more quickly. In fact, the motions of a fighter aircraft can be quite violent to the “passengers.” As we will discuss later in this section, we can determine that a system is stable (in the absolute sense) by determining that all transfer function poles lie in the left-half  $s$ -plane, or equivalently, that all the eigenvalues of the system matrix  $\mathbf{A}$  lie in the left-half  $s$ -plane. Given that all the poles (or eigenvalues) are in the left-half  $s$ -plane, we investigate relative-stability by examining the relative locations of the poles (or eigenvalues).

A **stable system** is defined as a system with a bounded (limited) system response. That is, if the system is subjected to a bounded input or disturbance and the response is bounded in magnitude, the system is said to be stable.

**A stable system is a dynamic system with a bounded response  
to a bounded input.**

The concept of stability can be illustrated by considering a right circular cone placed on a plane horizontal surface. If the cone is resting on its base and is tipped slightly, it returns to its original equilibrium position. This position and response are said to be stable. If the cone rests on its side and is displaced slightly, it rolls with no tendency to leave the position on its side. This position is designated as the neutral stability. On the other hand, if the cone is placed on its tip and released, it falls onto its side. This position is said to be unstable. These three positions are illustrated in Figure 6.1.

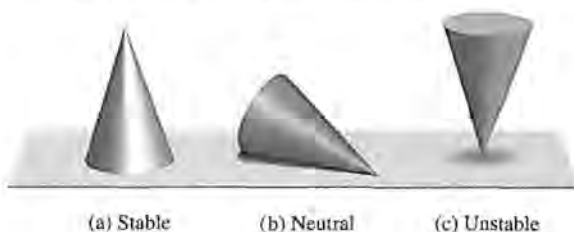


**FIGURE 6.1**  
The stability of a cone.

The stability of a dynamic system is defined in a similar manner. The response to a displacement, or initial condition, will result in either a decreasing, neutral, or increasing response. Specifically, it follows from the definition of stability that a linear system is stable if and only if the absolute value of its impulse response  $g(t)$ , integrated over an infinite range, is finite. That is, in terms of the convolution integral Equation (5.2) for a bounded input,  $\int_0^\infty |g(t)| dt$  must be finite.

The location in the  $s$ -plane of the poles of a system indicates the resulting transient response. The poles in the left-hand portion of the  $s$ -plane result in a decreasing response for disturbance inputs. Similarly, poles on the  $j\omega$ -axis and in the right-hand plane result in a neutral and an increasing response, respectively, for a disturbance input. This division of the  $s$ -plane is shown in Figure 6.2. Clearly, the poles of desirable dynamic systems must lie in the left-hand portion of the  $s$ -plane [1–3].

A common example of the potential destabilizing effect of feedback is that of feedback in audio amplifier and speaker systems used for public address in auditoriums. In this case, a loudspeaker produces an audio signal that is an amplified version of the sounds picked up by a microphone. In addition to other audio inputs, the sound coming from the speaker itself may be sensed by the microphone. The strength of this particular signal depends upon the distance between the loudspeaker and the microphone. Because of the attenuating properties of air, a larger distance will cause a weaker signal to reach the microphone. Due to the finite propagation speed of sound waves, there will also be a time delay between the signal produced by the loudspeaker and the signal sensed by the microphone. In this case, the output from the feedback path is added to the external input. This is an example of positive feedback.

As the distance between the loudspeaker and the microphone decreases, we find that if the microphone is placed too close to the speaker, then the system will be unstable. The result of this instability is an excessive amplification and distortion of audio signals and an oscillatory squeal.

Another example of an unstable system is shown in Figure 6.3. The first bridge across the Tacoma Narrows at Puget Sound, Washington, was opened to traffic on July 1, 1940. The bridge was found to oscillate whenever the wind blew. After four

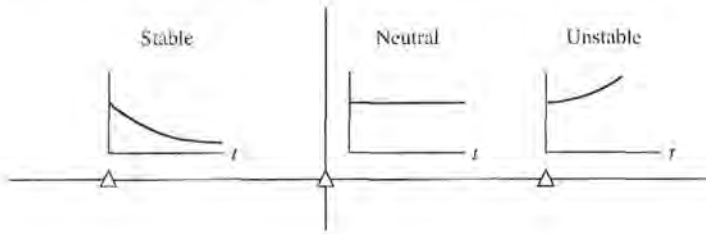


**FIGURE 6.2**  
Stability in the  $s$ -plane.



(a)



(b)

**FIGURE 6.3**  
Tacoma Narrows  
Bridge (a) as  
oscillation begins  
(b) at catastrophic  
failure.

months, on November 7, 1940, a wind produced an oscillation that grew in amplitude until the bridge broke apart. Figure 6.3(a) shows the condition at the beginning of oscillation; Figure 6.3(b) shows the catastrophic failure [5].

In terms of linear systems, we recognize that the stability requirement may be defined in terms of the location of the poles of the closed-loop transfer function. The closed-loop system transfer function is written as

$$T(s) = \frac{p(s)}{q(s)} = \frac{K \prod_{i=1}^M (s + z_i)}{s^N \prod_{k=1}^Q (s + \sigma_k) \prod_{m=1}^R [s^2 + 2\alpha_m s + (\alpha_m^2 + \omega_m^2)]}, \quad (6.1)$$

where  $q(s) = \Delta(s) = 0$  is the characteristic equation whose roots are the poles of the closed-loop system. The output response for an impulse function input (when  $N = 0$ ) is then

$$y(t) = \sum_{k=1}^Q A_k e^{-\sigma_k t} + \sum_{m=1}^R B_m \left( \frac{1}{\omega_m} \right) e^{-\alpha_m t} \sin(\omega_m t + \theta_m), \quad (6.2)$$

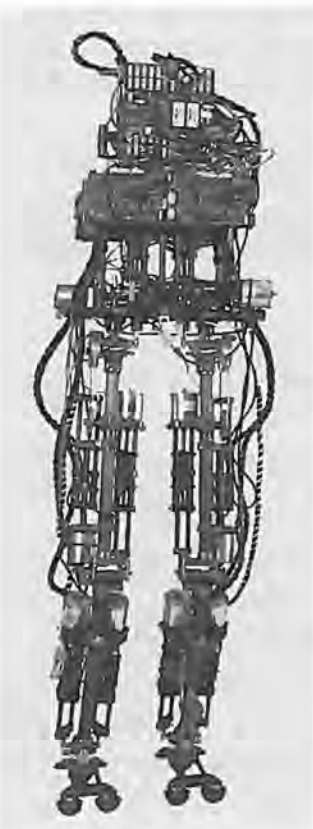
where  $A_k$  and  $B_m$  are constants that depend on  $\sigma_k$ ,  $z_i$ ,  $\alpha_m$ ,  $K$ , and  $\omega_m$ . To obtain a bounded response, the poles of the closed-loop system must be in the left-hand portion of the  $s$ -plane. Thus, a **necessary and sufficient condition for a feedback system to be stable is that all the poles of the system transfer function have negative real parts**. A system is stable if all the poles of the transfer function are in the left-hand  $s$ -plane. A system is not stable if not all the roots are in the left-hand plane. If the characteristic equation has simple roots on the imaginary axis ( $j\omega$ -axis) with all other roots in the left half-plane, the steady-state output will be sustained oscillations for a bounded input, unless the input is a sinusoid (which is bounded) whose frequency is equal to the magnitude of the  $j\omega$ -axis roots. For this case, the output becomes unbounded. Such a system is called **marginally stable**, since only certain bounded inputs (sinusoids of the frequency of the poles) will cause the output to become unbounded. For an unstable system, the characteristic equation has at least one root in the right half of the  $s$ -plane or repeated  $j\omega$  roots; for this case, the output will become unbounded for any input.

For example, if the characteristic equation of a closed-loop system is

$$(s + 10)(s^2 + 16) = 0,$$

then the system is said to be marginally stable. If this system is excited by a sinusoid of frequency  $\omega = 4$ , the output becomes unbounded.

To ascertain the stability of a feedback control system, we could determine the roots of the characteristic polynomial  $q(s)$ . However, we are first interested in determining the answer to the question, Is the system stable? If we calculate the roots of the characteristic equation in order to answer this question, we have determined much more information than is necessary. Therefore, several methods have been developed that provide the required yes or no answer to the stability question. The three approaches to the question of stability are (1) the  $s$ -plane approach, (2) the frequency plane ( $j\omega$ ) approach, and (3) the time-domain approach. The real frequency ( $j\omega$ ) approach is outlined in Chapter 9, and the discussion of the time-domain approach is considered in Section 6.4.

**FIGURE 6.4**

The M2 robot is more energy-efficient but less stable than many other designs that are well-balanced but consume much more power.  
(Courtesy of Professor Gill Pratt, Olin College.)

There are about one million robots in service throughout the world [10]. As the capability of robots increases, it is reasonable to assume that the numbers in service will continue to rise. Especially interesting are robots with human characteristics, particularly those that can walk upright. A class of robots that utilize series-elastic actuators as mechanical muscles emerged in the late 1990s. The M2 robot depicted in Figure 6.4 is more energy-efficient but less stable than many other designs that are well-balanced but consume much more power [21]. Examining the M2 robot in Figure 6.4, one can imagine that it is not inherently stable and that active control is required to keep it upright during the walking motion. In the next sections we present the Routh–Hurwitz stability criterion to investigate system stability by analyzing the characteristic equation without direct computation of the roots.

## 6.2 THE ROUTH–HURWITZ STABILITY CRITERION

The discussion and determination of stability has occupied the interest of many engineers. Maxwell and Vyshnegradskii first considered the question of stability of dynamic systems. In the late 1800s, A. Hurwitz and E. J. Routh independently

published a method of investigating the stability of a linear system [6, 7]. The Routh–Hurwitz stability method provides an answer to the question of stability by considering the characteristic equation of the system. The characteristic equation in the Laplace variable is written as

$$\Delta(s) = q(s) = a_n s^n + a_{n-1} s^{n-1} + \cdots + a_1 s + a_0 = 0. \quad (6.3)$$

To ascertain the stability of the system, it is necessary to determine whether any one of the roots of  $q(s)$  lies in the right half of the  $s$ -plane. If Equation (6.3) is written in factored form, we have

$$a_n(s - r_1)(s - r_2) \cdots (s - r_n) = 0, \quad (6.4)$$

where  $r_i$  =  $i$ th root of the characteristic equation. Multiplying the factors together, we find that

$$\begin{aligned} q(s) &= a_n s^n - a_n(r_1 + r_2 + \cdots + r_n)s^{n-1} \\ &\quad + a_n(r_1r_2 + r_2r_3 + r_1r_3 + \cdots)s^{n-2} \\ &\quad - a_n(r_1r_2r_3 + r_1r_2r_4 \cdots)s^{n-3} + \cdots \\ &\quad + a_n(-1)^n r_1r_2r_3 \cdots r_n = 0. \end{aligned} \quad (6.5)$$

In other words, for an  $n$ th-degree equation, we obtain

$$\begin{aligned} q(s) &= a_n s^n - a_n (\text{sum of all the roots}) s^{n-1} \\ &\quad + a_n (\text{sum of the products of the roots taken 2 at a time}) s^{n-2} \\ &\quad - a_n (\text{sum of the products of the roots taken 3 at a time}) s^{n-3} \\ &\quad + \cdots + a_n(-1)^n (\text{product of all } n \text{ roots}) = 0. \end{aligned} \quad (6.6)$$

Examining Equation (6.5), we note that all the coefficients of the polynomial must have the same sign if all the roots are in the left-hand plane. Also, it is necessary that all the coefficients for a stable system be nonzero. These requirements are necessary but not sufficient. That is, we immediately know the system is unstable if they are not satisfied; yet if they are satisfied, we must proceed further to ascertain the stability of the system. For example, when the characteristic equation is

$$q(s) = (s + 2)(s^2 - s + 4) = (s^3 + s^2 + 2s + 8), \quad (6.7)$$

the system is unstable, and yet the polynomial possesses all positive coefficients.

The **Routh–Hurwitz criterion** is a necessary and sufficient criterion for the stability of linear systems. The method was originally developed in terms of determinants, but we shall use the more convenient array formulation.

The Routh–Hurwitz criterion is based on ordering the coefficients of the characteristic equation

$$a_n s^n + a_{n-1} s^{n-1} + a_{n-2} s^{n-2} + \cdots + a_1 s + a_0 = 0 \quad (6.8)$$

into an array or schedule as follows [4]:

$$\begin{array}{c|ccc} s^n & a_n & a_{n-2} & a_{n-4} \cdots \\ s^{n-1} & a_{n-1} & a_{n-3} & a_{n-5} \cdots \end{array}$$

Further rows of the schedule are then completed as

$$\begin{array}{c|ccc} s^n & a_n & a_{n-2} & a_{n-4} \\ s^{n-1} & a_{n-1} & a_{n-3} & a_{n-5} \\ s^{n-2} & b_{n-1} & b_{n-3} & b_{n-5} \\ s^{n-3} & c_{n-1} & c_{n-3} & n_{n-5} \\ \vdots & \vdots & \vdots & \vdots \\ s^0 & h_{n-1} & & \end{array}$$

where

$$b_{n-1} = \frac{a_{n-1}a_{n-2} - a_n a_{n-3}}{a_{n-1}} = \frac{-1}{a_{n-1}} \begin{vmatrix} a_n & a_{n-2} \\ a_{n-1} & a_{n-3} \end{vmatrix},$$

$$b_{n-3} = -\frac{1}{a_{n-1}} \begin{vmatrix} a_n & a_{n-4} \\ a_{n-1} & a_{n-5} \end{vmatrix},$$

$$c_{n-1} = \frac{-1}{b_{n-1}} \begin{vmatrix} a_{n-1} & a_{n-3} \\ b_{n-1} & b_{n-3} \end{vmatrix},$$

and so on. The algorithm for calculating the entries in the array can be followed on a determinant basis or by using the form of the equation for  $b_{n-1}$ .

**The Routh-Hurwitz criterion states that the number of roots of  $q(s)$  with positive real parts is equal to the number of changes in sign of the first column of the Routh array.** This criterion requires that there be no changes in sign in the first column for a stable system. This requirement is both necessary and sufficient.

Four distinct cases or configurations of the first column array must be considered, and each must be treated separately and requires suitable modifications of the array calculation procedure: (1) No element in the first column is zero; (2) there is a zero in the first column, but some other elements of the row containing the zero in the first column are nonzero; (3) there is a zero in the first column, and the other elements of the row containing the zero are also zero; and (4) as in the third case, but with repeated roots on the  $j\omega$ -axis.

To illustrate this method clearly, several examples will be presented for each case.

### Case 1. No element in the first column is zero.

#### EXAMPLE 6.1 Second-order system

The characteristic polynomial of a second-order system is

$$q(s) = a_2 s^2 + a_1 s + a_0.$$

The Routh array is written as

$$\begin{array}{c|cc} s^2 & a_2 & a_0 \\ s^1 & a_1 & 0 \\ s^0 & b_1 & 0 \end{array}$$

where

$$b_1 = \frac{a_1 a_0 - (0)a_2}{a_1} = \frac{-1}{a_1} \begin{vmatrix} a_2 & a_0 \\ a_1 & 0 \end{vmatrix} = a_0.$$

Therefore, the requirement for a stable second-order system is simply that all the coefficients be positive or all the coefficients be negative. ■

### EXAMPLE 6.2 Third-order system

The characteristic polynomial of a third-order system is

$$q(s) = a_3 s^3 + a_2 s^2 + a_1 s + a_0.$$

The Routh array is

$s^3$	$a_3$	$a_1$
$s^2$	$a_2$	$a_0$
$s^1$	$b_1$	0
$s^0$	$c_1$	0

where

$$b_1 = \frac{a_2 a_1 - a_0 a_3}{a_2} \quad \text{and} \quad c_1 = \frac{b_1 a_0}{b_1} = a_0.$$

For the third-order system to be stable, it is necessary and sufficient that the coefficients be positive and  $a_2 a_1 > a_0 a_3$ . The condition when  $a_2 a_1 = a_0 a_3$  results in a marginal stability case, and one pair of roots lies on the imaginary axis in the  $s$ -plane. This marginal case is recognized as Case 3 because there is a zero in the first column when  $a_2 a_1 = a_0 a_3$ . It will be discussed under Case 3.

As a final example of characteristic equations that result in no zero elements in the first row, let us consider the polynomial

$$q(s) = (s - 1 + j\sqrt{7})(s - 1 - j\sqrt{7})(s + 3) = s^3 + s^2 + 2s + 24. \quad (6.9)$$

The polynomial satisfies all the necessary conditions because all the coefficients exist and are positive. Therefore, utilizing the Routh array, we have

$s^3$	1	2
$s^2$	1	24
$s^1$	-22	0
$s^0$	24	0

Because two changes in sign appear in the first column, we find that two roots of  $q(s)$  lie in the right-hand plane, and our prior knowledge is confirmed. ■

**Case 2. There is a zero in the first column, but some other elements of the row containing the zero in the first column are nonzero.** If only one element in the array is zero, it may be replaced with a small positive number,  $\epsilon$ , that is allowed to

approach zero after completing the array. For example, consider the following characteristic polynomial:

$$q(s) = s^5 + 2s^4 + 2s^3 + 4s^2 + 11s + 10. \quad (6.10)$$

The Routh array is then

$s^5$	1	2	11
$s^4$	2	4	10
$s^3$	$\epsilon$	6	0
$s^2$	$c_1$	10	0
$s^1$	$d_1$	0	0
$s^0$	10	0	0

where

$$c_1 = \frac{4\epsilon - 12}{\epsilon} = \frac{-12}{\epsilon} \quad \text{and} \quad d_1 = \frac{6c_1 - 10\epsilon}{c_1} \rightarrow 6.$$

There are two sign changes due to the large negative number in the first column,  $c_1 = -12/\epsilon$ . Therefore, the system is unstable, and two roots lie in the right half of the plane.

### EXAMPLE 6.3 Unstable system

As a final example of the type of Case 2, consider the characteristic polynomial

$$q(s) = s^4 + s^3 + s^2 + s + K, \quad (6.11)$$

where we desire to determine the gain  $K$  that results in marginal stability. The Routh array is then

$s^4$	1	1	$K$
$s^3$	1	1	0
$s^2$	$\epsilon$	$K$	0
$s^1$	$c_1$	0	0
$s^0$	$K$	0	0

where

$$c_1 = \frac{\epsilon - K}{\epsilon} \rightarrow \frac{-K}{\epsilon}.$$

Therefore, for any value of  $K$  greater than zero, the system is unstable. Also, because the last term in the first column is equal to  $K$ , a negative value of  $K$  will result in an unstable system. Consequently, the system is unstable for all values of gain  $K$ . ■

**Case 3. There is a zero in the first column, and the other elements of the row containing the zero are also zero.** Case 3 occurs when all the elements in one row are zero or when the row consists of a single element that is zero. This condition occurs when the polynomial contains singularities that are symmetrically located about the origin of the  $s$ -plane. Therefore, Case 3 occurs when factors such as  $(s + \sigma)(s - \sigma)$

or  $(s + j\omega)(s - j\omega)$  occur. This problem is circumvented by utilizing the **auxiliary polynomial**,  $U(s)$ , which immediately precedes the zero entry in the Routh array. The order of the auxiliary polynomial is always even and indicates the number of symmetrical root pairs.

To illustrate this approach, let us consider a third-order system with the characteristic polynomial

$$q(s) = s^3 + 2s^2 + 4s + K, \quad (6.12)$$

where  $K$  is an adjustable loop gain. The Routh array is then

$s^3$	1	4
$s^2$	2	$K$
$s^1$	$\frac{8-K}{2}$	0
$s^0$	2	
	$K$	0

For a stable system, we require that

$$0 < K < 8.$$

When  $K = 8$ , we have two roots on the  $j\omega$ -axis and a marginal stability case. Note that we obtain a row of zeros (Case 3) when  $K = 8$ . The auxiliary polynomial,  $U(s)$ , is the equation of the row preceding the row of zeros. The equation of the row preceding the row of zeros is, in this case, obtained from the  $s^2$ -row. We recall that this row contains the coefficients of the even powers of  $s$ , and therefore we have

$$U(s) = 2s^2 + Ks^0 = 2s^2 + 8 = 2(s^2 + 4) = 2(s + j2)(s - j2). \quad (6.13)$$

To show that the auxiliary polynomial,  $U(s)$ , is indeed a factor of the characteristic polynomial, we divide  $q(s)$  by  $U(s)$  to obtain

$$\begin{array}{r} \frac{\frac{1}{2}s + 1}{2s^2 + 8} \\ \hline s^3 & + 4s \\ \hline 2s^2 & + 8 \\ 2s^2 & + 8 \end{array} .$$

When  $K = 8$ , the factors of the characteristic polynomial are

$$q(s) = (s + 2)(s + j2)(s - j2). \quad (6.14)$$

The marginal case response is an unacceptable oscillation.

**Case 4. Repeated roots of the characteristic equation on the  $j\omega$ -axis.** If the  $j\omega$ -axis roots of the characteristic equation are simple, the system is neither stable nor unstable; it is instead called marginally stable, since it has an undamped sinusoidal mode. If the  $j\omega$ -axis roots are repeated, the system response will be unstable with a form  $t \sin(\omega t + \phi)$ . The Routh–Hurwitz criteria will not reveal this form of instability [20].

Consider the system with a characteristic polynomial

$$q(s) = (s + 1)(s + j)(s - j)(s + j)(s - j) = s^5 + s^4 + 2s^3 + 2s^2 + s + 1.$$

The Routh array is

$s^5$	1	2	1
$s^4$	1	2	1
$s^3$	$\epsilon$	$\epsilon$	0
$s^2$	1	1	,
$s^1$	$\epsilon$	0	
$s^0$	1		

where  $\epsilon \rightarrow 0$ . Note the absence of sign changes, a condition that falsely indicates that the system is marginally stable. The impulse response of the system increases with time as  $t \sin(t + \phi)$ . The auxiliary polynomial at the  $s^2$  line is  $s^2 + 1$ , and the auxiliary polynomial at the  $s^4$  line is  $s^4 + 2s^2 + 1 = (s^2 + 1)^2$ , indicating the repeated roots on the  $j\omega$ -axis.

#### EXAMPLE 6.4 Fifth-order system with roots on the $j\omega$ -axis

Consider the characteristic polynomial

$$q(s) = s^5 + s^4 + 4s^3 + 24s^2 + 3s + 63. \quad (6.15)$$

The Routh array is

$s^5$	1	4	3
$s^4$	1	24	63
$s^3$	-20	-60	0.
$s^2$	21	63	0
$s^1$	0	0	0

Therefore, the auxiliary polynomial is

$$U(s) = 21s^2 + 63 = 21(s^2 + 3) = 21(s + j\sqrt{3})(s - j\sqrt{3}), \quad (6.16)$$

which indicates that two roots are on the imaginary axis. To examine the remaining roots, we divide by the auxiliary polynomial to obtain

$$\frac{q(s)}{s^2 + 3} = s^3 + s^2 + s + 21.$$

Establishing a Routh array for this equation, we have

$s^3$	1	1
$s^2$	1	21
$s^1$	-20	0
$s^0$	21	0

The two changes in sign in the first column indicate the presence of two roots in the right-hand plane, and the system is unstable. The roots in the right-hand plane are  $s = +1 \pm j\sqrt{6}$ . ■

### EXAMPLE 6.5 Welding control

Large welding robots are used in today's auto plants. The welding head is moved to different positions on the auto body, and a rapid, accurate response is required. A block diagram of a welding head positioning system is shown in Figure 6.5. We desire to determine the range of  $K$  and  $a$  for which the system is stable. The characteristic equation is

$$1 + G(s) = 1 + \frac{K(s + a)}{s(s + 1)(s + 2)(s + 3)} = 0.$$

Therefore,  $q(s) = s^4 + 6s^3 + 11s^2 + (K + 6)s + Ka = 0$ . Establishing the Routh array, we have

$s^4$	1	11	$Ka$
$s^3$	6	$K + 6$	
$s^2$	$b_3$	$Ka$	,
$s^1$	$c_3$		
$s^0$	$Ka$		

where

$$b_3 = \frac{60 - K}{6} \quad \text{and} \quad c_3 = \frac{b_3(K + 6) - 6Ka}{b_3}.$$

The coefficient  $c_3$  sets the acceptable range of  $K$  and  $a$ , while  $b_3$  requires that  $K$  be less than 60. Requiring  $c_3 \geq 0$ , we obtain

$$(K - 60)(K + 6) + 36Ka \leq 0.$$

The required relationship between  $K$  and  $a$  is then

$$a \leq \frac{(60 - K)(K + 6)}{36K}$$

when  $a$  is positive. Therefore, if  $K = 40$ , we require  $a \leq 0.639$ . ■

The general form of the characteristic equation of an  $n$ th-order system is

$$s^n + a_{n-1}s^{n-1} + a_{n-2}s^{n-2} + \dots + a_1s + \omega_n^n = 0.$$

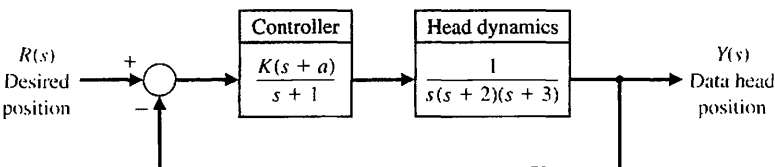


**FIGURE 6.5**  
Welding head  
position control.

**Table 6.1 The Routh–Hurwitz Stability Criterion**

<i>n</i>	Characteristic Equation	Criterion
2	$s^2 + bs + 1 = 0$	$b > 0$
3	$s^3 + bs^2 + cs + 1 = 0$	$bc - 1 > 0$
4	$s^4 + bs^3 + cs^2 + ds + 1 = 0$	$bcd - d^2 - b^2 > 0$
5	$s^5 + bs^4 + cs^3 + ds^2 + es + 1 = 0$	$bcd + b - d^2 - b^2e > 0$
6	$s^6 + bs^5 + cs^4 + ds^3 + es^2 + fs + 1 = 0$	$(bcd + bf - d^2 - b^2e)e + b^2c - bd - bc^2f - f^2 + bfe + cdf > 0$

Note: The equations are normalized by  $(\omega_n)^n$ .

We divide through by  $\omega_n^n$  and use  $\hat{s} = s/\omega_n$  to obtain the normalized form of the characteristic equation:

$$\hat{s}^n + b\hat{s}^{n-1} + c\hat{s}^{n-2} + \dots + 1 = 0.$$

For example, we normalize

$$s^3 + 5s^2 + 2s + 8 = 0$$

by dividing through by  $8 = \omega_n^3$ , obtaining

$$\frac{s^3}{\omega_n^3} + \frac{5}{2} \frac{s^2}{\omega_n^2} + \frac{2}{4} \frac{s}{\omega_n} + 1 = 0,$$

or

$$\hat{s}^3 + 2.5\hat{s}^2 + 0.5\hat{s} + 1 = 0,$$

where  $\hat{s} = s/\omega_n$ . In this case,  $b = 2.5$  and  $c = 0.5$ . Using this normalized form of the characteristic equation, we summarize the stability criterion for up to a sixth-order characteristic equation, as provided in Table 6.1. Note that  $bc = 1.25$  and the system is stable.

## 6.3 THE RELATIVE STABILITY OF FEEDBACK CONTROL SYSTEMS

The verification of stability using the Routh–Hurwitz criterion provides only a partial answer to the question of stability. The Routh–Hurwitz criterion ascertains the absolute stability of a system by determining whether any of the roots of the characteristic equation lie in the right half of the *s*-plane. However, if the system satisfies the Routh–Hurwitz criterion and is absolutely stable, it is desirable to determine the **relative stability**; that is, it is necessary to investigate the relative damping of each root of the characteristic equation. The relative stability of a system can be defined as the property that is measured by the relative real part of each root or pair of roots. Thus, root  $r_2$  is relatively more stable than the roots  $r_1, \hat{r}_1$ , as shown in Figure 6.6. The relative stability of a system can also be defined in terms of the relative damping coefficients  $\zeta$  of each complex root pair and, therefore, in terms of the speed of response and overshoot instead of settling time.

Hence, the investigation of the relative stability of each root is clearly necessary because, as we found in Chapter 5, the location of the closed-loop poles in the *s*-plane determines the performance of the system. Thus, it is imperative that we

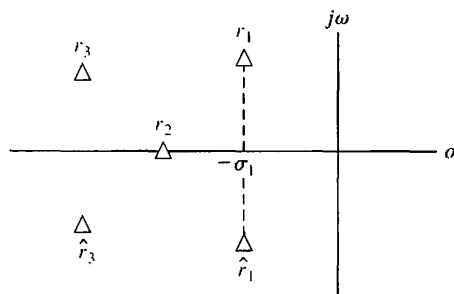


**FIGURE 6.6**  
Root locations in  
the  $s$ -plane.

reexamine the characteristic polynomial  $q(s)$  and consider several methods for the determination of relative stability.

Because the relative stability of a system is dictated by the location of the roots of the characteristic equation, a first approach using an  $s$ -plane formulation is to extend the Routh–Hurwitz criterion to ascertain relative stability. This can be simply accomplished by utilizing a change of variable, which shifts the  $s$ -plane axis in order to utilize the Routh–Hurwitz criterion. Examining Figure 6.6, we notice that a shift of the vertical axis in the  $s$ -plane to  $-\sigma_1$  will result in the roots  $r_1, \hat{r}_1$  appearing on the shifted axis. The correct magnitude to shift the vertical axis must be obtained on a trial-and-error basis. Then, without solving the fifth-order polynomial  $q(s)$ , we may determine the real part of the dominant roots  $r_1, \hat{r}_1$ .

#### EXAMPLE 6.6 Axis shift

Consider the simple third-order characteristic equation

$$q(s) = s^3 + 4s^2 + 6s + 4. \quad (6.17)$$

As a first try, let  $s_n = s + 1/2$  and note that we obtain a Routh array without a zero occurring in the first column. However, upon setting the shifted variable  $s_n$  equal to  $s + 1$ , we obtain

$$(s_n - 1)^3 + 4(s_n - 1)^2 + 6(s_n - 1) + 4 = s_n^3 + s_n^2 + s_n + 1. \quad (6.18)$$

Then the Routh array is established as

$s_n^3$	1	1
$s_n^2$	1	1
$s_n^1$	0	0
$s_n^0$	1	0

There are roots on the shifted imaginary axis that can be obtained from the auxiliary polynomial

$$U(s_n) = s_n^2 + 1 = (s_n + j)(s_n - j) = (s + 1 + j)(s + 1 - j). \quad (6.19) \blacksquare$$

The shifting of the  $s$ -plane axis to ascertain the relative stability of a system is a very useful approach, particularly for higher-order systems with several pairs of closed-loop complex conjugate roots.

## 6.4 THE STABILITY OF STATE VARIABLE SYSTEMS

The stability of a system modeled by a state variable flow graph model can be readily ascertained. The stability of a system with an input–output transfer function  $T(s)$  can be determined by examining the denominator polynomial of  $T(s)$ . Therefore, if the transfer function is written as

$$T(s) = \frac{p(s)}{q(s)},$$

where  $p(s)$  and  $q(s)$  are polynomials in  $s$ , then the stability of the system is represented by the roots of  $q(s)$ . The polynomial  $q(s)$ , when set equal to zero, is called the characteristic equation. The roots of the characteristic equation must lie in the left-hand  $s$ -plane for the system to exhibit a stable time response. Therefore, to ascertain the stability of a system represented by a transfer function, we investigate the characteristic equation and utilize the Routh–Hurwitz criterion. If the system we are investigating is represented by a signal-flow graph state model, we obtain the characteristic equation by evaluating the flow graph determinant. If the system is represented by a block diagram model we obtain the characteristic equation using the block diagram reduction methods. As an illustration of these methods, let us investigate the stability of the system of Example 3.2.

### EXAMPLE 6.7 Stability of a system

The transfer function  $T(s)$  examined in Example 3.2 is

$$T(s) = \frac{2s^2 + 8s + 6}{s^3 + 8s^2 + 16s + 6}. \quad (6.20)$$

The characteristic polynomial for this system is

$$q(s) = s^3 + 8s^2 + 16s + 6. \quad (6.21)$$

This characteristic polynomial is also readily obtained from either the flow graph model or block diagram model shown in Figure 3.11 or the ones shown in Figure 3.13. Using the Routh–Hurwitz criterion, we find that the system is stable and that all the roots of  $q(s)$  lie in the left-hand  $s$ -plane. ■

We often determine the flow graph or block diagram model directly from a set of state differential equations. We can use the flow graph directly to determine the stability of the system by obtaining the characteristic equation from the flow graph determinant  $\Delta(s)$ . Similarly, we can use block diagram reduction to define the characteristic equation. An illustration of these approaches will aid in comprehending these methods.

### EXAMPLE 6.8 Stability of a second-order system

A second-order system is described by the two first-order differential equations

$$\dot{x}_1 = -3x_1 + x_2 \quad \text{and} \quad \dot{x}_2 = +1x_2 - Kx_1 + Ku,$$

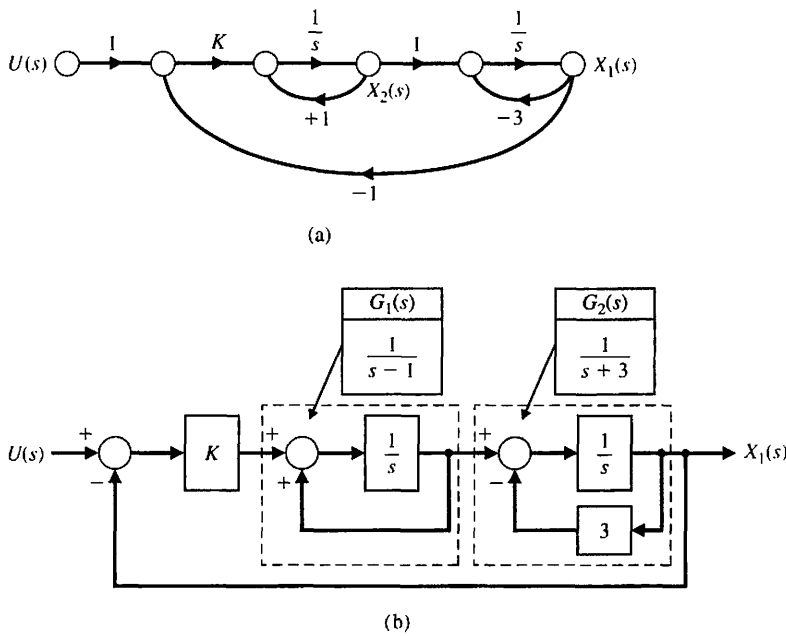


**FIGURE 6.7**  
 (a) Flow graph model for state variable equations of Example 6.8.  
 (b) Block diagram model.

where the dot notation implies the first derivative and  $u(t)$  is the input. The flow graph model of this set of differential equations is shown in Figure 6.7(a) and the block diagram model is shown in Figure 6.7(b).

Using Mason's signal-flow gain formula, we note three loops:

$$L_1 = s^{-1}, \quad L_2 = -3s^{-1}, \quad \text{and} \quad L_3 = -Ks^{-2},$$

where  $L_1$  and  $L_2$  do not share a common node. Therefore, the determinant is

$$\Delta = 1 - (L_1 + L_2 + L_3) + L_1 L_2 = 1 - (s^{-1} - 3s^{-1} - Ks^{-2}) + (-3s^{-2}).$$

We multiply by  $s^2$  to obtain the characteristic equation

$$s^2 + 2s + (K - 3) = 0.$$

Since all coefficients must be positive, we require  $K > 3$  for stability. A similar analysis can be undertaken using the block diagram. Closing the two feedback loops yields the two transfer functions

$$G_1(s) = \frac{1}{s-1} \quad \text{and} \quad G_2(s) = \frac{1}{s+3},$$

as illustrated in Figure 6.7(b). The closed loop transfer function is thus

$$T(s) = \frac{KG_1(s)G_2(s)}{1 + KG_1(s)G_2(s)}.$$

Therefore, the characteristic equation is

$$\Delta(s) = 1 + KG_1(s)G_2(s) = 0,$$

or

$$\Delta(s) = (s - 1)(s + 3) + K = s^2 + 2s + (K - 3) = 0.$$

This confirms the results obtained using signal-flow graph techniques. ■

A method of obtaining the characteristic equation directly from the vector differential equation is based on the fact that the solution to the unforced system is an exponential function. The vector differential equation without input signals is

$$\dot{\mathbf{x}} = \mathbf{Ax}, \quad (6.22)$$

where  $\mathbf{x}$  is the state vector. The solution is of exponential form, and we can define a constant  $\lambda$  such that the solution of the system for one state can be of the form  $x_i(t) = k_i e^{\lambda t}$ . The  $\lambda_i$  are called the characteristic roots or eigenvalues of the system, which are simply the roots of the characteristic equation. If we let  $\mathbf{x} = \mathbf{k}e^{\lambda t}$  and substitute into Equation (6.22), we have

$$\lambda \mathbf{k}e^{\lambda t} = \mathbf{A} \mathbf{k}e^{\lambda t}, \quad (6.23)$$

or

$$\lambda \mathbf{x} = \mathbf{Ax}. \quad (6.24)$$

Equation (6.24) can be rewritten as

$$(\lambda \mathbf{I} - \mathbf{A})\mathbf{x} = \mathbf{0}, \quad (6.25)$$

where  $\mathbf{I}$  equals the identity matrix and  $\mathbf{0}$  equals the null matrix. This set of simultaneous equations has a nontrivial solution if and only if the determinant vanishes—that is, only if

$$\det(\lambda \mathbf{I} - \mathbf{A}) = 0. \quad (6.26)$$

The  $n$ th-order equation in  $\lambda$  resulting from the evaluation of this determinant is the characteristic equation, and the stability of the system can be readily ascertained. Let us consider again the third-order system described in Example 3.3 to illustrate this approach.

#### EXAMPLE 6.9 Closed epidemic system

The vector differential equation of the epidemic system is given in Equation (3.63) and repeated here as

$$\frac{d\mathbf{x}}{dt} = \begin{bmatrix} -\alpha & -\beta & 0 \\ \beta & -\gamma & 0 \\ \alpha & \gamma & 0 \end{bmatrix} \mathbf{x} + \begin{bmatrix} 1 & 0 \\ 0 & 1 \\ 0 & 0 \end{bmatrix} \begin{bmatrix} u_1 \\ u_2 \end{bmatrix}.$$

The characteristic equation is then

$$\begin{aligned} \det(\lambda \mathbf{I} - \mathbf{A}) &= \det \left\{ \begin{bmatrix} \lambda & 0 & 0 \\ 0 & \lambda & 0 \\ 0 & 0 & \lambda \end{bmatrix} - \begin{bmatrix} -\alpha & -\beta & 0 \\ \beta & -\gamma & 0 \\ \alpha & \gamma & 0 \end{bmatrix} \right\} \\ &= \det \begin{bmatrix} \lambda + \alpha & \beta & 0 \\ -\beta & \lambda + \gamma & 0 \\ -\alpha & -\gamma & \lambda \end{bmatrix} \end{aligned}$$

$$\begin{aligned}
 &= \lambda[(\lambda + \alpha)(\lambda + \gamma) + \beta^2] \\
 &= \lambda[\lambda^2 + (\alpha + \gamma)\lambda + (\alpha\gamma + \beta^2)] = 0.
 \end{aligned}$$

Thus, we obtain the characteristic equation of the system, and it is similar to that obtained in Equation (3.65) by flow graph methods. The additional root  $\lambda = 0$  results from the definition of  $x_3$  as the integral of  $\alpha x_1 + \gamma x_2$ , and  $x_3$  does not affect the other state variables. Thus, the root  $\lambda = 0$  indicates the integration connected with  $x_3$ . The characteristic equation indicates that the system is marginally stable when  $\alpha + \gamma > 0$  and  $\alpha\gamma + \beta^2 > 0$ . ■

As another example, consider again the inverted pendulum described in Example 3.4. The system matrix is

$$\mathbf{A} = \begin{bmatrix} 0 & 1 & 0 & 0 \\ 0 & 0 & -mg/M & 0 \\ 0 & 0 & 0 & 1 \\ 0 & 0 & g/l & 0 \end{bmatrix}.$$

The characteristic equation can be obtained from the determinant of  $(\lambda\mathbf{I} - \mathbf{A})$  as follows:

$$\det \begin{bmatrix} \lambda & -1 & 0 & 0 \\ 0 & \lambda & mg/M & 0 \\ 0 & 0 & \lambda & -1 \\ 0 & 0 & -g/l & \lambda \end{bmatrix} = \lambda \left[ \lambda \left( \lambda^2 - \frac{g}{l} \right) \right] = \lambda^2 \left( \lambda^2 - \frac{g}{l} \right) = 0.$$

The characteristic equation indicates that there are two roots at  $\lambda = 0$ : a root at  $\lambda = +\sqrt{g/l}$  and a root at  $\lambda = -\sqrt{g/l}$ . Hence, the system is unstable, because there is a root in the right-hand plane at  $\lambda = +\sqrt{g/l}$ . The two roots at  $\lambda = 0$  will also result in an unbounded response.

## 6.5 DESIGN EXAMPLES

In this section we present two illustrative examples. The first example is a tracked vehicle control problem. In this first example, stability issues are addressed employing the Routh-Hurwitz stability criterion and the outcome is the selection of two key system parameters. The second example illustrates the stability problem robot-controlled motorcycle and how Routh-Hurwitz can be used in the selection of controller gains during the design process. The robot-controlled motorcycle example highlights the design process with special attention to the impact of key controller parameters on stability.

### EXAMPLE 6.10 Tracked vehicle turning control

The design of a turning control for a tracked vehicle involves the selection of two parameters [8]. In Figure 6.8, the system shown in part (a) has the model shown in part (b). The two tracks are operated at different speeds in order to turn the vehicle.

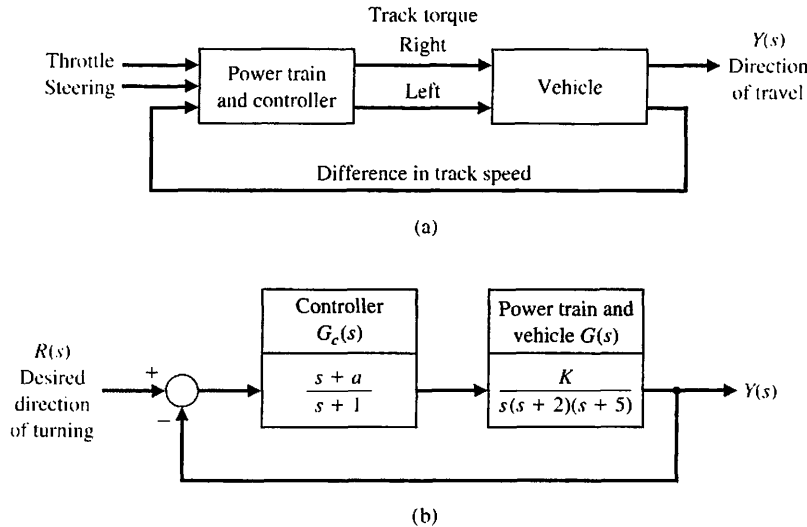


**FIGURE 6.8**  
(a) Turning control system for a two-track vehicle.  
(b) Block diagram.

We must select  $K$  and  $a$  so that the system is stable and the steady-state error for a ramp command is less than or equal to 24% of the magnitude of the command.

The characteristic equation of the feedback system is

$$1 + G_c G(s) = 0,$$

or

$$1 + \frac{K(s+a)}{s(s+1)(s+2)(s+5)} = 0. \quad (6.27)$$

Therefore, we have

$$s(s+1)(s+2)(s+5) + K(s+a) = 0,$$

or

$$s^4 + 8s^3 + 17s^2 + (K+10)s + Ka = 0. \quad (6.28)$$

To determine the stable region for  $K$  and  $a$ , we establish the Routh array as

$s^4$	1	17	$Ka$
$s^3$	8	$K+10$	0
$s^2$	$b_3$	$Ka$	,
$s^1$	$c_3$		
$s^0$	$Ka$		

where

$$b_3 = \frac{126 - K}{8} \quad \text{and} \quad c_3 = \frac{b_3(K+10) - 8Ka}{b_3}.$$

For the elements of the first column to be positive, we require that  $Ka$ ,  $b_3$ , and  $c_3$  be positive. Therefore, we require that

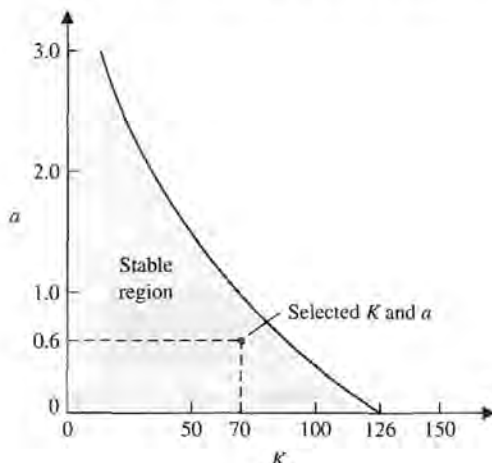


**FIGURE 6.9**  
The stable region.

$$\begin{aligned}K &< 126, \\Ka &> 0, \text{ and}\end{aligned}$$

$$(K + 10)(126 - K) - 64Ka > 0. \quad (6.29)$$

The region of stability for  $K > 0$  is shown in Figure 6.9. The steady-state error to a ramp input  $r(t) = At$ ,  $t > 0$  is

$$e_{ss} = A/K_v,$$

where

$$K_v = \lim_{s \rightarrow 0} sG_c G = Ka/10.$$

Therefore, we have

$$e_{ss} = \frac{10A}{Ka}. \quad (6.30)$$

When  $e_{ss}$  is equal to 23.8% of  $A$ , we require that  $Ka = 42$ . This can be satisfied by the selected point in the stable region when  $K = 70$  and  $a = 0.6$ , as shown in Figure 6.9. Another acceptable design would be attained when  $K = 50$  and  $a = 0.84$ . We can calculate a series of possible combinations of  $K$  and  $a$  that can satisfy  $Ka = 42$  and that lie within the stable region, and all will be acceptable design solutions. However, not all selected values of  $K$  and  $a$  will lie within the stable region. Note that  $K$  cannot exceed 126. ■

#### EXAMPLE 6.11 Robot-controlled motorcycle

Consider the robot-controlled motorcycle shown in Figure 6.10. The motorcycle will move in a straight line at constant forward speed  $v$ . Let  $\phi$  denote the angle between the plane of symmetry of the motorcycle and the vertical. The desired angle  $\phi_d$  is equal to zero:

$$\phi_d(s) = 0.$$

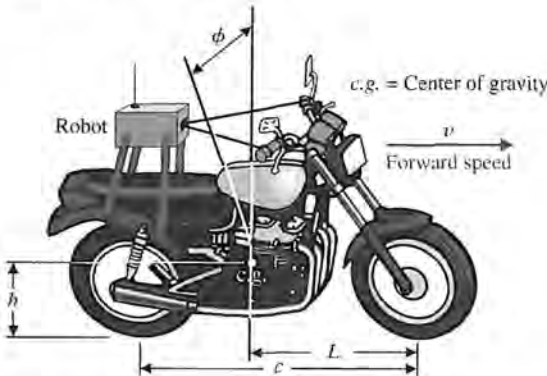


**FIGURE 6.10**  
The robot-controlled motorcycle.

The design elements highlighted in this example are illustrated in Figure 6.11. Using the Routh–Hurwitz stability criterion will allow us to get to the heart of the matter, that is, to develop a strategy for computing the controller gains while ensuring closed-loop stability.

The control goal is

#### Control Goal

Control the motorcycle in the vertical position, and maintain the prescribed position in the presence of disturbances.

The variable to be controlled is

#### Variable to Be Controlled

The motorcycle position from vertical ( $\phi$ ).

Since our focus here is on stability rather than transient response characteristics, the control specifications will be related to stability only; transient performance is an issue that we need to address once we have investigated all the stability issues. The control design specification is

#### Design Specification

**DS1** The closed-loop system must be stable.

The main components of the robot-controlled motorcycle are the motorcycle and robot, the controller, and the feedback measurements. The main subject of the chapter is not modeling, so we do not concentrate on developing the motorcycle dynamics model. We rely instead on the work of others (see [22]). The motorcycle model is given by

$$G(s) = \frac{1}{s^2 - \alpha_1}, \quad (6.31)$$

where  $\alpha_1 = g/h$ ,  $g = 9.806 \text{ m/s}^2$ , and  $h$  is the height of the motorcycle center of gravity above the ground (see Figure 6.10). The motorcycle is unstable with poles at  $s = \pm\sqrt{\alpha_1}$ . The controller is given by

$$G_c(s) = \frac{\alpha_2 + \alpha_3 s}{\tau s + 1}, \quad (6.32)$$

Topics emphasized in this example

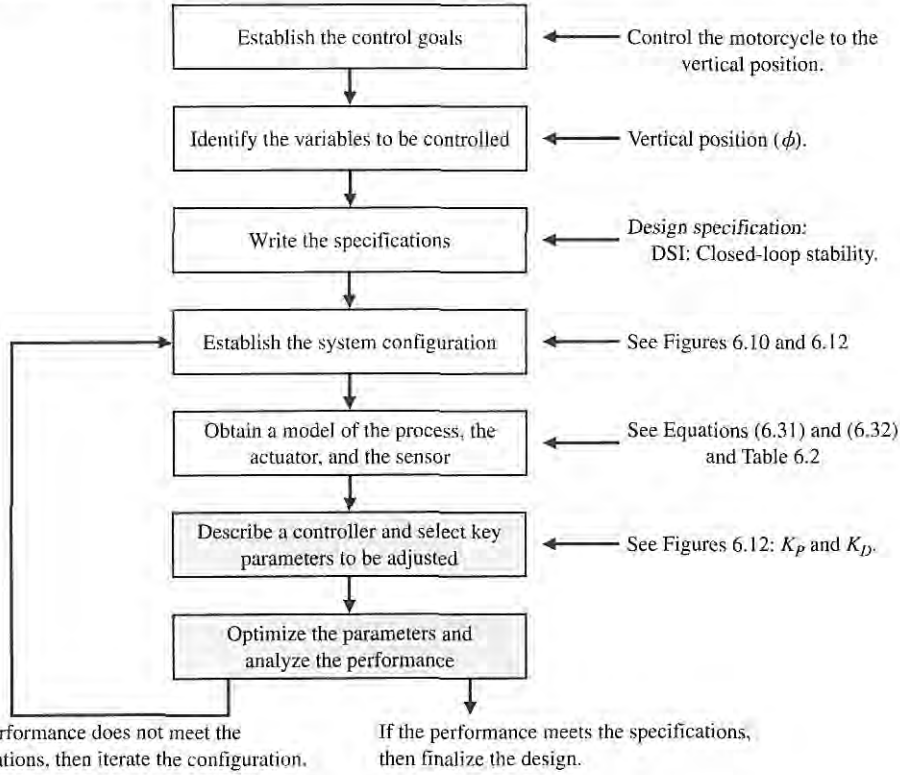


**FIGURE 6.11** Elements of the control system design process emphasized in this robot-controlled motorcycle example.

where

$$\alpha_2 = v^2/(hc)$$

and

$$\alpha_3 = vL/(hc).$$

The forward speed of the motorcycle is denoted by  $v$ , and  $c$  denotes the wheel-base (the distance between the wheel centers). The length,  $L$ , is the horizontal distance between the front wheel axle and the motorcycle center of gravity. The time-constant of the controller is denoted by  $\tau$ . This term represents the speed of response of the controller; smaller values of  $\tau$  indicate an increased speed of response. Many simplifying assumptions are necessary to obtain the simple transfer function models in Equations (6.31) and (6.32).

Control is accomplished by turning the handlebar. The front wheel rotation about the vertical is not evident in the transfer functions. Also, the transfer functions assume a constant forward speed  $v$  which means that we must have another control system at work regulating the forward speed. Nominal motorcycle and robot controller parameters are given in Table 6.2.

Assembling the components of the feedback system gives us the system configuration shown in Figure 6.12. Examination of the configuration reveals that the robot controller block is a function of the physical system ( $h$ ,  $c$ , and  $L$ ), the operating conditions ( $v$ ), and the robot time-constant ( $\tau$ ). No parameters need adjustment unless we physically change the motorcycle parameters and/or speed. In fact, in this example the parameters we want to adjust are in the feedback loop:

### Select Key Tuning Parameters

Feedback gains  $K_P$  and  $K_D$ .

The key tuning parameters are not always in the forward path; in fact they may exist in any subsystem in the block diagram.

We want to use the Routh–Hurwitz technique to analyze the closed-loop system stability. What values of  $K_P$  and  $K_D$  lead to closed-loop stability? A related question that we can pose is, given specific values of  $K_P$  and  $K_D$  for the nominal system (that is, nominal values of  $\alpha_1$ ,  $\alpha_2$ ,  $\alpha_3$ , and  $\tau$ ), how can the parameters themselves vary while still retaining closed-loop stability?

**Table 6.2 Physical Parameters**

$\tau$	0.2 s
$\alpha_1$	9 1/s <sup>2</sup>
$\alpha_2$	2.7 1/s <sup>2</sup>
$\alpha_3$	1.35 1/s
$h$	1.09 m
$V$	2.0 m/s
$L$	1.0 m
$c$	1.36 m

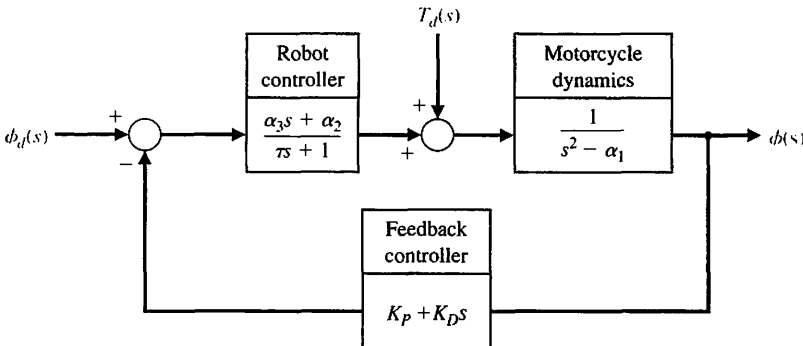


**FIGURE 6.12**

The robot-controlled motorcycle feedback system block diagram.

The closed-loop transfer function from  $\phi_d(s)$  to  $\phi(s)$  is

$$T(s) = \frac{\alpha_2 + \alpha_3 s}{\Delta(s)},$$

where

$$\Delta(s) = \tau s^3 + (1 + K_D \alpha_3)s^2 + (K_D \alpha_2 + K_P \alpha_3 - \tau \alpha_1)s + K_P \alpha_2 - \alpha_1.$$

The characteristic equation is

$$\Delta(s) = 0.$$

The question that we need to answer is for what values of  $K_P$  and  $K_D$  does the characteristic equation  $\Delta(s) = 0$  have all roots in the left half-plane?

We can set up the following Routh array:

$s^3$	$\tau$	$K_D \alpha_2 + K_P \alpha_3 - \tau \alpha_1$
$s^2$	$1 + K_D \alpha_3$	$K_P \alpha_2 - \alpha_1$
$s$	$a$	
1	$K_P \alpha_2 - \alpha_1$	

where

$$a = \frac{(1 + K_D \alpha_3)(K_D \alpha_2 + K_P \alpha_3 - \tau \alpha_1) - \tau(\alpha_2 K_P - \alpha_1)}{1 + K_D \alpha_3}.$$

By inspecting column 1, we determine that for stability we require

$$\tau > 0, K_D > -1/\alpha_3, K_P > \alpha_1/\alpha_2, \text{ and } a > 0.$$

Choosing  $K_D > 0$  satisfies the second inequality (note that  $\alpha_3 > 0$ ). In the event  $\tau = 0$ , we would reformulate the characteristic equation and rework the Routh array.

The computational difficulty arises in determining the conditions on  $K_P$  and  $K_D$  such that  $a > 0$ . We find that  $a > 0$  implies that the following relationship must be satisfied:

$$f = \alpha_2 \alpha_3 K_D^2 + (\alpha_2 - \tau \alpha_1 \alpha_3 + \alpha_3^2 K_P) K_D + (\alpha_3 - \tau \alpha_2) K_P > 0. \quad (6.33)$$

Using the nominal values of the parameters  $\alpha_1$ ,  $\alpha_2$ ,  $\alpha_3$ , and  $\tau$  (see Table 6.2), the stability region is shown in Figure 6.13. For all  $K_D > 0$  and  $K_P > 3.33$ , the function  $f > 0$ , hence  $a > 0$ . Taking into account all the inequalities, a valid region for selecting the gains is  $K_D > 0$  and  $K_P > \alpha_1/\alpha_2 = 3.33$ .

Selecting any point  $(K_P, K_D)$  in the stability region yields a valid (that is, stable) set of gains for the feedback loop. For example, selecting

$$K_P = 10 \text{ and } K_D = 5$$

yields a stable closed-loop system. The closed-loop poles are

$$s_1 = -35.2477, s_2 = -2.4674, \text{ and } s_3 = -1.0348.$$

Since all the poles have negative real parts, we know the system response to any bounded input will be bounded.

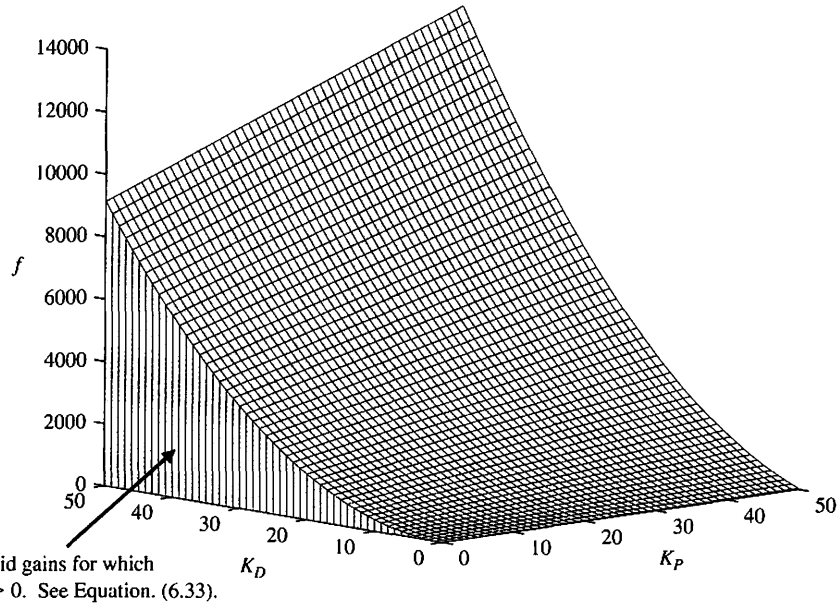


**FIGURE 6.13**  
Region of valid gains  $(K_D, K_P)$  for which the inequality in Equation (6.33) is satisfied.

For this robot-controlled motorcycle, we do not expect to have to respond to nonzero command inputs (that is,  $\phi_d \neq 0$ ) since we want the motorcycle to remain upright, and we certainly want to remain upright in the presence of external disturbances. The transfer function for the disturbance  $T_d(s)$  to the output  $\phi(s)$  without feedback is

$$\phi(s) = \frac{1}{s^2 - \alpha_1} T_d(s).$$

The characteristic equation is

$$q(s) = s^2 - \alpha_1 = 0.$$

The system poles are

$$s_1 = -\sqrt{\alpha_1} \text{ and } s_2 = +\sqrt{\alpha_1}.$$

Thus we see that the motorcycle is unstable; it possesses a pole in the right half-plane. Without feedback control, any external disturbance will result in the motorcycle falling over. Clearly the need for a control system (usually provided by the human rider) is necessary. With the feedback and robot controller in the loop, the closed-loop transfer function from the disturbance to the output is

$$\frac{\phi(s)}{T_d(s)} = \frac{\tau s + 1}{\tau s^3 + (1 + K_D \alpha_3)s^2 + (K_D \alpha_2 + K_P \alpha_3 - \tau \alpha_1)s + K_P \alpha_2 - \alpha_1}.$$

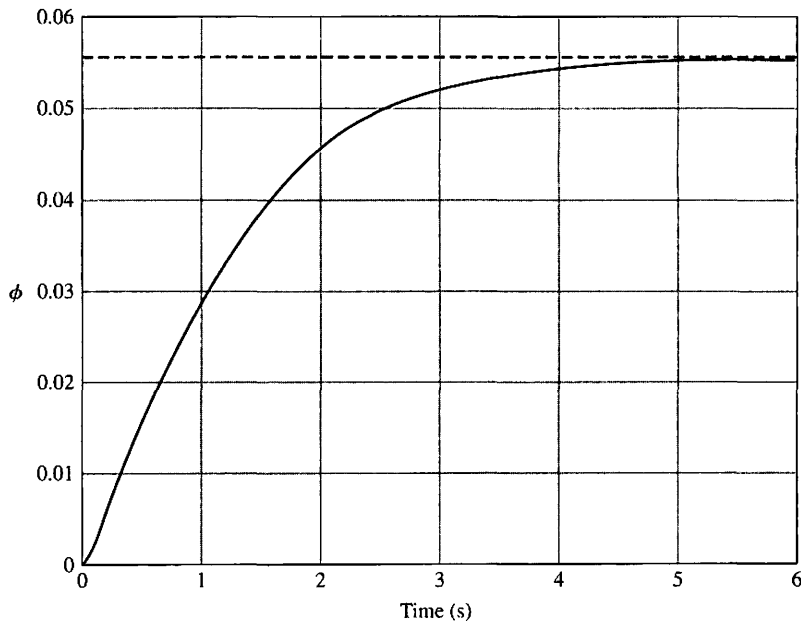


**FIGURE 6.14**  
Disturbance  
response with  
 $K_P = 10$  and  
 $K_D = 5$ .

The response to a step disturbance

$$T_d(s) = \frac{1}{s},$$

is shown in Figure 6.14; the response is stable. The control system manages to keep the motorcycle upright, although it is tilted at about  $\phi = 0.055$  rad = 3.18 deg.

It is important to give the robot the ability to control the motorcycle over a wide range of forward speeds. Is it possible for the robot, with the feedback gains as selected ( $K_P = 10$  and  $K_D = 5$ ), to control the motorcycle as the velocity varies? From experience we know that at slower speeds a bicycle becomes more difficult to control. We expect to see the same characteristics in the stability analysis of our system. Whenever possible, we try to relate the engineering problem at hand to real-life experiences. This helps to develop intuition that can be used as a reasonableness check on our solution.

A plot of the roots of the characteristic equation as the forward speed  $v$  varies is shown in Figure 6.15. The data in the plot were generated using the nominal values of the feedback gains,  $K_P = 10$  and  $K_D = 5$ . We selected these gains for the case where  $v = 2$  m/s. Figure 6.15 shows that as  $v$  increases, the roots of the characteristic equation remain stable (that is, in the left half-plane) with all points negative. But as the motorcycle forward speed decreases, the roots move toward zero, with one root becoming positive at  $v = 1.15$  m/s. At the point where one root is positive, the motorcycle is unstable. ■

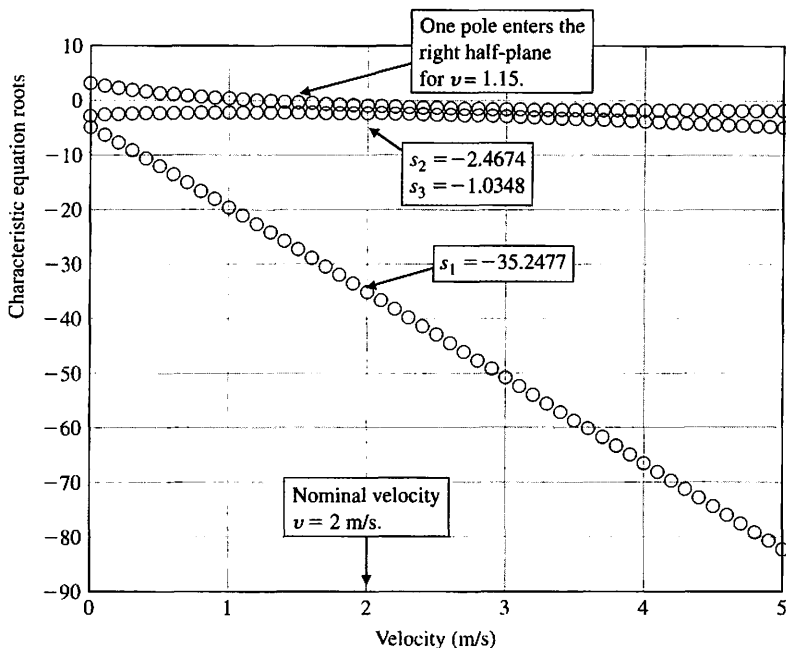


**FIGURE 6.15**  
Roots of the characteristic equation as the motorcycle velocity varies.

## 6.6 SYSTEM STABILITY USING CONTROL DESIGN SOFTWARE

This section begins with a discussion of the Routh–Hurwitz stability method. We will see how the computer can assist us in the stability analysis by providing an easy and accurate method for computing the poles of the characteristic equation. For the case of the characteristic equation as a function of a single parameter, it will be possible to generate a plot displaying the movement of the poles as the parameter varies. The section concludes with an example.

The function introduced in this section is the `for` function, which is used to repeat a number of statements a specific number of times.

**Routh–Hurwitz Stability.** As stated earlier, the Routh–Hurwitz criterion is a necessary and sufficient criterion for stability. Given a characteristic equation with fixed coefficients, we can use Routh–Hurwitz to determine the number of roots in the right half-plane. For example, consider the characteristic equation

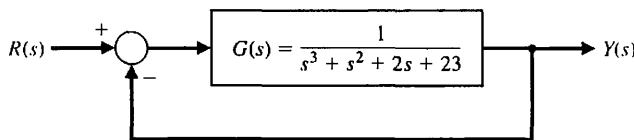
$$q(s) = s^3 + s^2 + 2s + 24 = 0$$

associated with the closed-loop control system shown in Figure 6.16. The corresponding Routh–Hurwitz array is shown in Figure 6.17. The two sign changes in the first column indicate that there are two roots of the characteristic polynomial in the right half-plane; hence, the closed-loop system is unstable. We can verify the Routh–Hurwitz result by directly computing the roots of the characteristic equation, as shown in Figure 6.18, using the `pole` function. Recall that the `pole` function computes the system poles.

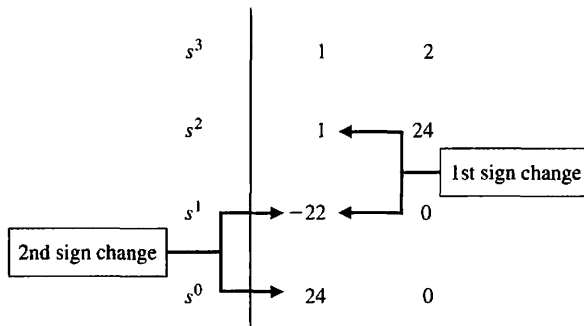
Whenever the characteristic equation is a function of a single parameter, the Routh–Hurwitz method can be utilized to determine the range of values that the

**FIGURE 6.16**

Closed-loop control system with  $T(s) = Y(s)/R(s) = 1/(s^3 + s^2 + 2s + 24)$ .

**FIGURE 6.17**

Routh array for the closed-loop control system with  $T(s) = Y(s)/R(s) = 1/(s^3 + s^2 + 2s + 24)$ .



parameter may take while maintaining stability. Consider the closed-loop feedback system in Figure 6.19. The characteristic equation is

$$q(s) = s^3 + 2s^2 + 4s + K = 0.$$

Using a Routh–Hurwitz approach, we find that we require  $0 < K < 8$  for stability (see Equation 6.12). We can verify this result graphically. As shown in Figure 6.20(b), we establish a vector of values for  $K$  at which we wish to compute the roots of the characteristic equation. Then using the roots function, we calculate and plot the roots of the characteristic equation, as shown in Figure 6.20(a). It can be seen that as  $K$  increases, the roots of the characteristic equation move toward the right half-plane as the gain tends toward  $K = 8$ , and eventually into the right half-plane when  $K > 8$ .

```

>>numg=[1]; deng=[1 1 2 23]; sysg=tf(numg,deng);
>>sys=feedback(sysg,[1]);
>>pole(sys)

ans =

-3.0000
1.0000 + 2.6458i
1.0000 - 2.6458i
    
```

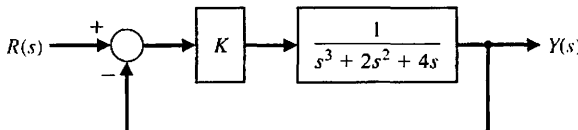
**Unstable poles**

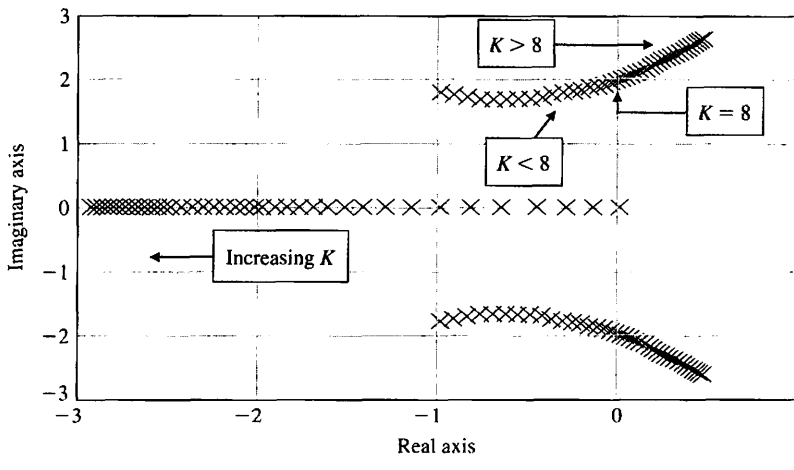
**FIGURE 6.18**

Using the pole function to compute the closed-loop control system poles of the system shown in Figure 6.16.

**FIGURE 6.19**

Closed-loop control system with  $T(s) = Y(s)/R(s) = K/(s^3 + 2s^2 + 4s + 4)$ .





(a)

```
% This script computes the roots of the characteristic
% equation q(s) = s^3 + 2 s^2 + 4 s + K for 0 < K < 20
%
K=[0:0.5:20];
for i=1:length(K)
    q=[1 2 4 K(i)];
    p(:,i)=roots(q);
end
plot(real(p),imag(p),'x'), grid
xlabel('Real axis'), ylabel('Imaginary axis')
```

Loop for roots as  
a function of K

(b)

**FIGURE 6.20**

(a) Plot of root locations of  $q(s) = s^3 + 2s^2 + 4s + K$  for  $0 \leq K \leq 20$ .  
(b) m-file script.

The script in Figure 6.20 contains the `for` function. This function provides a mechanism for repeatedly executing a series of statements a given number of times. The `for` function connected to an `end` statement sets up a repeating calculation loop. Figure 6.21 describes the `for` function format and provides an illustrative example of its usefulness. The example sets up a loop that repeats ten times. During the  $i$ th iteration, where  $1 \leq i \leq 10$ , the  $i$ th element of the vector  $\mathbf{a}$  is set equal to 20, and the scalar  $b$  is recomputed.

The Routh–Hurwitz method allows us to make definitive statements regarding absolute stability of a linear system. The method does not address the issue of relative stability, which is directly related to the location of the roots of the characteristic equation. Routh–Hurwitz tells us how many poles lie in the right half-plane, but not the specific location of the poles. With control design software, we can easily calculate the poles explicitly, thus allowing us to comment on the relative stability.

#### **EXAMPLE 6.12 Tracked vehicle control**

The block diagram of the control system for the two-track vehicle is shown in Figure 6.8. The design objective is to find  $a$  and  $K$  such that the system is stable and the steady-state error for a ramp input is less than or equal to 24% of the command.

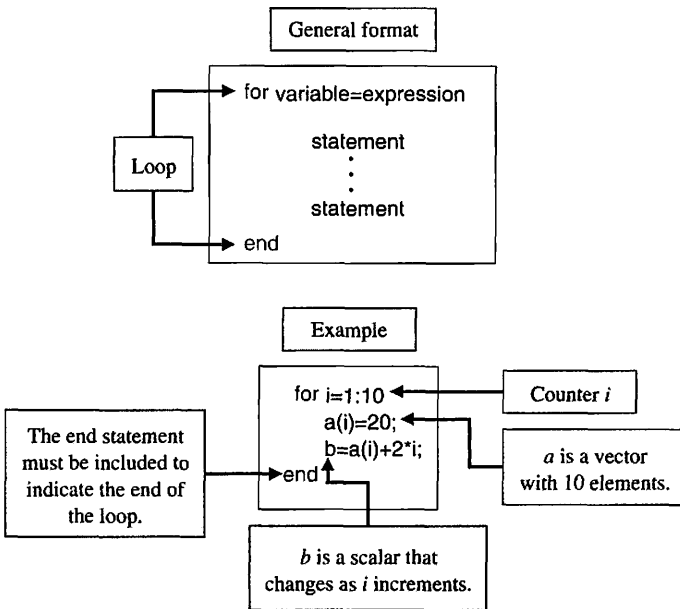


**FIGURE 6.21**  
The *for* function  
and an illustrative  
example.

We can use the Routh–Hurwitz method to aid in the search for appropriate values of  $a$  and  $K$ . The closed-loop characteristic equation is

$$q(s) = s^4 + 8s^3 + 17s^2 + (K + 10)s + aK = 0.$$

Using the Routh array, we find that, for stability, we require that

$$K < 126, \frac{126 - K}{8}(K + 10) - 8aK > 0, \text{ and } aK > 0.$$

For positive  $K$ , it follows that we can restrict our search to  $0 < K < 126$  and  $a > 0$ . Our approach will be to use the computer to help find a parameterized  $a$  versus  $K$  region in which stability is assured. Then we can find a set of  $(a, K)$  belonging to the stable region such that the steady-state error specification is met. This procedure, shown in Figure 6.22, involves selecting a range of values for  $a$  and  $K$  and computing the roots of the characteristic polynomial for specific values of  $a$  and  $K$ . For each value of  $K$ , we find the first value of  $a$  that results in at least one root of the characteristic equation in the right half-plane. The process is repeated until the entire selected range of  $a$  and  $K$  is exhausted. The plot of the  $(a, K)$  pairs defines the separation between the stable and unstable regions. The region to the left of the plot of  $a$  versus  $K$  in Figure 6.22 is the stable region.

If we assume that  $r(t) = At$ ,  $t > 0$ , then the steady-state error is

$$e_{ss} = \lim_{s \rightarrow 0} s \cdot \frac{s(s + 1)(s + 2)(s + 5)}{s(s + 1)(s + 2)(s + 5) + K(s + a)} \cdot \frac{A}{s^2} = \frac{10A}{aK},$$

where we have used the fact that

$$E(s) = \frac{1}{1 + G_c G(s)} R(s) = \frac{s(s + 1)(s + 2)(s + 5)}{s(s + 1)(s + 2)(s + 5) + K(s + a)} R(s).$$

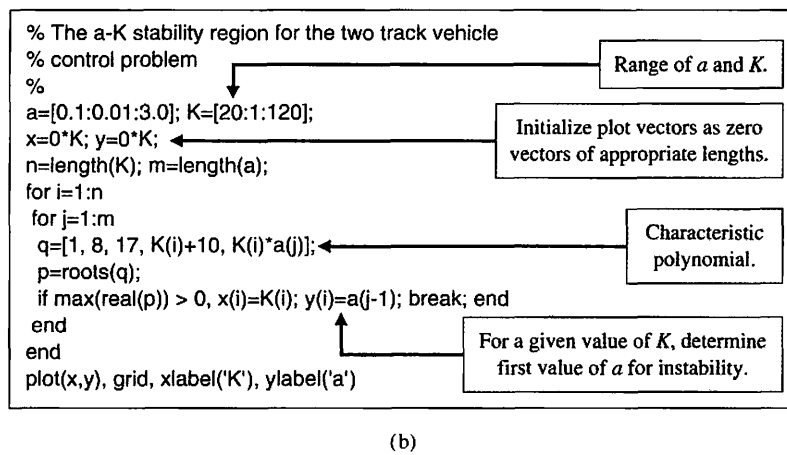
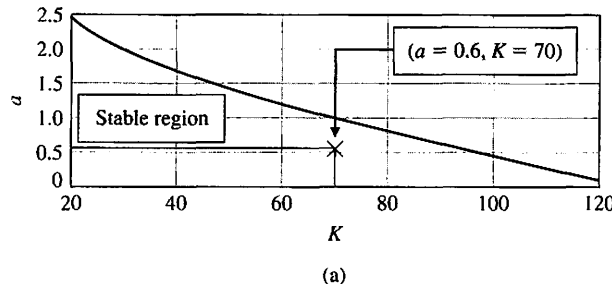


**FIGURE 6.22**  
(a) Stability region  
for  $a$  and  $K$  for two-track vehicle turning control. (b) m-file  
script.

Given the steady-state specification,  $e_{ss} < 0.24A$ , we find that the specification is satisfied when

$$\frac{10A}{aK} < 0.24A,$$

or

$$aK > 41.67. \quad (6.34)$$

Any values of  $a$  and  $K$  that lie in the stable region in Figure 6.22 and satisfy Equation (6.34) will lead to an acceptable design. For example,  $K = 70$  and  $a = 0.6$  will satisfy all the design requirements. The closed-loop transfer function (with  $a = 0.6$  and  $K = 70$ ) is

$$T(s) = \frac{70s + 42}{s^4 + 8s^3 + 17s^2 + 80s + 42}.$$

The associated closed-loop poles are

$$s = -7.0767,$$

$$s = -0.5781,$$

$$s = -0.1726 + 3.1995i, \text{ and}$$

$$s = -0.1726 - 3.1995i.$$

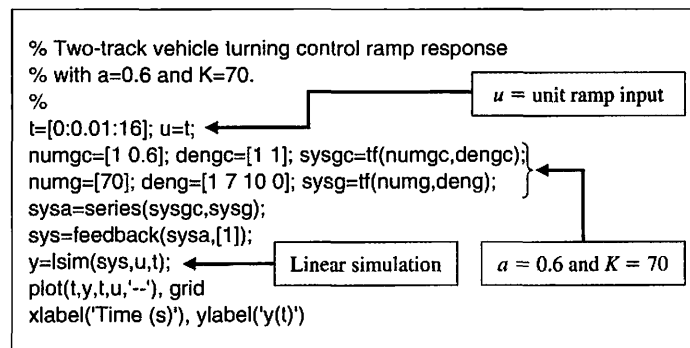
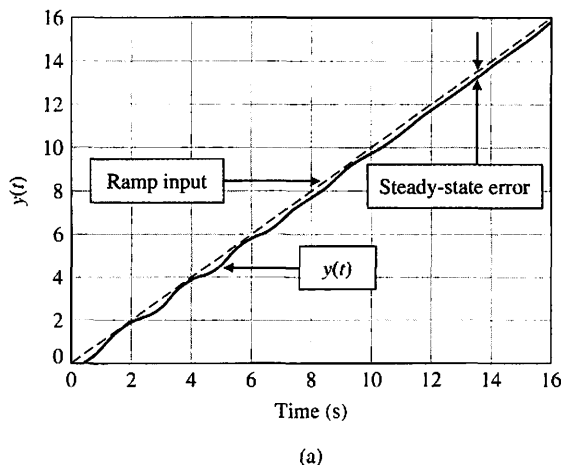


**FIGURE 6.23**  
 (a) Ramp response  
 for  $a = 0.6$  and  
 $K = 70$  for two-  
track vehicle  
turning control.  
(b) m-file script.

The corresponding unit ramp input response is shown in Figure 6.23. The steady-state error is less than 0.24, as desired. ■

**The Stability of State Variable Systems.** Now let us turn to determining the stability of systems described in state variable form. Suppose we have a system in state-space form as in Equation (6.22). The stability of the system can be evaluated with the characteristic equation associated with the system matrix  $\mathbf{A}$ . The characteristic equation is

$$\det(s\mathbf{I} - \mathbf{A}) = 0. \quad (6.35)$$

The left-hand side of the characteristic equation is a polynomial in  $s$ . If all of the roots of the characteristic equation have negative real parts (i.e.,  $\operatorname{Re}(s_i) < 0$ ), then the system is stable.

When the system model is given in state variable form, we must calculate the characteristic polynomial associated with the  $\mathbf{A}$  matrix. In this regard, we have several options. We can calculate the characteristic equation directly from Equation (6.35) by manually computing the determinant of  $s\mathbf{I} - \mathbf{A}$ . Then, we can compute the roots using the `roots` function to check for stability, or alternatively, we can use

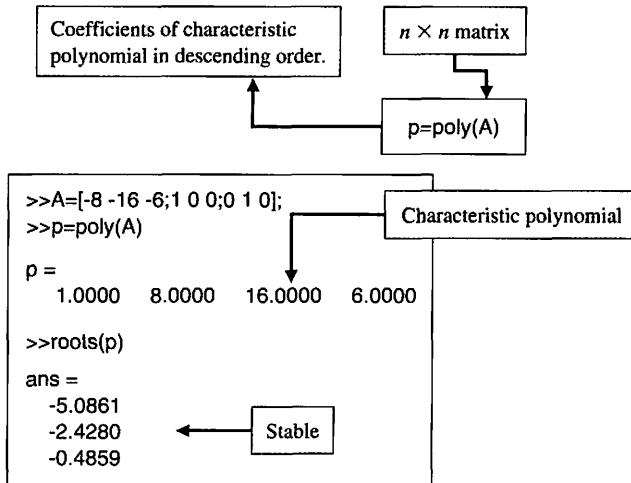


**FIGURE 6.24**  
 Computing the characteristic polynomial of  $\mathbf{A}$  with the **poly** function.

the Routh–Hurwitz method to detect any unstable roots. Unfortunately, the manual computations can become lengthy, especially if the dimension of  $\mathbf{A}$  is large. We would like to avoid this manual computation if possible. As it turns out, the computer can assist in this endeavor.

The **poly** function described in Section 2.9 can be used to compute the characteristic equation associated with  $\mathbf{A}$ . Recall that **poly** is used to form a polynomial from a vector of roots. It can also be used to compute the characteristic equation of  $\mathbf{A}$ , as illustrated in Figure 6.24. The input matrix  $\mathbf{A}$  is

$$\mathbf{A} = \begin{bmatrix} -8 & -16 & -6 \\ 1 & 0 & 0 \\ 0 & 1 & 0 \end{bmatrix},$$

and the associated characteristic polynomial is

$$s^3 + 8s^2 + 16s + 6 = 0.$$

If  $\mathbf{A}$  is an  $n \times n$  matrix,  $\text{poly}(\mathbf{A})$  is an  $n + 1$  element row vector whose elements are the coefficients of the characteristic equation  $\det(s\mathbf{I} - \mathbf{A}) = 0$ .

#### EXAMPLE 6.13 Stability region for an unstable process

A jump-jet aircraft has a control system as shown in Figure 6.25 [16]. Assume that  $z > 0$  and  $p > 0$ . The system is open-loop unstable (without feedback), since the characteristic equation of the process and controller is

$$s(s - 1)(s + p) = s[s^2 + (p - 1)s - p] = 0.$$

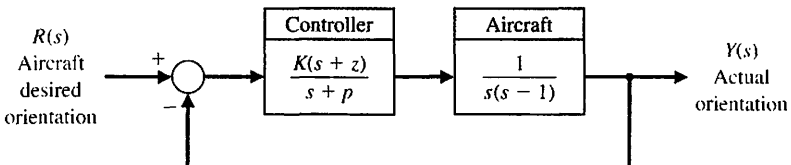


**FIGURE 6.25**  
 Control system for jump-jet aircraft.  
 Assume that  $z > 0$  and  $p > 0$ .

Note that since one term within the bracket has a negative coefficient, the characteristic equation has at least one root in the right-hand  $s$ -plane. The characteristic equation of the closed-loop system is

$$s^3 + (p - 1)s^2 + (K - p)s + Kz = 0.$$

The goal is to determine the region of stability for  $K$ ,  $p$ , and  $z$ . The Routh array is

$$\begin{array}{c|cc} s^3 & 1 & K - p \\ s^2 & p - 1 & Kz \\ s^1 & b_2 \\ s^0 & Kz \end{array},$$

where

$$b_2 = \frac{(p - 1)(K - p) - Kz}{p - 1}.$$

From the Routh–Hurwitz criterion, we find that we require  $Kz > 0$  and  $p > 1$ . Setting  $b_2 > 0$ , we have

$$(p - 1)(K - p) - Kz = K[(p - 1) - z] - p(p - 1) > 0.$$

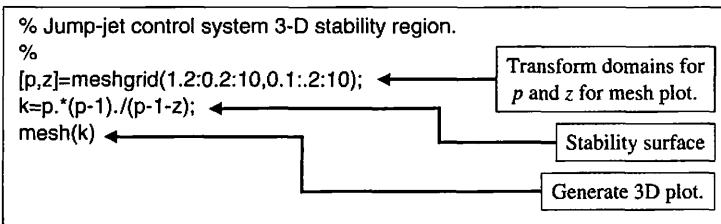
Consider two cases:

1.  $z \geq p - 1$ : there is no  $0 < K < \infty$  that leads to stability.
2.  $z < p - 1$ : any  $0 < K < \infty$  satisfying the stability condition for a given  $p$  and  $z$  will result in stability:

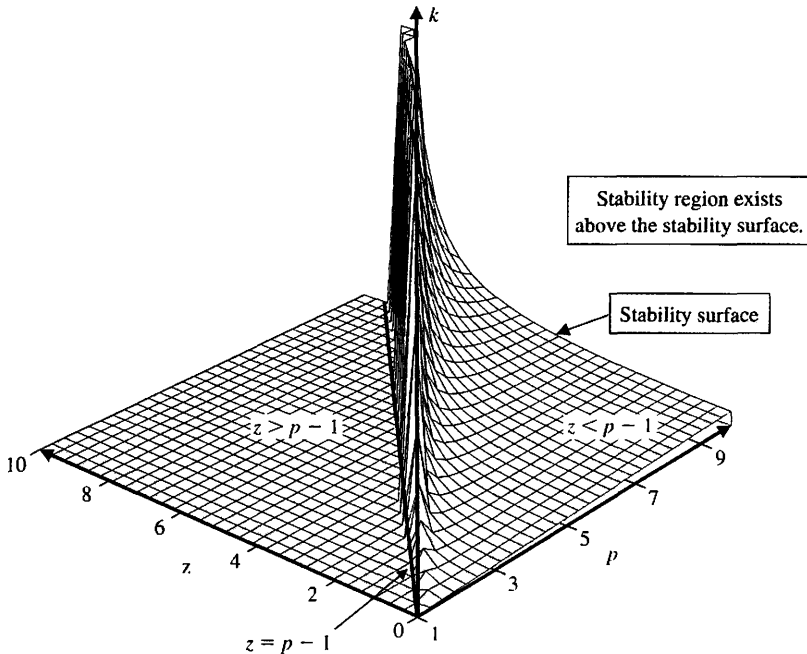
$$K > \frac{p(p - 1)}{(p - 1) - z}. \quad (6.36)$$

The stability conditions can be depicted graphically. The m-file script used to generate a three-dimensional stability surface is shown in Figure 6.26. This script uses `mesh` to create the three-dimensional surface and `meshgrid` to generate arrays for use with the mesh surface.

The three-dimensional plot of the stability region for  $K$ ,  $p$ , and  $z$  is shown in Figure 6.27. One acceptable stability point is  $z = 1$ ,  $p = 10$ , and  $K = 15$ . ■



**FIGURE 6.26**  
m-file script for stability region.

**FIGURE 6.27**

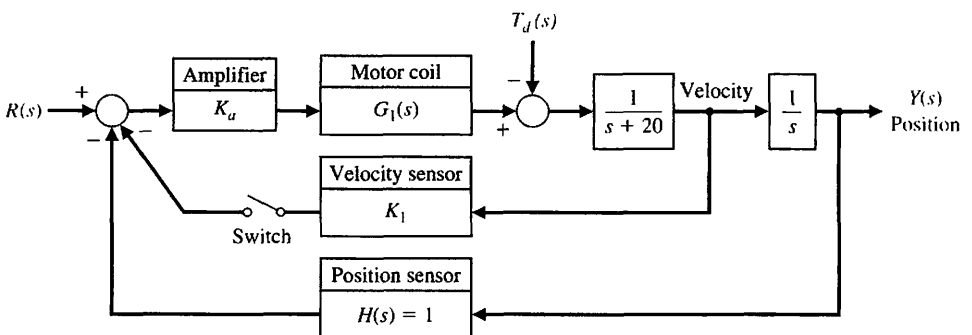
The three-dimensional region of stability lies above the surface shown.

## 6.7 SEQUENTIAL DESIGN EXAMPLE: DISK DRIVE READ SYSTEM



In Section 5.11, we examined the design of the head reader system with an adjustable gain  $K_a$ . In this section, we will examine the stability of the system as  $K_a$  is adjusted and then reconfigure the system.

Let us consider the system as shown in Figure 6.28. This is the same system with a model of the motor and load as considered in Chapter 5, except that the velocity

**FIGURE 6.28**

The closed-loop disk drive head system with an optional velocity feedback.

feedback sensor was added, as shown in Figure 6.28. Initially, we consider the case where the switch is open. Then the closed-loop transfer function is

$$\frac{Y(s)}{R(s)} = \frac{K_a G_1(s) G_2(s)}{1 + K_a G_1(s) G_2(s)}, \quad (6.37)$$

where

$$G_1(s) = \frac{5000}{s + 1000}$$

and

$$G_2(s) = \frac{1}{s(s + 20)}.$$

The characteristic equation is

$$s(s + 20)(s + 1000) + 5000K_a = 0, \quad (6.38)$$

or

$$s^3 + 1020s^2 + 20000s + 5000K_a = 0.$$

We use the Routh array

$$\begin{array}{c|cc} s^3 & 1 & 20000 \\ s^2 & 1020 & 5000K_a \\ s^1 & b_1 \\ s^0 & 5000K_a \end{array},$$

where

$$b_1 = \frac{(20000)1020 - 5000K_a}{1020}.$$

The case  $b_1 = 0$  results in marginal stability when  $K_a = 4080$ . Using the auxiliary equation, we have

$$1020s^2 + 5000(4080) = 0,$$

or the roots of the  $j\omega$ -axis are  $s = \pm j141.4$ . In order for the system to be stable,  $K_a < 4080$ .

Now let us add the velocity feedback by closing the switch in the system of Figure 6.28. The closed-loop transfer function for the system is then

$$\frac{Y(s)}{R(s)} = \frac{K_a G_1(s) G_2(s)}{1 + [K_a G_1(s) G_2(s)](1 + K_1 s)}, \quad (6.39)$$

since the feedback factor is equal to  $1 + K_1 s$ , as shown in Figure 6.29.

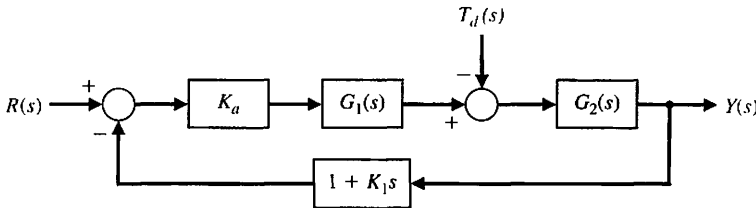


**FIGURE 6.29**  
Equivalent system with the velocity feedback switch closed.

The characteristic equation is then

$$1 + [K_a G_1(s) G_2(s)](1 + K_1 s) = 0,$$

or

$$s(s + 20)(s + 1000) + 5000K_a(1 + K_1 s) = 0.$$

Therefore, we have

$$s^3 + 1020s^2 + [20000 + 5000K_aK_1]s + 5000K_a = 0.$$

Then the Routh array is

$$\begin{array}{c|cc} s^3 & 1 & 20000 + 5000K_aK_1 \\ s^2 & 1020 & 5000K_a \\ s^1 & b_1 & \\ s^0 & 5000K_a & \end{array},$$

where

$$b_1 = \frac{1020(20000 + 5000K_aK_1) - 5000K_a}{1020}.$$

To guarantee stability, it is necessary to select the pair  $(K_a, K_1)$  such that  $b_1 > 0$ , where  $K_a > 0$ . When  $K_1 = 0.05$  and  $K_a = 100$ , we can determine the system response using the script shown in Figure 6.30. The settling time (with a 2% criterion) is approximately 260 ms, and the percent overshoot is zero. The system performance is summarized in Table 6.3. The performance specifications are nearly satisfied, and some iteration of  $K_1$  is necessary to obtain the desired 250 ms settling time.

**Table 6.3 Performance of the Disk Drive System Compared to the Specifications**

Performance Measure	Desired Value	Actual Response
Percent overshoot	Less than 5%	0%
Settling time	Less than 250 ms	260 ms
Maximum response to a unit disturbance	Less than $5 \times 10^{-3}$	$2 \times 10^{-3}$

```

Ka=100; K1=0.05; ←
ng1=[5000]; dg1=[1 1000]; sys1=tf(ng1,dg1);
ng2=[1]; dg2=[1 20 0]; sys2=tf(ng2,dg2);
nc=[K1 1]; dc=[0 1]; sysc=tf(nc,dc);
syso=series(Ka*sys1,sys2);
sys=feedback(syso,sysc); sys=minreal(sys);
t=[0:0.001:0.5];
y=step(sys,t); plot(t,y)
ylabel('y(t)'), xlabel('Time (s)'), grid

```

Select the velocity feedback gain  $K_1$  and amplifier gain  $K_a$ .

(a)

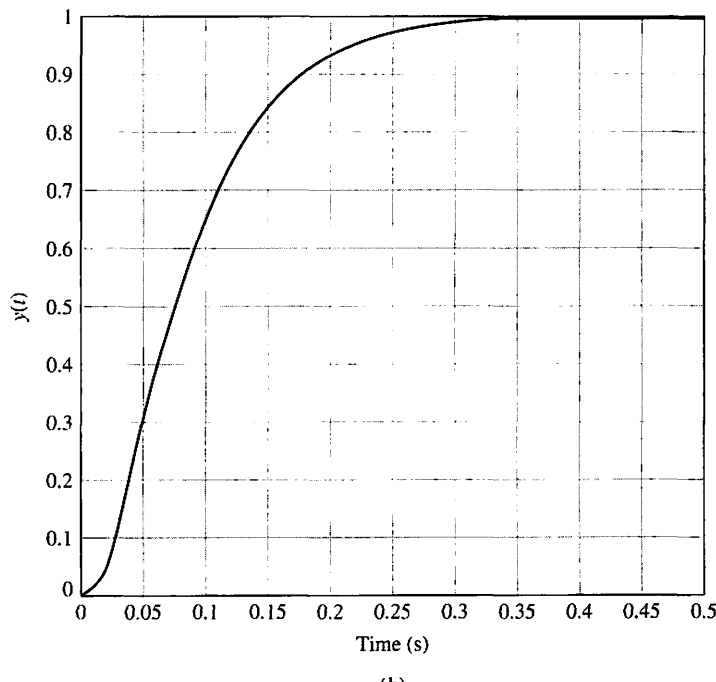


**FIGURE 6.30**  
Response of the system with velocity feedback.  
(a) m-file script.  
(b) Response with  $K_a = 100$  and  $K_1 = 0.05$ .

## 6.8 SUMMARY

In this chapter, we have considered the concept of the stability of a feedback control system. A definition of a stable system in terms of a bounded system response was outlined and related to the location of the poles of the system transfer function in the  $s$ -plane.

The Routh–Hurwitz stability criterion was introduced, and several examples were considered. The relative stability of a feedback control system was also considered in terms of the location of the poles and zeros of the system transfer function in the  $s$ -plane. The stability of state variable systems was considered.



## SKILLS CHECK

In this section, we provide three sets of problems to test your knowledge: True or False, Multiple Choice, and Word Match. To obtain direct feedback, check your answers with the answer key provided at the conclusion of the end-of-chapter problems. Use the block diagram in Figure 6.31 as specified in the various problem statements.

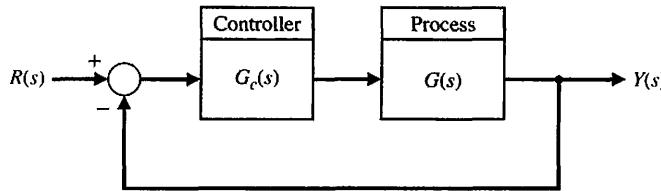


**FIGURE 6.31** Block diagram for the Skills Check.

In the following **True or False** and **Multiple Choice** problems, circle the correct answer.

- |   |               |
|---|---------------|
| 1. A stable system is a dynamic system with a bounded output response for any input.                                    | True or False |
| 2. A marginally stable system has poles on the $j\omega$ -axis.   | True or False |
| 3. A system is stable if all poles lie in the right half-plane.   | True or False |
| 4. The Routh-Hurwitz criterion is a necessary and sufficient criterion for determining the stability of linear systems. | True or False |
| 5. Relative stability characterizes the degree of stability.  | True or False |
| 6. A system has the characteristic equation   | True or False |

$$q(s) = s^3 + 4Ks^2 + (5 + K)s + 10 = 0.$$

The range of  $K$  for a stable system is:

- a.  $K > 0.46$
  - b.  $K < 0.46$
  - c.  $0 < K < 0.46$
  - d. Unstable for all  $K$
7. Utilizing the Routh-Hurwitz criterion, determine whether the following polynomials are stable or unstable:

$$p_1(s) = s^2 + 10s + 5 = 0,$$

$$p_2(s) = s^4 + s^3 + 5s^2 + 20s + 10 = 0.$$

- a.  $p_1(s)$  is stable,  $p_2(s)$  is stable
  - b.  $p_1(s)$  is unstable,  $p_2(s)$  is stable
  - c.  $p_1(s)$  is stable,  $p_2(s)$  is unstable
  - d.  $p_1(s)$  is unstable,  $p_2(s)$  is unstable
8. Consider the feedback control system block diagram in Figure 6.31. Investigate closed-loop stability for  $G_c(s) = K(s + 1)$  and  $G(s) = \frac{1}{(s + 2)(s - 1)}$ , for the two cases where  $K = 1$  and  $K = 3$ .
- a. Unstable for  $K = 1$  and stable for  $K = 3$

- b. Unstable for  $K = 1$  and unstable for  $K = 3$   
 c. Stable for  $K = 1$  and unstable for  $K = 3$   
 d. Stable for  $K = 1$  and stable for  $K = 3$
9. Consider a unity negative feedback system in Figure 6.31 with loop transfer function where

$$L(s) = G_c(s)G(s) = \frac{K}{(1 + 0.5s)(1 + 0.5s + 0.25s^2)}.$$

Determine the value of  $K$  for which the closed-loop system is marginally stable.

- a.  $K = 10$   
 b.  $K = 3$   
 c. The system is unstable for all  $K$   
 d. The system is stable for all  $K$

10. A system is represented by  $\dot{\mathbf{x}} = \mathbf{Ax}$ , where

$$\mathbf{A} = \begin{bmatrix} 0 & 1 & 0 \\ 0 & 0 & 1 \\ -5 & -K & 10 \end{bmatrix}.$$

The values of  $K$  for a stable system are

- a.  $K < 1/2$   
 b.  $K > 1/2$   
 c.  $K = 1/2$   
 d. The system is stable for all  $K$

11. Use the Routh array to assist in computing the roots of the polynomial

$$q(s) = 2s^3 + 2s^2 + s + 1 = 0.$$

- a.  $s_1 = -1; s_{2,3} = \pm \frac{\sqrt{2}}{2}j$   
 b.  $s_1 = 1; s_{2,3} = \pm \frac{\sqrt{2}}{2}j$   
 c.  $s_1 = -1; s_{2,3} = 1 \pm \frac{\sqrt{2}}{2}j$   
 d.  $s_1 = -1; s_{2,3} = 1$

12. Consider the following unity feedback control system in Figure 6.31 where

$$G(s) = \frac{1}{(s - 2)(s^2 + 10s + 45)} \text{ and } G_c(s) = \frac{K(s + 0.3)}{s}.$$

The range of  $K$  for stability is

- a.  $K < 260.68$   
 b.  $50.06 < K < 123.98$   
 c.  $100.12 < K < 260.68$   
 d. The system is unstable for all  $K > 0$

In Problems 13 and 14, consider the system represented in a state-space form

$$\dot{\mathbf{x}} = \begin{bmatrix} 0 & 1 & 0 \\ 0 & 0 & 1 \\ -5 & -10 & -5 \end{bmatrix} \mathbf{x} + \begin{bmatrix} 0 \\ 0 \\ 20 \end{bmatrix} u$$

$$y = [1 \ 0 \ 1] \mathbf{x}.$$

13. The characteristic equation is:
- $q(s) = s^3 + 5s^2 - 10s - 6$
  - $q(s) = s^3 + 5s^2 + 10s + 5$
  - $q(s) = s^3 - 5s^2 + 10s - 5$
  - $q(s) = s^2 - 5s + 10$
14. Using the Routh-Hurwitz criterion, determine whether the system is stable, unstable, or marginally stable.
- Stable
  - Unstable
  - Marginally stable
  - None of the above
15. A system has the block diagram representation as shown in Figure 6.31, where  $G(s) = \frac{10}{(s + 15)^2}$  and  $G_c(s) = \frac{K}{s + 80}$ , where  $K$  is always positive. The limiting gain for a stable system is:
- $0 < K < 28875$
  - $0 < K < 27075$
  - $0 < K < 25050$
  - Stable for all  $K > 0$

In the following **Word Match** problems, match the term with the definition by writing the correct letter in the space provided.

a. Routh-Hurwitz criterion	A performance measure of a system.	_____
b. Auxiliary polynomial	A dynamic system with a bounded system response to a bounded input.	_____
c. Marginally stable	The property that is measured by the relative real part of each root or pair of roots of the characteristic equation.	_____
d. Stable system	A criterion for determining the stability of a system by examining the characteristic equation of the transfer function.	_____
e. Stability	The equation that immediately precedes the zero entry in the Routh array.	_____
f. Relative stability	A system description that reveals whether a system is stable or not stable without consideration of other system attributes such as degree of stability.	_____
g. Absolute stability	A system possesses this type of stability if the zero input response remains bounded as $t \rightarrow \infty$ .	_____

## EXERCISES

**E6.1** A system has a characteristic equation  $s^3 + Ks^2 + (1 + K)s + 6 = 0$ . Determine the range of  $K$  for a stable system.

*Answer:*  $K > 2$

**E6.2** A system has a characteristic equation  $s^3 + 10s^2 + 2s + 30 = 0$ . Using the Routh-Hurwitz criterion, show that the system is unstable.

**E6.3** A system has the characteristic equation  $s^4 + 10s^3 + 32s^2 + 37s + 20 = 0$ . Using the Routh-Hurwitz criterion, determine if the system is stable.

**E6.4** A control system has the structure shown in Figure E6.4. Determine the gain at which the system will become unstable.

*Answer:*  $K = 20/7$

**E6.5** A unity feedback system has a loop transfer function

$$L(s) = \frac{K}{(s+1)(s+3)(s+6)},$$

where  $K = 20$ . Find the roots of the closed-loop system's characteristic equation.

**E6.6** For the feedback system of Exercise E6.5, find the value of  $K$  when two roots lie on the imaginary axis. Determine the value of the three roots.

*Answer:*  $s = -10, \pm j5.2$

**E6.7** A negative feedback system has a loop transfer function

$$L(s) = \frac{K(s+2)}{s(s-1)}.$$

(a) Find the value of the gain when the  $\zeta$  of the closed-loop roots is equal to 0.707. (b) Find the value of the gain when the closed-loop system has two roots on the imaginary axis.

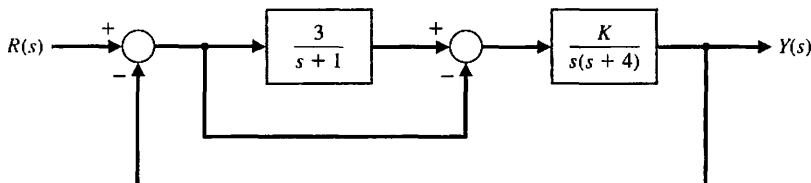


**FIGURE E6.4**  
Feedforward system.

**E6.8** Designers have developed small, fast, vertical-take-off fighter aircraft that are invisible to radar (stealth aircraft). This aircraft concept uses quickly turning jet nozzles to steer the airplane [16]. The control system for the heading or direction control is shown in Figure E6.8. Determine the maximum gain of the system for stable operation.

**E6.9** A system has a characteristic equation

$$s^3 + 2s^2 + (K + 1)s + 8 = 0.$$

Find the range of  $K$  for a stable system.

*Answer:*  $K > 3$

**E6.10** We all use our eyes and ears to achieve balance. Our orientation system allows us to sit or stand in a desired position even while in motion. This orientation system is primarily run by the information received in the inner ear, where the semicircular canals sense angular acceleration and the otoliths measure linear acceleration. But these acceleration measurements need to be supplemented by visual signals. Try the following experiment: (a) Stand with one foot in front of another, with your hands resting on your hips and your elbows bowed outward. (b) Close your eyes. Did you experience a low-frequency oscillation that grew until you lost balance? Is this orientation position stable with and without the use of your eyes?

**E6.11** A system with a transfer function  $Y(s)/R(s)$  is

$$\frac{Y(s)}{R(s)} = \frac{24(s+1)}{s^4 + 6s^3 + 2s^2 + s + 3}.$$

Determine the steady-state error to a unit step input. Is the system stable?

**E6.12** A system has the second-order characteristic equation

$$s^2 + as + b = 0,$$

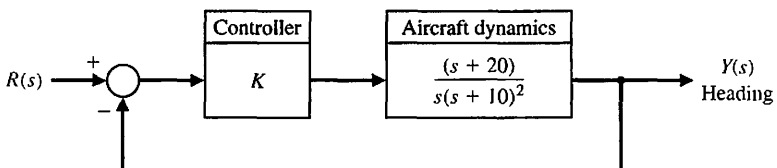
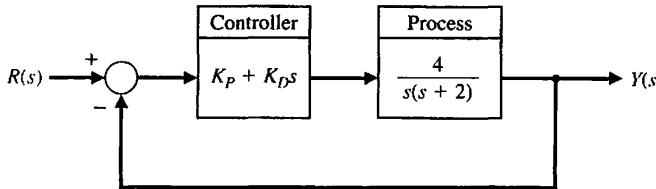


**FIGURE E6.8**  
Aircraft heading control.

**FIGURE E6.13**

Closed-loop system with a proportional plus derivative controller  
 $G_c(s) = K_P + K_Ds$ .



where  $a$  and  $b$  are constant parameters. Determine the necessary and sufficient conditions for the system to be stable. Is it possible to determine stability of a second-order system just by inspecting the coefficients of the characteristic equation?

**E6.13.** Consider the feedback system in Figure E6.13. Determine the range of  $K_P$  and  $K_D$  for stability of the closed-loop system.

**E6.14** By using magnetic bearings, a rotor is supported contactless. The technique of contactless support for rotors becomes more important in light and heavy industrial applications [14]. The matrix differential equation for a magnetic bearing system is

$$\dot{\mathbf{x}} = \begin{bmatrix} 0 & 1 & 0 \\ -3 & -1 & 0 \\ -2 & -1 & -2 \end{bmatrix} \mathbf{x},$$

where  $\mathbf{x}^T = [y, dy/dt, i]$ ,  $y$  = bearing gap, and  $i$  is the electromagnetic current. Determine whether the system is stable.

**Answer:** The system is stable.

**E6.15** A system has a characteristic equation

$$\begin{aligned} q(s) = s^6 + 9s^5 + 31.25s^4 + 61.25s^3 \\ + 67.75s^2 + 14.75s + 15 = 0. \end{aligned}$$

(a) Determine whether the system is stable, using the Routh-Hurwitz criterion. (b) Determine the roots of the characteristic equation.

**Answer:** (a) The system is marginally stable.  
(b)  $s = -3, -4, -1 \pm 2j, \pm 0.5j$

**E6.16** A system has a characteristic equation

$$q(s) = s^4 + 9s^3 + 45s^2 + 87s + 50 = 0.$$

(a) Determine whether the system is stable, using the Routh-Hurwitz criterion. (b) Determine the roots of the characteristic equation.

**E6.17** The matrix differential equation of a state variable model of a system has

$$\mathbf{A} = \begin{bmatrix} 0 & 1 & -1 \\ -8 & -12 & 8 \\ -8 & -12 & 5 \end{bmatrix}.$$

- (a) Determine the characteristic equation. (b) Determine whether the system is stable. (c) Determine the roots of the characteristic equation.

**Answer:** (a)  $q(s) = s^3 + 7s^2 + 36s + 24 = 0$

**E6.18** A system has a characteristic equation

$$q(s) = s^3 + 20s^2 + 5s + 100 = 0.$$

- (a) Determine whether the system is stable, using the Routh-Hurwitz criterion. (b) Determine the roots of the characteristic equation.

**E6.19** Determine whether the systems with the following characteristic equations are stable or unstable:

- (a)  $s^3 + 4s^2 + 6s + 100 = 0$ ,  
(b)  $s^4 + 6s^3 + 10s^2 + 17s + 6 = 0$ , and  
(c)  $s^2 + 6s + 3 = 0$ .

**E6.20** Find the roots of the following polynomials:

- (a)  $s^3 + 5s^2 + 8s + 4 = 0$  and  
(b)  $s^3 + 9s^2 + 27s + 27 = 0$ .

**E6.21** A system has the characteristic equation

$$q(s) = s^3 + 10s^2 + 29s + K = 0.$$

Shift the vertical axis to the right by 2 by using  $s = s_n - 2$ , and determine the value of gain  $K$  so that the complex roots are  $s = -2 \pm j$ .

**E6.22** A system has a transfer function  $Y(s)/R(s) = T(s) = 1/s$ . (a) Is this system stable? (b) If  $r(t)$  is a unit step input, determine the response  $y(t)$ .

**E6.23** A system is represented by Equation (6.22) where

$$\mathbf{A} = \begin{bmatrix} 0 & 1 & 0 \\ 0 & 0 & 1 \\ -8 & -k & -4 \end{bmatrix}.$$

Find the range of  $k$  where the system is stable.

**E6.24** Consider the system represented in state variable form

$$\dot{\mathbf{x}} = \mathbf{Ax} + \mathbf{Bu}$$

$$\mathbf{y} = \mathbf{Cx} + \mathbf{Du},$$

where

$$\mathbf{A} = \begin{bmatrix} 0 & 1 & 0 \\ 0 & 0 & 1 \\ -k & -k & -k \end{bmatrix}, \mathbf{B} = \begin{bmatrix} 0 \\ 0 \\ 1 \end{bmatrix}$$

$$\mathbf{C} = [1 \ 0 \ 0], \mathbf{D} = [0].$$

- (a) What is the system transfer function? (b) For what values of  $K$  is the system stable?

**E6.25** A closed-loop feedback system is shown in Figure E6.25. For what range of values of the parameters  $K$  and  $p$  is the system stable?

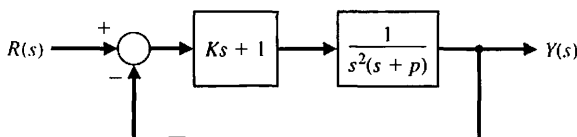
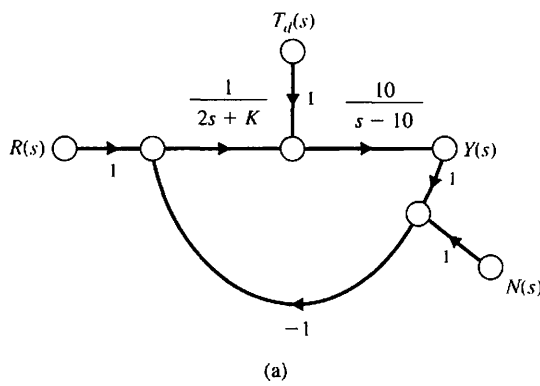


**FIGURE E6.25** Closed-loop system with parameters  $K$  and  $p$ .

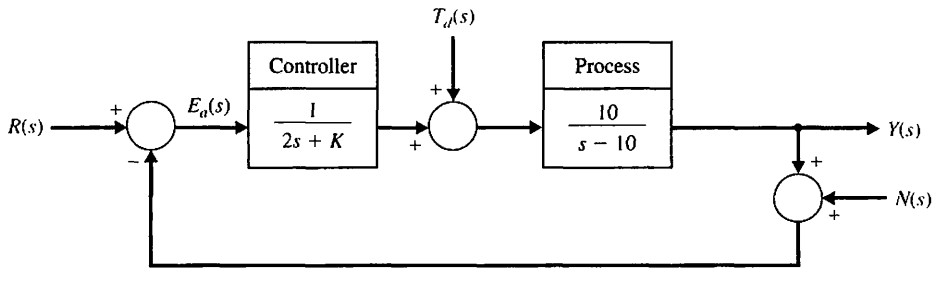
- E6.26** Consider the closed-loop system in Figure E6.26, where

$$G(s) = \frac{10}{s - 10} \quad \text{and} \quad G_c(s) = \frac{1}{2s + K}.$$

- (a) Determine the characteristic equation associated with the closed-loop system.  
 (b) Determine the values of  $K$  for which the closed-loop system is stable.



(a)



(b)

**FIGURE E6.26**  
Closed-loop  
feedback control  
system with  
parameter  $K$ .

## PROBLEMS

**P6.1** Utilizing the Routh-Hurwitz criterion, determine the stability of the following polynomials:

- (a)  $s^2 + 5s + 2$
- (b)  $s^3 + 4s^2 + 8s + 4$
- (c)  $s^3 + 2s^2 - 6s + 20$
- (d)  $s^4 + s^3 + 2s^2 + 12s + 10$

(e)  $s^4 + s^3 + 3s^2 + 2s + K$

(f)  $s^5 + s^4 + 2s^3 + s + 6$

(g)  $s^5 + s^4 + 2s^3 + s^2 + s + K$

Determine the number of roots, if any, in the right-hand plane. If it is adjustable, determine the range of  $K$  that results in a stable system.

**P6.2** An antenna control system was analyzed in Problem P4.5, and it was determined that, to reduce the effect of wind disturbances, the gain of the magnetic amplifier,  $k_a$ , should be as large as possible. (a) Determine the limiting value of gain for maintaining a stable system. (b) We want to have a system settling time equal to 1.5 seconds. Using a shifted axis and the Routh–Hurwitz criterion, determine the value of the gain that satisfies this requirement. Assume that the complex roots of the closed-loop system dominate the transient response. (Is this a valid approximation in this case?)

**P6.3** Arc welding is one of the most important areas of application for industrial robots [11]. In most manufacturing welding situations, uncertainties in dimensions of the part, geometry of the joint, and the welding process itself require the use of sensors for maintaining weld quality. Several systems use a vision system to measure the geometry of the puddle of melted metal, as shown in Figure P6.3. This system uses a constant rate of feeding the wire to be melted. (a) Calculate the maximum value for  $K$  for the system that will result in a stable system. (b) For half of the maximum value of  $K$  found in part (a), determine the roots of the characteristic equation. (c) Estimate the overshoot of the system of part (b) when it is subjected to a step input.

**P6.4** A feedback control system is shown in Figure P6.4. The controller and process transfer functions are given by

$$G_c(s) = K \text{ and } G(s) = \frac{s + 40}{s(s + 10)}$$

and the feedback transfer function is  $H(s) = 1/(s + 20)$ .

(a) Determine the limiting value of gain  $K$  for a stable system. (b) For the gain that results in marginal stability, determine the magnitude of the imaginary roots. (c) Reduce the gain to half the magnitude of the marginal value and determine the relative stability of the system (1) by shifting the axis and using the Routh–Hurwitz criterion and (2) by determining the root locations. Show the roots are between  $-1$  and  $-2$ .

**P6.5** Determine the relative stability of the systems with the following characteristic equations (1) by shifting the axis in the  $s$ -plane and using the Routh–Hurwitz criterion, and (2) by determining the location of the complex roots in the  $s$ -plane:

$$(a) s^3 + 3s^2 + 4s + 2 = 0.$$

$$(b) s^4 + 9s^3 + 30s^2 + 42s + 20 = 0.$$

$$(c) s^3 + 19s^2 + 110s + 200 = 0.$$

**P6.6** A unity-feedback control system is shown in Figure P6.6. Determine the relative stability of the

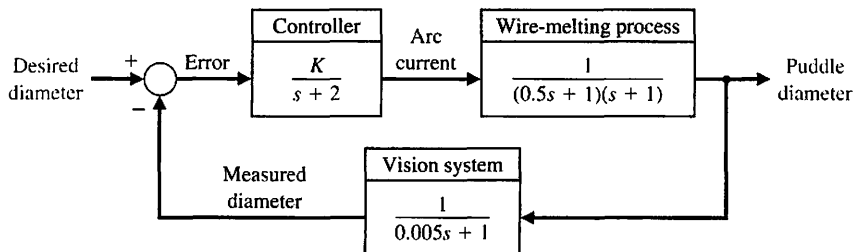


**FIGURE P6.3**  
Welder control.

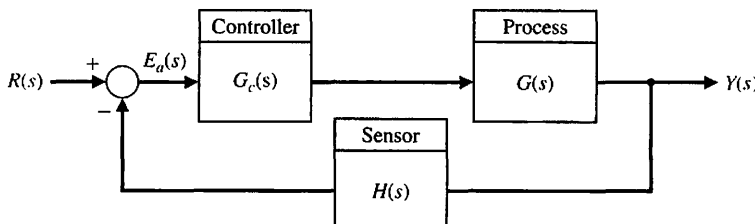


**FIGURE P6.4**  
Nonunity feedback system.

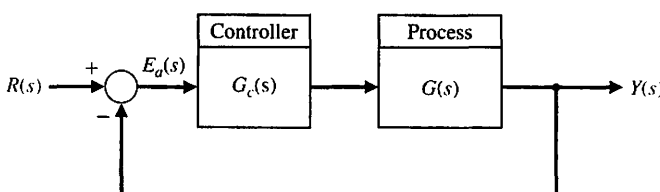


**FIGURE P6.6**  
Unity feedback system.

system with the following transfer functions by locating the complex roots in the  $s$ -plane:

$$(a) G_c(s)G(s) = \frac{10s + 2}{s^2(s + 1)}$$

$$(b) G_c(s)G(s) = \frac{24}{s(s^3 + 10s^2 + 35s + 50)}$$

$$(c) G_c(s)G(s) = \frac{(s + 2)(s + 3)}{s(s + 4)(s + 6)}$$

**P6.7** The linear model of a phase detector (phase-lock loop) can be represented by Figure P6.7 [9]. The phase-lock systems are designed to maintain zero difference in phase between the input carrier signal and a local voltage-controlled oscillator. Phase-lock loops find application in color television, missile tracking, and space telemetry. The filter for a particular application is chosen as

$$F(s) = \frac{10(s + 10)}{(s + 1)(s + 100)}.$$

We want to minimize the steady-state error of the system for a ramp change in the phase information signal. (a) Determine the limiting value of the gain  $K_aK = K_v$  in order to maintain a stable system. (b) A steady-state error equal to  $1^\circ$  is acceptable for a

ramp signal of  $100 \text{ rad/s}$ . For that value of gain  $K_v$ , determine the location of the roots of the system.

**P6.8** A very interesting and useful velocity control system has been designed for a wheelchair control system. We want to enable people paralyzed from the neck down to drive themselves in motorized wheelchairs. A proposed system utilizing velocity sensors mounted in a headgear is shown in Figure P6.8. The headgear sensor provides an output proportional to the magnitude of the head movement. There is a sensor mounted at  $90^\circ$  intervals so that forward, left, right, or reverse can be commanded. Typical values for the time constants are  $\tau_1 = 0.5 \text{ s}$ ,  $\tau_3 = 1 \text{ s}$ , and  $\tau_4 = \frac{1}{4} \text{ s}$ .

- (a) Determine the limiting gain  $K = K_1K_2K_3$  for a stable system.
- (b) When the gain  $K$  is set equal to one-third of the limiting value, determine whether the settling time (to within  $2\%$  of the final value of the system) is less than  $4 \text{ s}$ .
- (c) Determine the value of gain that results in a system with a settling time of  $4 \text{ s}$ . Also, obtain the value of the roots of the characteristic equation when the settling time is equal to  $4 \text{ s}$ .

**P6.9** A cassette tape storage device has been designed for mass-storage [1]. It is necessary to control the velocity of the tape accurately. The speed control of the tape drive is represented by the system shown in Figure P6.9.

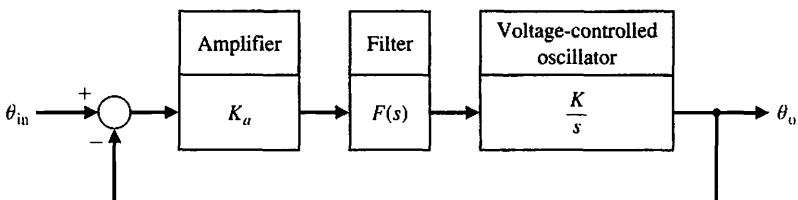


**FIGURE P6.7**  
Phase-lock loop system.

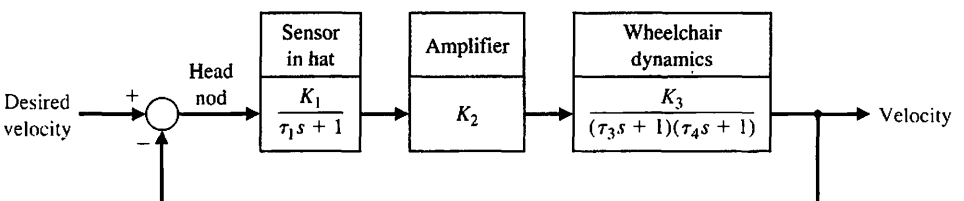


**FIGURE P6.8**  
Wheelchair control system.

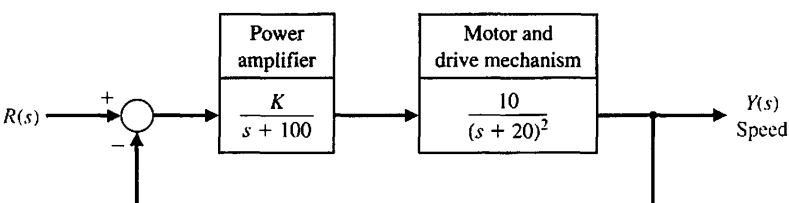


**FIGURE P6.9**  
Tape drive control.

- (a) Determine the limiting gain for a stable system.  
 (b) Determine a suitable gain so that the overshoot to a step command is approximately 5%.

**P6.10** Robots can be used in manufacturing and assembly operations that require accurate, fast, and versatile manipulation [10, 11]. The open-loop transfer function of a direct-drive arm may be approximated by

$$G(s)H(s) = \frac{K(s + 10)}{s(s + 3)(s^2 + 4s + 8)}.$$

- (a) Determine the value of gain  $K$  when the system oscillates. (b) Calculate the roots of the closed-loop system for the  $K$  determined in part (a).

**P6.11** A feedback control system has a characteristic equation

$$s^3 + (1 + K)s^2 + 10s + (5 + 15K) = 0.$$

The parameter  $K$  must be positive. What is the maximum value  $K$  can assume before the system becomes unstable? When  $K$  is equal to the maximum value, the system oscillates. Determine the frequency of oscillation.

**P6.12.** A system has the third-order characteristic equation

$$s^3 + as^2 + bs + c = 0,$$

where  $a$ ,  $b$ , and  $c$  are constant parameters. Determine the necessary and sufficient conditions for the system to be stable. Is it possible to determine stability of the system by just inspecting the coefficients of the characteristic equation?

**P6.13.** Consider the system in Figure P6.13. Determine the conditions on  $K$ ,  $p$ , and  $z$  that must be satisfied for closed-loop stability. Assume that  $K > 0$ ,  $\zeta > 0$ , and  $\omega_n > 0$ .

**P6.14** A feedback control system has a characteristic equation

$$s^6 + 2s^5 + 12s^4 + 4s^3 + 21s^2 + 2s + 10 = 0.$$

Determine whether the system is stable, and determine the values of the roots.

**P6.15** The stability of a motorcycle and rider is an important area for study because many motorcycle designs result in vehicles that are difficult to control [12, 13]. The handling characteristics of a motorcycle must include a model of the rider as well as one of the vehicle. The dynamics of one motorcycle and rider can be represented by a loop transfer function (Figure P6.4)

$$L(s) = \frac{K(s^2 + 30s + 1125)}{s(s + 20)(s^2 + 10s + 125)(s^2 + 60s + 3400)}.$$

- (a) As an approximation, calculate the acceptable range of  $K$  for a stable system when the numerator polynomial (zeros) and the denominator polynomial ( $s^2 + 60s + 3400$ ) are neglected. (b) Calculate the actual range of acceptable  $K$ , account for all zeros and poles.

**P6.16** A system has a closed-loop transfer function

$$T(s) = \frac{1}{s^3 + 5s^2 + 20s + 6}.$$

- (a) Determine whether the system is stable. (b) Determine the roots of the characteristic equation. (c) Plot the response of the system to a unit step input.

**P6.17** The elevator in Yokohama's 70-story Landmark Tower operates at a peak speed of 45 km/hr. To reach such a speed without inducing discomfort in passengers, the elevator accelerates for longer periods, rather than more precipitously. Going up, it reaches full speed only at the 27th floor; it begins decelerating 15 floors later. The result is a peak acceleration similar to that of other skyscraper elevators—a bit less than a tenth of the force of gravity. Admirable ingenuity has gone into making this safe and comfortable. Special ceramic brakes had to be developed; iron ones would melt. Computer-controlled systems damp out vibrations. The lift has been streamlined to reduce the wind noise as it speeds up and down [19]. One proposed control system for the elevator's vertical position is shown in Figure P6.17. Determine the range of  $K$  for a stable system.

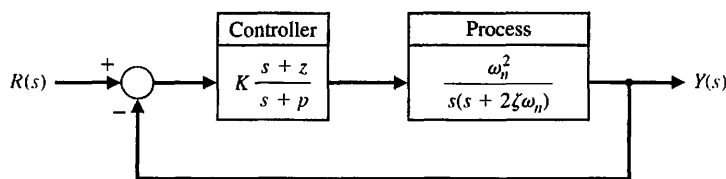


**FIGURE P6.13**  
Control system  
with controller with  
three parameters  
 $K$ ,  $p$ , and  $z$ .

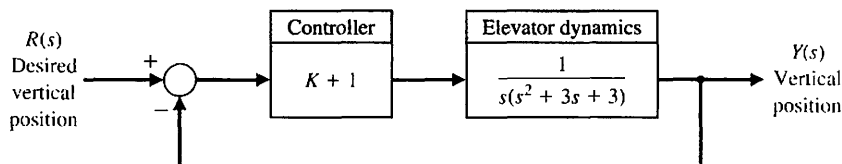


**FIGURE P6.17**  
Elevator control  
system.

- P6.18** Consider the case of rabbits and foxes in Australia. The number of rabbits is  $x_1$  and, if left alone, it would grow indefinitely (until the food supply was exhausted) so that

$$\dot{x}_1 = kx_1.$$

However, with foxes present on the continent, we have

$$\dot{x}_1 = kx_1 - ax_2,$$

where  $x_2$  is the number of foxes. Now, if the foxes must have rabbits to exist, we have

$$\dot{x}_2 = -hx_2 + bx_1.$$

Determine whether this system is stable and thus decays to the condition  $x_1(t) = x_2(t) = 0$  at  $t = \infty$ . What are the requirements on  $a, b, h$ , and  $k$  for a stable system? What is the result when  $k$  is greater than  $h$ ?

- P6.19** The goal of vertical takeoff and landing (VTOL) aircraft is to achieve operation from relatively small airports and yet operate as a normal aircraft in level

flight [16]. An aircraft taking off in a form similar to a missile (on end) is inherently unstable (see Example 3.4 for a discussion of the inverted pendulum). A control system using adjustable jets can control the vehicle, as shown in Figure P6.19. (a) Determine the range of gain for which the system is stable. (b) Determine the gain  $K$  for which the system is marginally stable and the roots of the characteristic equation for this value of  $K$ .

- P6.20** A personal vertical take-off and landing (VTOL) aircraft is shown in Figure P6.20(a). A possible control system for aircraft altitude is shown in Figure P6.20(b). (a) For  $K = 6$ , determine whether the system is stable. (b) Determine a range of stability, if any, for  $K > 0$ .

- P6.21** Consider the system described in state variable form by

$$\begin{aligned}\dot{\mathbf{x}}(t) &= \mathbf{A}\mathbf{x}(t) + \mathbf{B}u(t) \\ y(t) &= \mathbf{C}\mathbf{x}(t)\end{aligned}$$

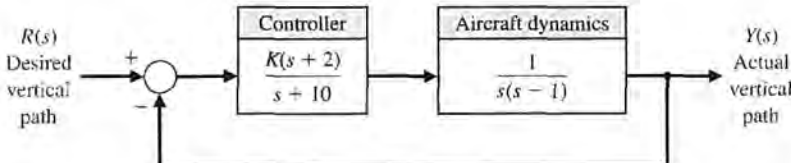
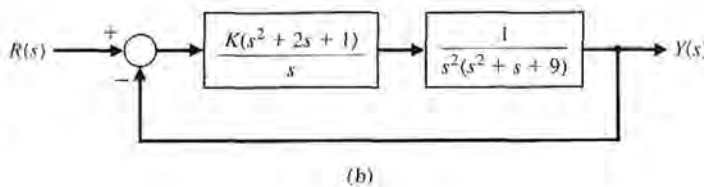


**FIGURE P6.19**  
Control of a jump-jet aircraft.



(a)

**FIGURE P6.20**  
(a) Personal VTOL aircraft. (Courtesy of Mirror Image Aerospace at [www.skywalkervtol.com](http://www.skywalkervtol.com))  
(b) Control system.



where

$$\mathbf{A} = \begin{bmatrix} 0 & 1 \\ -k_1 & -k_2 \end{bmatrix}, \mathbf{B} = \begin{bmatrix} 0 \\ 1 \end{bmatrix}, \text{ and } \mathbf{C} = [1 \quad -1],$$

and where  $k_1 \neq k_2$  and both  $k_1$  and  $k_2$  are real numbers.

- (a) Compute the state transition matrix  $\Phi(t, 0)$ .
- (b) Compute the eigenvalues of the system matrix  $\mathbf{A}$ .
- (c) Compute the roots of the characteristic polynomial.
- (d) Discuss the results of parts (a)–(c) in terms of stability of the system.

## ADVANCED PROBLEMS

**AP6.1** A teleoperated control system incorporates both a person (operator) and a remote machine. The normal teleoperation system is based on a one-way link to the machine and limited feedback to the operator. However, two-way coupling using bilateral information exchange enables better operation [18]. In the case of remote control of a robot, force feedback plus position feedback is useful. The characteristic equation for a teleoperated system, as shown in Figure AP6.1, is

$$s^4 + 20s^3 + K_1s^2 + 4s + K_2 = 0,$$

where  $K_1$  and  $K_2$  are feedback gain factors. Determine and plot the region of stability for this system for  $K_1$  and  $K_2$ .

**AP6.2** Consider the case of a navy pilot landing an aircraft on an aircraft carrier. The pilot has three basic tasks. The first task is guiding the aircraft's approach to the ship along the extended centerline of the runway. The second task is maintaining the aircraft on the correct glideslope. The third task is maintaining the correct speed. A model of a lateral position control system is shown in Figure AP6.2. Determine the range of stability for  $K \geq 0$ .

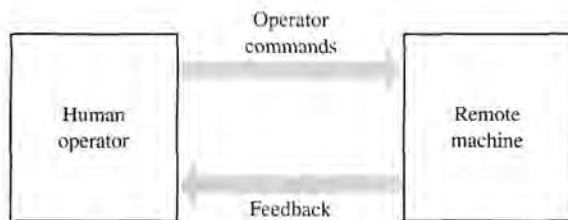


**FIGURE AP6.1** Model of a teleoperated machine.

**AP6.3** A control system is shown in Figure AP6.3. We want the system to be stable and the steady-state error for a unit step input to be less than or equal to 0.05 (5%). (a) Determine the range of  $\alpha$  that satisfies the error requirement. (b) Determine the range of  $\alpha$  that satisfies the stability requirement. (c) Select an  $\alpha$  that meets both requirements.

**AP6.4** A bottle-filling line uses a feeder screw mechanism, as shown in Figure AP6.4. The tachometer feedback is used to maintain accurate speed control. Determine and plot the range of  $K$  and  $p$  that permits stable operation.

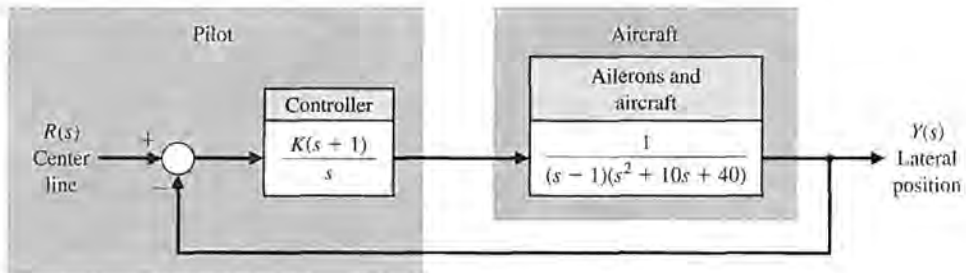


**FIGURE AP6.2**  
Lateral position control for landing on an aircraft carrier.

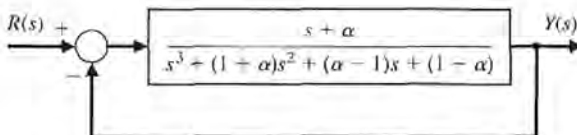


**FIGURE AP6.3**  
Third-order unity feedback system.

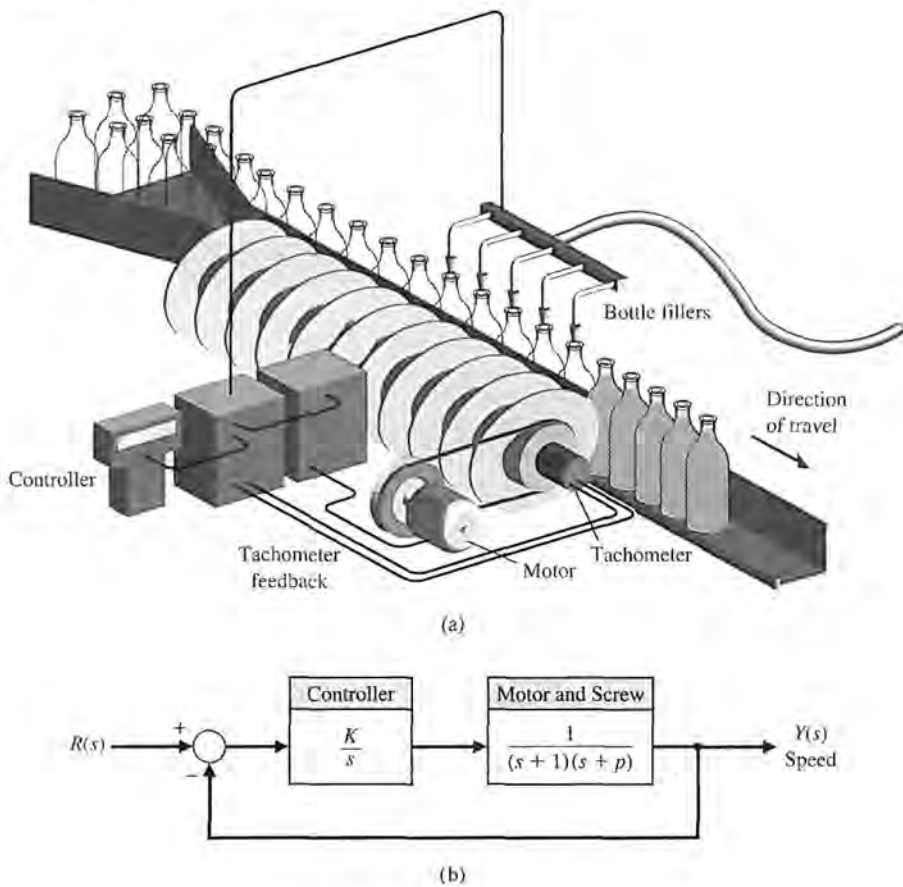


**FIGURE AP6.4**  
Speed control of a bottle-filling line.  
(a) System layout.  
(b) Block diagram.

**AP6.5** Consider the closed-loop system in Figure AP6.5. Suppose that all gains are positive, that is,  $K_1 > 0$ ,  $K_2 > 0$ ,  $K_3 > 0$ ,  $K_4 > 0$ , and  $K_5 > 0$ .

- Determine the closed-loop transfer function  $T(s) = Y(s)/R(s)$ .
- Obtain the conditions on selecting the gains  $K_1, K_2, K_3, K_4$ , and  $K_5$ , so that the closed-loop system is guaranteed to be stable.
- Using the results of part (b), select values of the five gains so that the closed-loop system is stable, and plot the unit step response.

**AP6.6** A spacecraft with a camera is shown in Figure AP6.6(a). The camera slews about  $16^\circ$  in a canted plane relative to the base. Reaction jets stabilize the base against the reaction torques from the slewing motors. Suppose that the rotational speed control for the camera slewing has a plant transfer function

$$G(s) = \frac{1}{(s+1)(s+2)(s+4)}$$

A proportional plus derivative controller is used in a system as shown in Figure AP6.6(b), where

$$G_c(s) = K_p + K_D s,$$

and where  $K_p > 0$  and  $K_D > 0$ . Obtain and plot the relationship between  $K_p$  and  $K_D$  that results in a stable closed-loop system.

**AP6.7** A human's ability to perform physical tasks is limited not by intellect but by physical strength. If, in an appropriate environment, a machine's mechanical power is closely integrated with a human arm's mechanical strength under the control of the human intellect, the resulting system will be superior to a loosely integrated combination of a human and a fully automated robot.

Extenders are defined as a class of robot manipulators that extend the strength of the human arm while maintaining human control of the task [23]. The defining characteristic of an extender is the transmission of both power and information signals. The extender is worn by the human; the physical contact between the extender

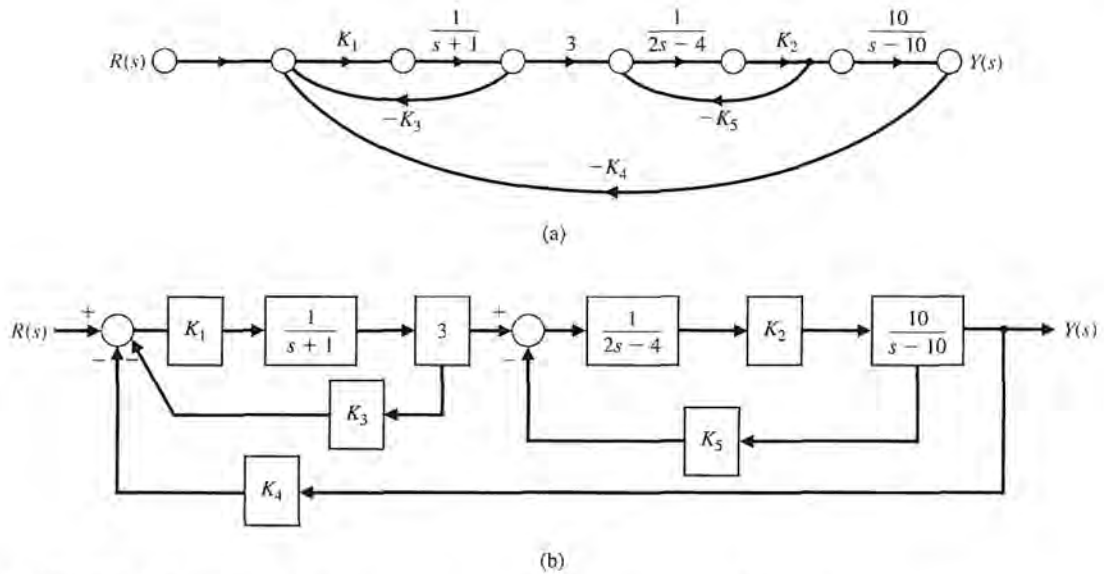


**FIGURE AP6.5** Multiloop feedback control system. (a) Signal flow graph. (b) Block diagram.

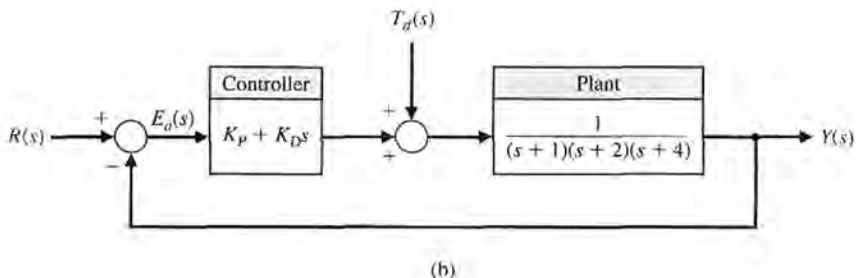
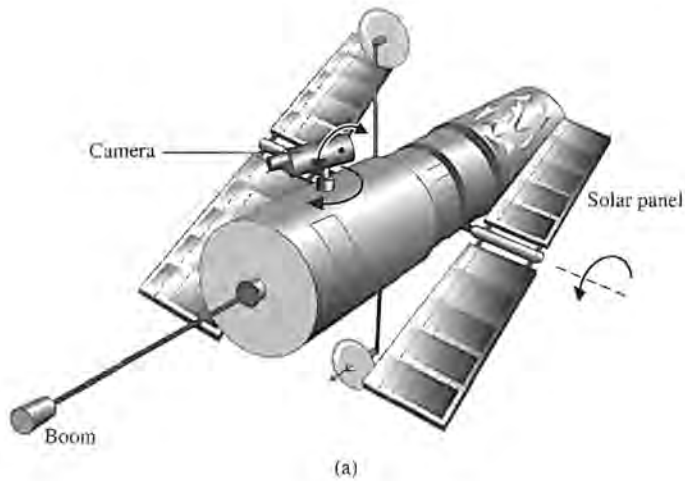


**FIGURE AP6.6**  
 (a) Spacecraft with a camera.  
 (b) Feedback control system.

and the human allows the direct transfer of mechanical power and information signals. Because of this unique interface, control of the extender trajectory can be accomplished without any type of joystick, keyboard, or master-slave system. The human provides a control system for the extender, while the extender actuators provide most of the strength necessary for the task. The human becomes a part of the extender and “feels” a scaled-down version of the load that the extender is carrying. The extender is distinguished from a conventional master-slave system; in that type of system, the human

operator is either at a remote location or close to the slave manipulator, but is not in direct physical contact with the slave in the sense of transfer of power. An extender is shown in Figure AP6.7(a) [23]. The block diagram of the system is shown in Figure AP6.7(b). Consider the proportional plus integral controller

$$G_c(s) = K_P + \frac{K_I}{s}$$

Determine the range of values of the controller gains  $K_P$  and  $K_I$  such that the closed-loop system is stable.



(a)

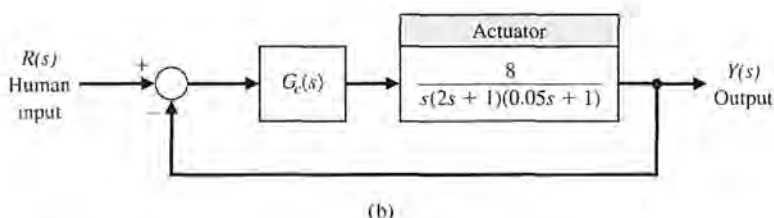


**FIGURE AP6.7**  
Extender robot  
control.

**CDP6.1** The capstan drive system of problem CDP5.1 uses the amplifier as the controller. Determine the maximum value of the gain  $K_b$  before the system becomes unstable.

**DP6.1** The control of the spark ignition of an automotive engine requires constant performance over a wide range of parameters [15]. The control system is shown in Figure DP6.1, with a controller gain  $K$  to be selected.

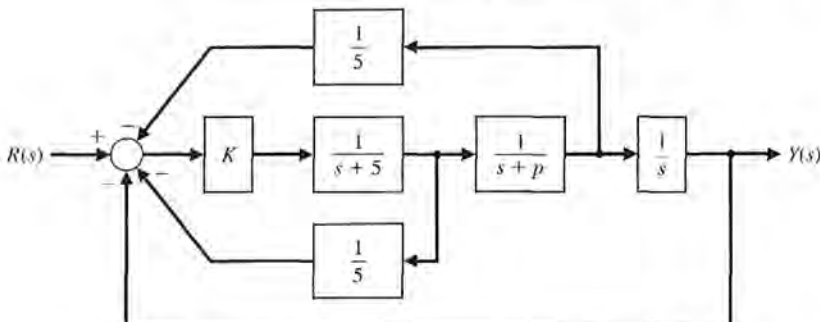


**FIGURE DP6.1**  
Automobile engine  
control.

The parameter  $p$  is equal to 2 for many autos but can equal zero for those with high performance. Select a gain  $K$  that will result in a stable system for both values of  $p$ .

**DP6.2** An automatically guided vehicle on Mars is represented by the system in Figure DP6.2. The system has a steerable wheel in both the front and back of the vehicle, and the design requires that  $H(s) = Ks + 1$ . Determine (a) the value of  $K$  required for stability, (b) the value of  $K$  when one root of the characteristic equation is equal to  $s = -5$ , and (c) the value of the two remaining roots for the gain selected in part (b). (d) Find the response of the system to a step command for the gain selected in part (b).

**DP6.3** A unity negative feedback system with

$$G_c(s)G(s) = \frac{K(s+2)}{s(1+\tau s)(1+2s)}$$

has two parameters to be selected. (a) Determine and plot the regions of stability for this system. (b) Select  $\tau$  and  $K$  so that the steady-state error to a ramp input is less than or equal to 25% of the input magnitude. (c) Determine the percent overshoot for a step input for the design selected in part (b).

**DP6.4** The attitude control system of a space shuttle rocket is shown in Figure DP6.4 [17]. (a) Determine

the range of gain  $K$  and parameter  $m$  so that the system is stable, and plot the region of stability. (b) Select the gain and parameter values so that the steady-state error to a ramp input is less than or equal to 10% of the input magnitude. (c) Determine the percent overshoot for a step input for the design selected in part (b).

**DP6.5** A traffic control system is designed to control the distance between vehicles, as shown in Figure DP6.5 [15]. (a) Determine the range of gain  $K$  for which the system is stable. (b) If  $K_m$  is the maximum value of  $K$  so that the characteristic roots are on the  $j\omega$ -axis, then let  $K = K_m/N$ , where  $6 < N < 7$ . We want the peak time to be less than 2 seconds and the percent overshoot to be less than 18%. Determine an appropriate value for  $N$ .

**DP6.6** Consider the single-input, single-output system as described by

$$\dot{\mathbf{x}}(t) = \mathbf{A}\mathbf{x}(t) + \mathbf{B}u(t)$$

$$y(t) = \mathbf{C}\mathbf{x}(t)$$

where

$$\mathbf{A} = \begin{bmatrix} 0 & 1 \\ 2 & -2 \end{bmatrix}, \mathbf{B} = \begin{bmatrix} 0 \\ 1 \end{bmatrix}, \mathbf{C} = [1 \quad 0].$$

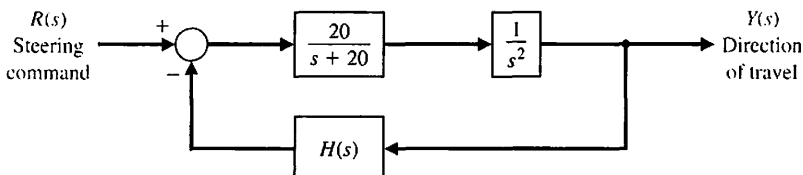


**FIGURE DP6.2**  
Mars guided vehicle control.

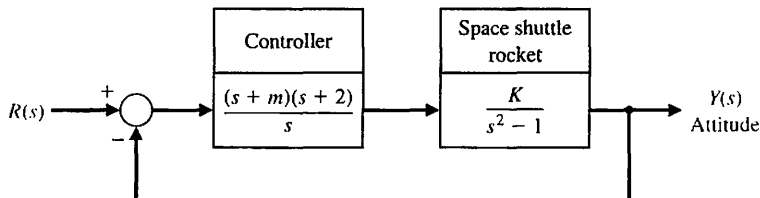


**FIGURE DP6.4**  
Shuttle attitude control.

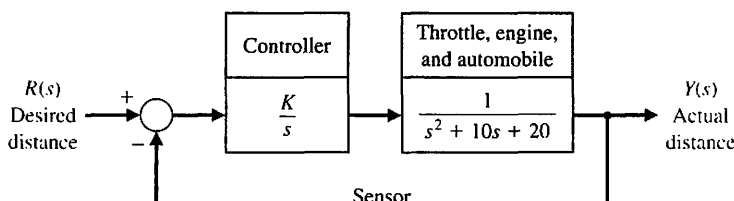


**FIGURE DP6.5**  
Traffic distance control.

Assume that the input is a linear combination of the states, that is,

$$u(t) = -\mathbf{K}\mathbf{x}(t) + r(t),$$

where  $r(t)$  is the reference input. The matrix  $\mathbf{K} = [K_1 \ K_2]$  is known as the gain matrix. If you substitute  $u(t)$  into the state variable equation you will obtain the closed-loop system

$$\dot{\mathbf{x}}(t) = [\mathbf{A} - \mathbf{B}\mathbf{K}]\mathbf{x}(t) + \mathbf{B}r(t)$$

$$y(t) = \mathbf{C}\mathbf{x}(t)$$

For what values of  $\mathbf{K}$  is the closed-loop system stable? Determine the region of the left half-plane where the desired closed-loop eigenvalues should be placed so that the percent overshoot to a unit step input,  $R(s) = 1/s$ , is less than  $P.O. < 5\%$  and the settling time is less than  $T_s < 4s$ . Select a gain matrix,  $\mathbf{K}$ , so that the system step response meets the specifications  $P.O. < 5\%$  and  $T_s < 4s$ .

**DP6.7** Consider the feedback control system in Figure DP6.7. The system has an inner loop and an outer loop.

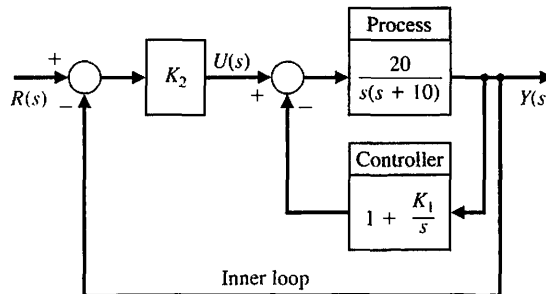


**FIGURE DP6.7**  
Feedback system  
with inner and outer  
loop.

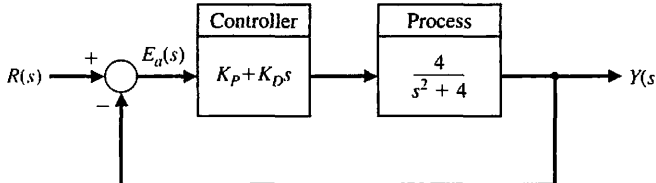


**FIGURE DP6.8**  
A marginally stable  
plant with a PD  
controller in the  
loop.

## COMPUTER PROBLEMS

**CP6.1** Determine the roots of the following characteristic equations:

- (a)  $q(s) = s^3 + 3s^2 + 10s + 14 = 0$ .
- (b)  $q(s) = s^4 + 8s^3 + 24s^2 + 32s + 16 = 0$ .
- (c)  $q(s) = s^4 + 2s^2 + 1 = 0$ .

**CP6.2** Consider a unity negative feedback system with

$$G_c(s) = K \text{ and } G(s) = \frac{s^2 - s + 2}{s^2 + 2s + 1}.$$

The inner loop must be stable and have a quick speed of response. (a) Consider the inner loop first. Determine the range of  $K_1$  resulting in a stable inner loop. That is, the transfer function  $Y(s)/U(s)$  must be stable. (b) Select the value of  $K_1$  in the stable range leading to the fastest step response. (c) For the value of  $K_1$  selected in (b), determine the range of  $K_2$  such that the closed-loop system  $T(s) = Y(s)/R(s)$  is stable.

**DP6.8** Consider the feedback system shown in Figure DP6.8. The process transfer function is marginally stable. The controller is the proportional-derivative (PD) controller

$$G_c(s) = K_P + K_D s.$$

Determine if it is possible to find values of  $K_P$  and  $K_D$  such that the closed-loop system is stable. If so, obtain values of the controller parameters such that the steady-state tracking error  $E(s) = R(s) - Y(s)$  to a unit step input  $R(s) = 1/s$  is  $e_{ss} = \lim_{t \rightarrow \infty} e(t) \leq 0.1$  and the damping of the closed-loop system is  $\zeta = \sqrt{2}/2$ .

Develop an m-file to compute the roots of the closed-loop transfer function characteristic polynomial for  $K = 1, 2$ , and  $5$ . For which values of  $K$  is the closed-loop system stable?

**CP6.3** A unity negative feedback system has the loop transfer function

$$G_c(s)G(s) = \frac{s + 1}{s^3 + 4s^2 + 6s + 10}.$$

Develop an m-file to determine the closed-loop transfer function and show that the roots of the characteristic equation are  $s_1 = -2.89$  and  $s_{2,3} = -0.55 \pm j1.87$ .

**CP6.4** Consider the closed-loop transfer function

$$T(s) = \frac{1}{s^5 + 2s^4 + 2s^3 + 4s^2 + s + 2}.$$

- (a) Using the Routh-Hurwitz method, determine whether the system is stable. If it is not stable, how many poles are in the right half-plane? (b) Compute the poles of  $T(s)$  and verify the result in part (a). (c) Plot the unit step response, and discuss the results.

**CP6.5** A “paper-pilot” model is sometimes utilized in aircraft control design and analysis to represent the pilot in the loop. A block diagram of an aircraft with a pilot “in the loop” is shown in Figure CP6.5. The variable  $\tau$  represents the pilot’s time delay. We can represent a slower pilot with  $\tau = 0.6$  and a faster pilot with  $\tau = 0.1$ . The remaining variables in the pilot model are assumed to be  $K = 1$ ,  $\tau_1 = 2$ , and  $\tau_2 = 0.5$ . Develop an m-file to compute the closed-loop system poles for the fast and slow pilots. Comment on the results. What is the maximum pilot time delay allowable for stability?

**CP6.6** Consider the feedback control system in Figure CP6.6. Using the `for` function, develop an m-file script

to compute the closed-loop transfer function poles for  $0 \leq K \leq 5$  and plot the results denoting the poles with the “ $\times$ ” symbol. Determine the maximum range of  $K$  for stability with the Routh-Hurwitz method. Compute the roots of the characteristic equation when  $K$  is the minimum value allowed for stability.

**CP6.7** Consider a system in state variable form:

$$\dot{\mathbf{x}} = \begin{bmatrix} 0 & 1 & 0 \\ 0 & 0 & 1 \\ -12 & -14 & -10 \end{bmatrix} \mathbf{x} + \begin{bmatrix} 0 \\ 0 \\ 12 \end{bmatrix} u,$$

$$y = [1 \ 1 \ 0] \mathbf{x}.$$

- (a) Compute the characteristic equation using the `poly` function. (b) Compute the roots of the characteristic equation, and determine whether the system is stable. (c) Obtain the response plot of  $y(t)$  when  $u(t)$  is a unit step and when the system has zero initial conditions.

**CP6.8** Consider the feedback control system in Figure CP6.8. (a) Using the Routh-Hurwitz method, determine the range of  $K_1$  resulting in closed-loop stability. (b) Develop an m-file to plot the pole locations as a function of  $0 < K_1 < 30$  and comment on the results.

**CP6.9** Consider a system represented in state variable form

$$\dot{\mathbf{x}} = \mathbf{A}\mathbf{x} + \mathbf{B}u$$

$$y = \mathbf{C}\mathbf{x} + \mathbf{D}u,$$

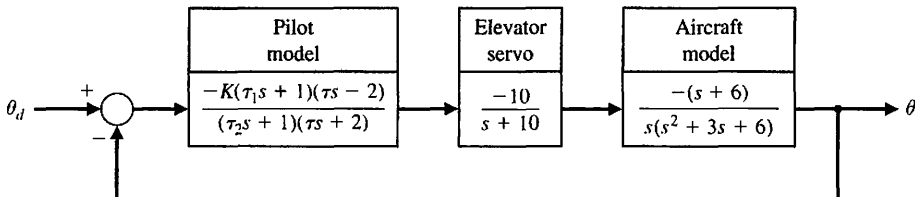


**FIGURE CP6.5**  
An aircraft with a pilot in the loop.

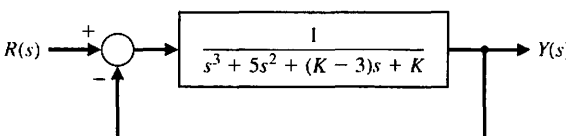


**FIGURE CP6.6**  
A single-loop feedback control system with parameter  $K$ .

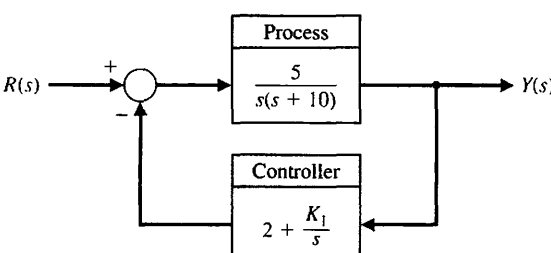


**FIGURE CP6.8**  
Nonunity feedback system with parameter  $K_1$ .

where

$$\mathbf{A} = \begin{bmatrix} 0 & 1 & 0 \\ 2 & 0 & 1 \\ -k & -3 & -2 \end{bmatrix}, \mathbf{B} = \begin{bmatrix} -1 \\ 0 \\ 1 \end{bmatrix},$$

$$\mathbf{C} = [1 \ 2 \ 0], \mathbf{D} = [0].$$

- (a) For what values of  $k$  is the system stable?
- (b) Develop an m-file to plot the pole locations as a function of  $0 < k < 10$  and comment on the results.



## ANSWERS TO SKILLS CHECK

True or False: (1) False; (2) True; (3) False; (4) True;  
 (5) True  
 Multiple Choice: (6) a; (7) c; (8) a; (9) b; (10) b;  
 (11) a; (12) a; (13) b; (14) a; (15) b

Word Match (in order, top to bottom): e, d, f, a, b,  
 g, c

## TERMS AND CONCEPTS

**Absolute stability** A system description that reveals whether a system is stable or not stable without consideration of other system attributes such as degree of stability.

**Auxiliary polynomial** The equation that immediately precedes the zero entry in the Routh array.

**Marginally stable** A system is marginally stable if and only if the zero input response remains bounded as  $t \rightarrow \infty$ .

**Relative stability** The property that is measured by the relative real part of each root or pair of roots of the characteristic equation.

**Routh–Hurwitz criterion** A criterion for determining the stability of a system by examining the characteristic equation of the transfer function. The criterion states that the number of roots of the characteristic equation with positive real parts is equal to the number of changes of sign of the coefficients in the first column of the Routh array.

**Stability** A performance measure of a system. A system is stable if all the poles of the transfer function have negative real parts.

**Stable system** A dynamic system with a bounded system response to a bounded input.

## **CHAPTER**

# **7**

# ***The Root Locus Method***

---

7.1	Introduction	444
7.2	The Root Locus Concept	444
7.3	The Root Locus Procedure	449
7.4	Parameter Design by the Root Locus Method	467
7.5	Sensitivity and the Root Locus	473
7.6	PID Controllers	480
7.7	Negative Gain Root Locus	492
7.8	Design Examples	496
7.9	The Root Locus Using Control Design Software	510
7.10	Sequential Design Example: Disk Drive Read System	516
7.11	Summary	518

### ***P R E V I E W***

The performance of a feedback system can be described in terms of the location of the roots of the characteristic equation in the  $s$ -plane. A graph showing how the roots of the characteristic equation move around the  $s$ -plane as a single parameter varies is known as a root locus plot. The root locus is a powerful tool for designing and analyzing feedback control systems. We will discuss practical techniques for obtaining a sketch of a root locus plot by hand. We also consider computer-generated root locus plots and illustrate their effectiveness in the design process. We will show that it is possible to use root locus methods for controller design when more than one parameter varies. This is important because we know that the response of a closed-loop feedback system can be adjusted to achieve the desired performance by judicious selection of one or more controller parameters. The popular PID controller is introduced as a practical controller structure. We will also define a measure of sensitivity of a specified root to a small incremental change in a system parameter. The chapter concludes with a controller design based on root locus methods for the Sequential Design Example: Disk Drive Read System.

### ***DESIRED OUTCOMES***

Upon completion of Chapter 7, students should:

- Understand the powerful concept of the root locus and its role in control system design.
- Know how to obtain a root locus plot by sketching or using computers.
- Be familiar with the PID controller as a key element of many feedback systems.
- Recognize the role of root locus plots in parameter design and system sensitivity analysis.
- Be able to design controllers to meet desired specifications using root locus methods.

## 7.1 INTRODUCTION

The relative stability and the transient performance of a closed-loop control system are directly related to the location of the closed-loop roots of the characteristic equation in the  $s$ -plane. It is frequently necessary to adjust one or more system parameters in order to obtain suitable root locations. Therefore, it is worthwhile to determine how the roots of the characteristic equation of a given system migrate about the  $s$ -plane as the parameters are varied; that is, it is useful to determine the **locus** of roots in the  $s$ -plane as a parameter is varied. The **root locus method** was introduced by Evans in 1948 and has been developed and utilized extensively in control engineering practice [1–3]. The root locus technique is a graphical method for sketching the locus of roots in the  $s$ -plane as a parameter is varied. In fact, the root locus method provides the engineer with a measure of the sensitivity of the roots of the system to a variation in the parameter being considered. The root locus technique may be used to great advantage in conjunction with the Routh–Hurwitz criterion.

The root locus method provides graphical information, and therefore an approximate sketch can be used to obtain qualitative information concerning the stability and performance of the system. Furthermore, the locus of roots of the characteristic equation of a multiloop system may be investigated as readily as for a single-loop system. If the root locations are not satisfactory, the necessary parameter adjustments often can be readily ascertained from the root locus [4].

## 7.2 THE ROOT LOCUS CONCEPT

The dynamic performance of a closed-loop control system is described by the closed-loop transfer function

$$T(s) = \frac{Y(s)}{R(s)} = \frac{p(s)}{q(s)}, \quad (7.1)$$

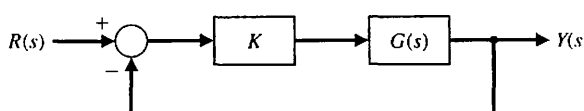
where  $p(s)$  and  $q(s)$  are polynomials in  $s$ . The roots of the characteristic equation  $q(s)$  determine the modes of response of the system. In the case of the simple single-loop system shown in Figure 7.1, we have the characteristic equation

$$1 + KG(s) = 0, \quad (7.2)$$

where  $K$  is a variable parameter and  $0 \leq K < \infty$ . The characteristic roots of the system must satisfy Equation (7.2), where the roots lie in the  $s$ -plane. Because  $s$  is a complex variable, Equation (7.2) may be rewritten in polar form as

$$|KG(s)| \angle KG(s) = -1 + j0, \quad (7.3)$$

**FIGURE 7.1**  
Closed-loop control system with a variable parameter  $K$ .



and therefore it is necessary that

$$|KG(s)| = 1$$

and

$$\angle KG(s) = 180^\circ + k360^\circ, \quad (7.4)$$

where  $k = 0, \pm 1, \pm 2, \pm 3, \dots$

**The root locus is the path of the roots of the characteristic equation traced out in the  $s$ -plane as a system parameter varies from zero to infinity.**

The simple second-order system considered in the previous chapters is shown in Figure 7.2. The characteristic equation representing this system is

$$\Delta(s) = 1 + KG(s) = 1 + \frac{K}{s(s+2)} = 0,$$

or, alternatively,

$$\Delta(s) = s^2 + 2s + K = s^2 + 2\zeta\omega_n s + \omega_n^2 = 0. \quad (7.5)$$

The locus of the roots as the gain  $K$  is varied is found by requiring that

$$|KG(s)| = \left| \frac{K}{s(s+2)} \right| = 1 \quad (7.6)$$

and

$$\angle KG(s) = \pm 180^\circ, \pm 540^\circ, \dots \quad (7.7)$$

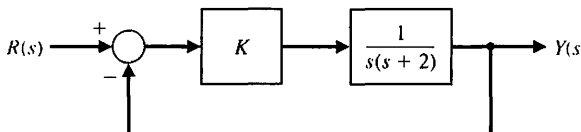
The gain  $K$  may be varied from zero to an infinitely large positive value. For a second-order system, the roots are

$$s_1, s_2 = -\zeta\omega_n \pm \omega_n\sqrt{\zeta^2 - 1}, \quad (7.8)$$

and for  $\zeta < 1$ , we know that  $\theta = \cos^{-1} \zeta$ . Graphically, for two open-loop poles as shown in Figure 7.3, the locus of roots is a vertical line for  $\zeta \leq 1$  in order to satisfy the angle requirement, Equation (7.7). For example, as shown in Figure 7.4, at a root  $s_1$ , the angles are

$$\left. \angle \frac{K}{s(s+2)} \right|_{s=s_1} = -\angle s_1 - \angle (s_1 + 2) = -[(180^\circ - \theta) + \theta] = -180^\circ. \quad (7.9)$$

**FIGURE 7.2**  
Unity feedback control system. The gain  $K$  is a variable parameter.



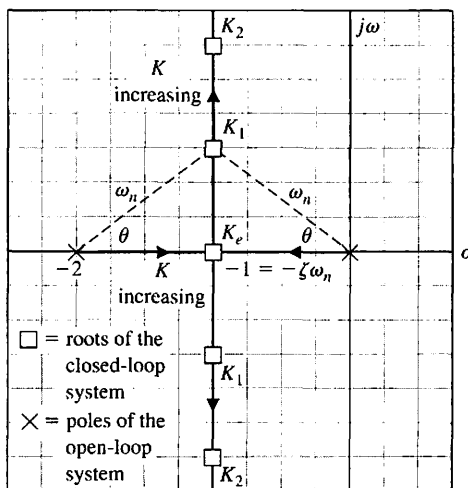


**FIGURE 7.3**  
Root locus for a second-order system when  $K_e < K_1 < K_2$ . The locus is shown as heavy lines, with arrows indicating the direction of increasing  $K$ . Note that roots of the characteristic equation are denoted by “□” on the root locus.

This angle requirement is satisfied at any point on the vertical line that is a perpendicular bisector of the line 0 to  $-2$ . Furthermore, the gain  $K$  at the particular points is found by using Equation (7.6) as

$$\left| \frac{K}{s(s + 2)} \right|_{s=s_1} = \frac{K}{|s_1||s_1 + 2|} = 1, \quad (7.10)$$

and thus

$$K = |s_1||s_1 + 2|, \quad (7.11)$$

where  $|s_1|$  is the magnitude of the vector from the origin to  $s_1$ , and  $|s_1 + 2|$  is the magnitude of the vector from  $-2$  to  $s_1$ .

For a multiloop closed-loop system, we found in Section 2.7 that by using Mason's signal-flow gain formula, we had

$$\Delta(s) = 1 - \sum_{n=1}^N L_n + \sum_{\substack{n, m \\ \text{nontouching}}} L_n L_m - \sum_{\substack{n, m, p \\ \text{nontouching}}} L_n L_m L_p + \dots, \quad (7.12)$$

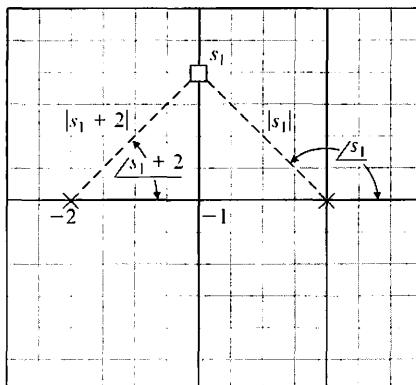


**FIGURE 7.4**  
Evaluation of the angle and gain at  $s_1$  for gain  $K = K_1$ .

where  $L_n$  equals the value of the  $n$ th self-loop transmittance. Hence, we have a characteristic equation, which may be written as

$$q(s) = \Delta(s) = 1 + F(s). \quad (7.13)$$

To find the roots of the characteristic equation, we set Equation (7.13) equal to zero and obtain

$$1 + F(s) = 0. \quad (7.14)$$

Equation (7.14) may be rewritten as

$$F(s) = -1 + j0, \quad (7.15)$$

and the roots of the characteristic equation must also satisfy this relation.

In general, the function  $F(s)$  may be written as

$$F(s) = \frac{K(s + z_1)(s + z_2)(s + z_3) \cdots (s + z_M)}{(s + p_1)(s + p_2)(s + p_3) \cdots (s + p_n)}.$$

Then the magnitude and angle requirement for the root locus are

$$|F(s)| = \frac{K|s + z_1||s + z_2| \cdots}{|s + p_1||s + p_2| \cdots} = 1 \quad (7.16)$$

and

$$\begin{aligned} \angle F(s) &= \angle s + z_1 + \angle s + z_2 + \cdots \\ &\quad - (\angle s + p_1 + \angle s + p_2 + \cdots) = 180^\circ + k360^\circ, \end{aligned} \quad (7.17)$$

where  $k$  is an integer. The magnitude requirement, Equation (7.16), enables us to determine the value of  $K$  for a given root location  $s_1$ . A test point in the  $s$ -plane,  $s_1$ , is verified as a root location when Equation (7.17) is satisfied. All angles are measured in a counterclockwise direction from a horizontal line.

To further illustrate the root locus procedure, let us consider again the second-order system of Figure 7.5(a). The effect of varying the parameter  $a$  can

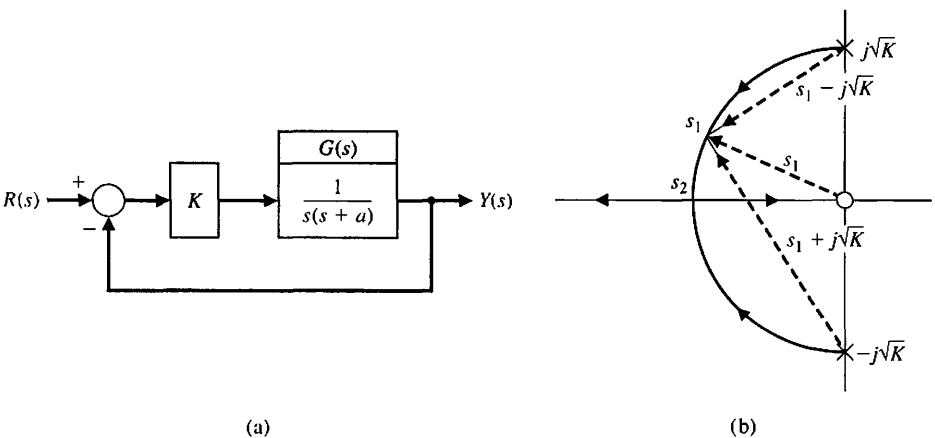


**FIGURE 7.5**  
 (a) Single-loop system. (b) Root locus as a function of the parameter  $a$ , where  $a > 0$ .

be effectively portrayed by rewriting the characteristic equation for the root locus form with  $a$  as the multiplying factor in the numerator. Then the characteristic equation is

$$1 + KG(s) = 1 + \frac{K}{s(s + a)} = 0,$$

or, alternatively,

$$s^2 + as + K = 0.$$

Dividing by the factor  $s^2 + K$ , we obtain

$$1 + \frac{as}{s^2 + K} = 0. \quad (7.18)$$

Then the magnitude criterion is satisfied when

$$\frac{a|s_1|}{|s_1^2 + K|} = 1 \quad (7.19)$$

at the root  $s_1$ . The angle criterion is

$$\angle s_1 - (\angle s_1 + j\sqrt{K} + \angle s_1 - j\sqrt{K}) = \pm 180^\circ, \pm 540^\circ, \dots$$

In principle, we could construct the root locus by determining the points in the  $s$ -plane that satisfy the angle criterion. In the next section, we will develop a multi-step procedure to sketch the root locus. The root locus for the characteristic equation in Equation (7.18) is shown in Figure 7.5(b). Specifically at the root  $s_1$ , the magnitude of the parameter  $a$  is found from Equation (7.19) as

$$a = \frac{|s_1 - j\sqrt{K}| |s_1 + j\sqrt{K}|}{|s_1|}. \quad (7.20)$$

The roots of the system merge on the real axis at the point  $s_2$  and provide a critically damped response to a step input. The parameter  $a$  has a magnitude at the critically damped roots,  $s_2 = \sigma_2$ , equal to

$$a = \frac{|\sigma_2 - j\sqrt{K}| |\sigma_2 + j\sqrt{K}|}{\sigma_2} = \frac{1}{\sigma_2} (\sigma_2^2 + K) = 2\sqrt{K}, \quad (7.21)$$

where  $\sigma_2$  is evaluated from the  $s$ -plane vector lengths as  $\sigma_2 = \sqrt{K}$ . As  $a$  increases beyond the critical value, the roots are both real and distinct; one root is larger than  $\sigma_2$ , and one is smaller.

In general, we desire an orderly process for locating the locus of roots as a parameter varies. In the next section, we will develop such an orderly approach to sketching a root locus diagram.

### 7.3 THE ROOT LOCUS PROCEDURE

The roots of the characteristic equation of a system provide a valuable insight concerning the response of the system. To locate the roots of the characteristic equation in a graphical manner on the  $s$ -plane, we will develop an orderly procedure of seven steps that facilitates the rapid sketching of the locus.

**Step 1:** Prepare the root locus sketch. Begin by writing the characteristic equation as

$$1 + F(s) = 0. \quad (7.22)$$

Rearrange the equation, if necessary, so that the parameter of interest,  $K$ , appears as the multiplying factor in the form,

$$1 + KP(s) = 0. \quad (7.23)$$

We are usually interested in determining the locus of roots as  $K$  varies as

$$0 \leq K \leq \infty.$$

In Section 7.7, we consider the case when  $K$  varies as  $-\infty < K \leq 0$ . Factor  $P(s)$ , and write the polynomial in the form of poles and zeros as follows:

$$1 + K \frac{\prod_{i=1}^M (s + z_i)}{\prod_{j=1}^n (s + p_j)} = 0. \quad (7.24)$$

Locate the poles  $-p_i$  and zeros  $-z_i$  on the  $s$ -plane with selected symbols. By convention, we use 'x' to denote poles and 'o' to denote zeros.

Rewriting Equation (7.24), we have

$$\prod_{j=1}^n (s + p_j) + K \prod_{i=1}^M (s + z_i) = 0. \quad (7.25)$$

Note that Equation (7.25) is another way to write the characteristic equation. When  $K = 0$ , the roots of the characteristic equation are the poles of  $P(s)$ . To see this, consider Equation (7.25) with  $K = 0$ . Then, we have

$$\prod_{j=1}^n (s + p_j) = 0.$$

When solved, this yields the values of  $s$  that coincide with the poles of  $P(s)$ . Conversely, as  $K \rightarrow \infty$ , the roots of the characteristic equation are the zeros of  $P(s)$ . To see this, first divide Equation (7.25) by  $K$ . Then, we have

$$\frac{1}{K} \prod_{j=1}^n (s + p_j) + \prod_{i=1}^M (s + z_i) = 0,$$

which, as  $K \rightarrow \infty$ , reduces to

$$\prod_{j=1}^M (s + z_j) = 0.$$

When solved, this yields the values of  $s$  that coincide with the zeros of  $P(s)$ . Therefore, we note that the locus of the roots of the characteristic equation  $1 + KP(s) = 0$  begins at the poles of  $P(s)$  and ends at the zeros of  $P(s)$  as  $K$  increases from zero to infinity. For most functions  $P(s)$  that we will encounter, several of the zeros of  $P(s)$  lie at infinity in the  $s$ -plane. This is because most of our functions have more poles than zeros. With  $n$  poles and  $M$  zeros and  $n > M$ , we have  $n - M$  branches of the root locus approaching the  $n - M$  zeros at infinity.

**Step 2:** Locate the segments of the real axis that are root loci. The root locus on the real axis always lies in a section of the real axis to the left of an odd number of poles and zeros. This fact is ascertained by examining the angle criterion of Equation (7.17). These two useful steps in plotting a root locus will be illustrated by a suitable example.

### EXAMPLE 7.1 Second-order system

A single-loop feedback control system possesses the characteristic equation

$$1 + GH(s) = 1 + \frac{K(\frac{1}{2}s + 1)}{\frac{1}{4}s^2 + s} = 0. \quad (7.26)$$

**STEP 1:** The characteristic equation can be written as

$$1 + K \frac{2(s + 2)}{s^2 + 4s} = 0,$$

where

$$P(s) = \frac{2(s + 2)}{s^2 + 4s}.$$

The transfer function,  $P(s)$ , is rewritten in terms of poles and zeros as

$$1 + K \frac{2(s + 2)}{s(s + 4)} = 0, \quad (7.27)$$

and the multiplicative gain parameter is  $K$ . To determine the locus of roots for the gain  $0 \leq K \leq \infty$ , we locate the poles and zeros on the real axis as shown in Figure 7.6(a).

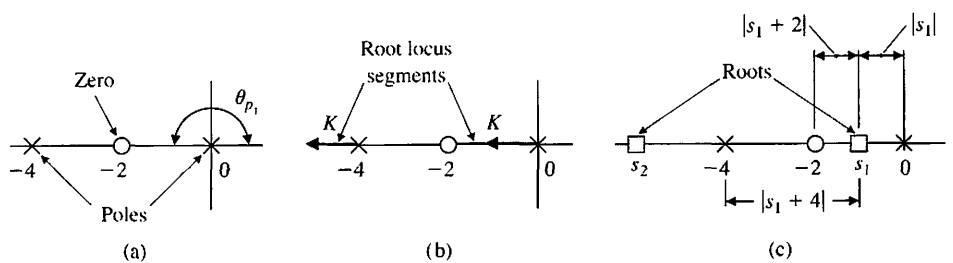


**FIGURE 7.6**  
 (a) The zero and poles of a second-order system,  
 (b) the root locus segments, and  
 (c) the magnitude of each vector at  $s_1$ .

**STEP 2:** The angle criterion is satisfied on the real axis between the points 0 and  $-2$ , because the angle from pole  $p_1$  at the origin is  $180^\circ$ , and the angle from the zero and pole  $p_2$  at  $s = -4$  is zero degrees. The locus begins at the pole and ends at the zeros, and therefore the locus of roots appears as shown in Figure 7.6(b), where the direction of the locus as  $K$  is increasing ( $K \uparrow$ ) is shown by an arrow. We note that because the system has two real poles and one real zero, the second locus segment ends at a zero at negative infinity. To evaluate the gain  $K$  at a specific root location on the locus, we use the magnitude criterion, Equation (7.16). For example, the gain  $K$  at the root  $s = s_1 = -1$  is found from (7.16) as

$$\frac{(2K)|s_1 + 2|}{|s_1||s_1 + 4|} = 1$$

or

$$K = \frac{|-1||-1 + 4|}{2|-1 + 2|} = \frac{3}{2}. \quad (7.28)$$

This magnitude can also be evaluated graphically, as shown in Figure 7.6(c). For the gain of  $K = \frac{3}{2}$ , one other root exists, located on the locus to the left of the pole at  $-4$ . The location of the second root is found graphically to be located at  $s = -6$ , as shown in Figure 7.6(c).

Now, we determine the number of separate loci,  $SL$ . Because the loci begin at the poles and end at the zeros, the **number of separate loci is equal to the number of poles** since the number of poles is greater than or equal to the number of zeros. Therefore, as we found in Figure 7.6, the number of separate loci is equal to two because there are two poles and one zero.

Note that the **root loci must be symmetrical with respect to the horizontal real axis** because the complex roots must appear as pairs of complex conjugate roots. ■

We now return to developing a general list of root locus steps.

**Step 3:** The loci proceed to the zeros at infinity along asymptotes centered at  $\sigma_A$  and with angles  $\phi_A$ . When the number of finite zeros of  $P(s)$ ,  $M$ , is less than the number of poles  $n$  by the number  $N = n - M$ , then  $N$  sections of loci must end at zeros at infinity. These sections of loci proceed to the zeros at infinity along **asymptotes** as  $K$  approaches infinity. These linear asymptotes are centered at a point on the real axis given by

$$\boxed{\sigma_A = \frac{\sum \text{poles of } P(s) - \sum \text{zeros of } P(s)}{n - M} = \frac{\sum_{j=1}^n (-p_j) - \sum_{i=1}^M (-z_i)}{n - M}.} \quad (7.29)$$

The **angle of the asymptotes** with respect to the real axis is

$$\boxed{\phi_A = \frac{2k + 1}{n - M} 180^\circ, \quad k = 0, 1, 2, \dots, (n - M - 1),} \quad (7.30)$$

where  $k$  is an integer index [3]. The usefulness of this rule is obvious for sketching the approximate form of a root locus. Equation (7.30) can be readily derived by considering a point on a root locus segment at a remote distance from the finite poles and zeros in the  $s$ -plane. The net phase angle at this remote point is  $180^\circ$ , because it is a point on a root locus segment. The finite poles and zeros of  $P(s)$  are a great distance from the remote point, and so the angles from each pole and zero,  $\phi$ , are essentially equal, and therefore the net angle is simply  $(n - M)\phi$ , where  $n$  and  $M$  are the number of finite poles and zeros, respectively. Thus, we have

$$(n - M)\phi = 180^\circ,$$

or, alternatively,

$$\phi = \frac{180^\circ}{n - M}.$$

Accounting for all possible root locus segments at remote locations in the  $s$ -plane, we obtain Equation (7.30).

The center of the linear asymptotes, often called the **asymptote centroid**, is determined by considering the characteristic equation in Equation (7.24). For large values of  $s$ , only the higher-order terms need be considered, so that the characteristic equation reduces to

$$1 + \frac{Ks^M}{s^n} = 0.$$

However, this relation, which is an approximation, indicates that the centroid of  $n - M$  asymptotes is at the origin,  $s = 0$ . A better approximation is obtained if we consider a characteristic equation of the form

$$1 + \frac{K}{(s - \sigma_A)^{n-M}} = 0$$

with a centroid at  $\sigma_A$ .

The centroid is determined by considering the first two terms of Equation (7.24), which may be found from the relation

$$1 + \frac{K \prod_{i=1}^M (s + z_i)}{\prod_{j=1}^n (s + p_j)} = 1 + K \frac{s^M + b_{M-1}s^{M-1} + \dots + b_0}{s^n + a_{n-1}s^{n-1} + \dots + a_0}.$$

From Chapter 6, especially Equation (6.5), we note that

$$b_{M-1} = \sum_{i=1}^M z_i \quad \text{and} \quad a_{n-1} = \sum_{j=1}^n p_j.$$

Considering only the first two terms of this expansion, we have

$$1 + \frac{K}{s^{n-M} + (a_{n-1} - b_{M-1})s^{n-M-1}} = 0.$$

The first two terms of

$$1 + \frac{K}{(s - \sigma_A)^{n-M}} = 0$$

are

$$1 + \frac{K}{s^{n-M} - (n-M)\sigma_A s^{n-M-1}} = 0.$$

Equating the term for  $s^{n-M-1}$ , we obtain

$$a_{n-1} - b_{M-1} = -(n-M)\sigma_A,$$

or

$$\sigma_A = \frac{\sum_{i=1}^n (-p_i) - \sum_{i=1}^M (-z_i)}{n - M}$$

which is Equation (7.29).

For example, reexamine the system shown in Figure 7.2 and discussed in Section 7.2. The characteristic equation is written as

$$1 + \frac{K}{s(s+2)} = 0.$$

Because  $n - M = 2$ , we expect two loci to end at zeros at infinity. The asymptotes of the loci are located at a center

$$\sigma_A = \frac{-2}{2} = -1$$

and at angles of

$$\phi_A = 90^\circ \text{ (for } k = 0\text{)} \quad \text{and} \quad \phi_A = 270^\circ \text{ (for } k = 1\text{).}$$

The root locus is readily sketched, and the locus shown in Figure 7.3 is obtained. An example will further illustrate the process of using the asymptotes.

### EXAMPLE 7.2 Fourth-order system

A single-loop feedback control system has a characteristic equation as follows:

$$1 + GH(s) = 1 + \frac{K(s+1)}{s(s+2)(s+4)^2}. \quad (7.31)$$

We wish to sketch the root locus in order to determine the effect of the gain  $K$ . The poles and zeros are located in the  $s$ -plane, as shown in Figure 7.7(a). The root loci on the real axis must be located to the left of an odd number of poles and zeros; they are shown as heavy lines in Figure 7.7(a). The intersection of the asymptotes is

$$\sigma_A = \frac{(-2) + 2(-4) - (-1)}{4 - 1} = \frac{-9}{3} = -3. \quad (7.32)$$

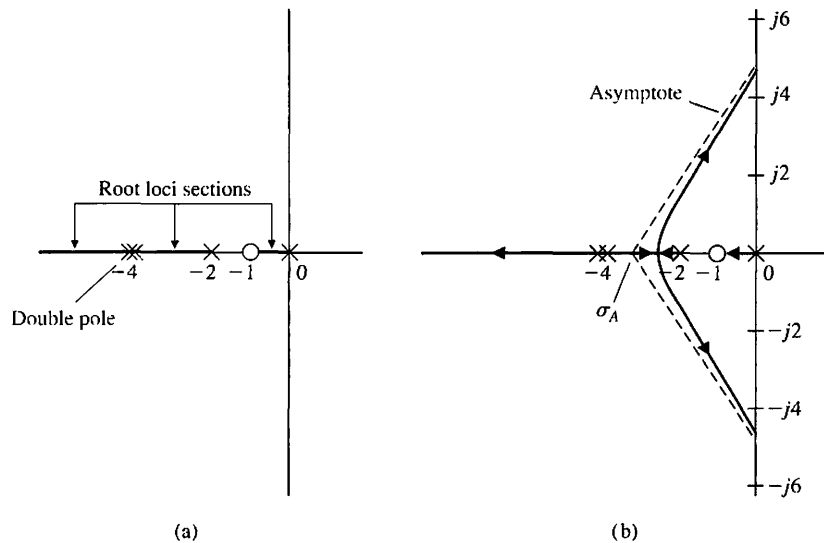


**FIGURE 7.7**  
A fourth-order system with (a) a zero and (b) root locus.

(a)

(b)

The angles of the asymptotes are

$$\begin{aligned}\phi_A &= +60^\circ \quad (k = 0), \\ \phi_A &= 180^\circ \quad (k = 1), \text{ and} \\ \phi_A &= 300^\circ \quad (k = 2),\end{aligned}$$

where there are three asymptotes, since  $n - M = 3$ . Also, we note that the root loci must begin at the poles; therefore, two loci must leave the double pole at  $s = -4$ . Then with the asymptotes sketched in Figure 7.7(b), we may sketch the form of the root locus as shown in Figure 7.7(b). The actual shape of the locus in the area near  $\sigma_A$  would be graphically evaluated, if necessary. ■

We now proceed to develop more steps for the process of determining the root loci.

**Step 4:** Determine where the locus crosses the imaginary axis (if it does so), using the Routh–Hurwitz criterion. **The actual point at which the root locus crosses the imaginary axis is readily evaluated by using the criterion.**

**Step 5:** Determine the breakaway point on the real axis (if any). The root locus in Example 7.2 left the real axis at a **breakaway point**. The locus breakaway from the real axis occurs where the net change in angle caused by a small displacement is zero. The locus leaves the real axis where there is a multiplicity of roots (typically, two). The breakaway point for a simple second-order system is shown in Figure 7.8(a) and, for a special case of a fourth-order system, is shown in Figure 7.8(b). In general, due to the phase criterion, **the tangents to the loci at the breakaway point are equally spaced over  $360^\circ$ . Therefore, in Figure 7.8(a), we find that the two loci at the breakaway point are spaced  $180^\circ$  apart, whereas in Figure 7.8(b), the four loci are spaced  $90^\circ$  apart.**

The breakaway point on the real axis can be evaluated graphically or analytically. The most straightforward method of evaluating the breakaway point involves

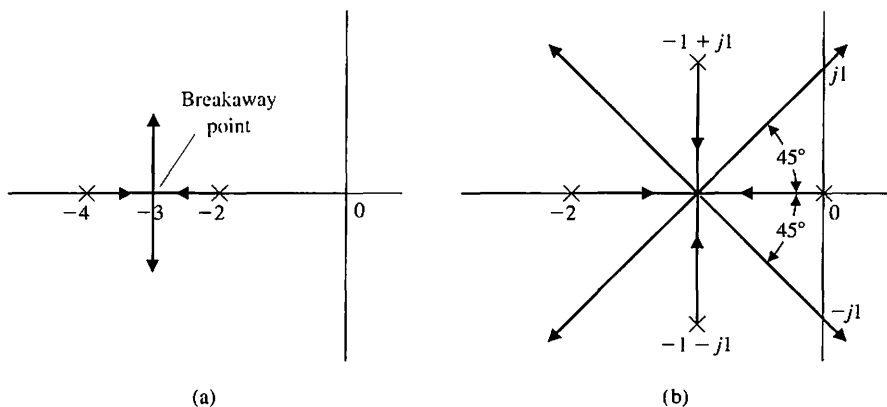


**FIGURE 7.8**  
Illustration of the  
breakaway point  
(a) for a simple  
second-order  
system and (b) for a  
fourth-order  
system.

the rearranging of the characteristic equation to isolate the multiplying factor  $K$ . Then the characteristic equation is written as

$$p(s) = K. \quad (7.33)$$

For example, consider a unity feedback closed-loop system with an open-loop transfer function

$$G(s) = \frac{K}{(s+2)(s+4)},$$

which has the characteristic equation

$$1 + G(s) = 1 + \frac{K}{(s+2)(s+4)} = 0. \quad (7.34)$$

Alternatively, the equation may be written as

$$K = p(s) = -(s + 2)(s + 4). \quad (7.35)$$

The root loci for this system are shown in Figure 7.8(a). We expect the breakaway point to be near  $s = \sigma = -3$  and plot  $p(s)|_{s=\sigma}$  near that point, as shown in Figure 7.9. In this case,  $p(s)$  equals zero at the poles  $s = -2$  and  $s = -4$ . The plot of  $p(s)$  versus  $s - \sigma$  is symmetrical, and the maximum point occurs at  $s = \sigma = -3$ , the breakaway point.

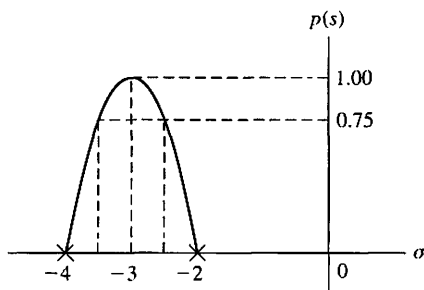


**FIGURE 7.9**  
A graphical evaluation of the breakaway point.

Analytically, the very same result may be obtained by determining the maximum of  $K = p(s)$ . To find the maximum analytically, we differentiate, set the differentiated polynomial equal to zero, and determine the roots of the polynomial. Therefore, we may evaluate

$$\frac{dK}{ds} = \frac{dp(s)}{ds} = 0 \quad (7.36)$$

in order to find the breakaway point. Equation (7.36) is an analytical expression of the graphical procedure outlined in Figure 7.9 and will result in an equation of only one degree less than the total number of poles and zeros  $n + M - 1$ .

The proof of Equation (7.36) is obtained from a consideration of the characteristic equation

$$1 + F(s) = 1 + \frac{KY(s)}{X(s)} = 0,$$

which may be written as

$$X(s) + KY(s) = 0. \quad (7.37)$$

For a small increment in  $K$ , we have

$$X(s) + (K + \Delta K)Y(s) = 0.$$

Dividing by  $X(s) + KY(s)$  yields

$$1 + \frac{\Delta KY(s)}{X(s) + KY(s)} = 0. \quad (7.38)$$

Because the denominator is the original characteristic equation, a multiplicity  $m$  of roots exists at a breakaway point, and

$$\frac{Y(s)}{X(s) + KY(s)} = \frac{C_i}{(s - s_i)^m} = \frac{C_i}{(\Delta s)^m}. \quad (7.39)$$

Then we may write Equation (7.38) as

$$1 + \frac{\Delta K C_i}{(\Delta s)^m} = 0, \quad (7.40)$$

or, alternatively,

$$\frac{\Delta K}{\Delta s} = \frac{-(\Delta s)^{m-1}}{C_i}. \quad (7.41)$$

Therefore, as we let  $\Delta s$  approach zero, we obtain

$$\frac{dK}{ds} = 0 \quad (7.42)$$

at the breakaway points.

Now, considering again the specific case where

$$G(s) = \frac{K}{(s + 2)(s + 4)},$$

we obtain

$$p(s) = K = -(s + 2)(s + 4) = -(s^2 + 6s + 8). \quad (7.43)$$

Then, when we differentiate, we have

$$\frac{dp(s)}{ds} = -(2s + 6) = 0, \quad (7.44)$$

or the breakaway point occurs at  $s = -3$ . A more complicated example will illustrate the approach and demonstrate the use of the graphical technique to determine the breakaway point.

### EXAMPLE 7.3 Third-order system

A feedback control system is shown in Figure 7.10. The characteristic equation is

$$1 + G(s)H(s) = 1 + \frac{K(s + 1)}{s(s + 2)(s + 3)} = 0. \quad (7.45)$$

The number of poles  $n$  minus the number of zeros  $M$  is equal to 2, and so we have two asymptotes at  $\pm 90^\circ$  with a center at  $\sigma_A = -2$ . The asymptotes and the sections of loci on the real axis are shown in Figure 7.11(a). A breakaway point occurs between  $s = -2$  and  $s = -3$ . To evaluate the breakaway point, we rewrite the characteristic equation so that  $K$  is separated; thus,

$$s(s + 2)(s + 3) + K(s + 1) = 0,$$

or

$$p(s) = \frac{-s(s + 2)(s + 3)}{s + 1} = K. \quad (7.46)$$

Then, evaluating  $p(s)$  at various values of  $s$  between  $s = -2$  and  $s = -3$ , we obtain the results of Table 7.1, as shown in Figure 7.11(b). Alternatively, we differentiate

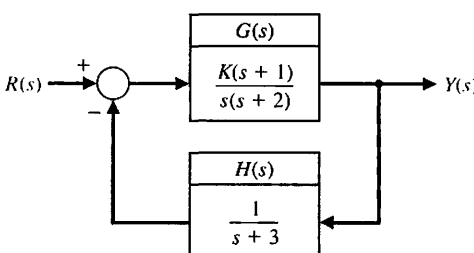


**FIGURE 7.10**  
Closed-loop system.

**Table 7.1**

$p(s)$	0	0.411	0.419	0.417	+0.390	0
$s$	-2.00	-2.40	-2.46	-2.50	-2.60	-3.0

Equation (7.46) and set it equal to zero to obtain

$$\frac{d}{ds} \left( \frac{-s(s+2)(s+3)}{(s+1)} \right) = \frac{(s^3 + 5s^2 + 6s) - (s+1)(3s^2 + 10s + 6)}{(s+1)^2} = 0$$

$$2s^3 + 8s^2 + 10s + 6 = 0. \quad (7.47)$$

Now to locate the maximum of  $p(s)$ , we locate the roots of Equation (7.47) to obtain  $s = -2.46, -0.77 \pm 0.79j$ . The only value of  $s$  on the real axis in the interval  $s = -2$  to  $s = -3$  is  $s = -2.46$ ; hence this must be the breakaway point. It is evident from this one example that the numerical evaluation of  $p(s)$  near the expected breakaway point provides an effective method of evaluating the breakaway point. ■

**Step 6:** Determine the angle of departure of the locus from a pole and the angle of arrival of the locus at a zero, using the phase angle criterion. The **angle of locus departure from a pole** is the difference between the net angle due to all other poles and zeros and the **criterion angle of  $\pm 180^\circ (2k + 1)$** , and similarly for the locus angle of arrival at a zero. The angle of departure (or arrival) is particularly of interest for complex poles (and zeros) because the information is helpful in completing the root locus. For example, consider the third-order open-loop transfer function

$$F(s) = G(s)H(s) = \frac{K}{(s + p_3)(s^2 + 2\zeta\omega_n s + \omega_n^2)}. \quad (7.48)$$

The pole locations and the vector angles at one complex pole  $-p_1$  are shown in Figure 7.12(a). The angles at a test point  $s_1$ , an infinitesimal distance from  $-p_1$ , must

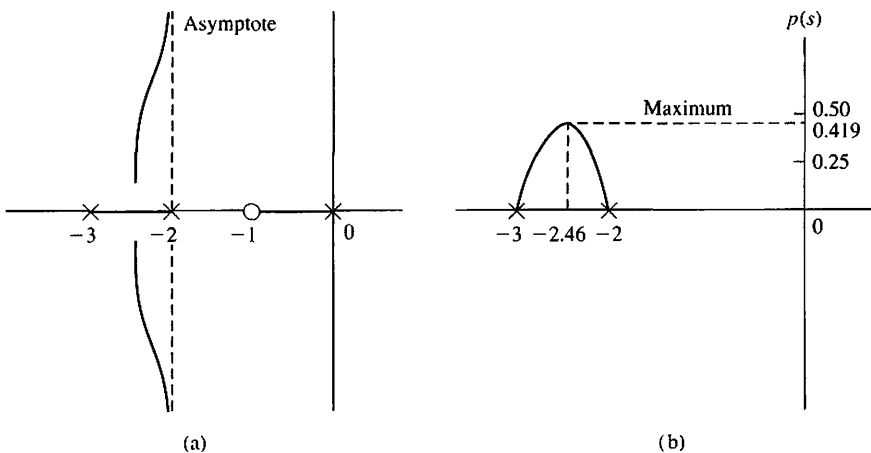


**FIGURE 7.11**  
Evaluation of the  
(a) asymptotes and  
(b) breakaway  
point.

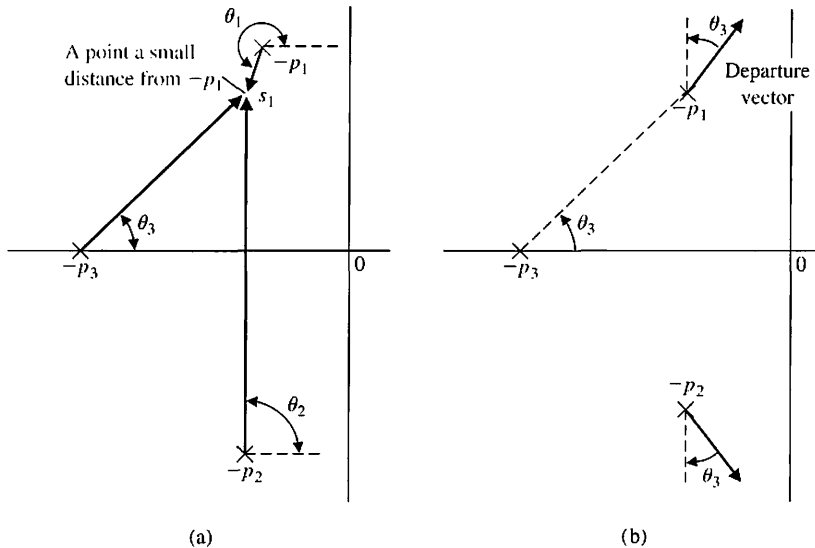


**FIGURE 7.12**  
Illustration of the angle of departure.  
(a) Test point infinitesimal distance from  $-p_1$ .  
(b) Actual departure vector at  $-p_1$ .

meet the angle criterion. Therefore, since  $\theta_2 = 90^\circ$ , we have

$$\theta_1 + \theta_2 + \theta_3 = \theta_1 + 90^\circ + \theta_3 = +180^\circ,$$

or the angle of departure at pole  $p_1$  is

$$\theta_1 = 90^\circ - \theta_3,$$

as shown in Figure 7.12(b). The departure at pole  $-p_2$  is the negative of that at  $-p_1$ , because  $-p_1$  and  $-p_2$  are complex conjugates. Another example of a departure angle is shown in Figure 7.13. In this case, the departure angle is found from

$$\theta_2 - (\theta_1 + \theta_3 + 90^\circ) = 180^\circ + k360^\circ.$$

Since  $\theta_2 - \theta_3 = \gamma$  in the diagram, we find that the departure angle is  $\theta_1 = 90^\circ + \gamma$ .

**Step 7:** The final step in the root locus sketching procedure is to complete the sketch. This entails sketching in all sections of the locus not covered in the previous

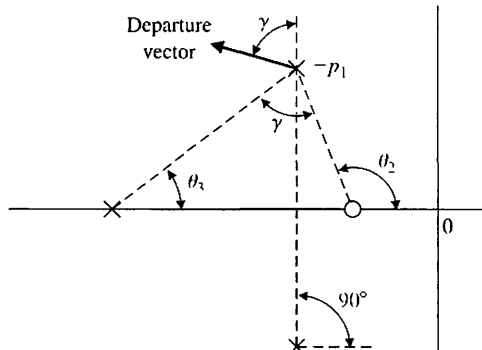


**FIGURE 7.13**  
Evaluation of the angle of departure.

six steps. If a more detailed root locus is required, we recommend using a computer-aided tool. (See Section 7.8.)

In some situation, we may want to determine a root location  $s_x$  and the value of the parameter  $K_x$  at that root location. Determine the root locations that satisfy the phase criterion at the root  $s_x$ ,  $x = 1, 2, \dots, n$ , using the phase criterion. The phase criterion, given in Equation (7.17), is

$$\angle P(s) = 180^\circ + k360^\circ, \text{ and } k = 0, \pm 1, \pm 2, \dots$$

To determine the parameter value  $K_x$  at a specific root  $s_x$ , we use the magnitude requirement (Equation 7.16). The magnitude requirement at  $s_x$  is

$$K_x = \left. \frac{\prod_{j=1}^n |s + p_j|}{\prod_{i=1}^M |s + z_i|} \right|_{s=s_x}.$$

It is worthwhile at this point to summarize the seven steps utilized in the root locus method (Table 7.2) and then illustrate their use in a complete example.

**Table 7.2 Seven Steps for Sketching a Root Locus**

Step	Related Equation or Rule
1. Prepare the root locus sketch.	
(a) Write the characteristic equation so that the parameter of interest, $K$ , appears as a multiplier.	$1 + KP(s) = 0$ .
(b) Factor $P(s)$ in terms of $n$ poles and $M$ zeros.	$1 + K \frac{\prod_{i=1}^M (s + z_i)}{\prod_{j=1}^n (s + p_j)} = 0$ .
(c) Locate the open-loop poles and zeros of $P(s)$ in the $s$ -plane with selected symbols.	$\times = \text{poles}, \bigcirc = \text{zeros}$ Locus begins at a pole and ends at a zero.
(d) Determine the number of separate loci, $SL$ .	$SL = n$ when $n \geq M$ ; $n$ = number of finite poles, $M$ = number of finite zeros.
(e) The root loci are symmetrical with respect to the horizontal real axis.	
2. Locate the segments of the real axis that are root loci.	Locus lies to the left of an odd number of poles and zeros.
3. The loci proceed to the zeros at infinity along asymptotes centered at $\sigma_A$ and with angles $\phi_A$ .	$\sigma_A = \frac{\sum(-p_j) - \sum(-z_i)}{n - M}$ .
	$\phi_A = \frac{2k + 1}{n - M} 180^\circ, k = 0, 1, 2, \dots (n - M - 1)$ .
4. Determine the points at which the locus crosses the imaginary axis (if it does so).	Use Routh-Hurwitz criterion (see Section 6.2).
5. Determine the breakaway point on the real axis (if any).	a) Set $K = p(s)$ . b) Determine roots of $dp(s)/ds = 0$ or use graphical method to find maximum of $p(s)$ . $\angle P(s) = 180^\circ + k360^\circ$ at $s = -p_j$ or $-z_i$ .
6. Determine the angle of locus departure from complex poles and the angle of locus arrival at complex zeros, using the phase criterion.	
7. Complete the root locus sketch.	

**EXAMPLE 7.4 Fourth-order system**

1. (a) We desire to plot the root locus for the characteristic equation of a system as  $K$  varies for  $K > 0$  when

$$1 + \frac{K}{s^4 + 12s^3 + 64s^2 + 128s} = 0.$$

- (b) Determining the poles, we have

$$1 + \frac{K}{s(s+4)(s+4+j4)(s+4-j4)} = 0 \quad (7.49)$$

as  $K$  varies from zero to infinity. This system has no finite zeros.

- (c) The poles are located on the  $s$ -plane as shown in Figure 7.14(a).  
 (d) Because the number of poles  $n$  is equal to 4, we have four separate loci.  
 (e) The root loci are symmetrical with respect to the real axis.

2. A segment of the root locus exists on the real axis between  $s = 0$  and  $s = -4$ .  
 3. The angles of the asymptotes are

$$\phi_A = \frac{(2k+1)}{4} 180^\circ, \quad k = 0, 1, 2, 3;$$

$$\phi_A = +45^\circ, 135^\circ, 225^\circ, 315^\circ.$$

The center of the asymptotes is

$$\sigma_A = \frac{-4 - 4 - 4}{4} = -3.$$

Then the asymptotes are drawn as shown in Figure 7.14(a).

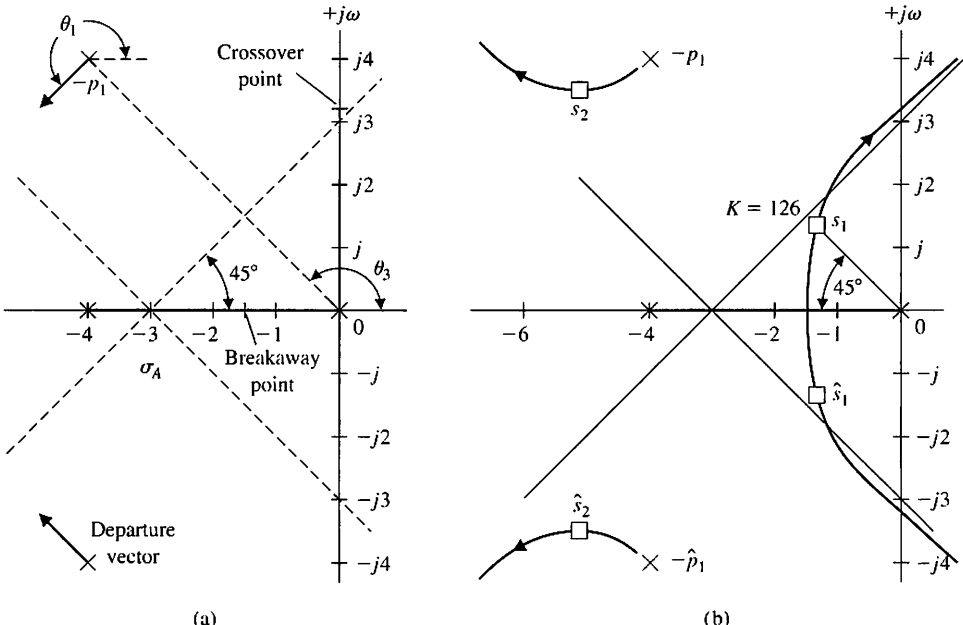


**FIGURE 7.14**  
 The root locus for Example 7.4.  
 Locating (a) the poles and (b) the asymptotes.

4. The characteristic equation is rewritten as

$$s(s + 4)(s^2 + 8s + 32) + K = s^4 + 12s^3 + 64s^2 + 128s + K = 0. \quad (7.50)$$

Therefore, the Routh array is

$$\begin{array}{c|ccc} s^4 & 1 & 64 & K \\ s^3 & 12 & 128 & \\ s^2 & b_1 & K & , \\ s^1 & c_1 & & \\ s^0 & K & & \end{array}$$

where

$$b_1 = \frac{12(64) - 128}{12} = 53.33 \quad \text{and} \quad c_1 = \frac{53.33(128) - 12K}{53.33}.$$

Hence, the limiting value of gain for stability is  $K = 568.89$ , and the roots of the auxiliary equation are

$$53.33s^2 + 568.89 = 53.33(s^2 + 10.67) = 53.33(s + j3.266)(s - j3.266). \quad (7.51)$$

The points where the locus crosses the imaginary axis are shown in Figure 7.14(a). Therefore, when  $K = 568.89$ , the root locus crosses the  $j\omega$ -axis at  $s = \pm j3.266$ .

5. The breakaway point is estimated by evaluating

$$K = p(s) = -s(s + 4)(s + 4 + j4)(s + 4 - j4)$$

between  $s = -4$  and  $s = 0$ . We expect the breakaway point to lie between  $s = -3$  and  $s = -1$ , so we search for a maximum value of  $p(s)$  in that region. The resulting values of  $p(s)$  for several values of  $s$  are given in Table 7.3. The maximum of  $p(s)$  is found to lie at approximately  $s = -1.577$ , as indicated in the table. A more accurate estimate of the breakaway point is normally not necessary. The breakaway point is then indicated on Figure 7.14(a).

6. The angle of departure at the complex pole  $p_1$  can be estimated by utilizing the angle criterion as follows:

$$\theta_1 + 90^\circ + 90^\circ + \theta_3 = 180^\circ + k360^\circ.$$

Here,  $\theta_3$  is the angle subtended by the vector from pole  $p_3$ . The angles from the pole at  $s = -4$  and  $s = -4 - j4$  are each equal to  $90^\circ$ . Since  $\theta_3 = 135^\circ$ , we find that

$$\theta_1 = -135^\circ = +225^\circ,$$

as shown in Figure 7.14(a).

7. Complete the sketch as shown in Figure 7.14(b).

**Table 7.3**

$p(s)$	0	51.0	68.44	80.0	83.57	75.0	0
$s$	-4.0	-3.0	-2.5	-2.0	-1.577	-1.0	0

Using the information derived from the seven steps of the root locus method, the complete root locus sketch is obtained by filling in the sketch as well as possible by visual inspection. The root locus for this system is shown in Figure 7.14(b). When the complex roots near the origin have a damping ratio of  $\zeta = 0.707$ , the gain  $K$  can be determined graphically as shown in Figure 7.14(b). The vector lengths to the root location  $s_1$  from the open-loop poles are evaluated and result in a gain at  $s_1$  of

$$K = |s_1||s_1 + 4||s_1 - p_1||s_1 - \hat{p}_1| = (1.9)(2.9)(3.8)(6.0) = 126. \quad (7.52)$$

The remaining pair of complex roots occurs at  $s_2$  and  $\hat{s}_2$ , when  $K = 126$ . The effect of the complex roots at  $s_2$  and  $\hat{s}_2$  on the transient response will be negligible compared to the roots  $s_1$  and  $\hat{s}_1$ . This fact can be ascertained by considering the damping of the response due to each pair of roots. The damping due to  $s_1$  and  $\hat{s}_1$  is

$$e^{-\zeta_1 \omega_{n_1} t} = e^{-\sigma_1 t},$$

and the damping factor due to  $s_2$  and  $\hat{s}_2$  is

$$e^{-\zeta_2 \omega_{n_2} t} = e^{-\sigma_2 t},$$

where  $\sigma_2$  is approximately five times as large as  $\sigma_1$ . Therefore, the transient response term due to  $s_2$  will decay much more rapidly than the transient response term due to  $s_1$ . Thus, the response to a unit step input may be written as

$$\begin{aligned} y(t) &= 1 + c_1 e^{-\sigma_1 t} \sin(\omega_1 t + \theta_1) + c_2 e^{-\sigma_2 t} \sin(\omega_2 t + \theta_2) \\ &\approx 1 + c_1 e^{-\sigma_1 t} \sin(\omega_1 t + \theta_1). \end{aligned} \quad (7.53)$$

The complex conjugate roots near the origin of the  $s$ -plane relative to the other roots of the closed-loop system are labeled the **dominant roots** of the system because they represent or dominate the transient response. The relative dominance of the complex roots, in a third-order system with a pair of complex conjugate roots, is determined by the ratio of the real root to the real part of the complex roots and will result in approximate dominance for ratios exceeding 5.

The dominance of the second term of Equation (7.53) also depends upon the relative magnitudes of the coefficients  $c_1$  and  $c_2$ . These coefficients, which are the residues evaluated at the complex roots, in turn depend upon the location of the zeros in the  $s$ -plane. Therefore, the concept of dominant roots is useful for estimating the response of a system, but must be used with caution and with a comprehension of the underlying assumptions. ■

#### EXAMPLE 7.5 Automatic self-balancing scale

The analysis and design of a control system can be accomplished by using the Laplace transform, a signal-flow diagram or block diagram, the  $s$ -plane, and the root locus method. At this point, it will be worthwhile to examine a control system and select suitable parameter values based on the root locus method.

Figure 7.15 shows an automatic self-balancing scale in which the weighing operation is controlled by the physical balance function through an electrical feedback loop [5]. The balance is shown in the equilibrium condition, and  $x$  is the travel of the counterweight  $W_c$  from an unloaded equilibrium condition. The weight  $W$  to be

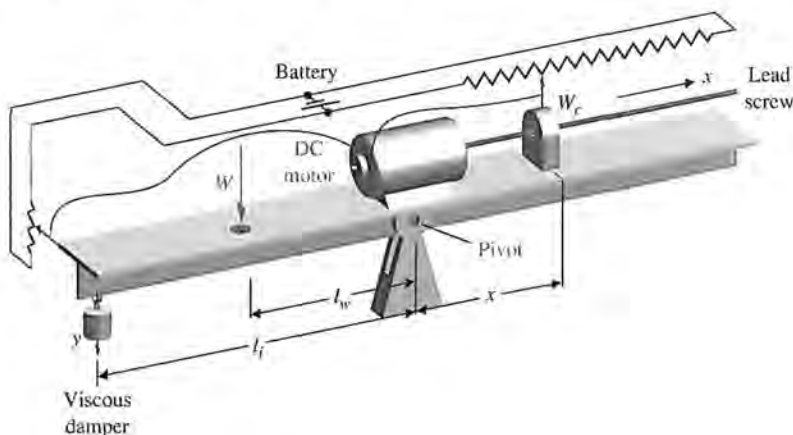


**FIGURE 7.15**  
An automatic self-balancing scale.  
(Reprinted with permission from J. H. Goldberg, *Automatic Controls*, Allyn and Bacon, Boston, 1964.)

measured is applied 5 cm from the pivot, and the length  $l_i$  of the beam to the viscous damper is 20 cm. We desire to accomplish the following:

1. Select the parameters and the specifications of the feedback system.
2. Obtain a model representing the system.
3. Select the gain  $K$  based on a root locus diagram.
4. Determine the dominant mode of response.

An inertia of the beam equal to  $0.05 \text{ kg m}^2$  will be chosen. We must select a battery voltage that is large enough to provide a reasonable position sensor gain, so we will choose  $E_b = 24$  volts. We will use a lead screw of 20 turns/cm and a potentiometer for  $x$  equal to 6 cm in length. Accurate balances are required; therefore, an input potentiometer 0.5 cm in length for  $y$  will be chosen. A reasonable viscous damper will be chosen with a damping constant  $b = 10\sqrt{3} \text{ N/(m/s)}$ . Finally, a counterweight  $W_c$  is chosen so that the expected range of weights  $W$  can be balanced. The parameters of the system are selected as listed in Table 7.4.

**Specifications.** A rapid and accurate response resulting in a small steady-state weight measurement error is desired. Therefore, we will require that the system be at least a type one so that a zero measurement error is obtained. An underdamped response to a step change in the measured weight  $W$  is satisfactory, so a dominant response with  $\zeta = 0.5$  will be specified. We want the settling time to be less than

**Table 7.4 Self-Balancing Scale Parameters**

$W_c = 2 \text{ N}$	$\text{Lead screw gain } K_s = \frac{1}{4000\pi} \text{ m/rad.}$
$I = 0.05 \text{ kg m}^2$	
$l_w = 5 \text{ cm}$	$\text{Input potentiometer gain } K_i = 4800 \text{ V/m.}$
$l_i = 20 \text{ cm}$	
$b = 10\sqrt{3} \text{ N m/s}$	$\text{Feedback potentiometer gain } K_f = 400 \text{ V/m.}$

**Table 7.5 Specifications**

Steady-state error	$K_p = \infty, e_{ss} = 0$ for a step input
Underdamped response	$\zeta = 0.5$
Settling time (2% criterion)	Less than 2 seconds

2 seconds in order to provide a rapid weight-measuring device. The settling time must be within 2% of the final value of the balance following the introduction of a weight to be measured. The specifications are summarized in Table 7.5.

The derivation of a model of the electromechanical system may be accomplished by obtaining the equations of motion of the balance. For small deviations from balance, the deviation angle is

$$\theta \approx \frac{y}{l_i}. \quad (7.54)$$

The motion of the beam about the pivot is represented by the torque equation

$$I \frac{d^2\theta}{dt^2} = \sum \text{torques}.$$

Therefore, in terms of the deviation angle, the motion is represented by

$$I \frac{d^2\theta}{dt^2} = l_w W - x W_c - l_i^2 b \frac{d\theta}{dt}. \quad (7.55)$$

The input voltage to the motor is

$$v_m(t) = K_i y - K_f x. \quad (7.56)$$

The lead screw motion and transfer function of the motor are described by

$$X(s) = K_s \theta_m(s) \quad \text{and} \quad \frac{\theta_m(s)}{V_m(s)} = \frac{K_m}{s(\tau s + 1)}, \quad (7.57)$$

where  $\tau$  will be negligible with respect to the time constants of the overall system, and  $\theta_m$  is the output shaft rotation. A signal-flow graph and block diagram representing Equations (7.54) through (7.57) is shown in Figure 7.16. Examining the forward path from  $W$  to  $X(s)$ , we find that the system is a type one due to the integration preceding  $Y(s)$ . Therefore, the steady-state error of the system is zero.

The closed-loop transfer function of the system is obtained by utilizing Mason's signal-flow gain formula and is found to be

$$\frac{X(s)}{W(s)} = \frac{l_w l_i K_i K_m K_s / (Is^3)}{1 + l_i^2 b / (Is) + (K_m K_s K_f / s) + l_i K_i K_m K_s W_c / (Is^3) + l_i^2 b K_m K_s K_f / (Is^2)}, \quad (7.58)$$

where the numerator is the path factor from  $W$  to  $X$ , the second term in the denominator is the loop  $L_1$ , the third term is the loop factor  $L_2$ , the fourth term is the loop

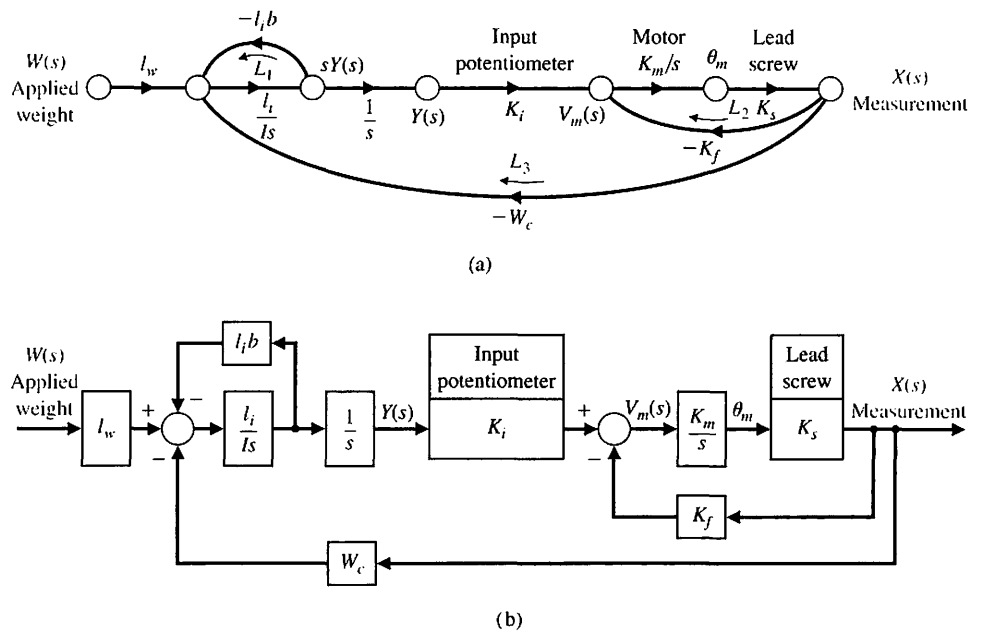


**FIGURE 7.16**  
Model of the automatic self-balancing scale.  
(a) Signal-flow graph. (b) Block diagram.

$L_3$ , and the fifth term is the two nontouching loops  $L_1L_2$ . Therefore, the closed-loop transfer function is

$$\frac{X(s)}{W(s)} = \frac{l_w l_i K_i K_m K_s}{s(Is + l_i^2 b)(s + K_m K_s K_f) + W_c K_m K_s K_i l_i}. \quad (7.59)$$

The steady-state gain of the system is then

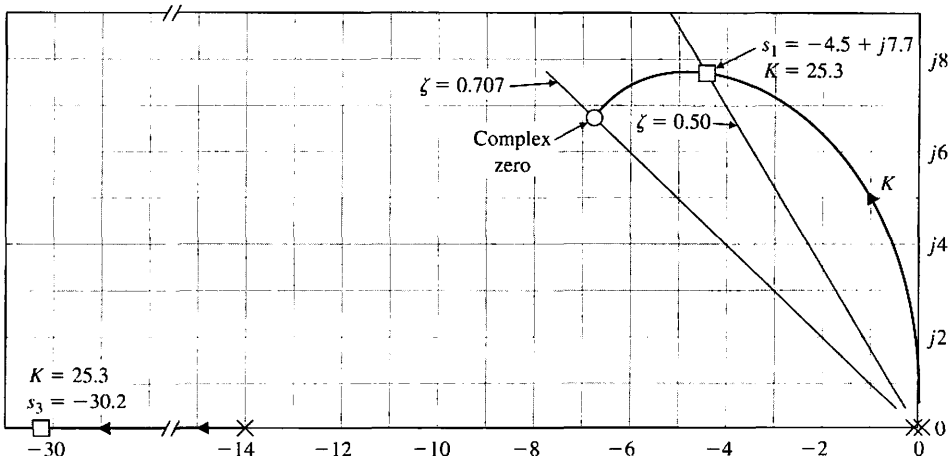
$$\lim_{t \rightarrow \infty} \frac{x(t)}{|W|} = \lim_{s \rightarrow 0} \frac{X(s)}{W(s)} = \frac{l_w}{W_c} = 2.5 \text{ cm/kg} \quad (7.60)$$

when  $W(s) = |W|/s$ . To obtain the root locus as a function of the motor constant  $K_m$ , we substitute the selected parameters into the characteristic equation, which is the denominator of Equation (7.59). Therefore, we obtain the following characteristic equation:

$$s(s + 8\sqrt{3})\left(s + \frac{K_m}{10\pi}\right) + \frac{96K_m}{10\pi} = 0. \quad (7.61)$$

Rewriting the characteristic equation in root locus form, we first isolate  $K_m$  as follows:

$$s^2(s + 8\sqrt{3}) + s(s + 8\sqrt{3})\frac{K_m}{10\pi} + \frac{96K_m}{10\pi} = 0. \quad (7.62)$$

**FIGURE 7.17**

Root locus as  $K_m$  varies (only upper halfplane shown). One locus leaves the two poles at the origin and goes to the two complex zeros as  $K$  increases. The other locus is to the left of the pole at  $s = -14$ .

Then, rewriting Equation (7.62) in root locus form, we have

$$1 + KP(s) = 1 + \frac{K_m/(10\pi)[s(s + 8\sqrt{3}) + 96]}{s^2(s + 8\sqrt{3})} = 0$$

$$= 1 + \frac{K_m/(10\pi)(s + 6.93 + j6.93)(s + 6.93 - j6.93)}{s^2(s + 8\sqrt{3})}. \quad (7.63)$$

The root locus as  $K_m$  varies is shown in Figure 7.17. The dominant roots can be placed at  $\zeta = 0.5$  when  $K = 25.3 = K_m/10\pi$ . To achieve this gain,

$$K_m = 795 \frac{\text{rad/s}}{\text{volt}} = 7600 \frac{\text{rpm}}{\text{volt}}, \quad (7.64)$$

an amplifier would be required to provide a portion of the required gain. The real part of the dominant roots is less than  $-4$ ; therefore, the settling time,  $4/\sigma$ , is less than 1 second, and the settling time requirement is satisfied. The third root of the characteristic equation is a real root at  $s = -30.2$ , and the underdamped roots clearly dominate the response. Therefore, the system has been analyzed by the root locus method and a suitable design for the parameter  $K_m$  has been achieved. The efficiency of the  $s$ -plane and root locus methods is clearly demonstrated by this example. ■

## 7.4 PARAMETER DESIGN BY THE ROOT LOCUS METHOD

Originally, the root locus method was developed to determine the locus of roots of the characteristic equation as the system gain,  $K$ , is varied from zero to infinity. However, as we have seen, the effect of other system parameters may be readily

investigated by using the root locus method. Fundamentally, the root locus method is concerned with a characteristic equation (Equation 7.22), which may be written as

$$1 + F(s) = 0. \quad (7.65)$$

Then the standard root locus method we have studied may be applied. The question arises: How do we investigate the effect of two parameters,  $\alpha$  and  $\beta$ ? It appears that the root locus method is a single-parameter method; fortunately, it can be readily extended to the investigation of two or more parameters. This method of **parameter design** uses the root locus approach to select the values of the parameters.

The characteristic equation of a dynamic system may be written as

$$a_n s^n + a_{n-1} s^{n-1} + \cdots + a_1 s + a_0 = 0. \quad (7.66)$$

Hence, the effect of the coefficient  $a_1$  may be ascertained from the root locus equation

$$1 + \frac{a_1 s}{a_n s^n + a_{n-1} s^{n-1} + \cdots + a_2 s^2 + a_0} = 0. \quad (7.67)$$

If the parameter of interest,  $\alpha$ , does not appear solely as a coefficient, the parameter may be isolated as

$$a_n s^n + a_{n-1} s^{n-1} + \cdots + (a_{n-q} - \alpha) s^{n-q} + \alpha s^{n-q} + \cdots + a_1 s + a_0 = 0. \quad (7.68)$$

For example, a third-order equation of interest might be

$$s^3 + (3 + \alpha) s^2 + 3s + 6 = 0. \quad (7.69)$$

To ascertain the effect of the parameter  $\alpha$ , we isolate the parameter and rewrite the equation in root locus form, as shown in the following steps:

$$s^3 + 3s^2 + \alpha s^2 + 3s + 6 = 0; \quad (7.70)$$

$$1 + \frac{\alpha s^2}{s^3 + 3s^2 + 3s + 6} = 0. \quad (7.71)$$

Then, to determine the effect of two parameters, we must repeat the root locus approach twice. Thus, for a characteristic equation with two variable parameters,  $\alpha$  and  $\beta$ , we have

$$\begin{aligned} a_n s^n + a_{n-1} s^{n-1} + \cdots + (a_{n-q} - \alpha) s^{n-q} + \alpha s^{n-q} + \cdots \\ + (a_{n-r} - \beta) s^{n-r} + \beta s^{n-r} + \cdots + a_1 s + a_0 = 0. \end{aligned} \quad (7.72)$$

The two variable parameters have been isolated, and the effect of  $\alpha$  will be determined. Then, the effect of  $\beta$  will be determined. For example, for a certain third-order characteristic equation with  $\alpha$  and  $\beta$  as parameters, we obtain

$$s^3 + s^2 + \beta s + \alpha = 0. \quad (7.73)$$

In this particular case, the parameters appear as the coefficients of the characteristic equation. The effect of varying  $\beta$  from zero to infinity is determined from the root

locus equation

$$1 + \frac{\beta s}{s^3 + s^2 + \alpha} = 0. \quad (7.74)$$

We note that the denominator of Equation (7.74) is the characteristic equation of the system with  $\beta = 0$ . Therefore, we must first evaluate the effect of varying  $\alpha$  from zero to infinity by using the equation

$$s^3 + s^2 + \alpha = 0,$$

rewritten as

$$1 + \frac{\alpha}{s^2(s + 1)} = 0, \quad (7.75)$$

where  $\beta$  has been set equal to zero in Equation (7.73). Then, upon evaluating the effect of  $\alpha$ , a value of  $\alpha$  is selected and used with Equation (7.74) to evaluate the effect of  $\beta$ . This two-step method of evaluating the effect of  $\alpha$  and then  $\beta$  may be carried out as two root locus procedures. First, we obtain a locus of roots as  $\alpha$  varies, and we select a suitable value of  $\alpha$ ; the results are satisfactory root locations. Then, we obtain the root locus for  $\beta$  by noting that the poles of Equation (7.74) are the roots evaluated by the root locus of Equation (7.75). A limitation of this approach is that we will not always be able to obtain a characteristic equation that is linear in the parameter under consideration (for example,  $\alpha$ ).

To illustrate this approach effectively, let us obtain the root locus for  $\alpha$  and then  $\beta$  for Equation (7.73). A sketch of the root locus as  $\alpha$  varies for Equation (7.75) is shown in Figure 7.18(a), where the roots for two values of gain  $\alpha$  are shown. If the gain  $\alpha$  is selected as  $\alpha_1$ , then the resultant roots of Equation (7.75) become the poles of Equation (7.74). The root locus of Equation (7.74) as  $\beta$  varies is shown in Figure 7.18(b), and a suitable  $\beta$  can be selected on the basis of the desired root locations.

Using the root locus method, we will further illustrate this parameter design approach by a specific design example.

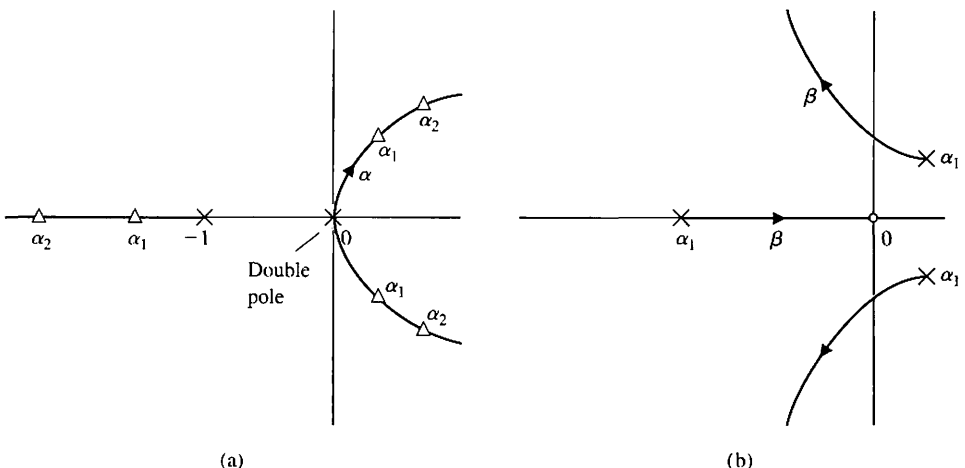


**FIGURE 7.18**

Root loci as a function of  $\alpha$  and  $\beta$ .  
 (a) Loci as  $\alpha$  varies.  
 (b) Loci as  $\beta$  varies for one value of  
 $\alpha = \alpha_1$ .

**EXAMPLE 7.6 Welding head control**

A welding head for an auto body requires an accurate control system for positioning the welding head [4]. The feedback control system is to be designed to satisfy the following specifications:

1. Steady-state error for a ramp input  $\leq 35\%$  of input slope
2. Damping ratio of dominant roots  $\geq 0.707$
3. Settling time to within 2% of the final value  $\leq 3$  seconds

The structure of the feedback control system is shown in Figure 7.19, where the amplifier gain  $K_1$  and the derivative feedback gain  $K_2$  are to be selected. The steady-state error specification can be written as

$$e_{ss} = \lim_{t \rightarrow \infty} e(t) = \lim_{s \rightarrow 0} sE(s) = \lim_{s \rightarrow 0} \frac{s(|R|/s^2)}{1 + G_2(s)}, \quad (7.76)$$

where  $G_2(s) = G(s)/(1 + G(s)H_1(s))$ . Therefore, the steady-state error requirement is

$$\frac{e_{ss}}{|R|} = \frac{2 + K_1 K_2}{K_1} \leq 0.35. \quad (7.77)$$

Thus, we will select a small value of  $K_2$  to achieve a low value of steady-state error. The damping ratio specification requires that the roots of the closed-loop system be below the line at  $45^\circ$  in the left-hand  $s$ -plane. The settling time specification can be rewritten in terms of the real part of the dominant roots as

$$T_s = \frac{4}{\sigma} \leq 3 \text{ s.} \quad (7.78)$$

Therefore, it is necessary that  $\sigma \geq \frac{4}{3}$ ; this area in the left-hand  $s$ -plane is indicated along with the  $\zeta$ -requirement in Figure 7.20. Note that  $\sigma \geq \frac{4}{3}$  implies that we want the dominant roots to lie to the left of the line defined by  $\sigma = -\frac{4}{3}$ . To satisfy the specifications, all the roots must lie within the shaded area of the left-hand plane.

The parameters to be selected are  $\alpha = K_1$  and  $\beta = K_2 K_1$ . The characteristic equation is

$$1 + GH(s) = s^2 + 2s + \beta s + \alpha = 0. \quad (7.79)$$

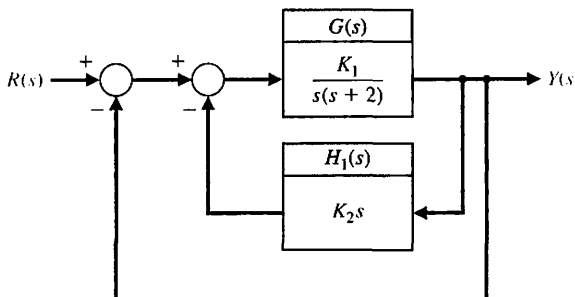


**FIGURE 7.19**  
Block diagram of  
welding head  
control system.

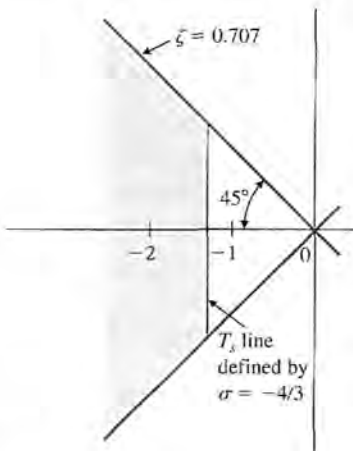


**FIGURE 7.20**  
A region in the  
s-plane for desired  
root location.

The locus of roots as  $\alpha = K_1$  varies (set  $\beta = 0$ ) is determined from the equation

$$1 + \frac{\alpha}{s(s+2)} = 0, \quad (7.80)$$

as shown in Figure 7.21(a). For a gain of  $K_1 = \alpha = 20$ , the roots are indicated on the locus. Then the effect of varying  $\beta = 20K_2$  is determined from the locus equation

$$1 + \frac{\beta s}{s^2 + 2s + \alpha} = 0, \quad (7.81)$$

where the poles of this root locus are the roots of the locus of Figure 7.21(a). The root locus for Equation (7.81) is shown in Figure 7.21(b), and roots with  $\zeta = 0.707$  are obtained when  $\beta = 4.3 = 20K_2$  or when  $K_2 = 0.215$ . The real part of these roots is

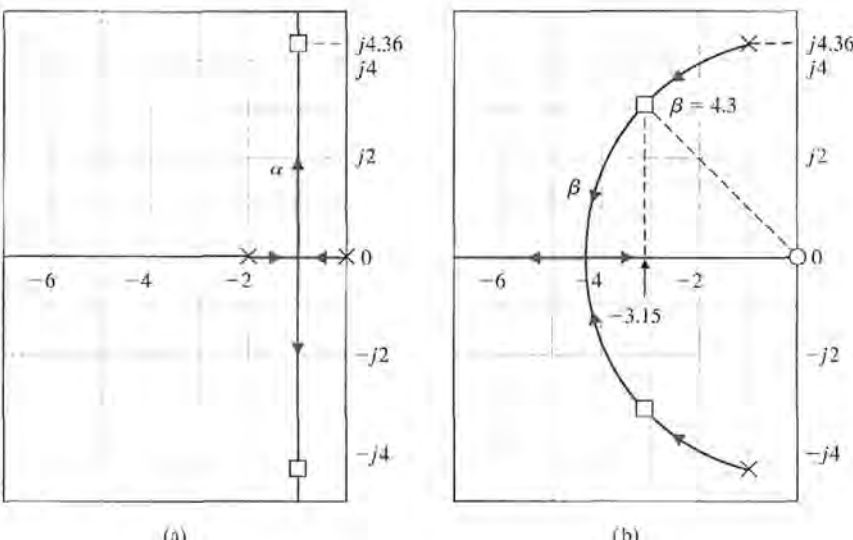


**FIGURE 7.21**  
Root loci as a  
function of (a)  $\alpha$   
and (b)  $\beta$ .

$\sigma = -3.15$ ; therefore, the time to settle (to within 2% of the final value) is equal to 1.27 seconds, which is considerably less than the specification of 3 seconds. ■

We can extend the root locus method to more than two parameters by extending the number of steps in the method outlined in this section. Furthermore, a family of root loci can be generated for two parameters in order to determine the total effect of varying two parameters. For example, let us determine the effect of varying  $\alpha$  and  $\beta$  of the following characteristic equation:

$$s^3 + 3s^2 + 2s + \beta s + \alpha = 0. \quad (7.82)$$

The root locus equation as a function of  $\alpha$  is (set  $\beta = 0$ )

$$1 + \frac{\alpha}{s(s+1)(s+2)} = 0. \quad (7.83)$$

The root locus as a function of  $\beta$  is

$$1 + \frac{\beta s}{s^3 + 3s^2 + 2s + \alpha} = 0. \quad (7.84)$$

The root locus for Equation (7.83) as a function of  $\alpha$  is shown in Figure 7.22 (unbroken lines). The roots of this locus, indicated by slashes, become the poles for the locus of Equation (7.84). Then the locus of Equation (7.84) is continued on Figure 7.22 (dotted lines), where the locus for  $\beta$  is shown for several selected values of  $\alpha$ . This family of loci, often called **root contours**, illustrates the effect of  $\alpha$  and  $\beta$  on the roots of the characteristic equation of a system [3].

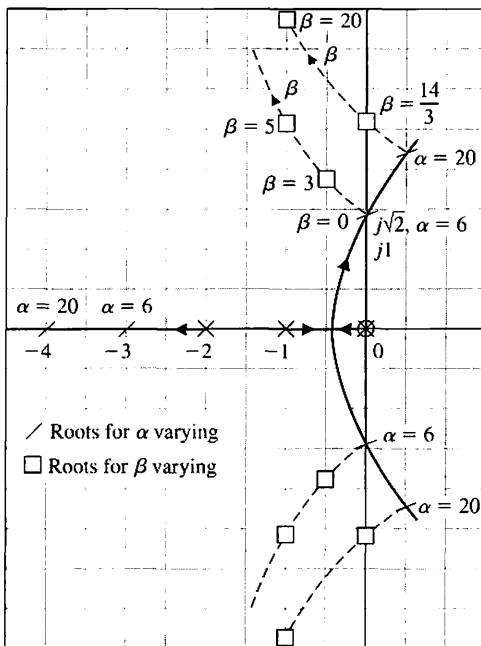


**FIGURE 7.22**  
Two-parameter root locus. The loci for  $\alpha$  varying are solid; the loci for  $\beta$  varying are dashed.

## 7.5 SENSITIVITY AND THE ROOT LOCUS

One of the prime reasons for the use of negative feedback in control systems is the reduction of the effect of parameter variations. The effect of parameter variations, as we found in Section 4.3, can be described by a measure of the sensitivity of the system performance to specific parameter changes. In Section 4.3, we defined the **logarithmic sensitivity** originally suggested by Bode as

$$S_K^T = \frac{\partial \ln T}{\partial \ln K} = \frac{\partial T/T}{\partial K/K}, \quad (7.85)$$

where the system transfer function is  $T(s)$  and the parameter of interest is  $K$ .

In recent years, there has been an increased use of the pole-zero ( $s$ -plane) approach. Therefore, it has become useful to define a sensitivity measure in terms of the positions of the roots of the characteristic equation [7–9]. Because these roots represent the dominant modes of transient response, the effect of parameter variations on the position of the roots is an important and useful measure of the sensitivity. The **root sensitivity** of a system  $T(s)$  can be defined as

$$S_K^{r_i} = \frac{\partial r_i}{\partial \ln K} = \frac{\partial r_i}{\partial K/K}, \quad (7.86)$$

where  $r_i$  equals the  $i$ th root of the system, so that

$$T(s) = \frac{K_1 \prod_{j=1}^M (s + z_j)}{\prod_{i=1}^n (s + r_i)} \quad (7.87)$$

and  $K$  is a parameter affecting the roots. The root sensitivity relates the changes in the location of the root in the  $s$ -plane to the change in the parameter. The root sensitivity is related to the logarithmic sensitivity by the relation

$$S_K^T = \frac{\partial \ln K_1}{\partial \ln K} - \sum_{i=1}^n \frac{\partial r_i}{\partial \ln K} \cdot \frac{1}{s + r_i} \quad (7.88)$$

when the zeros of  $T(s)$  are independent of the parameter  $K$ , so that

$$\frac{\partial z_j}{\partial \ln K} = 0.$$

This logarithmic sensitivity can be readily obtained by determining the derivative of  $T(s)$ , Equation (7.87), with respect to  $K$ . For this particular case, when the gain of the system is independent of the parameter  $K$ , we have

$$S_K^T = - \sum_{i=1}^n S_K^{r_i} \cdot \frac{1}{s + r_i}, \quad (7.89)$$

and the two sensitivity measures are directly related.

The evaluation of the root sensitivity for a control system can be readily accomplished by utilizing the root locus methods of the preceding section. The root sensitivity  $S_K^{r_i}$  may be evaluated at root  $-r_i$  by examining the root contours for the parameter  $K$ . We can change  $K$  by a small finite amount  $\Delta K$  and determine the modified root  $-(r_i + \Delta r_i)$  at  $K + \Delta K$ . Then, using Equation (7.86), we have

$$S_K^{r_i} \approx \frac{\Delta r_i}{\Delta K/K}. \quad (7.90)$$

Equation (7.90) is an approximation that approaches the actual value of the sensitivity as  $\Delta K \rightarrow 0$ . An example will illustrate the process of evaluating the root sensitivity.

#### EXAMPLE 7.7 Root sensitivity of a control system

The characteristic equation of the feedback control system shown in Figure 7.23 is

$$1 + \frac{K}{s(s + \beta)} = 0,$$

or, alternatively,

$$s^2 + \beta s + K = 0. \quad (7.91)$$

The gain  $K$  will be considered to be the parameter  $\alpha$ . Then the effect of a change in each parameter can be determined by utilizing the relations

$$\alpha = \alpha_0 \pm \Delta\alpha \quad \text{and} \quad \beta = \beta_0 \pm \Delta\beta,$$

where  $\alpha_0$  and  $\beta_0$  are the nominal or desired values for the parameters  $\alpha$  and  $\beta$ , respectively. We shall consider the case when the nominal pole value is  $\beta_0 = 1$  and the desired gain is  $\alpha_0 = K = 0.5$ . Then the root locus can be obtained as a function of  $\alpha = K$  by utilizing the root locus equation

$$1 + \frac{K}{s(s + \beta_0)} = 1 + \frac{K}{s(s + 1)} = 0, \quad (7.92)$$

as shown in Figure 7.24. The nominal value of gain  $K = \alpha_0 = 0.5$  results in two complex roots,  $-r_1 = -0.5 + j0.5$  and  $-r_2 = -\hat{r}_1$ , as shown in Figure 7.24. To evaluate the effect of unavoidable changes in the gain, the characteristic equation with  $\alpha = \alpha_0 \pm \Delta\alpha$  becomes

$$s^2 + s + \alpha_0 \pm \Delta\alpha = s^2 + s + 0.5 \pm \Delta\alpha. \quad (7.93)$$

Therefore, the effect of changes in the gain can be evaluated from the root locus of Figure 7.24. For a 20% change in  $\alpha$ , we have  $\Delta\alpha = \pm 0.1$ . The root locations for a

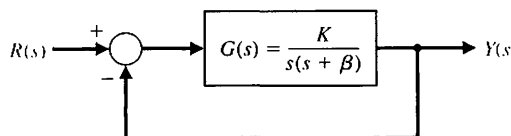


**FIGURE 7.23**  
A feedback control system.

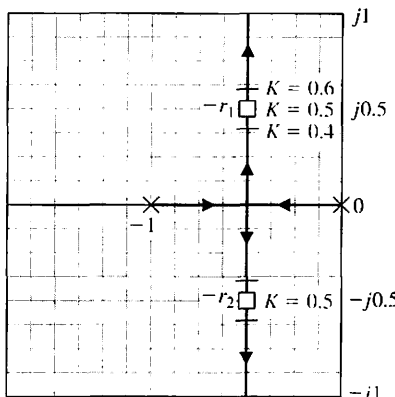


**FIGURE 7.24**  
The root locus  
for  $K$ .

gain  $\alpha = 0.4$  and  $\alpha = 0.6$  are readily determined by root locus methods, and the root locations for  $\Delta\alpha = \pm 0.1$  are shown in Figure 7.24. When  $\alpha = K = 0.6$ , the root in the second quadrant of the  $s$ -plane is

$$(-r_1) + \Delta r_1 = -0.5 + j0.59,$$

and the change in the root is  $\Delta r_1 = +j0.09$ . When  $\alpha = K = 0.4$ , the root in the second quadrant is

$$-(r_1) + \Delta r_1 = -0.5 + j0.387,$$

and the change in the root is  $-\Delta r_1 = -j0.11$ . Thus, the root sensitivity for  $r_1$  is

$$S_{K+}^{r_1} = \frac{\Delta r_1}{\Delta K/K} = \frac{+j0.09}{+0.2} = j0.45 = 0.45 \angle +90^\circ \quad (7.94)$$

for positive changes of gain. For negative increments of gain, the sensitivity is

$$S_{K-}^{r_1} = \frac{\Delta r_1}{\Delta K/K} = \frac{-j0.11}{+0.2} = -j0.55 = 0.55 \angle -90^\circ.$$

For infinitesimally small changes in the parameter  $K$ , the sensitivity will be equal for negative or positive increments in  $K$ . The angle of the root sensitivity indicates the direction the root moves as the parameter varies. The angle of movement for  $+\Delta\alpha$  is always  $180^\circ$  from the angle of movement for  $-\Delta\alpha$  at the point  $\alpha = \alpha_0$ .

The pole  $\beta$  varies due to environmental changes, and it may be represented by  $\beta = \beta_0 + \Delta\beta$ , where  $\beta_0 = 1$ . Then the effect of variation of the poles is represented by the characteristic equation

$$s^2 + s + \Delta\beta s + K = 0,$$

or, in root locus form,

$$1 + \frac{\Delta\beta s}{s^2 + s + K} = 0. \quad (7.95)$$

The denominator of the second term is the unchanged characteristic equation when  $\Delta\beta = 0$ . The root locus for the unchanged system ( $\Delta\beta = 0$ ) is shown in Figure 7.24 as a function of  $K$ . For a design specification requiring  $\zeta = 0.707$ , the complex roots lie at

$$-r_1 = -0.5 + j0.5 \quad \text{and} \quad -r_2 = -\hat{r}_1 = -0.5 - j0.5.$$

Then, because the roots are complex conjugates, the root sensitivity for  $r_1$  is the conjugate of the root sensitivity for  $\hat{r}_1 = r_2$ . Using the parameter root locus techniques discussed in the preceding section, we obtain the root locus for  $\Delta\beta$  as shown in Figure 7.25. We are normally interested in the effect of a variation for the parameter so that  $\beta = \beta_0 \pm \Delta\beta$ , for which the locus as  $\beta$  decreases is obtained from the root locus equation

$$1 + \frac{-(\Delta\beta)s}{s^2 + s + K} = 0.$$

We note that the equation is of the form

$$1 - \Delta\beta P(s) = 0.$$

Comparing this equation with Equation (7.23) in Section 7.3, we find that the sign preceding the gain  $\Delta\beta$  is negative in this case. In a manner similar to the development of the root locus method in Section 7.3, we require that the root locus satisfy the equations

$$|\Delta\beta P(s)| = 1 \quad \text{and} \quad \angle P(s) = 0^\circ \pm k360^\circ,$$

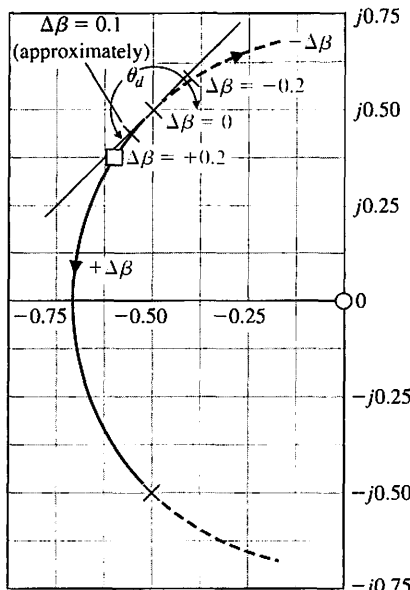


**FIGURE 7.25**  
The root locus for the parameter  $\beta$ .

where  $k$  is an integer. The locus of roots follows a zero-degree locus in contrast with the  $180^\circ$  locus considered previously. However, the root locus rules of Section 7.3 may be altered to account for the zero-degree phase angle requirement, and then the root locus may be obtained as in the preceding sections. Therefore, to obtain the effect of reducing  $\beta$ , we determine the zero-degree locus in contrast to the  $180^\circ$  locus, as shown by a dotted locus in Figure 7.25. To find the effect of a 20% change of the parameter  $\beta$ , we evaluate the new roots for  $\Delta\beta = \pm 0.20$ , as shown in Figure 7.25. The root sensitivity is readily evaluated graphically and, for a positive change in  $\beta$ , is

$$S_{\beta+}^{r_1} = \frac{\Delta r_1}{\Delta\beta/\beta} = \frac{0.16 \angle -128^\circ}{0.20} = 0.80 \angle -128^\circ.$$

The root sensitivity for a negative change in  $\beta$  is

$$S_{\beta-}^{r_1} = \frac{\Delta r_1}{\Delta\beta/\beta} = \frac{0.125 \angle 39^\circ}{0.20} = 0.625 \angle +39^\circ.$$

As the percentage change  $\Delta\beta/\beta$  decreases, the sensitivity measures  $S_{\beta+}^{r_1}$  and  $S_{\beta-}^{r_1}$  will approach equality in magnitude and a difference in angle of  $180^\circ$ . Thus, for small changes when  $\Delta\beta/\beta \leq 0.10$ , the sensitivity measures are related as

$$|S_{\beta+}^{r_1}| = |S_{\beta-}^{r_1}|$$

and

$$\angle S_{\beta+}^{r_1} = 180^\circ + \angle S_{\beta-}^{r_1}.$$

Often, the desired root sensitivity measure is desired for small changes in the parameter. When the relative change in the parameter is of the order  $\Delta\beta/\beta = 0.10$ , we can estimate the increment in the root change by approximating the root locus with the line at the angle of departure  $\theta_d$ . This approximation is shown in Figure 7.25 and is accurate for only relatively small changes in  $\Delta\beta$ . However, the use of this approximation allows the analyst to avoid sketching the complete root locus diagram. Therefore, for Figure 7.25, the root sensitivity may be evaluated for  $\Delta\beta/\beta = 0.10$  along the departure line, and we obtain

$$S_{\beta+}^{r_1} = \frac{0.075 \angle -132^\circ}{0.10} = 0.75 \angle -132^\circ. \quad (7.96)$$

The root sensitivity measure for a parameter variation is useful for comparing the sensitivity for various design parameters and at different root locations. Comparing Equation (7.96) for  $\beta$  with Equation (7.94) for  $\alpha$ , we find (a) that the sensitivity for  $\beta$  is greater in magnitude by approximately 50% and (b) that the angle for  $S_{\beta-}^{r_1}$  indicates that the approach of the root toward the  $j\omega$ -axis is more sensitive for changes in  $\beta$ . Therefore, the tolerance requirements for  $\beta$  would be more stringent than for  $\alpha$ . This information provides the designer with a comparative measure of the required tolerances for each parameter. ■

**EXAMPLE 7.8 Root sensitivity to a parameter**

A unity feedback control system has a forward transfer function

$$G(s) = \frac{20.7(s + 3)}{s(s + 2)(s + \beta)},$$

where  $\beta = \beta_0 + \Delta\beta$  and  $\beta_0 = 8$ . The characteristic equation, as a function of  $\Delta\beta$ , is

$$s(s + 2)(s + 8 + \Delta\beta) + 20.7(s + 3) = 0,$$

or

$$s(s + 2)(s + 8) + \Delta\beta s(s + 2) + 20.7(s + 3) = 0.$$

When  $\Delta\beta = 0$ , the roots are

$$-r_1 = -2.36 + j2.48, \quad -r_2 = \hat{r}_1, \quad \text{and} \quad -r_3 = -5.27.$$

The root locus for  $\Delta\beta$  is determined by using the root locus equation

$$1 + \frac{\Delta\beta s(s + 2)}{(s + r_1)(s + \hat{r}_1)(s + r_3)} = 0. \quad (7.97)$$

The roots and zeros of Equation (7.97) are shown in Figure 7.26. The angle of departure at  $r_1$  is evaluated from the angles as follows:

$$\begin{aligned} 180^\circ &= -(\theta_d + 90^\circ + \theta_{p_3}) + (\theta_{z_1} + \theta_{z_2}) \\ &= -(\theta_d + 90^\circ + 40^\circ) + (133^\circ + 98^\circ). \end{aligned}$$

Therefore,  $\theta_d = -80^\circ$  and the locus is approximated near  $-r_1$  by the line at an angle of  $\theta_d$ . For a change of  $\Delta r_1 = 0.2$  along the departure line, the  $+\Delta\beta$  is evaluated by determining the vector lengths from the poles and zeros. Then we have

$$+\Delta\beta = \frac{4.8(3.75)(0.2)}{(3.25)(2.3)} = 0.48.$$

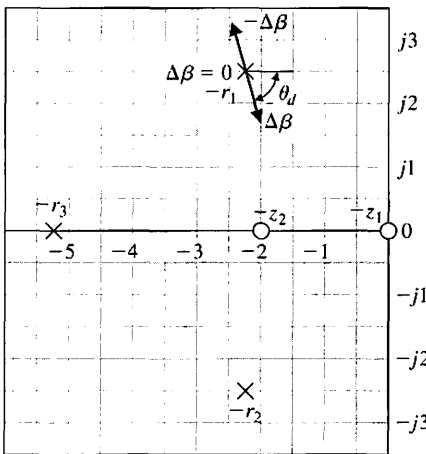


**FIGURE 7.26**  
Pole and zero  
diagram for the  
parameter  $\beta$ .

Therefore, the sensitivity at  $r_1$  is

$$S_{\beta}^{r_1} = \frac{\Delta r_1}{\Delta \beta / \beta} = \frac{0.2 / -80^\circ}{0.48/8} = 3.34 / -80^\circ,$$

which indicates that the root is quite sensitive to this 6% change in the parameter  $\beta$ . For comparison, it is worthwhile to determine the sensitivity of the root  $-r_1$  to a change in the zero  $s = -3$ . Then the characteristic equation is

$$s(s + 2)(s + 8) + 20.7(s + 3 + \Delta\gamma) = 0,$$

or

$$1 + \frac{20.7 \Delta\gamma}{(s + r_1)(s + \hat{r}_1)(s + r_3)} = 0. \quad (7.98)$$

The pole-zero diagram for Equation (7.98) is shown in Figure 7.27. The angle of departure at root  $-r_1$  is  $180^\circ = -(\theta_d + 90^\circ + 40^\circ)$ , or

$$\theta_d = +50^\circ.$$

For a change of  $\Delta r_1 = 0.2 / +50^\circ$ , the  $\Delta\gamma$  is positive. Obtaining the vector lengths, we find that

$$|\Delta\gamma| = \frac{5.22(4.18)(0.2)}{20.7} = 0.21.$$

Therefore, the sensitivity at  $r_1$  for  $+\Delta\gamma$  is

$$S_{\gamma}^{r_1} = \frac{\Delta r_1}{\Delta\gamma/\gamma} = \frac{0.2 / +50^\circ}{0.21/3} = 2.84 / +50^\circ.$$

Thus, we find that the magnitude of the root sensitivity for the pole  $\beta$  and the zero  $\gamma$  is approximately equal. However, the sensitivity of the system to the pole can be considered to be less than the sensitivity to the zero because the angle of the sensitivity,  $S_{\gamma}^{r_1}$ , is equal to  $+50^\circ$  and the direction of the root change is toward the  $j\omega$ -axis.

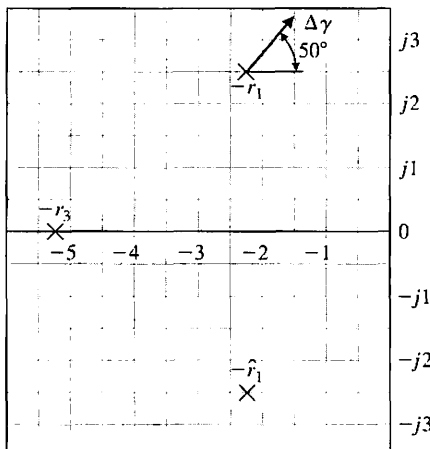


**FIGURE 7.27**  
Pole-zero diagram  
for the parameter  $\gamma$ .

Evaluating the root sensitivity in the manner of the preceding paragraphs, we find that the sensitivity for the pole  $s = -\delta_0 = -2$  is

$$S_{\delta}^{rL} = 2.1 / +27^\circ.$$

Thus, for the parameter  $\delta$ , the magnitude of the sensitivity is less than for the other parameters, but the direction of the change of the root is more important than for  $\beta$  and  $\gamma$ . ■

To utilize the root sensitivity measure for the analysis and design of control systems, a series of calculations must be performed; they will determine the various selections of possible root configurations and the zeros and poles of the open-loop transfer function. Therefore, the root sensitivity measure as a design technique is somewhat limited by two things: the relatively large number of calculations required and the lack of an obvious direction for adjusting the parameters in order to provide a minimized or reduced sensitivity. However, the root sensitivity measure can be utilized as an analysis measure, which permits the designer to compare the sensitivity for several system designs based on a suitable method of design. The root sensitivity measure is a useful index of the system's sensitivity to parameter variations expressed in the  $s$ -plane. The weakness of the sensitivity measure is that it relies on the ability of the root locations to represent the performance of the system. As we have seen in the preceding chapters, the root locations represent the performance quite adequately for many systems, but due consideration must be given to the location of the zeros of the closed-loop transfer function and the dominancy of the pertinent roots. The root sensitivity measure is a suitable measure of system performance sensitivity and can be used reliably for system analysis and design.

## 7.6 PID CONTROLLERS

One form of controller widely used in industrial process control is the three-term, **PID controller** [4, 10]. This controller has a transfer function

$$G_c(s) = K_p + \frac{K_I}{s} + K_D s.$$

The equation for the output in the time domain is

$$u(t) = K_p e(t) + K_I \int e(t) dt + K_D \frac{de(t)}{dt}.$$

The three-term controller is called a PID controller because it contains a proportional, an integral, and a derivative term represented by  $K_p$ ,  $K_I$ , and  $K_D$ , respectively. The transfer function of the derivative term is actually

$$G_d(s) = \frac{K_D s}{\tau_d s + 1},$$

but  $\tau_d$  is usually much smaller than the time constants of the process itself, so it is neglected.

If we set  $K_D = 0$ , then we have the **proportional plus integral (PI) controller**

$$G_c(s) = K_p + \frac{K_I}{s}.$$

When  $K_I = 0$ , we have

$$G_c(s) = K_p + K_D s,$$

which is called a **proportional plus derivative (PD) controller**.

The PID controller can also be viewed as a cascade of the PI and the PD controllers. Consider the PI controller

$$G_{PI}(s) = \hat{K}_P + \frac{\hat{K}_I}{s}$$

and the PD controller

$$G_{PD}(s) = \bar{K}_P + \bar{K}_D s,$$

where  $\hat{K}_P$  and  $\hat{K}_I$  are the PI controller gains and  $\bar{K}_P$  and  $\bar{K}_D$  are the PD controller gains. Cascading the two controllers (that is, placing them in series) yields

$$\begin{aligned} G_c(s) &= G_{PI}(s)G_{PD}(s) \\ &= \left( \hat{K}_P + \frac{\hat{K}_I}{s} \right) (\bar{K}_P + \bar{K}_D s) \\ &= (\bar{K}_P \hat{K}_P + \hat{K}_I \bar{K}_D) + \hat{K}_P \bar{K}_D s + \frac{\hat{K}_I \bar{K}_D}{s} \\ &= K_P + K_D s + \frac{K_I}{s}, \end{aligned}$$

where we have the following relationships between the PI and PD controller gains and the PID controller gains

$$\begin{aligned} K_P &= \bar{K}_P \hat{K}_P + \hat{K}_I \bar{K}_D \\ K_D &= \hat{K}_P \bar{K}_D \\ K_I &= \hat{K}_I \bar{K}_D. \end{aligned}$$

Consider the PID controller

$$\begin{aligned} G_c(s) &= K_P + \frac{K_I}{s} + K_D s = \frac{K_D s^2 + K_P s + K_I}{s} \\ &= \frac{K_D(s^2 + as + b)}{s} = \frac{K_D(s + z_1)(s + z_2)}{s}, \end{aligned}$$

where  $a = K_P/K_D$  and  $b = K_I/K_D$ . Therefore, a PID controller introduces a transfer function with one pole at the origin and two zeros that can be located anywhere in the  $s$ -plane.

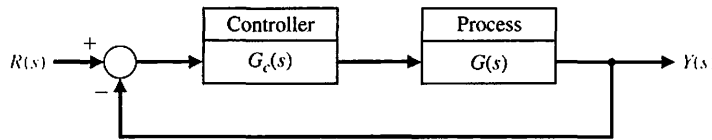


**FIGURE 7.28**  
Closed-loop system with a controller.

Recall that a root locus begins at the poles and ends at the zeros. If we have a system, as shown in Figure 7.28, with

$$G(s) = \frac{1}{(s + 2)(s + 3)},$$

and we use a PID controller with complex zeros  $-z_1$  and  $-z_2$ , where  $-z_1 = -3 + j1$  and  $-z_2 = -\hat{z}_1$ , we can plot the root locus as shown in Figure 7.29. As the gain,  $K_D$ , of the controller is increased, the complex roots approach the zeros. The closed-loop transfer function is

$$\begin{aligned} T(s) &= \frac{G(s)G_c(s)}{1 + G(s)G_c(s)} \\ &= \frac{K_D(s + z_1)(s + \hat{z}_1)}{(s + r_2)(s + r_1)(s + \hat{r}_1)}. \end{aligned}$$

The response of this system will be attractive. The percent overshoot to a step will be less than 2%, and the steady-state error for a step input will be zero. The settling time will be approximately 1 second. If a shorter settling time is desired, then we select  $z_1$  and  $z_2$  to lie further left in the left-hand  $s$ -plane and set  $K_D$  to drive the roots near the complex zeros.

Many industrial processes are controlled using PID controllers. The popularity of PID controllers can be attributed partly to their good performance in a wide range of operating conditions and partly to their functional simplicity that allows

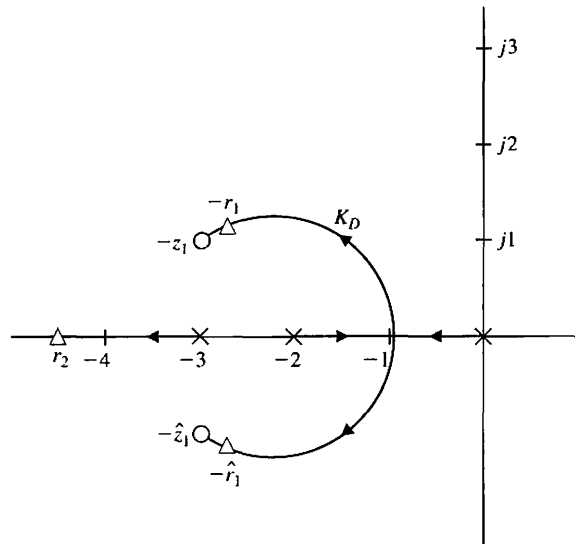


**FIGURE 7.29**  
Root locus for plant with a PID controller with complex zeros.

**Table 7.6 Effect of Increasing the PID Gains  $K_P$ ,  $K_I$ , and  $K_D$  on the Step Response**

PID Gain	Percent Overshoot	Settling Time	Steady-State Error
Increasing $K_P$	Increases	Minimal impact	Decreases
Increasing $K_I$	Increases	Increases	Zero steady-state error
Increasing $K_D$	Decreases	Decreases	No impact

engineers to operate them in a simple, straightforward manner. To implement the PID controller, three parameters must be determined, the proportional gain, denoted by  $K_P$ , integral gain, denoted by  $K_I$ , and derivative gain denoted by  $K_D$  [10].

There are many methods available to determine acceptable values of the PID gains. The process of determining the gains is often called **PID tuning**. A common approach to tuning is to use **manual PID tuning** methods, whereby the PID control gains are obtained by trial-and-error with minimal analytic analysis using step responses obtained via simulation, or in some cases, actual testing on the system and deciding on the gains based on observations and experience. A more analytic method is known as the **Ziegler-Nichols tuning** method. The Ziegler-Nichols tuning method actually has several variations. We discuss in this section a Ziegler-Nichols tuning method based on open-loop responses to a step input and a related a Ziegler-Nichols tuning method based on closed-loop response to a step input.

One approach to manual tuning is to first set  $K_I = 0$  and  $K_D = 0$ . This is followed by slowly increasing the gain  $K_P$  until the output of the closed-loop system oscillates just on the edge of instability. This can be done either in simulation or on the actual system if it cannot be taken off-line. Once the value of  $K_P$  (with  $K_I = 0$  and  $K_D = 0$ ) is found that brings the closed-loop system to the edge of stability, you reduce the value of gain  $K_P$  to achieve what is known as the **quarter amplitude decay**. That is, the amplitude of the closed-loop response is reduced approximately to one-fourth of the maximum value in one oscillatory period. A rule-of-thumb is to start by reducing the proportional gain  $K_P$  by one-half. The next step of the design process is to increase  $K_I$  and  $K_D$  manually to achieve a desired step response. Table 7.6 describes in general terms the effect of increasing  $K_I$  and  $K_D$ .

### EXAMPLE 7.9 Manual PID tuning

Consider the closed-loop system in Figure 7.30 with

$$G(s) = \frac{1}{s(s + b)(s + 2\zeta\omega_n)},$$

where  $b = 10$ ,  $\zeta = 0.707$ , and  $\omega_n = 4$ .

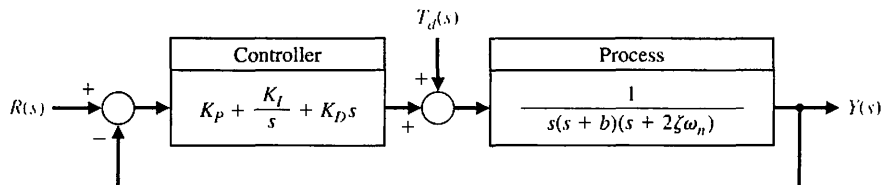


**FIGURE 7.30**  
Unity feedback control system with PID controller.

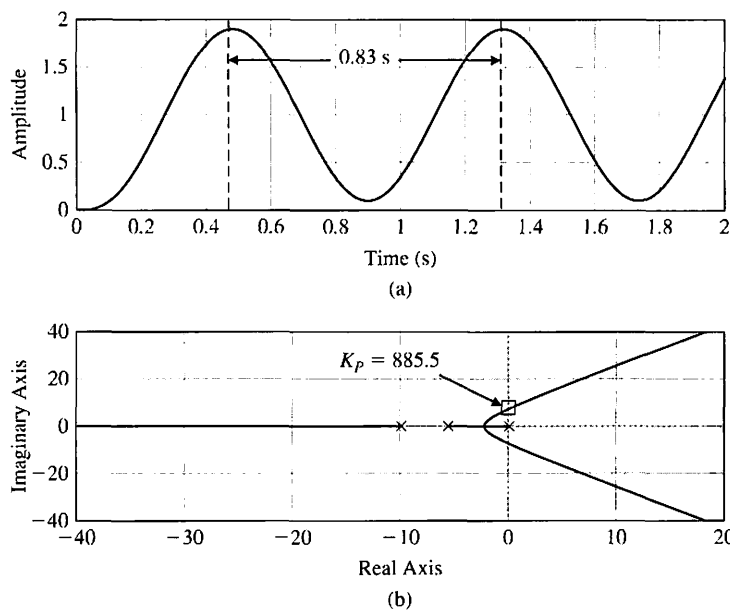


**FIGURE 7.31**  
 (a) Step response with  $K_P = 885.5$ ,  $K_D = 0$ , and  $K_I = 0$ .  
 (b) Root locus showing  $K_P = 885.5$  results in marginal stability with  $s = \pm 7.5j$ .

To begin the manual tuning process, set  $K_I = 0$  and  $K_D = 0$  and increase  $K_P$  until the closed-loop system has sustained oscillations. As can be seen in Figure 7.31a, when  $K_P = 885.5$ , we have a sustained oscillation of magnitude  $A = 1.9$  and period  $P = 0.83$  s. The root locus shown in Figure 7.31b corresponds to the characteristic equation

$$1 + K_P \left[ \frac{1}{s(s + 10)(s + 5.66)} \right] = 0.$$

The root locus shown in Figure 7.31b illustrates that when  $K_P = 885.5$ , we have closed-loop poles at  $s = \pm 7.5j$  leading to the oscillatory behavior in the step response in Figure 7.31a.

Reduce  $K_P = 885.5$  by half as a first step to achieving a step response with approximately a quarter amplitude decay. You may have to iterate on the value  $K_P = 442.75$ . The step response is shown in Figure 7.32 where we note that the peak amplitude is reduced to one-fourth of the maximum value in one period, as desired. To accomplish this reduction, we refined the value of  $K_P$  by slowly reducing the value from  $K_P = 442.75$  to  $K_P = 370$ .

The root locus for  $K_P = 370$ ,  $K_I = 0$ , and  $0 \leq K_D < \infty$  is shown in Figure 7.33. In this case, the characteristic equation is

$$1 + K_D \left[ \frac{s}{(s + 10)(s + 5.66) + K_P} \right] = 0.$$

We see in Figure 7.33 that as  $K_D$  increases, the root locus shows that the closed-loop complex poles move left, and in doing so, increases the associated damping ratio and thereby decreases the percent overshoot. The movement of the complex poles to the left also increases the associated  $\zeta\omega_n$ , thereby reducing the settling time. These

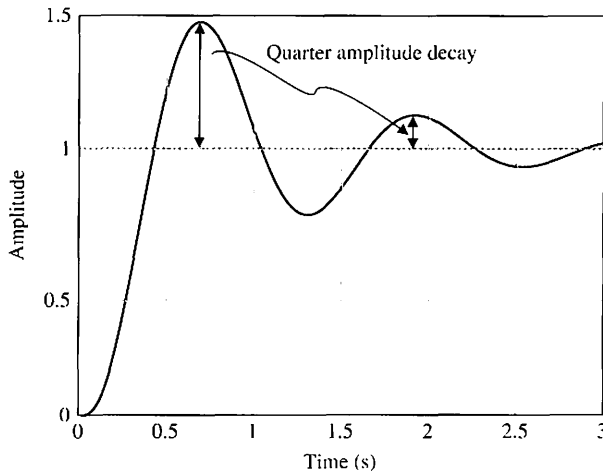


**FIGURE 7.32**  
Step response with  
 $K_P = 370$  showing  
the quarter  
amplitude decay.

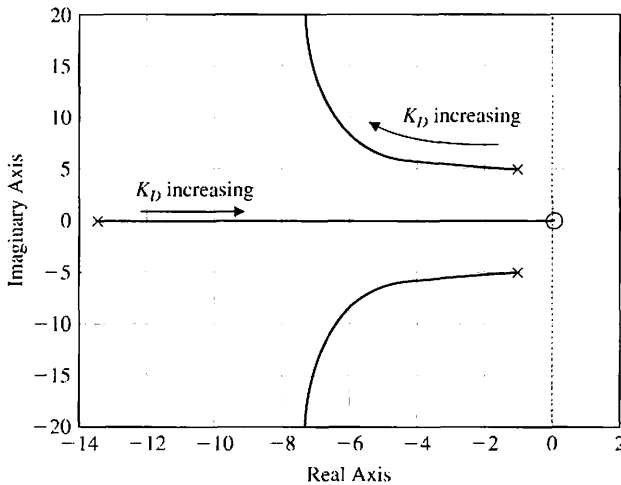


**FIGURE 7.33**  
Root locus for  
 $K_P = 370$ ,  
 $K_I = 0$ , and  
 $0 \leq K_D < \infty$ .

effects of varying  $K_D$  are consistent with information provided in Table 7.6. As  $K_D$  increases (when  $K_D > 75$ ), the real root begins to dominate the response and the trends described in Table 7.6 become less accurate. The percent overshoot and settling time as a function of  $K_D$  are shown in Figure 7.34.

The root locus for  $K_P = 370$ ,  $K_D = 0$ , and  $0 \leq K_I < \infty$  is shown in Figure 7.35. The characteristic equation is

$$1 + K_I \left[ \frac{1}{s(s(s + 10)(s + 5.66) + K_P)} \right] = 0.$$

We see in Figure 7.35 that as  $K_I$  increases, the root locus shows that the closed-loop complex pair poles move right. This decreases the associated damping ratio and thereby increasing the percent overshoot. In fact, when  $K_I = 778.2$ , the system is marginally stable with closed-loop poles at  $s = \pm 4.86j$ . The movement of the

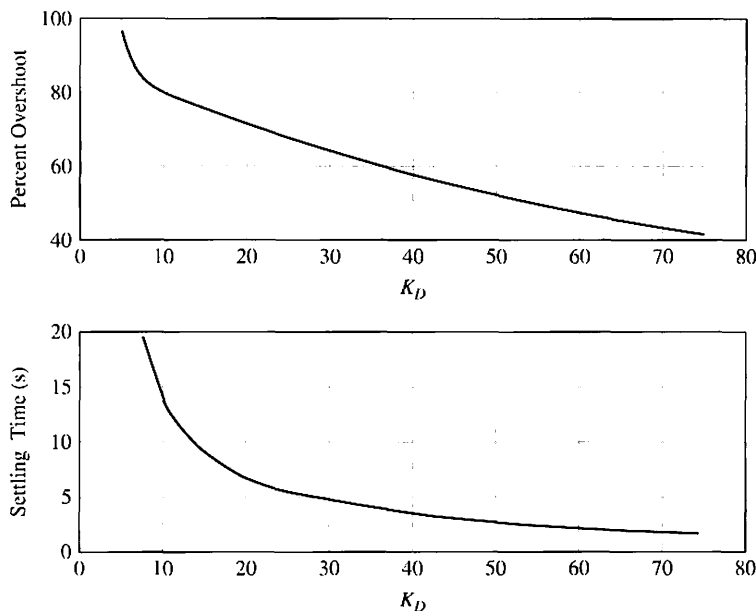


**FIGURE 7.34**  
 Percent overshoot and settling time with  $K_P = 370$ ,  $K_I = 0$ , and  $5 \leq K_D < 75$ .

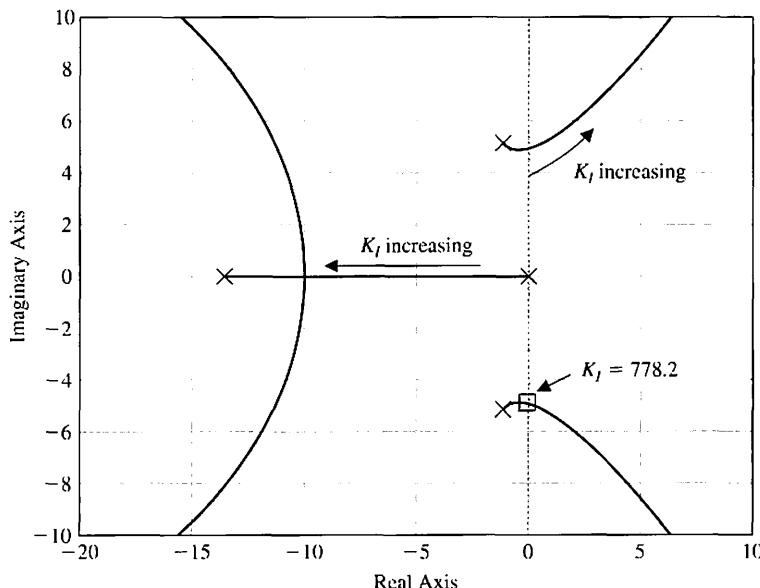


**FIGURE 7.35**  
 Root locus for  $K_P = 370$ ,  $K_D = 0$ , and  $0 \leq K_I < \infty$ .

complex poles to the right also decreases the associated  $\zeta\omega_n$ , thereby increasing the settling time. The percent overshoot and settling time as a function of  $K_I$  are shown in Figure 7.36. The trends in Figure 7.36 are consistent with Table 7.6.

To meet the percent overshoot and settling time specifications, we can select  $K_P = 370$ ,  $K_D = 60$ , and  $K_I = 100$ . The step response shown in Figure 7.37 indicates a  $T_s = 2.4$  s and  $P.O. = 12.8\%$  meeting the specifications. ■

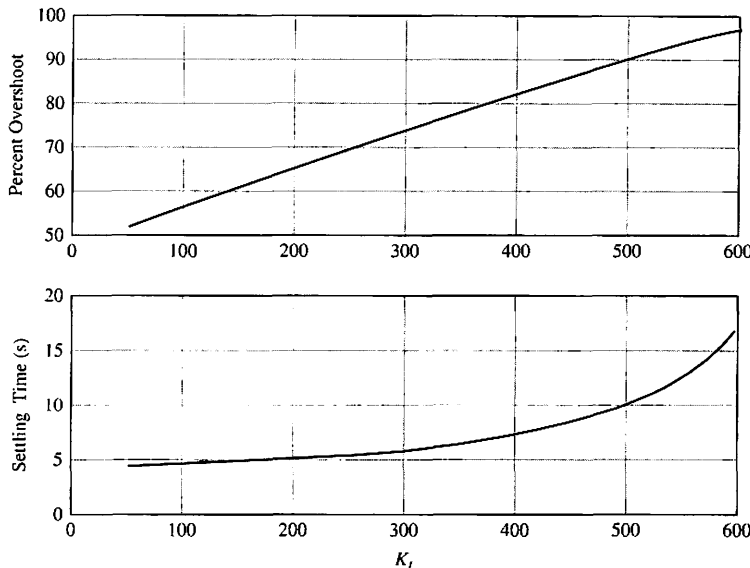


**FIGURE 7.36**  
Percent overshoot  
and settling time  
with  $K_P = 370$ ,  
 $K_D = 0$ , and  
 $50 \leq K_I < 600$ .

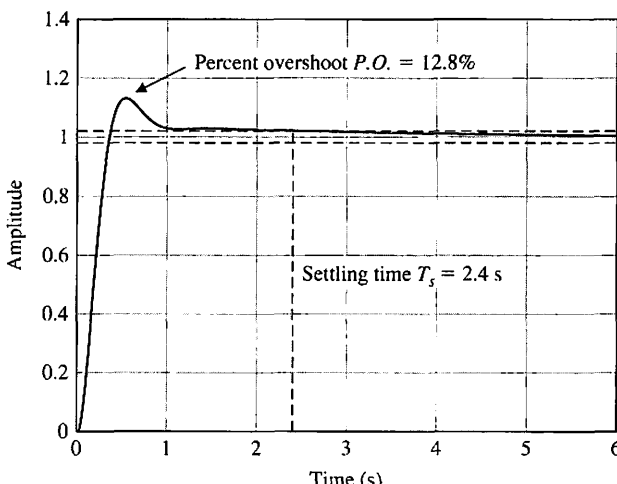


**FIGURE 7.37**  
Percent overshoot  
and settling time  
with final design  
 $K_P = 370$ ,  $K_D = 60$ ,  
and  $K_I = 100$ .

Two important PID controller gain tuning methods were published in 1942 by John G. Ziegler and Nathaniel B. Nichols intended to achieve a fast closed-loop step response without excessive oscillations and excellent disturbance rejection. The two approaches are classified under the general heading of Ziegler-Nichols tuning methods. The first approach is based on closed-loop concepts requiring the computation of the **ultimate gain** and **ultimate period**. The second approach is based on open-loop concepts relying on **reaction curves**. The Ziegler-Nichols tuning methods are based on assumed forms of the models of the process, but the models do not have to be precisely known. This makes the tuning approach very practical in process

**Table 7.7 Ziegler-Nichols PID Tuning Using Ultimate Gain,  $K_U$ , and Oscillation Period,  $P_U$** 

Ziegler-Nichols PID Controller Gain Tuning Using Closed-loop Concepts			
Controller Type	$K_P$	$K_I$	$K_D$
Proportional (P) $G_c(s) = K_P$	$0.5K_U$	-	-
Proportional-plus-integral (PI) $G_c(s) = K_P + \frac{K_I}{s}$	$0.45K_U$	$\frac{0.54K_U}{T_U}$	-
Proportional-plus-integral-plus-derivative (PID) $G_c(s) = K_P + \frac{K_I}{s} + K_D s$	$0.6K_U$	$\frac{1.2K_U}{T_U}$	$\frac{0.6K_U T_U}{8}$

control applications. Our suggestion is to consider the Ziegler-Nichols rules to obtain initial controller designs followed by design iteration and refinement. Remember that the Ziegler-Nichols rules will not work with all plants or processes.

The closed-loop Ziegler-Nichols tuning method considers the closed-loop system response to a step input (or step disturbance) with the PID controller in the loop. Initially the derivative and integral gains,  $K_D$  and  $K_I$ , respectively, are set to zero. The proportional gain  $K_P$  is increased (in simulation or on the actual system) until the closed-loop system reaches the boundary of instability. The gain on the border of instability, denoted by  $K_U$ , is called the ultimate gain. The period of the sustained oscillations, denoted by  $P_U$ , is called the ultimate period. Once  $K_U$  and  $P_U$  are determined, the PID gains are computed using the relationships in Table 7.7 according to the Ziegler-Nichols tuning method.

#### EXAMPLE 7.10 Closed-loop Ziegler-Nichols PID tuning

Re-consider the system in Example 7.9. The plant is

$$G(s) = \frac{1}{s(s + b)(s + 2\zeta\omega_n)},$$

where  $b = 10$ ,  $\zeta = 0.707$ , and  $\omega_n = 4$ . The controller is a PID controller

$$G_c(s) = K_P + \frac{K_I}{s} + K_D s,$$

where the gains  $K_P$ ,  $K_D$ , and  $K_I$  are computed using the formulas in Table 7.7. We found in Example 7.9 that  $K_U = 885.5$  and  $T_U = 0.83$  s. By using the Ziegler-Nichols formulas we obtain

$$K_P = 0.6K_U = 531.3, \quad K_I = \frac{1.2K_U}{T_U} = 1280.2, \quad \text{and} \quad K_D = \frac{0.6K_U T_U}{8} = 55.1.$$

Comparing the step response in Figures 7.37 and 7.38 we note that the settling time is approximately the same for the manually tuned and the Ziegler-Nichols tuned PID controllers. However, the percent overshoot of the manually tuned controller is less than that of the Ziegler-Nichols tuning. This is due to the fact that the

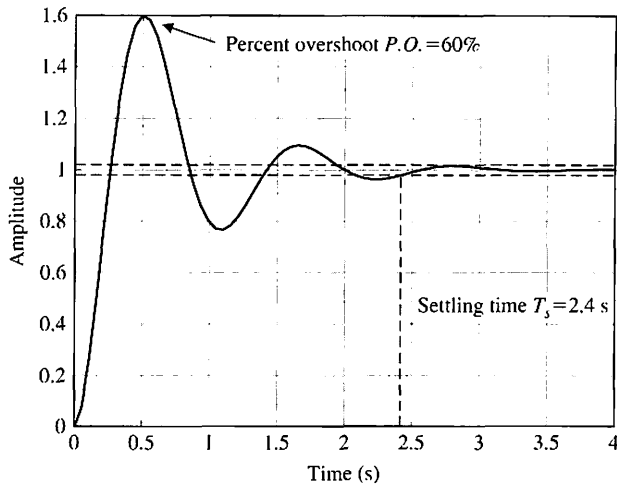


**FIGURE 7.38**  
Time response for the Ziegler-Nichols PID tuning with  $K_P = 531.3$ ,  $K_I = 1280.2$ , and  $K_D = 55.1$ .

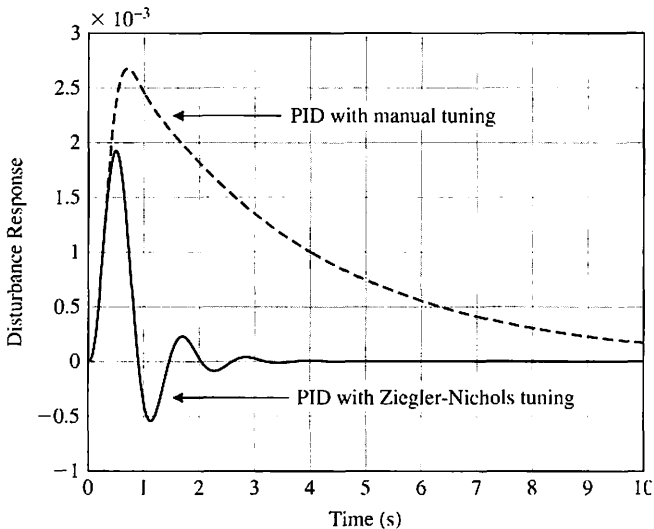


**FIGURE 7.39**  
Disturbance response for the Ziegler-Nichols PID tuning versus the manual tuning in Example 7.9.

Ziegler-Nichols tuning is designed to provide the best disturbance rejection performance rather than the best input response performance.

In Figure 7.39, we see that the step disturbance performance of the Ziegler-Nichols PID controller is indeed better than the manually tuned controller. While Ziegler-Nichols approach provides a structured procedure for obtaining the PID controller gains, the appropriateness of the Ziegler-Nichols tuning depends on the requirements of the problem under investigation. ■

The open-loop Ziegler-Nichols tuning method utilizes a reaction curve obtained by taking the controller off-line (that is, out of the loop) and introducing a step input (or step disturbance). This approach is very commonly used in process control applications. The measured output is the reaction curve and is assumed to

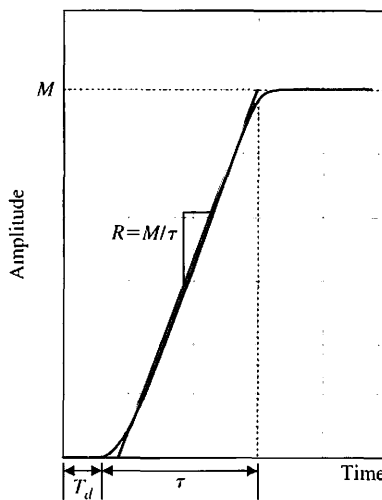


**FIGURE 7.40**  
Reaction curve illustrating parameters  $R$  and  $T_d$  required for the Ziegler-Nichols open-loop tuning method.

have the general shape shown in Figure 7.40. The response in Figure 7.40 implies that the process is a first-order system with a transport delay. If the actual system does not match the assumed form, then another approach to PID tuning should be considered. However, if the underlying system is linear and lethargic (or sluggish and characterized by delay), the assumed model may suffice to obtain a reasonable PID gain selection using the open-loop Ziegler-Nichols tuning method.

The reaction curve is characterized by the transport delay,  $T_d$ , and the reaction rate,  $R$ . Generally, the reaction curve is recorded and numerical analysis is performed to obtain estimates of the parameters  $T_d$  and  $R$ . A system possessing the reaction curve shown in Figure 7.40 can be approximated by a first-order system with a transport delay as

$$G(s) = M \left[ \frac{p}{s + p} \right] e^{-T_d s},$$

**Table 7.8 Ziegler-Nichols PID Tuning Using Reaction Curve Characterized by Time Delay,  $T_d$ , and Reaction Rate,  $R$**

Ziegler-Nichols PID Controller Gain Tuning Using Open-loop Concepts			
Controller Type	$K_P$	$K_I$	$K_D$
Proportional (P) $G_c(s) = K_P$	$\frac{1}{RT_d}$	—	—
Proportional-plus-integral (PI) $G_c(s) = K_P + \frac{K_I}{s}$	$\frac{0.9}{RT_d}$	$\frac{0.27}{RT_d^2}$	—
Proportional-plus-integral-plus-derivative (PID) $G_c(s) = K_P + \frac{K_I}{s} + K_D s$	$\frac{1.2}{RT_d}$	$\frac{0.6}{RT_d^2}$	$\frac{0.6}{R}$

where  $M$  is the magnitude of the response at steady-state,  $T_d$  is the transport delay, and  $p$  is related to the slope of the reaction curve. The parameters  $M$ ,  $\tau$ , and  $T_d$  can be estimated from the open-loop step response and then utilized to compute  $R = M/\tau$ . Once that is accomplished, the PID gains are computed as shown in Table 7.8. You can also use the Ziegler-Nichols open-loop tuning method to design a proportional controller or a proportional-plus-integral controller.

#### EXAMPLE 7.11 Open-loop Ziegler-Nichols PI controller tuning

Consider the reaction curve shown in Figure 7.41. We estimate the transport lag to be  $T_d = 0.1$  s and the reaction rate  $R = 0.8$ .

Using the Ziegler-Nichols tuning for the PI controller gains we have

$$K_P = \frac{0.9}{RT_d} = 11.25 \quad \text{and} \quad K_I = \frac{0.27}{RT_d^2} = 33.75.$$

The closed-loop system step response (assuming unity feedback) is shown in Figure 7.42. The settling time is  $T_s = 1.28$  s and the percent overshoot is  $P.O. = 78\%$ . Since we are using a PI controller, the steady-state is zero, as expected. ■

The manual tuning method and the two Ziegler-Nichols tuning approaches presented here will not always lead to the desired closed-loop performance. The three methods do provide structured design steps leading to candidate PID gains and should be viewed as first steps in the design iteration. Since the PID (and the related PD and PI) controllers are in wide use today in a variety of applications, it is important to become familiar with various design approaches. We will use the PD controller later in this chapter to control the hard disk drive sequential design problem (see Section 7.10).

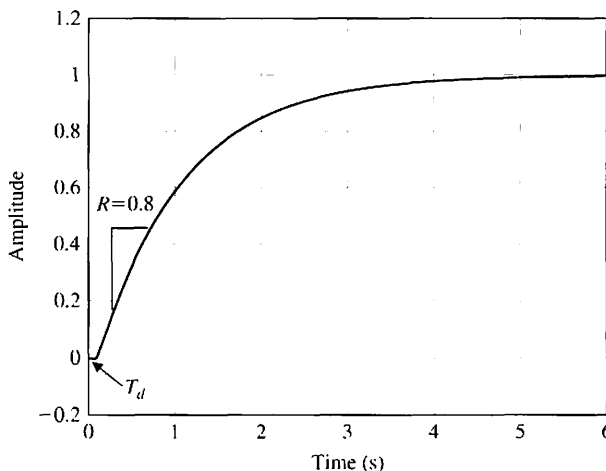


**FIGURE 7.41**  
Reaction curve with  
 $T_d = 0.1$  s and  
 $R = 0.8$ .

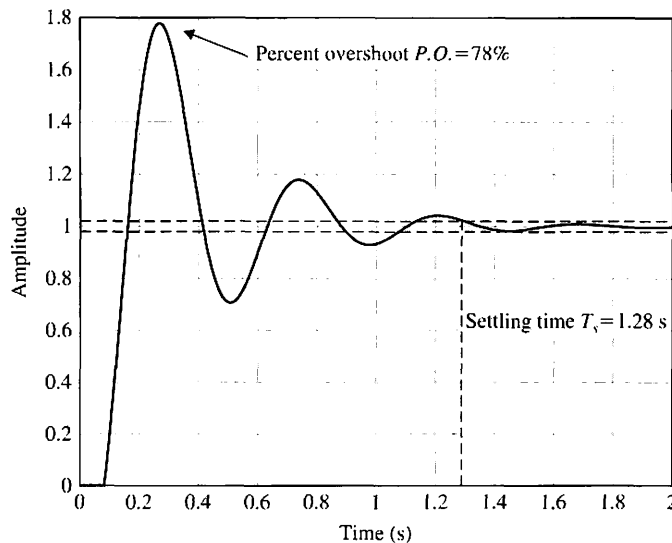


**FIGURE 7.42**  
Time response for the Ziegler-Nichols PI tuning with  $K_P = 11.25$  and  $K_I = 33.75$ .

## 7.7 NEGATIVE GAIN ROOT LOCUS

As discussed in Section 7.2, the dynamic performance of a closed-loop control system is described by the closed-loop transfer function, that is, by the poles and zeros of the closed-loop system. The root locus is a graphical illustration of the variation of the roots of the characteristic equation as a single parameter of interest varies. We know that the roots of the characteristic equation and the closed-loop poles are one in the same. In the case of the single-loop negative unity feedback system shown in Figure 7.1, the characteristic equation is

$$1 + KG(s) = 0, \quad (7.99)$$

where  $K$  is the parameter of interest. The orderly seven-step procedure for sketching the root locus described in Section 7.3 and summarized in Table 7.2 is valid for the case where  $0 \leq K < \infty$ . Sometimes the situation arises where we are interested in the root locus for negative values of the parameter of interest where  $-\infty < K \leq 0$ . We refer to this as the **negative gain root locus**. Our objective here is to develop an orderly procedure for sketching the negative gain root locus using familiar concepts from root locus sketching as described in Section 7.2.

Rearranging Equation (7.99) yields

$$G(s) = -\frac{1}{K}.$$

Since  $K$  is negative, it follows that

$$|KG(s)| = 1 \quad \text{and} \quad KG(s) = 0^\circ + k360^\circ \quad (7.100)$$

where  $k = 0, \pm 1, \pm 2, \pm 3, \dots$ . The magnitude and phase conditions in Equation (7.100) must both be satisfied for all points on the negative gain root locus. Note

that the phase condition in Equation (7.100) is different from the phase condition in Equation (7.4). As we will show, the new phase condition leads to several key modifications in the root locus sketching steps from those summarized in Table 7.2.

### EXAMPLE 7.12 Negative gain root locus

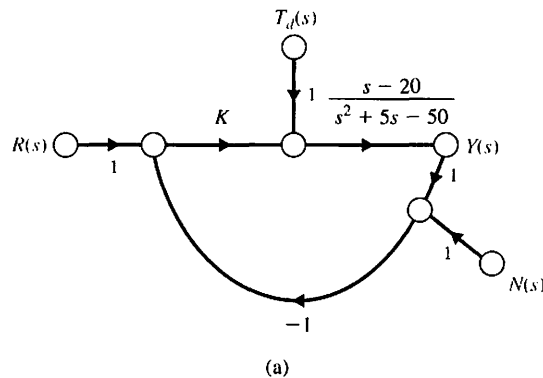
Consider the system shown in Figure 7.43. The loop transfer function is

$$L(s) = KG(s) = K \frac{s - 20}{s^2 + 5s - 50}$$

and the characteristic equation is

$$1 + K \frac{s - 20}{s^2 + 5s - 50} = 0.$$

Sketching the root locus yields the plot shown in Figure 7.44a where it can be seen that the closed-loop system is not stable for any  $0 \leq K < \infty$ . The negative gain root locus is shown in Figure 7.44b. Using the negative gain root locus in Figure 7.44b we find that the stability is  $-5.0 < K < -2.5$ . The system in Figure 7.43 can thus be stabilized with only negative gain,  $K$ . ■



(a)

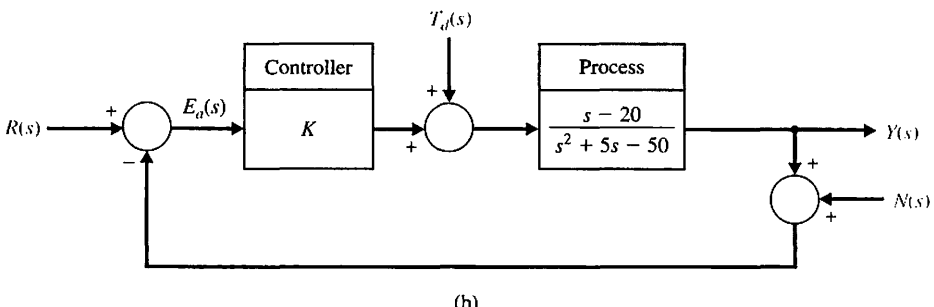


**FIGURE 7.43**  
 (a) Signal flow graph and (b) block diagram of unity feedback system with controller gain,  $K$ .

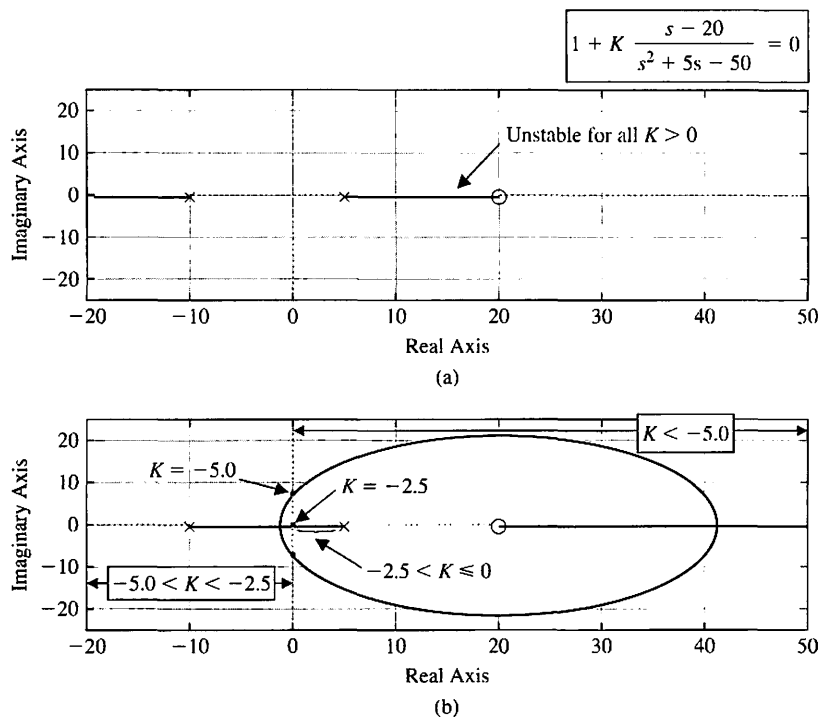


**FIGURE 7.44**  
 (a) Root locus for  $0 \leq K < \infty$ .  
 (b) Negative gain root locus for  $-\infty < K \leq 0$ .

To locate the roots of the characteristic equation in a graphical manner on the  $s$ -plane for negative values of the parameter of interest, we will re-visit the seven steps summarized in Table 7.2 to obtain a similar orderly procedure to facilitate the rapid sketching of the locus.

**Step 1:** Prepare the root locus sketch. As before, you begin by writing the characteristic equation and rearranging, if necessary, so that the parameter of interest,  $K$ , appears as the multiplying factor in the form,

$$1 + KP(s) = 0. \quad (7.101)$$

For the negative gain root locus, we are interested in determining the locus of roots of the characteristic equation in Equation (7.101) for  $-\infty < K \leq 0$ . As in Equation (7.24), factor  $P(s)$  in Equation (7.101) in the form of poles and zeros and locate the poles and zeros on the  $s$ -plane with 'x' to denote poles and 'o' to denote zeros.

When  $K = 0$ , the roots of the characteristic equation are the poles of  $P(s)$ , and when  $K \rightarrow -\infty$  the roots of the characteristic equation are the zeros of  $P(s)$ . Therefore, the locus of the roots of the characteristic equation begins at the poles of  $P(s)$  when  $K = 0$  and ends at the zeros of  $P(s)$  as  $K \rightarrow -\infty$ . If  $P(s)$  has  $n$  poles and  $M$  zeros and  $n > M$ , we have  $n - M$  branches of the root locus approaching the zeros at infinity and the number of separate loci is equal to the number of poles. The root loci are symmetrical with respect to the horizontal real axis because the complex roots must appear as pairs of complex conjugate roots.

**Step 2:** Locate the segments of the real axis that are root loci. The root locus on the real axis always lies in a section of the real axis to the left of an **even** number of poles and zeros. This follows from the angle criterion of Equation (7.100).

**Step 3:** When  $n > M$ , we have  $n - M$  branches heading to the zeros at infinity as  $K \rightarrow -\infty$  along asymptotes centered at  $\sigma_A$  and with angles  $\phi_A$ . The linear asymptotes are centered at a point on the real axis given by

$$\sigma_A = \frac{\sum \text{poles of } P(s) - \sum \text{zeros of } P(s)}{n - M} = \frac{\sum_{j=1}^n (-p_j) - \sum_{i=1}^M (-z_i)}{n - M}. \quad (7.102)$$

The angle of the asymptotes with respect to the real axis is

$$\phi_A = \frac{2k + 1}{n - M} 360^\circ \quad k = 0, 1, 2, \dots, (n - M - 1), \quad (7.103)$$

where  $k$  is an integer index.

**Step 4:** Determine where the locus crosses the imaginary axis (if it does so), using the Routh-Hurwitz criterion.

**Step 5:** Determine the breakaway point on the real axis (if any). In general, due to the phase criterion, the tangents to the loci at the breakaway point are equally spaced over  $360^\circ$ . The breakaway point on the real axis can be evaluated graphically or analytically. The breakaway point can be computed by rearranging the characteristic equation

$$1 + K \frac{n(s)}{d(s)} = 0$$

as

$$p(s) = K,$$

where  $p(s) = -d(s)/n(s)$  and finding the values of  $s$  that maximize  $p(s)$ . This is accomplished by solving the equation

$$n(s) \frac{d[d(s)]}{ds} - d(s) \frac{d[n(s)]}{ds} = 0. \quad (7.104)$$

Equation (7.104) yields a polynomial equation in  $s$  of degree  $n + M - 1$ , where  $n$  is the number of poles and  $M$  is the number of zeros. Hence the number of solutions is  $n + M - 1$ . The solutions that exist on the root locus are the breakaway points.

**Step 6:** Determine the angle of departure of the locus from a pole and the angle of arrival of the locus at a zero using the phase angle criterion. The angle of locus departure from a pole or angle of arrival at a zero is the difference between the net angle due to all other poles and zeros and the criterion angle of  $\pm k 360^\circ$ .

**Step 7:** The final step is to complete the sketch by drawing in all sections of the locus not covered in the previous six steps.

The seven steps for sketching a negative gain root locus are summarized in Table 7.9.

**Table 7.9 Seven Steps for Sketching a Negative Gain Root Locus (color text denotes changes from root locus steps in Table 7.2)**

Step	Related Equation or Rule
1. Prepare the root locus sketch.	
(a) Write the characteristic equation so that the parameter of interest, $K$ , appears as a multiplier.	(a) $1 + KP(s) = 0$
(b) Factor $P(s)$ in terms of $n$ poles and $M$ zeros	(b) $1 + K \frac{\prod_{i=1}^M (s + z_i)}{\prod_{j=1}^n (s + p_j)} = 0$
(c) Locate the open-loop poles and zeros of $P(s)$ in the $s$ -plane with selected symbols.	(c) $\times$ = poles, $\circ$ = zeros
(d) Determine the number of separate loci, $SL$ .	(d) Locus begins at a pole and ends at a zero. $SL = n$ when $n \geq M$ ; $n$ = number of finite poles, $M$ = number of finite zeros.
(e) The root loci are symmetrical with respect to the horizontal real axis.	
2. Locate the segments of the real axis that are root loci.	Locus lies to the left of an even number of poles and zeros.
3. The loci proceed to the zeros at infinity along asymptotes centered at $\sigma_A$ and with angles $\phi_A$ .	$\sigma_A = \frac{\sum_{j=1}^n (-p_j) - \sum_{i=1}^M (-z_i)}{n - M}$
4. Determine the points at which the locus crosses the imaginary axis (if it does so).	$\phi_A = \frac{2k + 1}{n - M} 360^\circ, k = 0, 1, 2, \dots (n - M - 1)$
5. Determine the breakaway point on the real axis (if any).	Use Routh-Hurwitz criterion (see Section 6.2).
6. Determine the angle of locus departure from complex at or poles and the angle of locus arrival at complex zeros using the phase criterion.	a) Set $K = p(s)$ b) Determine roots of $dp(s)/ds = 0$ or use graphical method to find maximum of $p(s)$ . $\angle P(s) = \pm k 360^\circ \text{ at } s = -p_j \text{ or } -z_i$
7. Complete the negative gain root locus sketch.	

## 7.8 DESIGN EXAMPLES

In this section we present four illustrative examples. The first example is a wind turbine control system. The feedback control system uses a PI controller to achieve a fast settling time and rise time while limiting the percent overshoot to a step input. The second example is a laser manipulator control system. Here the root locus method is used to show how the closed-loop system poles move in the  $s$ -plane as the proportional controller amplifier gain varies. The second example considers a simplified robotic replication facility. In the example, the system is represented by a fifth-order transfer function model. The feedback control strategy employs a velocity feedback coupled with a controller in the forward loop. Root locus design methods are used to select the two feedback controller gains. In the final example, the

automatic control of the velocity of an automobile is considered. In this example, the root locus method is extended from one parameter to three parameters as the three gains of a PID controller are determined. The design process is emphasized, including considering the control goals and associated variables to be controlled, the design specifications, and the PID controller design using root locus methods.

#### EXAMPLE 7.13 Wind turbine speed control

Wind energy conversion to electric power is achieved by wind energy turbines connected to electric generators. Of particular interest are wind turbines, as shown in Figure 7.45, that are located offshore [33]. The new concept is to allow the wind turbine to float rather than positioning the structure on a tower tied deep into the ocean floor. This allows the wind turbine structure to be placed in deeper waters up to 100 miles offshore far enough not to burden the landscape with unsightly structures [34]. Moreover, the wind is generally stronger on the open ocean potentially leading to the production of 5 MW versus the more typical 1.5 MW for wind turbines onshore. However, the irregular character of wind direction and power results in the need for reliable, steady electric energy by using control systems for the wind turbines. The goal of these control devices is to reduce the effects of wind intermittency and of wind direction change. The rotor and generator speed control can be achieved by adjusting the pitch angle of the blades.

A basic model of the generator speed control system is shown in Figure 7.46 [35]. A linearized model from the collective pitch to the generator speed is given by<sup>1</sup>

$$G(s) = \frac{4.2158(s - 827.1)(s^2 - 5.489s + 194.4)}{(s + 0.195)(s^2 + 0.101s + 482.6)}. \quad (7.105)$$

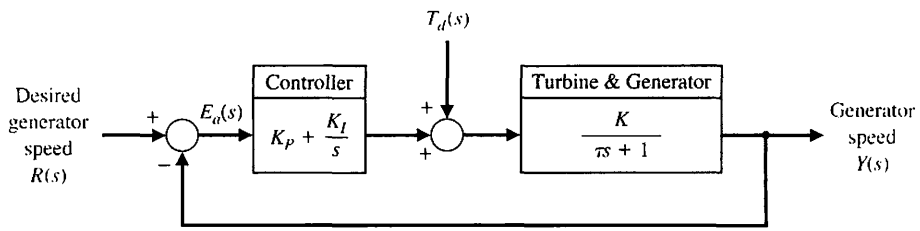
The model corresponds to a 600 KW turbine with hub height = 36.6 m, rotor diameter = 40 m, rated rotor speed = 41.7 rpm, rated generator speed = 1800 rpm,



**FIGURE 7.45**  
Wind turbine placed offshore can help alleviate the energy needs. (Photo courtesy of Alamy Images.)

<sup>1</sup> Provided by Dr. Lucy Pao and Jason Laks in private correspondence.

**FIGURE 7.46**  
Wind turbine generator speed control system.



and maximum pitch rate = 18.7 deg/sec. Note that the linearized model in Equation (7.105) has zeros in the right half-plane at  $s_1 = 827.1$  and  $s_{2,3} = 0.0274 \pm 0.1367j$  making this a nonminimum phase system (see Chapter 8 for more information on nonminimum phase systems).

A simplified version of the model in Equation (7.105) is given by the transfer function

$$G(s) = \frac{K}{\tau s + 1}, \quad (7.106)$$

where  $\tau = 5$  seconds and  $K = -7200$ . We will design a PI controller to control the speed of the turbine generator using the simplified first-order model in Equation (7.106) and confirm that the design specifications are satisfied for both the first-order model and the third-order model in Equation (7.105). The PI controller, denoted by  $G_c(s)$ , is given by

$$G_c(s) = K_P + \frac{K_I}{s} = K_P \left[ \frac{s + \tau_c}{s} \right],$$

where  $\tau_c = K_I/K_P$  and the gains  $K_P$  and  $K_I$  are to be determined. A stability analysis indicates that negative gains  $K_I < 0$  and  $K_P < 0$  will stabilize the system. The main design specification is to have a settling time  $T_s < 4$  seconds to a unit step input. We also desire a limited percent overshoot ( $P.O. < 25\%$ ) and a short rise time ( $T_r < 1$  s) while meeting the settling time specification. To this end, we will target the damping ratio of the dominant roots to be  $\zeta > 0.4$  and the natural frequency  $\omega_n > 2.5$  rad/s.

The root locus is shown in Figure 7.47 for the characteristic equation

$$1 + \hat{K}_P \left[ \frac{s + \tau_c}{s} \frac{7200}{5s + 1} \right] = 0,$$

where  $\tau_c = 2$  and  $\hat{K}_P = -K_P > 0$ . The placement of the controller zero at  $s = -\tau_c = -2$  is a design parameter. We select the value of  $\hat{K}_P$  such that the damping ratio of the closed-loop complex poles is  $\zeta = 0.707$ . Selecting  $\hat{K}_P = 0.0025$  yields  $K_P = -0.0025$  and  $K_I = -0.005$ . The PI controller is

$$G_c(s) = K_P + \frac{K_I}{s} = -0.0025 \left[ \frac{s + 2}{s} \right].$$

The step response is shown in Figure 7.48 using the simplified first-order model in Equation (7.106). The step response has  $T_s = 1.8$  seconds,  $T_r = 0.34$  seconds, and  $\zeta = 0.707$  which translates to  $P.O. = 19\%$ . The PI controller is able to meet all the control specifications. The step response using the third-order model in Equation (7.105) is shown in Figure 7.49 where we see the effect of the neglected components in the design as small oscillations in the speed response. The closed-loop impulse disturbance response in Figure 7.50 shows fast and accurate rejection of the disturbance in less than 3 seconds due to a  $1^\circ$  pitch angle change. ■

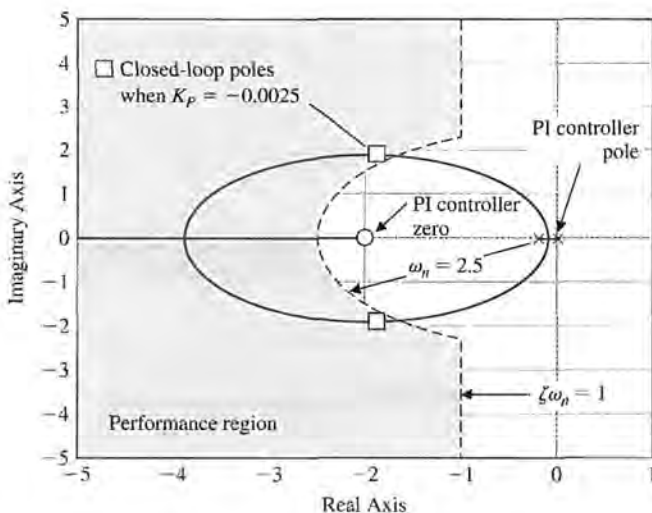


**FIGURE 7.47**  
Wind turbine  
generator speed  
control root locus  
with a PI controller.

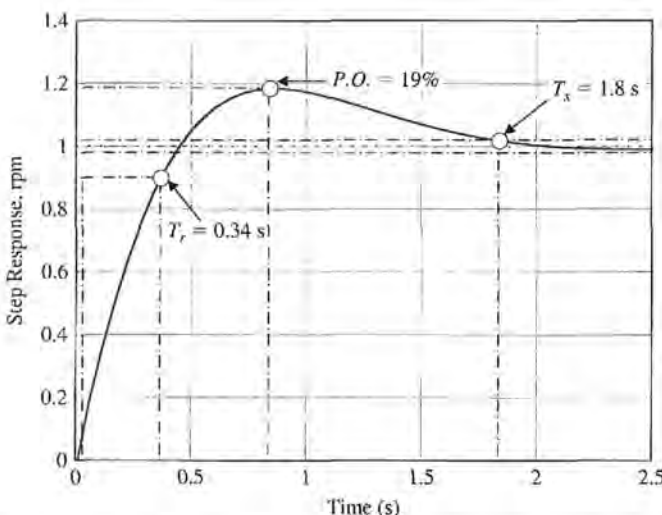


**FIGURE 7.48** Step response of the wind turbine generator speed control system using the first-order model in Equation (7.106) with the designed PI controller showing all specifications are satisfied with  $P.O. = 19\%$ ,  $T_s = 1.8$  s, and  $T_r = 0.34$  s.

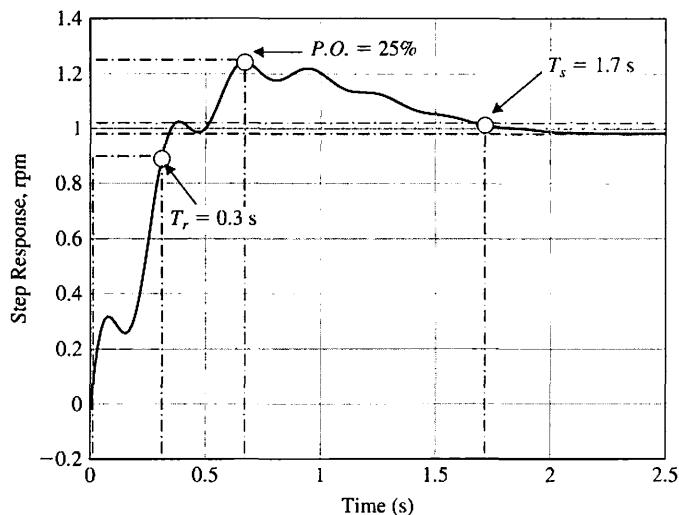


**FIGURE 7.49** Step response of the third-order model in Equation (7.105) with the PI controller showing that all specifications are satisfied with  $P.O. = 25\%$ ,  $T_s = 1.7$  s, and  $T_r = 0.3$  s.

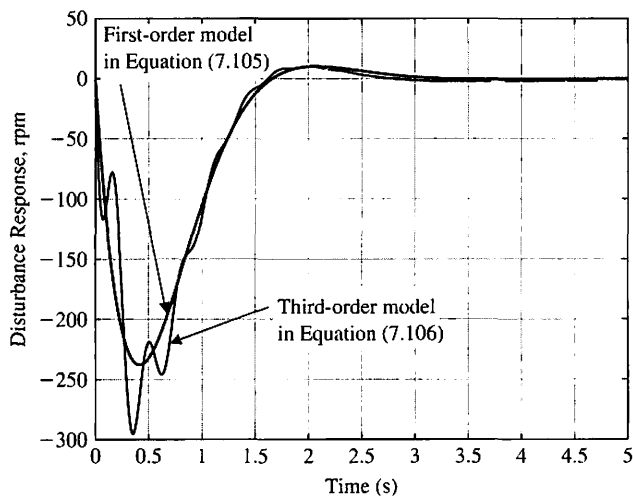


**FIGURE 7.50** Disturbance response of the wind turbine generator speed control system with a PI controller shows excellent disturbance rejection characteristics.

#### EXAMPLE 7.14 Laser manipulator control system

Lasers can be used to drill the hip socket for the appropriate insertion of an artificial hip joint. The use of lasers for surgery requires high accuracy for position and velocity response. Let us consider the system shown in Figure 7.51, which uses a DC motor manipulator for the laser. The amplifier gain  $K$  must be adjusted so that the steady-state error for a ramp input,  $r(t) = At$  (where  $A = 1$  mm/s), is less than or equal to 0.1 mm, while a stable response is maintained.

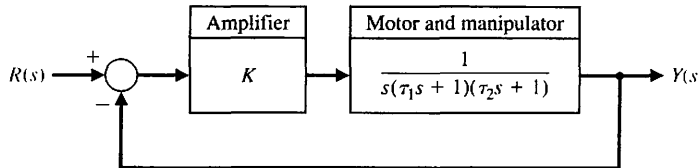


**FIGURE 7.51**  
Laser manipulator control system.

To obtain the steady-state error required and a good response, we select a motor with a field time constant  $\tau_1 = 0.1$  s and a motor-plus-load time constant  $\tau_2 = 0.2$  s. We then have

$$\begin{aligned} T(s) &= \frac{KG(s)}{1 + KG(s)} = \frac{K}{s(\tau_1 s + 1)(\tau_2 s + 1) + K} \\ &= \frac{K}{0.02s^3 + 0.3s^2 + s + K} = \frac{50K}{s^3 + 15s^2 + 50s + 50K}. \end{aligned} \quad (7.107)$$

The steady-state error for a ramp,  $R(s) = A/s^2$ , from Equation (5.29), is

$$e_{ss} = \frac{A}{K_v} = \frac{A}{K}.$$

Since we desire  $e_{ss} = 0.1$  mm (or less) and  $A = 1$  mm, we require  $K = 10$  (or greater).

To ensure a stable system, we obtain the characteristic equation from Equation (7.107) as

$$s^3 + 15s^2 + 50s + 50K = 0.$$

Establishing the Routh array, we have

$s^3$	1	50	
$s^2$	15	$50K$	
$s^1$	$b_1$	0	,
$s_0$	50K		

where

$$b_1 = \frac{750 - 50K}{15}.$$

Therefore, the system is stable for

$$0 \leq K \leq 15.$$

The characteristic equation can be written as

$$1 + K \frac{50}{s^3 + 15s^2 + 50s} = 0.$$

The root locus for  $K > 0$  is shown in Figure 7.52. Using  $K = 10$  results in a stable system that also satisfies the steady-state tracking error specification. The roots at  $K = 10$  are  $-r_2 = -13.98$ ,  $-r_1 = -0.51 + j5.96$ , and  $-\hat{r}_1$ . The  $\zeta$  of the complex

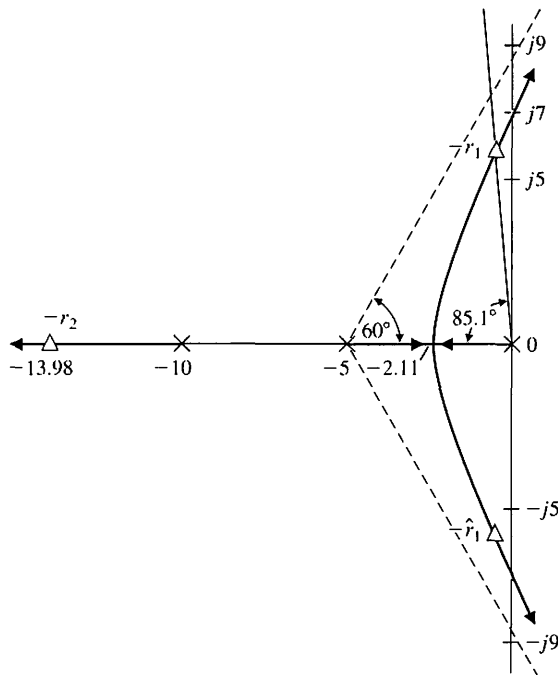


**FIGURE 7.52**  
Root locus for a  
laser control  
system.

roots is 0.085 and  $\zeta\omega_n = 0.51$ . Thus, assuming that the complex roots are dominant, we expect (using Equation 5.16 and 5.13) a step input to have an overshoot of 76% and a settling time (to within 2% of the final value) of

$$T_s = \frac{4}{\zeta\omega_n} = \frac{4}{0.51} = 7.8 \text{ s.}$$

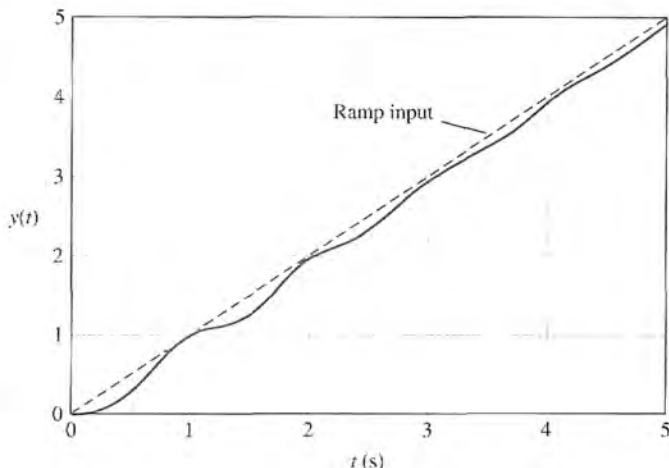
Plotting the actual system response, we find that the overshoot is 70% and the settling time is 7.5 seconds. Thus, the complex roots are essentially dominant. The system response to a step input is highly oscillatory and cannot be tolerated for laser surgery. The command signal must be limited to a low-velocity ramp signal. The response to a ramp signal is shown in Figure 7.53. ■

#### EXAMPLE 7.15 Robot control system

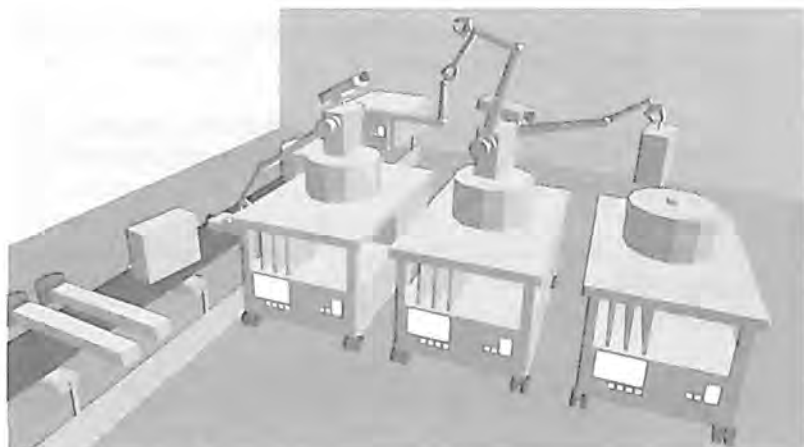
The concept of robot replication is relatively easy to grasp. The central idea is that robots replicate themselves and develop a factory that automatically produces robots. An example of a robot replication facility is shown in Figure 7.54. To achieve the rapid and accurate control of a robot, it is important to keep the robotic arm stiff and yet lightweight [6].

The specifications for controlling the motion of the arm are (1) a settling time to within 2% of the final value of less than 2 seconds, (2) a percent overshoot of less than 10% for a step input, and (3) a steady-state error of zero for a step input.

The block diagram of the proposed system with a controller is shown in Figure 7.55. The configuration proposes the use of velocity feedback as well as

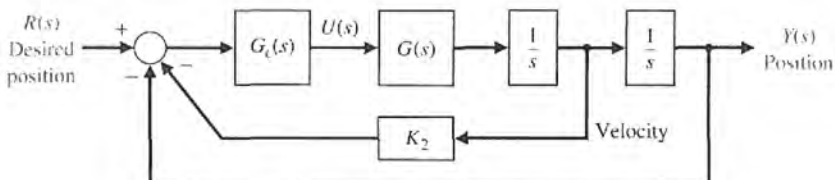
**FIGURE 7.53**

The response to a ramp input for a laser control system.

**FIGURE 7.54**

A robot replication facility.

**FIGURE 7.55**  
Proposed configuration for control of the lightweight robotic arm.



the use of a controller  $G_c(s)$ . The transfer function of the arm is

$$\frac{Y(s)}{U(s)} = \frac{1}{s^2} G(s)$$

where

$$G(s) = \frac{(s^2 + 4s + 10004)(s^2 + 12s + 90036)}{(s + 10)(s^2 + 2s + 2501)(s^2 + 6s + 22509)}$$

The complex zeros are located at

$$s = -2 \pm j100 \quad \text{and} \quad s = -6 \pm j300.$$

The complex poles are located at

$$s = -1 \pm j50 \quad \text{and} \quad s = -3 \pm j150.$$

A sketch of the root locus when  $K_2 = 0$  and the controller is an adjustable gain,  $G_c(s) = K_1$ , is shown in Figure 7.56. The system is unstable since two roots of the characteristic equation appear in the right-hand  $s$ -plane for  $K_1 > 0$ .

It is clear that we need to introduce the use of velocity feedback by setting  $K_2$  to a positive magnitude. Then we have  $H(s) = 1 + K_2s$ ; therefore, the loop transfer function is

$$\frac{1}{s^2} G_c(s) G(s) H(s) = \frac{K_1 K_2 \left( s + \frac{1}{K_2} \right) (s^2 + 4s + 10004)(s^2 + 12s + 90036)}{s^2(s + 10)(s^2 + 2s + 2501)(s^2 + 6s + 22509)},$$

where  $K_1$  is the gain of  $G_c(s)$ . We now have available two parameters,  $K_1$  and  $K_2$ , that we may adjust. We select  $5 < K_2 < 10$  in order to place the adjustable zero near the origin.

When  $K_2 = 5$  and  $K_1$  is varied, we obtain the root locus sketched in Figure 7.57. When  $K_1 = 0.8$  and  $K_2 = 5$ , we obtain a step response with a percent overshoot of 12% and a settling time of 1.8 seconds. This is the optimum achievable response. If we try  $K_2 = 7$  or  $K_2 = 4$ , the overshoot will be larger than desired. Therefore, we have achieved the best performance with this system. If we desired to continue the design process, we would use a controller  $G_c(s)$  with a pole and zero in addition to retaining the velocity feedback with  $K_2 = 5$ .

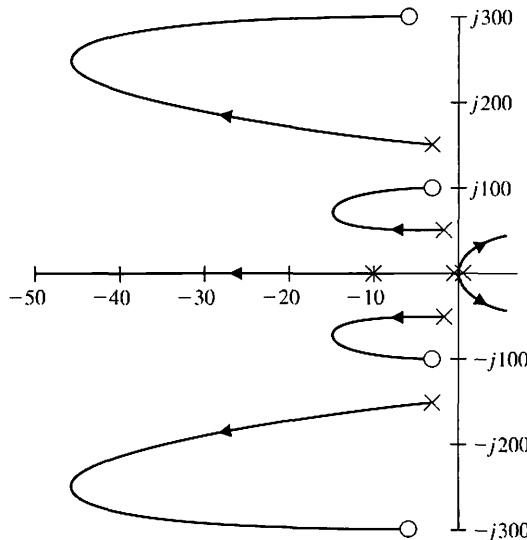


**FIGURE 7.56**  
Root locus of the system if  
 $K_2 = 0$ ,  $K_1$  is varied from  $K_1 = 0$  to  $K_1 = \infty$ , and  $G_c(s) = K_1$ .

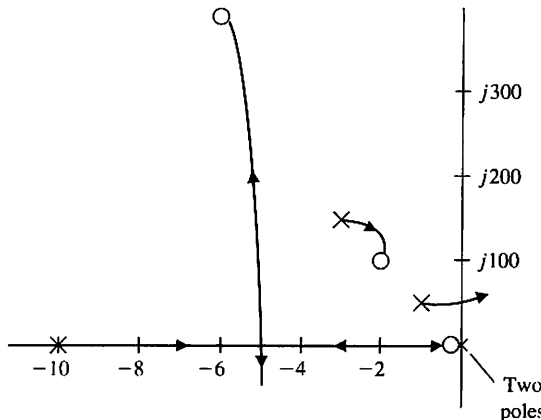


**FIGURE 7.57**  
Root locus for the robot controller with a zero inserted at  $s = -0.2$  with  $G_c(s) = K_1$ .

One possible selection of a controller is

$$G_c(s) = \frac{K_1(s + z)}{s + p}.$$

If we select  $z = 1$  and  $p = 5$ , then, when  $K_1 = 5$ , we obtain a step response with an overshoot of 8% and a settling time of 1.6 seconds. ■

#### EXAMPLE 7.16 Automobile velocity control

The automotive electronics market is expected to reach \$243 billion by 2015. It is predicted that there will be growth of about 6.4% up to the year 2015 in electronic braking, steering, and driver information. Much of the additional computing power will be used for new technology for smart cars and smart roads, such as IVHS (intelligent vehicle/highway systems) [14, 30, 31]. New systems on-board the automobile will support semi-autonomous automobiles, safety enhancements, emission reduction, and other features including intelligent cruise control, and brake by wire systems eliminating the hydraulics [32].

The term IVHS refers to a varied assortment of electronics that provides real-time information on accidents, congestion, and roadside services to drivers and traffic controllers. IVHS also encompasses devices that make vehicles more autonomous: collision-avoidance systems and lane-tracking technology that alert drivers to impending disasters and allow a car to drive itself.

An example of an automated highway system is shown in Figure 7.58. A velocity control system for maintaining the velocity between vehicles is shown in Figure 7.59. The output  $Y(s)$  is the relative velocity of the two automobiles; the input  $R(s)$  is the desired relative velocity between the two vehicles. Our design goal is to develop a controller that can maintain the prescribed velocity between the vehicles and maneuver the active vehicle (in this case the rearward automobile) as commanded. The elements of the design process emphasized in this example are depicted in Figure 7.60.

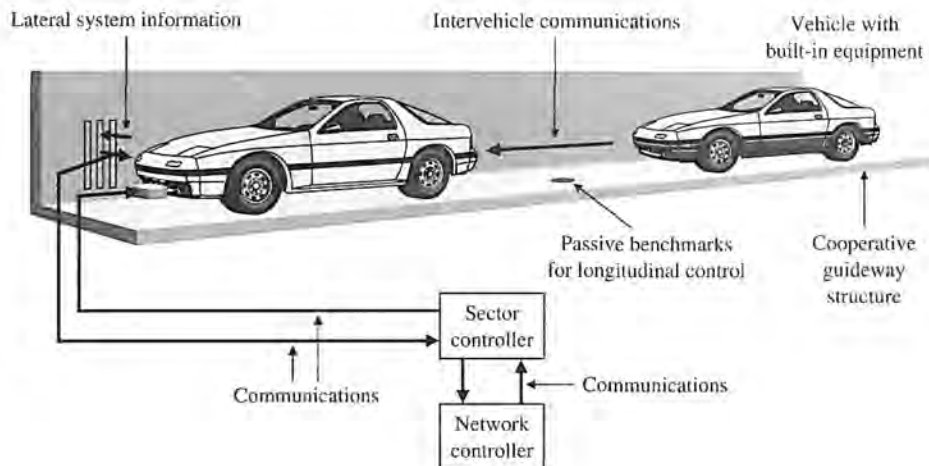
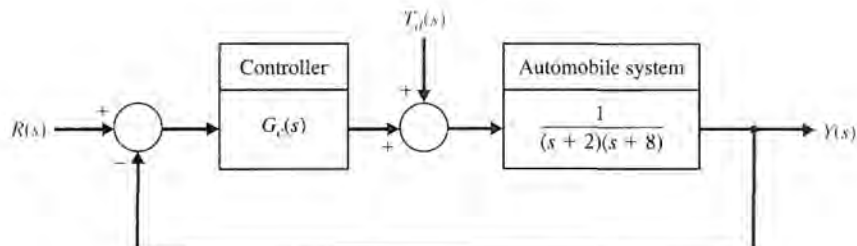


**FIGURE 7.58**  
Automated  
highway system.



The control goal is

#### Control Goal

Maintain the prescribed velocity between the two vehicles, and maneuver the active vehicle as commanded.

The variable to be controlled is the relative velocity between the two vehicles:

#### Variable to Be Controlled

The relative velocity between vehicles, denoted by  $y(t)$ .

The design specifications are

#### Design Specifications

**DS1** Zero steady-state error to a step input.

**DS2** Steady-state error due to a ramp input of less than 25% of the input magnitude.

**DS3** Percent overshoot less than 5% to a step input.

**DS4** Settling time less than 1.5 seconds to a step input (using a 2% criterion to establish settling time).

From the design specifications and knowledge of the open-loop system, we find that we need a type 1 system to guarantee a zero steady-state error to a step input. The open-loop system transfer function is a type 0 system; therefore, the controller

Topics emphasized in this example

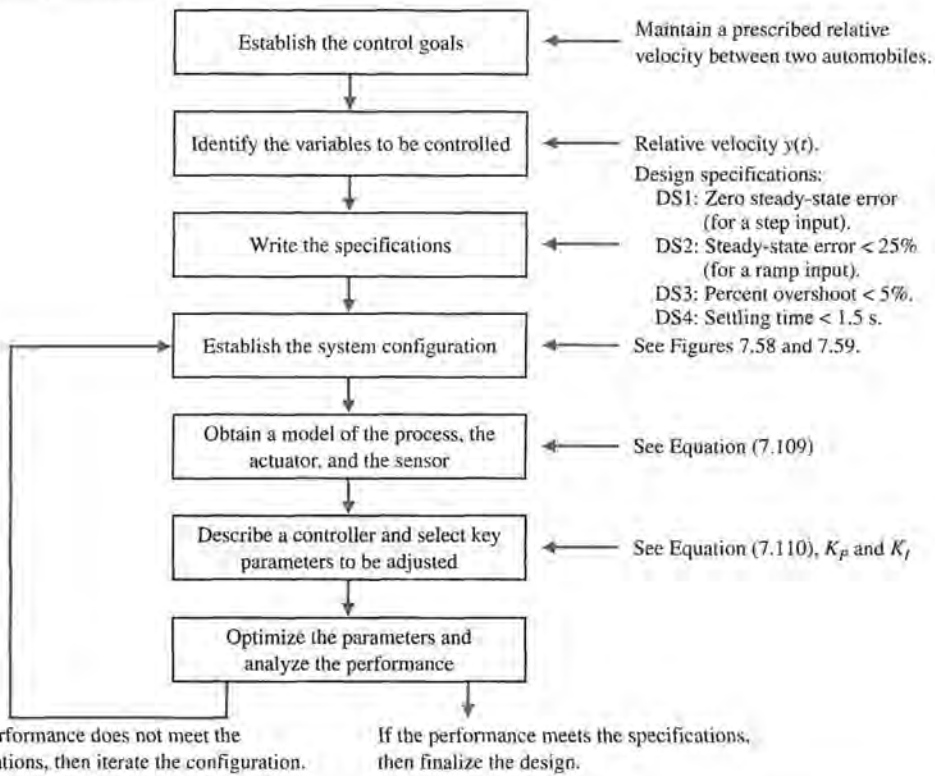


**FIGURE 7.60** Elements of the control system design process emphasized in the automobile velocity control example.

needs to increase the system type by at least 1. A type 1 controller (that is, a controller with one integrator) satisfies DS1. To meet DS2 we need to have the velocity error constant (see Equation (5.29))

$$K_v = \lim_{s \rightarrow 0} sG_c(s)G(s) \geq \frac{1}{0.25} = 4, \quad (7.108)$$

where

$$G(s) = \frac{1}{(s + 2)(s + 8)}, \quad (7.109)$$

and  $G_c(s)$  is the controller (yet to be specified).

The percent overshoot specification DS3 allows us to define a target damping ratio (see Figure 5.8):

$$P.O. \leq 5\% \text{ implies } \zeta \geq 0.69.$$

Similarly from the settling time specification DS4 we have (see Equation (5.13))

$$T_s \approx \frac{4}{\zeta \omega_n} \leq 1.5.$$

Solving for  $\zeta \omega_n$  yields  $\zeta \omega_n \geq 2.6$ .

The desired region for the poles of the closed-loop transfer function is shown in Figure 7.61. Using a proportional controller  $G_c(s) = K_p$ , is not reasonable, because DS2 cannot be satisfied. We need at least one pole at the origin to track a ramp input. Consider the PI controller

$$G_c(s) = \frac{K_p s + K_I}{s} = K_p \frac{s + \frac{K_I}{K_p}}{s}. \quad (7.110)$$

The question is where to place the zero at  $s = -K_I/K_p$ .

We ask for what values of  $K_p$  and  $K_I$  is the system stable. The closed-loop transfer function is

$$T(s) = \frac{K_p s + K_I}{s^3 + 10s^2 + (16 + K_p)s + K_I}.$$

The corresponding Routh array is

$s^3$	1	$16 + K_p$
$s^2$	10	$K_I$
$s$	$10(K_p + 16) - K_I$	0
1	10	
	$K_I$	

The first requirement for stability (from column one, row four) is

$$K_I > 0. \quad (7.111)$$

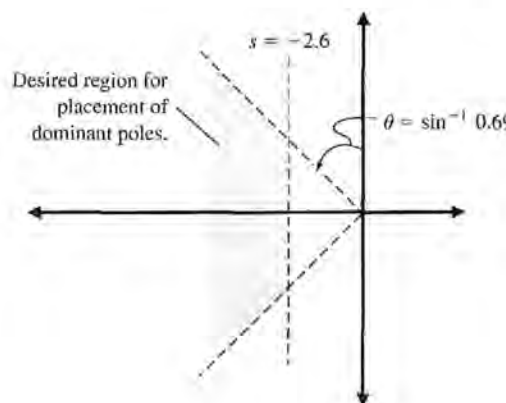


**FIGURE 7.61**  
Desired region in  
the complex plane  
for locating the  
dominant system  
poles.

From the first column, third row, we have the inequality

$$K_P > \frac{K_I}{10} - 16. \quad (7.112)$$

It follows from DS2 that

$$K_v = \lim_{s \rightarrow 0} sG_c(s)G(s) = \lim_{s \rightarrow 0} s \frac{K_P \left( s + \frac{K_I}{K_P} \right)}{s} \frac{1}{(s+2)(s+8)} = \frac{K_I}{16} > 4.$$

Therefore, the integral gain must satisfy

$$K_I > 64. \quad (7.113)$$

If we select  $K_I > 64$ , then the inequality in Equation (7.103) is satisfied. The valid region for  $K_P$  is then given by Equation (7.112), where  $K_I > 64$ .

We need to consider DS4. Here we want to have the dominant poles to the left of the  $s = -2.6$  line. We know from our experience sketching the root locus that since we have three poles (at  $s = 0, -2$ , and  $-8$ ) and one zero (at  $s = -K_I/K_P$ ), we expect two branches of the loci to go to infinity along two asymptotes at  $\phi = -90^\circ$  and  $+90^\circ$  centered at

$$\sigma_A = \frac{\sum(-p_i) - \sum(-z_i)}{n_p - n_z},$$

where  $n_p = 3$  and  $n_z = 1$ . In our case

$$\sigma_A = \frac{-2 - 8 - \left( -\frac{K_I}{K_P} \right)}{2} = -5 + \frac{1}{2} \frac{K_I}{K_P}.$$

We want to have  $\alpha < -2.6$  so that the two branches will bend into the desired regions. Therefore,

$$-5 + \frac{1}{2} \frac{K_I}{K_P} < -2.6,$$

or

$$\frac{K_I}{K_P} < 4.7. \quad (7.114)$$

So as a first design, we can select  $K_P$  and  $K_I$  such that

$$K_I > 64, K_P > \frac{K_I}{10} - 16, \text{ and } \frac{K_I}{K_P} < 4.7.$$

Suppose we choose  $K_I/K_P = 2.5$ . Then the closed-loop characteristic equation is

$$1 + K_P \frac{s + 2.5}{s(s+2)(s+8)} = 0.$$

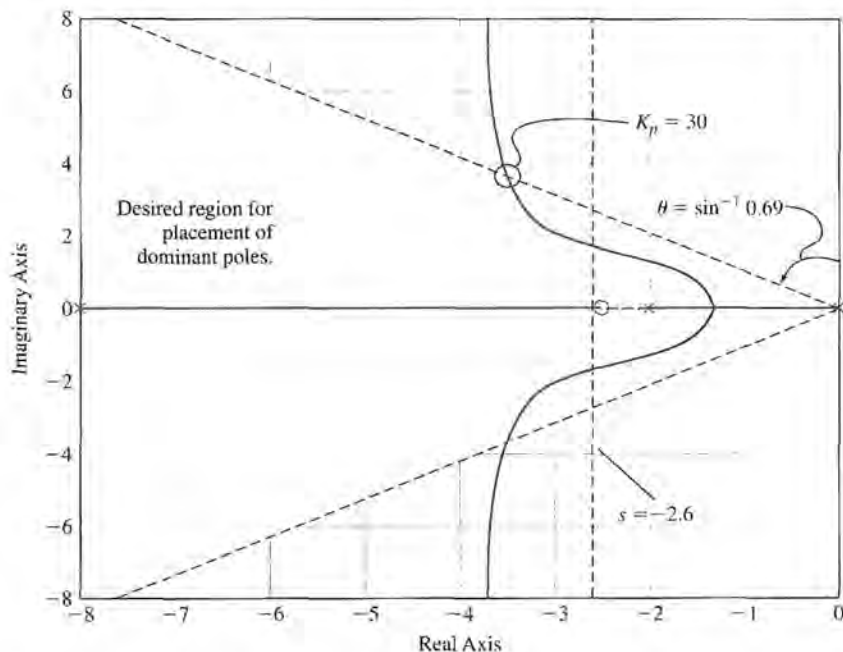


**FIGURE 7.62**  
Root locus for  
 $K_I/K_P = 2.5$ .

The root locus is shown in Figure 7.62. To meet the  $\zeta = 0.69$  (which evolved from DS3), we need to select  $K_P < 30$ . We selected the value at the boundary of the performance region (see Figure 7.62) as carefully as possible.

Selecting  $K_P = 26$ , we have  $K_I/K_P = 2.5$  which implies  $K_I = 65$ . This satisfies the steady-state tracking error specification (DS2) since  $K_I = 65 > 64$ .

The resulting PI controller is

$$G_c(s) = 26 + \frac{65}{s}. \quad (7.115)$$

The step response is shown in Figure 7.63.

The percent overshoot is  $P.O. = 8\%$ , and the settling time is  $T_s = 1.45$  s. The percent overshoot specification is not precisely satisfied, but the controller in Equation (7.115) represents a very good first design. We can iteratively refine it. Even though the closed-loop poles lie in the desired region, the response does not exactly meet the specifications because the controller zero influences the response. The closed-loop system is a third-order system and does not have the performance of a second-order system. We might consider moving the zero to  $s = -2$  (by choosing  $K_I/K_P = 2$ ) so that the pole at  $s = -2$  is cancelled and the resulting system is a second-order system. ■

## 7.9 THE ROOT LOCUS USING CONTROL DESIGN SOFTWARE

An approximate root locus sketch can be obtained by applying the orderly procedure summarized in Table 7.2. Alternatively, we can use control design software to obtain an accurate root locus plot. However, we should not be tempted to rely solely on the computer for obtaining root locus plots while neglecting the manual steps in developing an

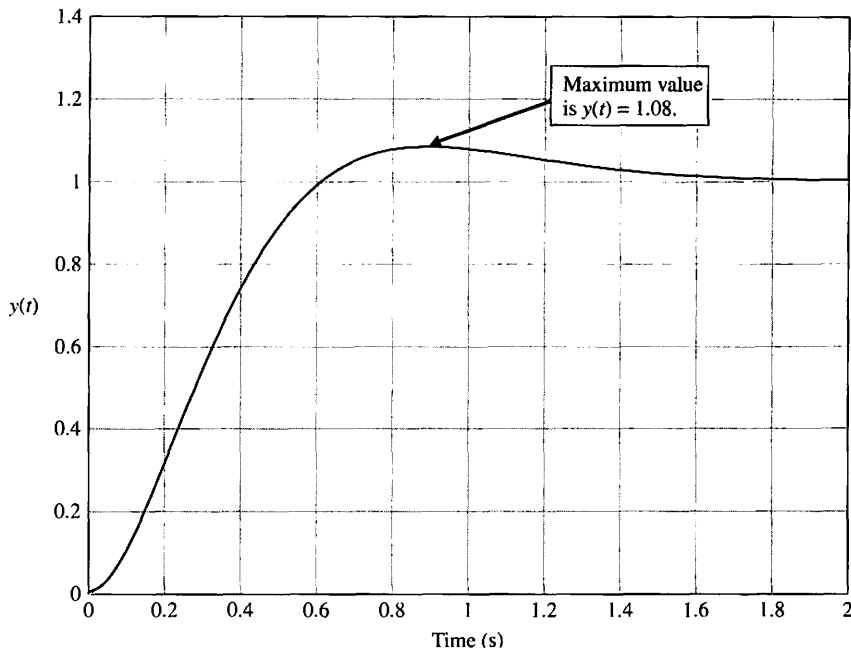


**FIGURE 7.63**  
Automobile velocity control using the PI controller in Equation (7.107).

approximate root locus. The fundamental concepts behind the root locus method are embedded in the manual steps, and it is essential to understand their application fully.

The section begins with a discussion on obtaining a computer-generated root locus plot. This is followed by a discussion of the connections between the partial fraction expansion, dominant poles, and the closed-loop system response. Root sensitivity is covered in the final paragraphs.

The functions covered in this section are `rlocus`, `rlocfind`, and `residue`. The functions `rlocus` and `rlocfind` are used to obtain root locus plots, and the `residue` function is utilized for partial fraction expansions of rational functions.

**Obtaining a Root Locus Plot.** Consider the closed-loop control system in Figure 7.10. The closed-loop transfer function is

$$T(s) = \frac{Y(s)}{R(s)} = \frac{K(s + 1)(s + 3)}{s(s + 2)(s + 3) + K(s + 1)}.$$

The characteristic equation can be written as

$$1 + K \frac{s + 1}{s(s + 2)(s + 3)} = 0. \quad (7.116)$$

The form of the characteristic equation in Equation (7.116) is necessary to use the `rlocus` function for generating root locus plots. The general form of the characteristic equation necessary for application of the `rlocus` function is

$$1 + KG(s) = 1 + K \frac{p(s)}{q(s)} = 0, \quad (7.117)$$

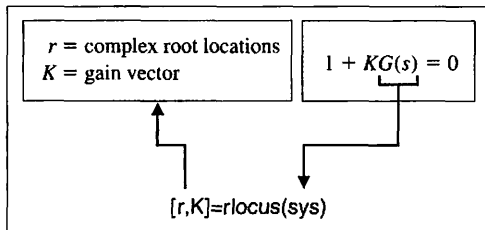


**FIGURE 7.64**  
The `rlocus` function.

where  $K$  is the parameter of interest to be varied from  $0 < K < \infty$ . The `rlocus` function is shown in Figure 7.64, where we define the transfer function object  $\text{sys} = G(s)$ . The steps to obtaining the root locus plot associated with Equation (7.116), along with the associated root locus plot, are shown in Figure 7.65. Invoking the `rlocus` function without left-hand arguments results in an automatic generation of the root locus plot. When invoked with left-hand arguments, the `rlocus` function returns a matrix of root locations and the associated gain vector.

The steps to obtain a computer-generated root locus plot are as follows:

1. Obtain the characteristic equation in the form given in Equation (7.117), where  $K$  is the parameter of interest.
2. Use the `rlocus` function to generate the plots.

Referring to Figure 7.65, we can see that as  $K$  increases, two branches of the root locus break away from the real axis. This means that, for some values of  $K$ , the closed-loop system characteristic equation will have two complex roots. Suppose we want to find the value of  $K$  corresponding to a pair of complex roots. We can use

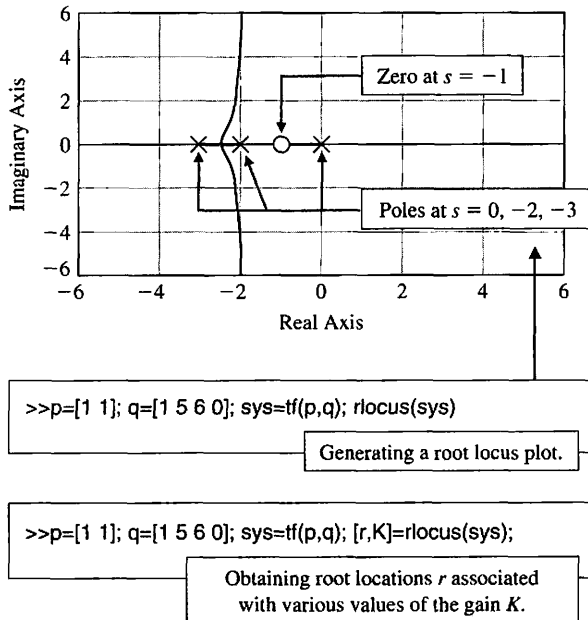


**FIGURE 7.65**  
The root locus for the characteristic equation, Equation (7.116).

the rlocfind function to do this, but only after a root locus has been obtained with the rlocus function. Executing the rlocfind function will result in a cross-hair marker appearing on the root locus plot. We move the cross-hair marker to the location on the locus of interest and hit the enter key. The value of the parameter  $K$  and the value of the selected point will then be displayed in the command display. The use of the rlocfind function is illustrated in Figure 7.66.



Control design software packages may respond differently when interacting with plots, such as with the rlocfind function on the root locus. The response of rlocfind in Figure 7.66 corresponds to MATLAB. Refer to the companion website for more information on other control design software applications.

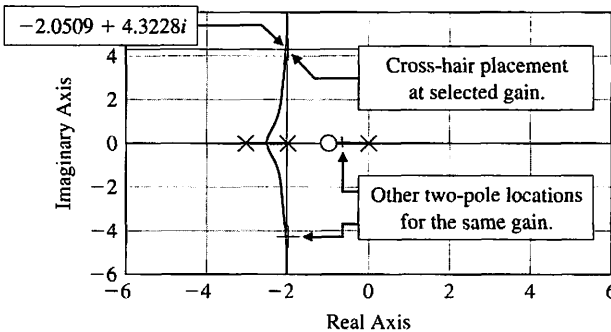
Continuing our third-order root locus example, we find that when  $K = 20.5775$ , the closed-loop transfer function has three poles and two zeros, at

$$\text{poles: } s = \begin{pmatrix} -2.0505 + j4.3227 \\ -2.0505 - j4.3227 \\ -0.8989 \end{pmatrix}; \quad \text{zeros: } s = \begin{pmatrix} -1 \\ -3 \end{pmatrix}.$$

Considering the closed-loop pole locations only, we would expect that the real pole at  $s = -0.8989$  would be the dominant pole. To verify this, we can study the closed-loop system response to a step input,  $R(s) = 1/s$ . For a step input, we have

$$Y(s) = \frac{20.5775(s+1)(s+3)}{s(s+2)(s+3) + 20.5775(s+1)} \cdot \frac{1}{s}. \quad (7.118)$$

Generally, the first step in computing  $y(t)$  is to expand Equation (7.118) in a partial fraction expansion. The residue function can be used to expand Equation (7.118), as shown in Figure 7.67. The residue function is described in Figure 7.68.



```
>>p=[1 1]; q=[1 5 6 0]; sys=tf(p,q); rlocus(sys)
>>rlocfind(sys) ← rlocfind follows the rlocus function.
Select a point in the graphics window
selected_point =
-2.0509 + 4.3228i
ans =
20.5775 ← Value of K at selected point
```

**FIGURE 7.66**  
Using the rlocfind function.

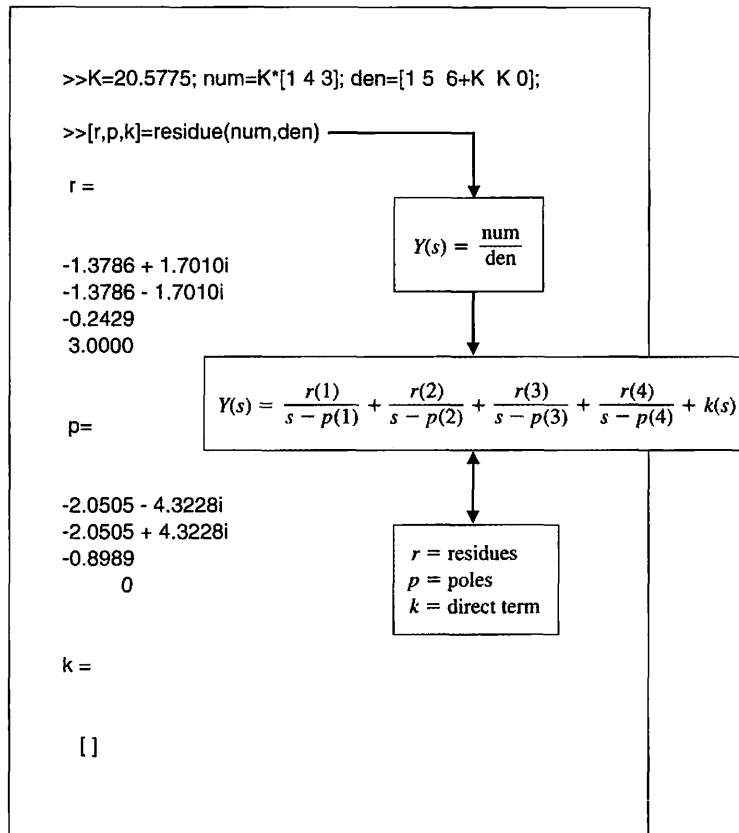


**FIGURE 7.67**  
Partial fraction expansion of Equation (7.118).

The partial fraction expansion of Equation (7.118) is

$$Y(s) = \frac{-1.3786 + j1.7010}{s + 2.0505 + j4.3228} + \frac{-1.3786 - j1.7010}{s + 2.0505 - j4.3228} + \frac{-0.2429}{s + 0.8989} + \frac{3}{s}$$

Comparing the residues, we see that the coefficient of the term corresponding to the pole at  $s = -0.8989$  is considerably smaller than the coefficient of the terms corresponding to the complex-conjugate poles at  $s = -2.0505 \pm j4.3227$ . From this, we expect that the influence of the pole at  $s = -0.8989$  on the output response  $y(t)$  is not dominant. The settling time (to within 2% of the final value) is then predicted by considering the complex-conjugate poles. The poles at  $s = -2.0505 \pm j4.3227$  correspond to a damping of  $\zeta = 0.4286$  and a natural frequency of  $\omega_n = 4.7844$ . Thus, the settling time is predicted to be

$$T_s \approx \frac{4}{\zeta\omega_n} = 1.95 \text{ s.}$$

Using the step function, as shown in Figure 7.69, we find that  $T_s = 1.6 \text{ s}$ . Hence, our approximation of settling time  $T_s \approx 1.95$  is a fairly good approximation. The percent overshoot can be predicted using Figure 5.13 since the zero of  $T(s)$  at  $s = -3$  will impact the system response. Using Figure 5.13, we predict an overshoot of 60%. As can be seen in Figure 7.48, the actual overshoot is 50%.

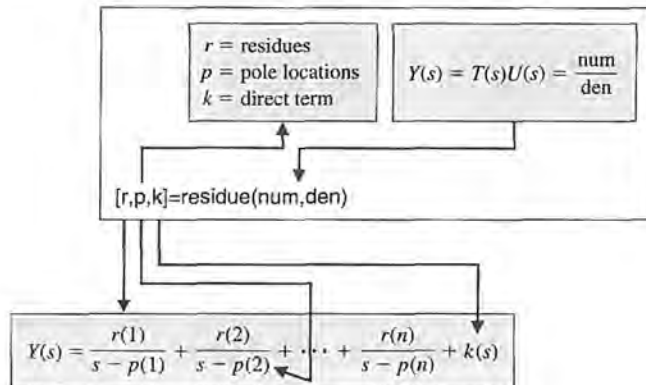


**FIGURE 7.68**  
The residue function.

When using the step function, we can right-click on the figure to access the pull-down menu, which allows us to determine the step response settling time and peak response, as illustrated in Figure 7.69. On the pull-down menu select “Characteristics” and select “Settling Time.” A dot will appear on the figure at the settling point. Place the cursor over the dot to determine the settling time.

In this example, the role of the system zeros on the transient response is illustrated. The proximity of the zero at  $s = -1$  to the pole at  $s = -0.8989$  reduces the impact of that pole on the transient response. The main contributors to the transient response are the complex-conjugate poles at  $s = -2.0505 \pm j4.3228$  and the zero at  $s = -3$ .

There is one final point regarding the residue function: We can convert the partial fraction expansion back to the polynomials num/den, given the residues  $r$ , the pole locations  $p$ , and the direct terms  $k$ , with the command shown in Figure 7.70.

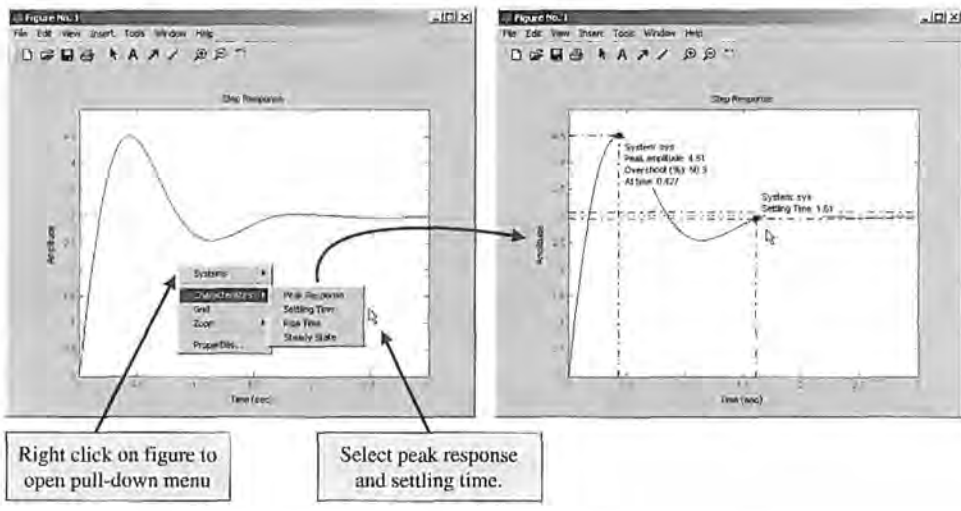
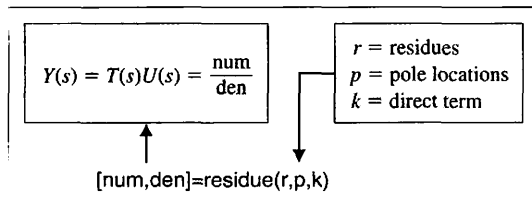


**FIGURE 7.69**  
Step response for the closed-loop system in Figure 7.10 with  $K = 20.5775$ .

```
>>K=20.5775;num=k*[1 4 3]; den=[1 5 6+K K]; sys=tf(num,den);
>>step(sys)
```

**FIGURE 7.70**  
Converting a partial fraction expansion back to a rational function.



**Sensitivity and the Root Locus.** The roots of the characteristic equation play an important role in defining the closed-loop system transient response. The effect of parameter variations on the roots of the characteristic equation is a useful measure of sensitivity. The root sensitivity is defined to be

$$\frac{\partial r_i}{\partial K/K}. \quad (7.119)$$

We can use Equation (7.119) to investigate the sensitivity of the roots of the characteristic equation to variations in the parameter  $K$ . If we change  $K$  by a small finite amount  $\Delta K$ , and evaluate the modified root  $r_i + \Delta r_i$ , it follows that

$$S_K^{r_i} \approx \frac{\Delta r_i}{\Delta K/K}. \quad (7.120)$$

The quantity  $S_K^{r_i}$  is a complex number. Referring back to the third-order example of Figure 7.10 (Equation 7.116), if we change  $K$  by a factor of 5%, we find that the dominant complex-conjugate pole at  $s = -2.0505 + j4.3228$  changes by

$$\Delta r_i = -0.0025 - j0.1168$$

when  $K$  changes from  $K = 20.5775$  to  $K = 21.6064$ . From Equation (7.120), it follows that

$$S_K^{r_i} = \frac{-0.0025 - j0.1168}{1.0289/20.5775} = -0.0494 - j2.3355.$$

The sensitivity  $S_K^{r_i}$  can also be written in the form

$$S_K^{r_i} = 2.34/\underline{268.79^\circ}.$$

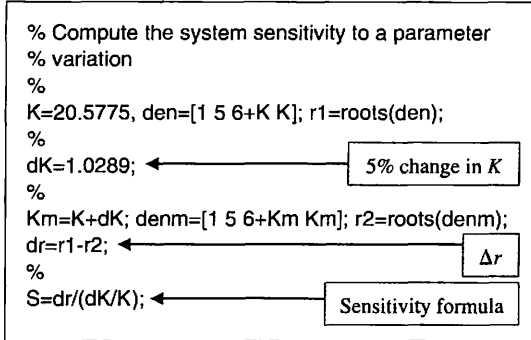
The magnitude and direction of  $S_K^{r_i}$  provides a measure of the root sensitivity. The script used to perform these sensitivity calculations is shown in Figure 7.71.

The root sensitivity measure may be useful for comparing the sensitivity for various system parameters at different root locations.

## 7.10 SEQUENTIAL DESIGN EXAMPLE: DISK DRIVE READ SYSTEM



In Chapter 6, we introduced a new configuration for the control system using velocity feedback. In this chapter, we will use the PID controller to obtain a desirable response. We will proceed with our model and then select a controller. Finally, we will optimize the parameters and analyze the performance. In this chapter, we will use the root locus method in the selection of the controller parameters.

**FIGURE 7.71**

Sensitivity calculations for the root locus for a 5% change in  $K = 20.5775$ .

We use the root locus to select the controller gains. The PID controller introduced in this chapter is

$$G_c(s) = K_P + \frac{K_I}{s} + K_D s.$$

Since the process model  $G_1(s)$  already possesses an integration, we set  $K_I = 0$ . Then we have the PD controller

$$G_c(s) = K_P + K_D s,$$

and our goal is to select  $K_P$  and  $K_D$  in order to meet the specifications. The system is shown in Figure 7.72. The closed-loop transfer function of the system is

$$\frac{Y(s)}{R(s)} = T(s) = \frac{G_c(s)G_1(s)G_2(s)}{1 + G_c(s)G_1(s)G_2(s)H(s)},$$

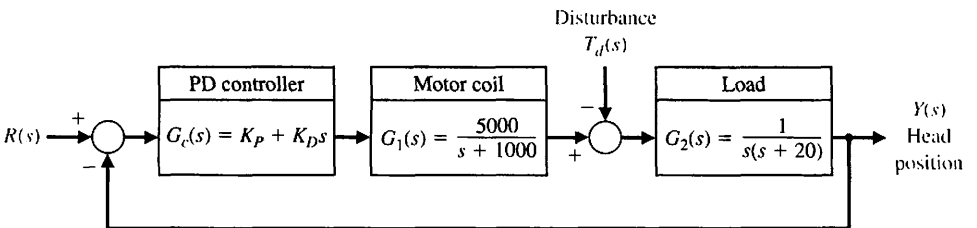
where  $H(s) = 1$ .

In order to obtain the root locus as a function of a parameter, we write  $G_c(s)G_1(s)G_2(s)H(s)$  as

$$G_c(s)G_1(s)G_2(s)H(s) = \frac{5000(K_P + K_D s)}{s(s + 20)(s + 1000)} = \frac{5000K_D(s + z)}{s(s + 20)(s + 1000)},$$

where  $z = K_P/K_D$ . We use  $K_P$  to select the location of the zero  $z$  and then sketch the locus as a function of  $K_D$ . Based on the insight developed in Section 6.7, we select  $z = 1$  so that

$$G_c(s)G_1(s)G_2(s)H(s) = \frac{5000K_D(s + 1)}{s(s + 20)(s + 1000)}.$$

**FIGURE 7.72**

Disk drive control system with a PD controller.

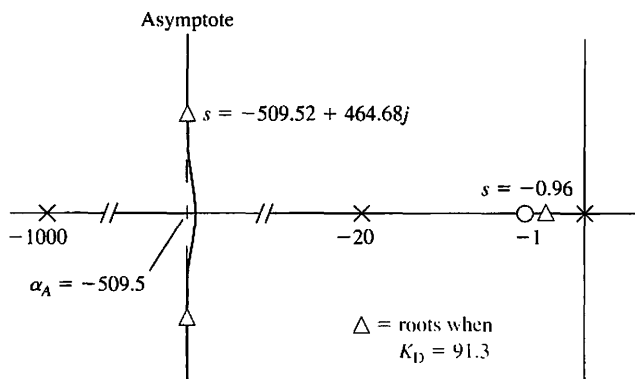


**FIGURE 7.73**  
Sketch of the root locus.

**Table 7.10 Disk Drive Control System Specifications and Actual Design Performance**

Performance Measure	Desired Value	Actual Response
Percent overshoot	Less than 5%	0%
Settling time	Less than 250 ms	20 ms
Maximum response to a unit disturbance	Less than $5 \times 10^{-3}$	$2 \times 10^{-3}$

The number of poles minus the number of zeros is 2, and we expect asymptotes at  $\phi_A = \pm 90^\circ$  with a centroid

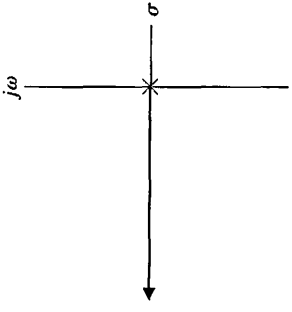
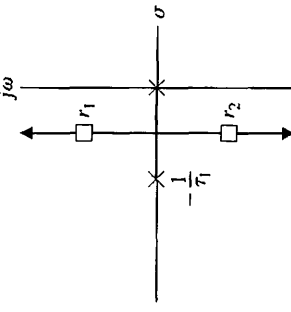
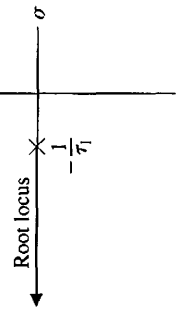
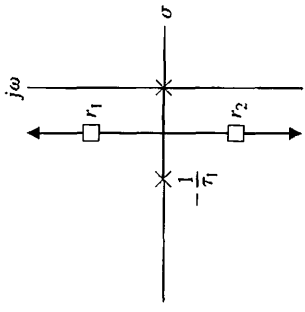
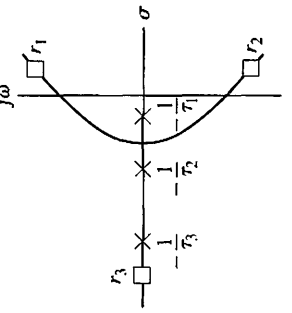
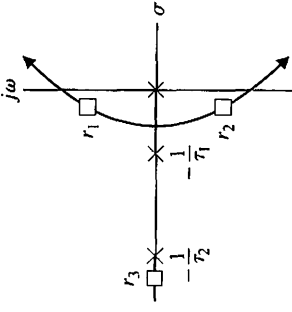
$$\sigma_A = \frac{-1020 + 1}{2} = -509.5,$$

as shown in Figure 7.73. We can quickly sketch the root locus, as shown in Figure 7.73. We use the computer-generated root locus to determine the root values for various values of  $K_D$ . When  $K_D = 91.3$ , we obtain the roots shown in Figure 7.73. Then, obtaining the system response, we achieve the actual response measures as listed in Table 7.10. As designed, the system meets all the specifications. It takes the system a settling time of 20 ms to “practically” reach the final value. In reality, the system drifts very slowly toward the final value after quickly achieving 97% of the final value.

## 7.11 SUMMARY

The relative stability and the transient response performance of a closed-loop control system are directly related to the location of the closed-loop roots of the characteristic equation. We investigated the movement of the characteristic roots on the  $s$ -plane as key system parameters (such as controller gains) are varied. The root locus and the negative gain root locus are graphical representations of the variation of the system closed-loop poles as one parameter varies. The plots can be sketched by hand using a given set of rules in order to analyze the initial design of a system and determine suitable alterations of the system structure and the parameter values. A computer is then commonly used to obtain the accurate root locus for use in the final design and analysis. A summary of fifteen typical root locus diagrams is shown in Table 7.11.

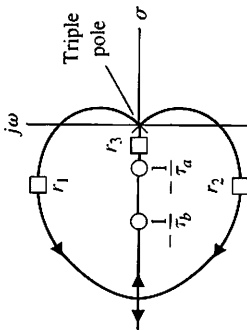
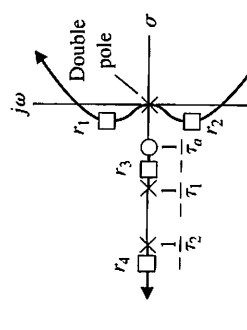
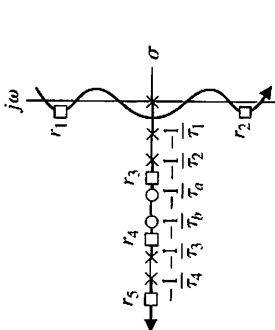
Table 7.11 Root Locus Plots for Typical Transfer Functions

$G(s)$	Root Locus	$G(s)$	Root Locus
$1. \frac{K}{s\tau_1 + 1}$		$4. \frac{K}{s}$	
$2. \frac{K}{(s\tau_1 + 1)(s\tau_2 + 1)}$		$5. \frac{K}{s(s\tau_1 + 1)}$	
$3. \frac{K}{(s\tau_1 + 1)(s\tau_2 + 1)(s\tau_3 + 1)}$		$6. \frac{K}{s(s\tau_1 + 1)(s\tau_2 + 1)}$	

**Table 7.11 (continued)**

$G(s)$	Root Locus	$G(s)$	Root Locus
$7. \frac{K(s\tau_a + 1)}{s(s\tau_1 + 1)(s\tau_2 + 1)}$		$8. \frac{K}{s^2}$	
$10. \frac{K(s\tau_a + 1)}{s^2(s\tau_1 + 1)}$ $\tau_a > \tau_1$		$11. \frac{K}{s^3}$	
$12. \frac{K(s\tau_a + 1)}{s^3}$			

Table 7.11 (continued)

$G(s)$	Root Locus	$G(s)$	Root Locus
$13. \frac{K(s\tau_a + 1)(s\tau_b + 1)}{\xi^3}$		$15. \frac{K(s\tau_a + 1)}{s^2(s\tau_1 + 1)(s\tau_2 + 1)}$	
			
		$14. \frac{K(s\tau_a + 1)(s\tau_b + 1)}{s(s\tau_1 + 1)(s\tau_2 + 1)(s\tau_3 + 1)(s\tau_4 + 1)}$	

Furthermore, we extended the root locus method for the design of several parameters for a closed-loop control system. Then the sensitivity of the characteristic roots was investigated for undesired parameter variations by defining a root sensitivity measure. It is clear that the root locus method is a powerful and useful approach for the analysis and design of modern control systems and will continue to be one of the most important procedures of control engineering.



### SKILLS CHECK

In this section, we provide three sets of problems to test your knowledge: True or False, Multiple Choice, and Word Match. To obtain direct feedback, check your answers with the answer key provided at the conclusion of the end-of-chapter problems. Use the block diagram in Figure 7.74 as specified in the various problem statements.

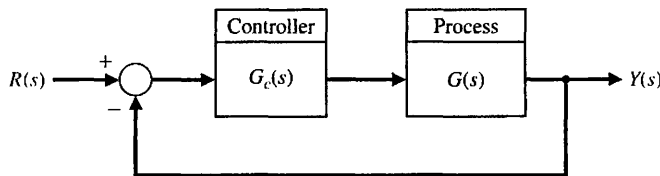


**FIGURE 7.74** Block diagram for the Skills Check.

In the following **True or False** and **Multiple Choice** problems, circle the correct answer.

1. The root locus is the path the roots of the characteristic equation (given by  $1 + KG(s) = 0$ ) trace out on the  $s$ -plane as the system parameter  $0 \leq K < \infty$  varies. *True or False*
2. On the root locus plot, the number of separate loci is equal to the number of poles of  $G(s)$ . *True or False*
3. The root locus always starts at the zeros and ends at the poles of  $G(s)$ . *True or False*
4. The root locus provides the control system designer with a measure of the sensitivity of the poles of the system to variations of a parameter of interest. *True or False*
5. The root locus provides valuable insight into the response of a system to various test inputs. *True or False*
6. Consider the control system in Figure 7.74, where the loop transfer function is

$$L(s) = G_c(s)G(s) = \frac{K(s^2 + 5s + 9)}{s^2(s + 3)}$$

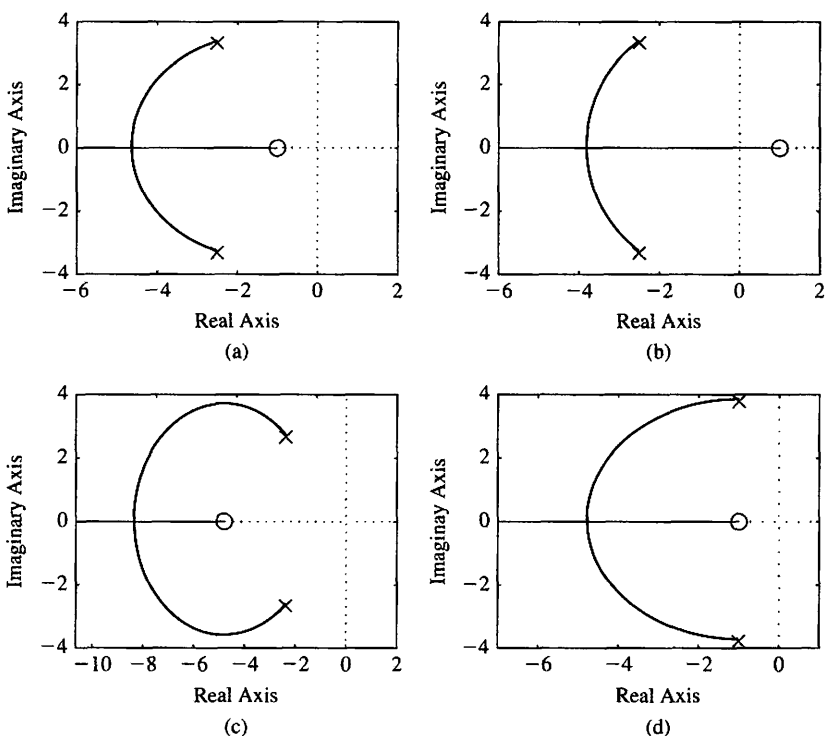
Using the root locus method, determine the value of  $K$  such that the dominant roots have a damping ratio  $\zeta = 0.5$ .

- a.  $K = 1.2$
- b.  $K = 4.5$
- c.  $K = 9.7$
- d.  $K = 37.4$

In Problems 7 and 8, consider the unity feedback system in Figure 7.74 with

$$L(s) = G_c(s)G(s) = \frac{K(s + 1)}{s^2 + 5s + 17.33}.$$

7. The approximate angles of departure of the root locus from the complex poles are
- $\phi_d = \pm 180^\circ$
  - $\phi_d = \pm 115^\circ$
  - $\phi_d = \pm 205^\circ$
  - None of the above
8. The root locus of this system is given by which of the following



9. A unity feedback system has the closed-loop transfer function given by

$$T(s) = \frac{K}{(s + 45)^2 + K}.$$

Using the root locus method, determine the value of the gain  $K$  so that the closed-loop system has a damping ratio  $\zeta = \sqrt{2}/2$ .

- $K = 25$
- $K = 1250$
- $K = 2025$
- $K = 10500$

10. Consider the unity feedback control system in Figure 7.74 where

$$L(s) = G_c(s)G(s) = \frac{10(s + z)}{s(s^2 + 4s + 8)}.$$

Using the root locus method, determine that maximum value of  $z$  for closed-loop stability.

- a.  $z = 7.2$
- b.  $z = 12.8$
- c. Unstable for all  $z > 0$
- d. Stable for all  $z > 0$

In Problems 11 and 12, consider the control system in Figure 7.74 where the model of the process is

$$G(s) = \frac{7500}{(s + 1)(s + 10)(s + 50)}.$$

11. Suppose that the controller is

$$G_c(s) = \frac{K(1 + 0.2s)}{1 + 0.025s}.$$

Using the root locus method, determine the maximum value of the gain  $K$  for closed-loop stability.

- a.  $K = 2.13$
- b.  $K = 3.88$
- c.  $K = 14.49$
- d. Stable for all  $K > 0$

12. Suppose that a simple proportional controller is utilized, that is,  $G_c(s) = K$ . Using the root locus method, determine the maximum controller gain  $K$  for closed-loop stability.

- a.  $K = 0.50$
- b.  $K = 1.49$
- c.  $K = 4.49$
- d. Unstable for  $K > 0$

13. Consider the unity feedback system in Figure 7.74 where

$$L(s) = G_c(s)G(s) = \frac{K}{s(s + 5)(s^2 + 6s + 17.76)}.$$

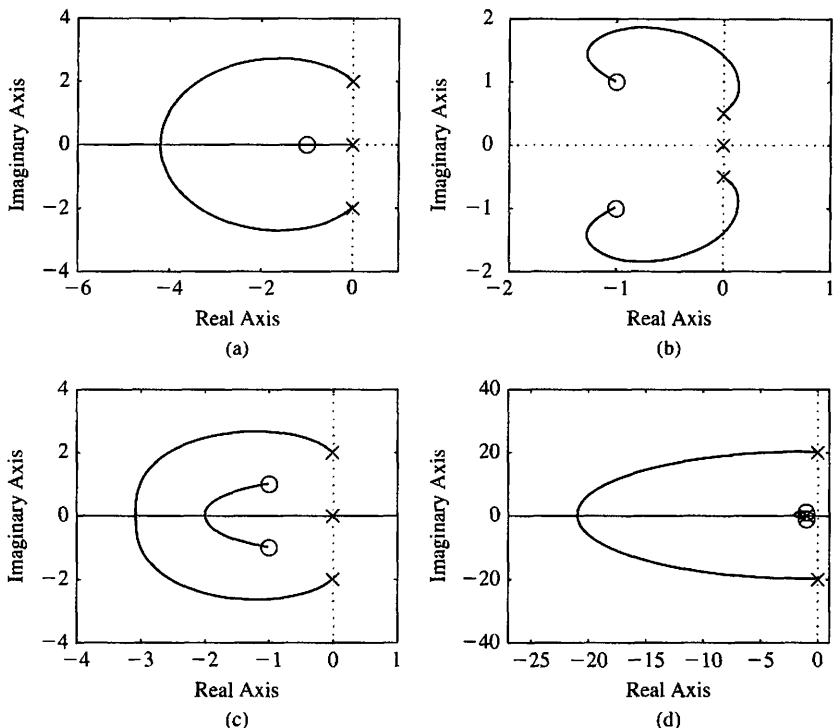
Determine the breakaway point on the real axis and the respective gain,  $K$ .

- a.  $s = -1.8, K = 58.75$
- b.  $s = -2.5, K = 4.59$
- c.  $s = 1.4, K = 58.75$
- d. None of the above

In Problems 14 and 15, consider the feedback system in Figure 7.74, where

$$L(s) = G_c(s)G(s) = \frac{K(s + 1 + j)(s + 1 - j)}{s(s + 2j)(s - 2j)}.$$

14. Which of the following is the associated root locus?



15. The departure angles from the complex poles and the arrival angles at the complex zeros are:

- a.  $\phi_D = \pm 180^\circ, \phi_A = 0^\circ$
- b.  $\phi_D = \pm 116.6^\circ, \phi_A = \pm 198.4^\circ$
- c.  $\phi_D = \pm 45.8^\circ, \phi_A = \pm 116.6^\circ$
- d. None of the above

In the following **Word Match** problems, match the term with the definition by writing the correct letter in the space provided.

a. Parameter design	The amplitude of the closed-loop response is reduced approximately to one-fourth of the maximum value in one oscillatory period.	_____
b. Root sensitivity	The path the root locus follows as the parameter becomes very large and approaches $\infty$ .	_____
c. Root locus	The center of the linear asymptotes, $\sigma_A$ .	_____
d. Root locus segments on the real axis	The process of determining the PID controller gains using one of several analytic methods based on open-loop and closed-loop responses to step inputs.	_____
e. Root locus method	A method of selecting one or two parameters using the root locus method.	_____

f. Asymptote centroid	The root locus lying in a section of the real axis to the left of an odd number of poles and zeros.	_____
g. Breakaway point	The root locus for negative values of the parameter of interest where $-\infty < K \leq 0$ .	_____
h. Locus	The angle at which a locus leaves a complex pole in the $s$ -plane.	_____
i. Angle of departure	A path or trajectory that is traced out as a parameter is changed.	_____
j. Number of separate loci	The locus or path of the roots traced out on the $s$ -plane as a parameter is changed.	_____
k. Asymptote	The sensitivity of the roots as a parameter changes from its normal value.	_____
l. Negative gain root locus	The method for determining the locus of roots of the characteristic equation $1 + KG(s) = 0$ as $0 \leq K < \infty$ .	_____
m. PID tuning	The process of determining the PID controller gains.	_____
n. Quarter amplitude decay	The point on the real axis where the locus departs from the real axis of the $s$ -plane.	_____
o. Ziegler-Nichols PID tuning method	Equal to the number of poles of the transfer function, assuming that the number of poles is greater than or equal to the number of zeros of the transfer function.	_____

## EXERCISES

**E7.1** Let us consider a device that consists of a ball rolling on the inside rim of a hoop [11]. This model is similar to the problem of liquid fuel sloshing in a rocket. The hoop is free to rotate about its horizontal principal axis as shown in Figure E7.1. The angular position of the hoop may be controlled via the torque  $T$  applied to the hoop from a torque motor attached to the hoop drive shaft. If negative feedback is used, the system characteristic equation is

$$1 + \frac{Ks(s+4)}{s^2 + 2s + 2} = 0.$$

(a) Sketch the root locus. (b) Find the gain when the roots are both equal. (c) Find these two equal roots.

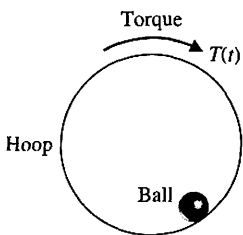


FIGURE E7.1 Hoop rotated by motor.

(d) Find the settling time of the system when the roots are equal.

**E7.2** A tape recorder has a speed control system so that  $H(s) = 1$  with negative feedback and

$$L(s) = G_c(s)G(s) = \frac{K}{s(s+2)(s^2 + 4s + 5)}.$$

- (a) Sketch a root locus for  $K$ , and show that the dominant roots are  $s = -0.35 \pm j0.80$  when  $K = 6.5$ .  
 (b) For the dominant roots of part (a), calculate the settling time and overshoot for a step input.

**E7.3** A control system for an automobile suspension tester has negative unity feedback and a process [12]

$$L(s) = G_c(s)G(s) = \frac{K(s^2 + 4s + 8)}{s^2(s+4)}.$$

We desire the dominant roots to have a  $\zeta$  equal to 0.5. Using the root locus, show that  $K = 7.35$  is required and the dominant roots are  $s = -1.3 \pm j2.2$ .

**E7.4** Consider a unity feedback system with

$$L(s) = G_c(s)G(s) = \frac{K(s+1)}{s^2 + 4s + 5}.$$

- (a) Find the angle of departure of the root locus from the complex poles. (b) Find the entry point for the root locus as it enters the real axis.

**Answers:**  $\pm 225^\circ$ ;  $-2.4$

- E7.5** Consider a unity feedback system with a loop transfer function

$$G_c(s)G(s) = \frac{s^2 + 2s + 10}{s^4 + 38s^3 + 515s^2 + 2950s + 6000}.$$

- (a) Find the breakaway points on the real axis. (b) Find the asymptote centroid. (c) Find the values of  $K$  at the breakaway points.

- E7.6** One version of a space station is shown in Figure E7.6 [28]. It is critical to keep this station in the proper orientation toward the Sun and the Earth for generating power and communications. The orientation controller may be represented by a unity feedback system with an actuator and controller, such as

$$G_c(s)G(s) = \frac{15K}{s(s^2 + 15s + 75)}.$$

Sketch the root locus of the system as  $K$  increases. Find the value of  $K$  that results in an unstable system.

**Answers:**  $K = 75$

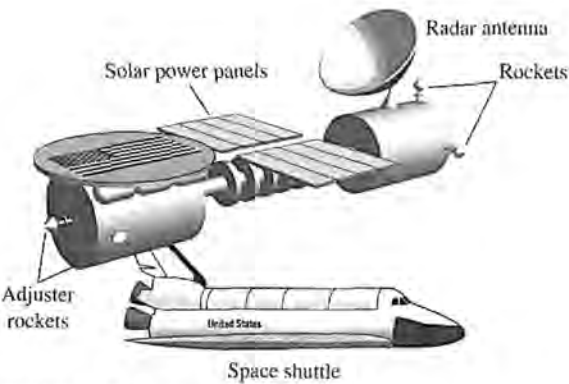


**FIGURE E7.6** Space station.

- E7.7** The elevator in a modern office building travels at a top speed of 25 feet per second and is still able to stop within one-eighth of an inch of the floor outside. The loop transfer function of the unity feedback elevator position control is

$$L(s) = G_c(s)G(s) = \frac{K(s+8)}{s(s+4)(s+6)(s+9)}.$$

Determine the gain  $K$  when the complex roots have a  $\zeta$  equal to 0.8.

- E7.8** Sketch the root locus for a unity feedback system with

$$L(s) = G_c(s)G(s) = \frac{K(s+1)}{s^2(s+9)}.$$

- (a) Find the gain when all three roots are real and equal. (b) Find the roots when all the roots are equal as in part (a).

**Answers:**  $K = 27$ ;  $s = -3$

- E7.9** The world's largest telescope is located in Hawaii. The primary mirror has a diameter of 10 m and consists of a mosaic of 36 hexagonal segments with the orientation of each segment actively controlled. This unity feedback system for the mirror segments has the loop transfer function

$$L(s) = G_c(s)G(s) = \frac{K}{s(s^2 + 2s + 5)}.$$

- (a) Find the asymptotes and draw them in the  $s$ -plane. (b) Find the angle of departure from the complex poles. (c) Determine the gain when two roots lie on the imaginary axis. (d) Sketch the root locus.

- E7.10** A unity feedback system has the loop transfer function

$$L(s) = KG(s) = \frac{K(s+2)}{s(s+1)}.$$

- (a) Find the breakaway and entry points on the real axis. (b) Find the gain and the roots when the real part of the complex roots is located at  $-2$ . (c) Sketch the locus.

**Answers:** (a)  $-0.59$ ,  $-3.41$ ; (b)  $K = 3$ ,  $s = -2 \pm j\sqrt{2}$

- E7.11** A robot force control system with unity feedback has a loop transfer function [6]

$$L(s) = KG(s) = \frac{K(s+2.5)}{(s^2 + 2s + 2)(s^2 + 4s + 5)}.$$

- (a) Find the gain  $K$  that results in dominant roots with a damping ratio of 0.707. Sketch the root locus. (b) Find the actual percent overshoot and peak time for the gain  $K$  of part (a).

- E7.12** A unity feedback system has a loop transfer function

$$L(s) = KG(s) = \frac{K(s+1)}{s(s^2 + 6s + 18)}.$$

- (a) Sketch the root locus for  $K > 0$ . (b) Find the roots when  $K = 10$  and  $20$ . (c) Compute the rise time, percent overshoot, and settling time (with a 2% criterion) of the system for a unit step input when  $K = 10$  and  $20$ .

**E7.13** A unity feedback system has a loop transfer function

$$L(s) = G_c(s)G(s) = \frac{4(s + z)}{s(s + 1)(s + 3)},$$

- (a) Draw the root locus as  $z$  varies from 0 to 100.
- (b) Using the root locus, estimate the percent overshoot and settling time (with a 2% criterion) of the system at  $z = 0.6, 2$ , and  $4$  for a step input. (c) Determine the actual overshoot and settling time at  $z = 0.6, 2$ , and  $4$ .

**E7.14** A unity feedback system has the loop transfer function

$$L(s) = G_c(s)G(s) = \frac{K(s + 10)}{s(s + 5)}.$$

- (a) Determine the breakaway and entry points of the root locus and sketch the root locus for  $K > 0$ .
- (b) Determine the gain  $K$  when the two characteristic roots have a  $\zeta$  of  $1/\sqrt{2}$ . (c) Calculate the roots.

**E7.15** (a) Plot the root locus for a unity feedback system with loop transfer function

$$L(s) = G_c(s)G(s) = \frac{K(s + 10)(s + 2)}{s^3}.$$

- (b) Calculate the range of  $K$  for which the system is stable. (c) Predict the steady-state error of the system for a ramp input.

*Answers:* (a)  $K > 1.67$ ; (b)  $e_{ss} = 0$

**E7.16** A negative unity feedback system has a loop transfer function

$$L(s) = G_c(s)G(s) = \frac{Ke^{-sT}}{s + 1},$$

where  $T = 0.1$  s. Show that an approximation for the time delay is

$$e^{-sT} \approx \frac{\frac{2}{T} - s}{\frac{2}{T} + s}.$$

Using

$$e^{-0.1s} = \frac{20 - s}{20 + s},$$

obtain the root locus for the system for  $K > 0$ . Determine the range of  $K$  for which the system is stable.

**E7.17** A control system, as shown in Figure E7.17, has a process

$$G(s) = \frac{1}{s(s - 1)}.$$

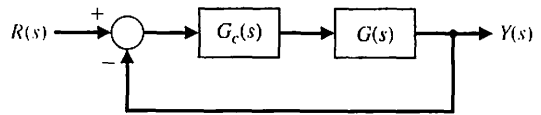


**FIGURE E7.17** Feedback system.

- (a) When  $G_c(s) = K$ , show that the system is always unstable by sketching the root locus. (b) When

$$G_c(s) = \frac{K(s + 2)}{s + 20},$$

sketch the root locus and determine the range of  $K$  for which the system is stable. Determine the value of  $K$  and the complex roots when two roots lie on the  $j\omega$ -axis.

**E7.18** A closed-loop negative unity feedback system is used to control the yaw of the A-6 Intruder attack jet. When the loop transfer function is

$$L(s) = G_c(s)G(s) = \frac{K}{s(s + 3)(s^2 + 2s + 2)},$$

determine (a) the root locus breakaway point and (b) the value of the roots on the  $j\omega$ -axis and the gain required for those roots. Sketch the root locus.

*Answers:* (a) Breakaway:  $s = -2.29$  (b)  $j\omega$ -axis:  $s = \pm j1.09, K = 8$

**E7.19** A unity feedback system has a loop transfer function

$$L(s) = G_c(s)G(s) = \frac{K}{s(s + 3)(s^2 + 6s + 64)}.$$

(a) Determine the angle of departure of the root locus at the complex poles. (b) Sketch the root locus. (c) Determine the gain  $K$  when the roots are on the  $j\omega$ -axis and determine the location of these roots.

**E7.20** A unity feedback system has a loop transfer function

$$L(s) = G_c(s)G(s) = \frac{K(s + 1)}{s(s - 2)(s + 6)}.$$

(a) Determine the range of  $K$  for stability. (b) Sketch the root locus. (c) Determine the maximum  $\zeta$  of the stable complex roots.

*Answers:* (a)  $K > 16$ ; (b)  $\zeta = 0.25$

**E7.21** A unity feedback system has a loop transfer function

$$L(s) = G_c(s)G(s) = \frac{Ks}{s^3 + 5s^2 + 10}.$$

Sketch the root locus. Determine the gain  $K$  when the complex roots of the characteristic equation have a  $\zeta$  approximately equal to 0.66.

- E7.22** A high-performance missile for launching a satellite has a unity feedback system with a loop transfer function

$$G_c(s)G(s) = \frac{K(s^2 + 18)(s + 2)}{(s^2 - 2)(s + 12)}.$$

Sketch the root locus as  $K$  varies from  $0 < K < \infty$ .

- E7.23** A unity feedback system has a loop transfer function

$$L(s) = G_c(s)G(s) = \frac{4(s^2 + 1)}{s(s + a)}.$$

Sketch the root locus for  $0 \leq a < \infty$ .

- E7.24** Consider the system represented in state variable form

$$\dot{x} = Ax + Bu$$

$$y = Cx + Du,$$

where

$$A = \begin{bmatrix} 0 & 1 \\ -4 & -k \end{bmatrix}, B = \begin{bmatrix} 0 \\ 1 \end{bmatrix},$$

$$C = [1 \quad 0], \text{ and } D = [0].$$

Determine the characteristic equation and then sketch the root locus as  $0 < k < \infty$ .

- E7.25** A closed-loop feedback system is shown in Figure E7.25. For what range of values of the parameters  $K$  is the system stable? Sketch the root locus as  $0 < K < \infty$ .

- E7.26** Consider the single-input, single-output system is described by

$$\dot{x}(t) = Ax(t) + Bu(t)$$

$$y(t) = Cx(t)$$

where

$$A = \begin{bmatrix} 0 & 1 \\ 3 - K & -2 - K \end{bmatrix}, B = \begin{bmatrix} 0 \\ 1 \end{bmatrix}, C = [1 \quad -1].$$

Compute the characteristic polynomial and plot the root locus as  $0 \leq K < \infty$ . For what values of  $K$  is the system stable?

- E7.27** Consider the unity feedback system in Figure E7.27. Sketch the root locus as  $0 \leq p < \infty$ .

- E7.28.** Consider the feedback system in Figure E7.28. Obtain the negative gain root locus as  $-\infty < K \leq 0$ . For what values of  $K$  is the system stable?

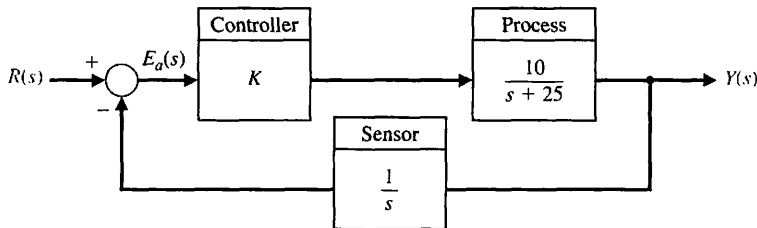


**FIGURE E7.25**  
Nonunity feedback system with parameter  $K$ .

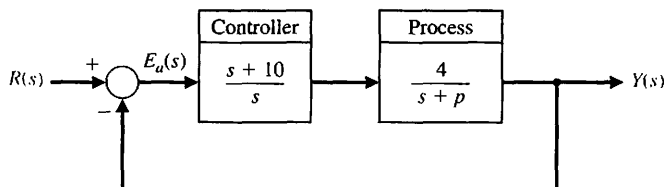


**FIGURE E7.27**  
Unity feedback system with parameter  $p$ .

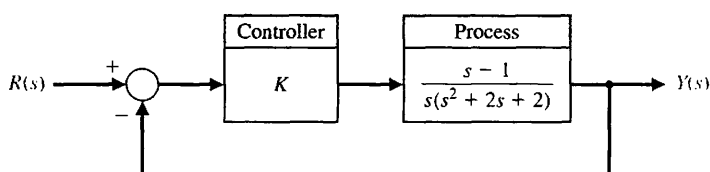


**FIGURE E7.28**  
Feedback system for negative gain root locus.

## PROBLEMS

**P7.1** Sketch the root locus for the following loop transfer functions of the system shown in Figure P7.1 when  $0 < K < \infty$ :

$$(a) G_c(s)G(s) = \frac{K}{s(s + 10)(s + 8)}$$

$$(b) G_c(s)G(s) = \frac{K}{(s^2 + 2s + 2)(s + 2)}$$

$$(c) G_c(s)G(s) = \frac{K(s + 5)}{s(s + 1)(s + 10)}$$

$$(d) G_c(s)G(s) = \frac{K(s^2 + 4s + 8)}{s^2(s + 1)}$$

**P7.2** The linear model of a phase detector was presented in Problem P6.7. Sketch the root locus as a function of the gain  $K_v = K_a K$ . Determine the value of  $K_v$  attained if the complex roots have a damping ratio equal to 0.60 [13].

**P7.3** A unity feedback system has the loop transfer function

$$G_c(s)G(s) = \frac{K}{s(s + 2)(s + 5)}.$$

Find (a) the breakaway point on the real axis and the gain  $K$  for this point, (b) the gain and the roots when two roots lie on the imaginary axis, and (c) the roots when  $K = 6$ . (d) Sketch the root locus.

**P7.4** The analysis of a large antenna was presented in Problem P4.5. Sketch the root locus of the system as

$0 < k_a < \infty$ . Determine the maximum allowable gain of the amplifier for a stable system.

**P7.5** Automatic control of helicopters is necessary because, unlike fixed-wing aircraft which possess a fair degree of inherent stability, the helicopter is quite unstable. A helicopter control system that utilizes an automatic control loop plus a pilot stick control is shown in Figure P7.5. When the pilot is not using the control stick, the switch may be considered to be open. The dynamics of the helicopter are represented by the transfer function

$$G(s) = \frac{25(s + 0.03)}{(s + 0.4)(s^2 - 0.36s + 0.16)}.$$

- (a) With the pilot control loop open (hands-off control), sketch the root locus for the automatic stabilization loop. Determine the gain  $K_2$  that results in a damping for the complex roots equal to  $\zeta = 0.707$ .
- (b) For the gain  $K_2$  obtained in part (a), determine the steady-state error due to a wind gust  $T_d(s) = 1/s$ .
- (c) With the pilot loop added, draw the root locus as  $K_1$  varies from zero to  $\infty$  when  $K_2$  is set at the value calculated in part (a). (d) Recalculate the steady-state error of part (b) when  $K_1$  is equal to a suitable value based on the root locus.

**P7.6** An attitude control system for a satellite vehicle within the earth's atmosphere is shown in Figure P7.6. The transfer functions of the system are

$$G(s) = \frac{K(s + 0.20)}{(s + 0.90)(s - 0.60)(s - 0.10)}$$

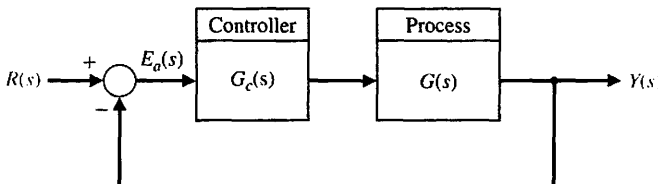


FIGURE P7.1

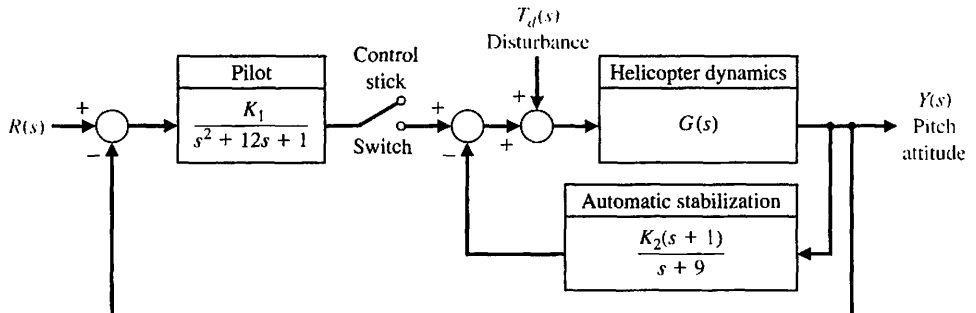
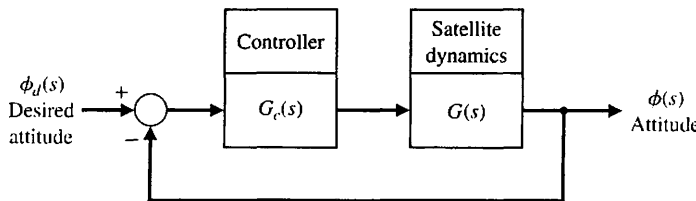


FIGURE P7.5  
Helicopter control.

**FIGURE P7.6**  
Satellite attitude control.



and

$$G_c(s) = \frac{(s + 2 + j1.5)(s + 2 - j1.5)}{s + 4.0}.$$

- (a) Draw the root locus of the system as  $K$  varies from 0 to  $\infty$ . (b) Determine the gain  $K$  that results in a system with a settling time (with a 2% criterion) less than 12 seconds and a damping ratio for the complex roots greater than 0.50.

**P7.7** The speed control system for an isolated power system is shown in Figure P7.7. The valve controls the steam flow input to the turbine in order to account for load changes  $\Delta L(s)$  within the power distribution network. The equilibrium speed desired results in a generator frequency equal to 60 cps. The effective rotary inertia  $J$  is equal to 4000 and the friction constant  $b$  is equal to 0.75. The steady-state speed regulation factor  $R$  is represented by the equation  $R \approx (\omega_0 - \omega_r)/\Delta L$ , where  $\omega_r$  equals the speed at rated load and  $\omega_0$  equals the speed at no load. We want to obtain a very small  $R$ , usually less than 0.10. (a) Using root locus techniques, determine the regulation  $R$  attainable when the damping ratio of the roots of the system must be greater than 0.60. (b) Verify that the steady-state speed deviation for a load torque change  $\Delta L(s) = \Delta L/s$  is, in fact, approximately equal to  $R\Delta L$  when  $R \leq 0.1$ .

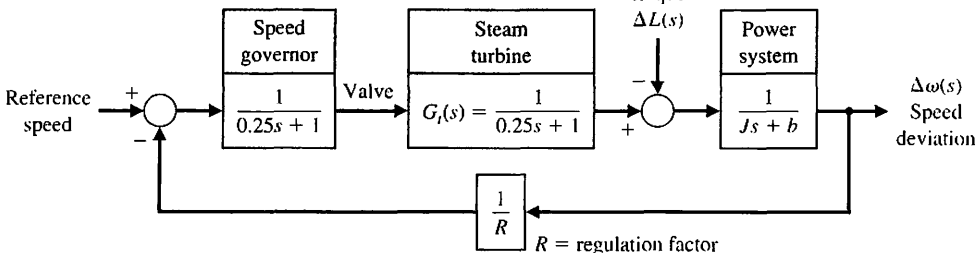


**FIGURE P7.7**  
Power system control.

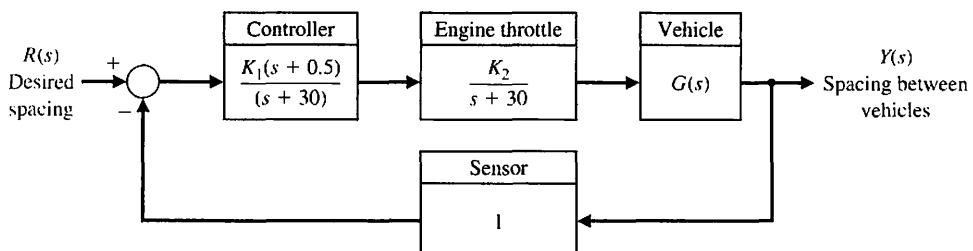


**FIGURE P7.9**  
Guided vehicle control.

**P7.8** Consider again the power control system of Problem P7.7 when the steam turbine is replaced by a hydroturbine. For hydroturbines, the large inertia of the water used as a source of energy causes a considerably larger time constant. The transfer function of a hydroturbine may be approximated by

$$G_t(s) = \frac{-\tau s + 1}{(\tau/2)s + 1},$$

where  $\tau = 1$  second. With the rest of the system remaining as given in Problem P7.7, repeat parts (a) and (b) of Problem P7.7.

**P7.9** The achievement of safe, efficient control of the spacing of automatically controlled guided vehicles is an important part of the future use of the vehicles in a manufacturing plant [14, 15]. It is important that the system eliminate the effects of disturbances (such as oil on the floor) as well as maintain accurate spacing between vehicles on a guideway. The system can be represented by the block diagram of Figure P7.9. The vehicle dynamics can be represented by

$$G(s) = \frac{(s + 0.1)(s^2 + 2s + 289)}{s(s - 0.4)(s + 0.8)(s^2 + 1.45s + 361)}.$$

(a) Sketch the root locus of the system. (b) Determine all the roots when the loop gain  $K = K_1 K_2$  is equal to 4000.

**P7.10** New concepts in passenger airliner design will have the range to cross the Pacific in a single flight and the efficiency to make it economical [16, 29]. These new designs will require the use of temperature-resistant, lightweight materials and advanced control systems. Noise control is an important issue in modern aircraft designs since most airports have strict noise level requirements. One interesting concept is the Boeing Sonic Cruiser depicted in Figure P7.10(a). It would seat 200 to 250 passengers and cruise at just below the speed of sound.

The flight control system must provide good handling characteristics and comfortable flying conditions. An automatic control system can be designed for the next generation passenger aircraft.

The desired characteristics of the dominant roots of the control system shown in Figure P7.10(b) have a

$\zeta = 0.707$ . The characteristics of the aircraft are  $\omega_n = 2.5$ ,  $\zeta = 0.30$ , and  $\tau = 0.1$ . The gain factor  $K_1$ , however, will vary over the range 0.02 at medium-weight cruise conditions to 0.20 at lightweight descent conditions. (a) Sketch the root locus as a function of the loop gain  $K_1 K_2$ . (b) Determine the gain  $K_2$  necessary to yield roots with  $\zeta = 0.707$  when the aircraft is in the medium-cruise condition. (c) With the gain  $K_2$  as found in part (b), determine the  $\zeta$  of the roots when the gain  $K_1$  results from the condition of light descent.

**P7.11** A computer system requires a high-performance magnetic tape transport system [17]. The environmental conditions imposed on the system result in a severe test of control engineering design. A direct-drive DC motor system for the magnetic tape reel system is shown in Figure P7.11, where  $r$  equals the reel radius, and  $J$  equals the reel and rotor inertia. A complete reversal of the tape reel direction is required in 6 ms, and the tape reel must follow a step command in 3 ms or less. The tape is normally operating at a speed of



(a)

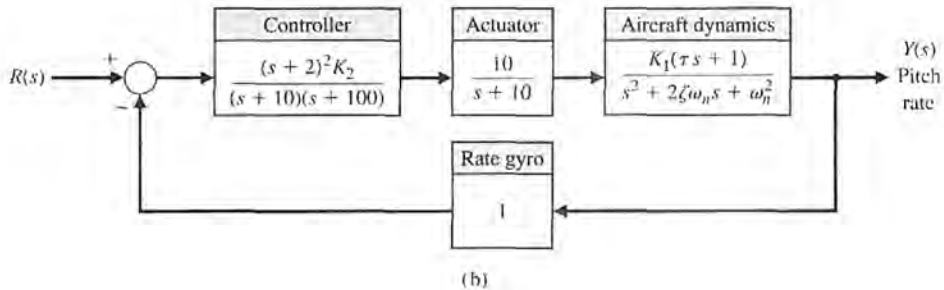


**FIGURE P7.10**  
 (a) A passenger jet aircraft of the future. (TM and © Boeing. Used under license.) (b) Control system.

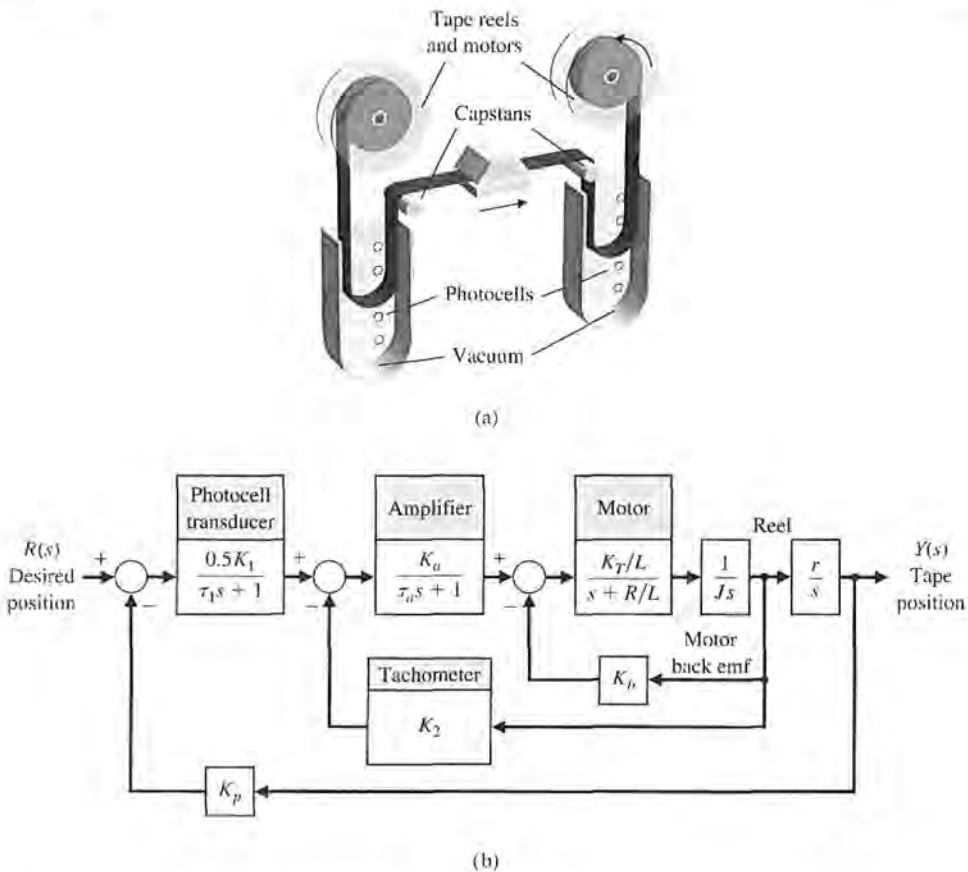


**FIGURE P7.11**  
(a) Tape control system. (b) Block diagram.

100 in/s. The motor and components selected for this system possess the following characteristics:

$$K_h = 0.40$$

$$K_p = 1$$

$$\tau_1 = \tau_a = 1 \text{ ms}$$

$$K_T/(LJ) = 2.0$$

$$r = 0.2$$

$$K_1 = 2.0$$

$$K_2 \text{ is adjustable.}$$

The inertia of the reel and motor rotor is  $2.5 \times 10^{-3}$  when the reel is empty, and  $5.0 \times 10^{-3}$  when the reel is full. A series of photocells is used as an error-sensing device. The time constant of the motor is  $L/R = 0.5 \text{ ms}$ . (a) Sketch the root locus for the system when  $K_2 = 10$  and  $J = 5.0 \times 10^{-3}$ ,  $0 < K_a < \infty$ . (b) Determine the gain  $K_a$  that results in a well-damped system so that the  $\zeta$  of all the roots is greater than or equal to 0.60. (c) With the  $K_a$  determined from part (b), sketch a root locus for  $0 < K_2 < \infty$ .

**P7.12** A precision speed control system (Figure P7.12) is required for a platform used in gyroscope and inertial system testing where a variety of closely controlled

speeds is necessary. A direct-drive DC torque motor system was utilized to provide (1) a speed range of  $0.01^\circ/\text{s}$  to  $600^\circ/\text{s}$ , and (2) 0.1% steady-state error maximum for a step input. The direct-drive DC torque motor avoids the use of a gear train with its attendant backlash and friction. Also, the direct-drive motor has a high-torque capability, high efficiency, and low motor time constants. The motor gain constant is nominally  $K_m = 1.8$ , but is subject to variations up to 50%. The amplifier gain  $K_a$  is normally greater than 10 and subject to a variation of 10%. (a) Determine the minimum loop gain necessary to satisfy the steady-state error requirement. (b) Determine the limiting value of gain for stability. (c) Sketch the root locus as  $K_a$  varies from 0 to  $\infty$ . (d) Determine the roots when  $K_a = 40$ , and estimate the response to a step input.

**P7.13** A unity feedback system has the loop transfer function

$$L(s) = G_c(s)G(s) = \frac{K}{s(s+3)(s^2 + 4s + 7.84)}.$$

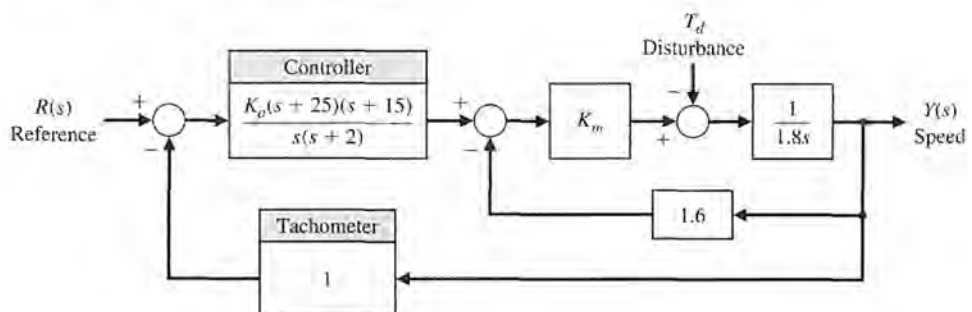


**FIGURE P7.12**  
Speed control.

- (a) Find the breakaway point on the real axis and the gain for this point. (b) Find the gain to provide two complex roots nearest the  $j\omega$ -axis with a damping ratio of 0.707. (c) Are the two roots of part (b) dominant? (d) Determine the settling time (with a 2% criterion) of the system when the gain of part (b) is used.

**P7.14** The loop transfer function of a single-loop negative feedback system is

$$L(s) = G_c(s)G(s) = \frac{K(s + 2.5)(s + 3.2)}{s^2(s + 1)(s + 10)(s + 30)}.$$

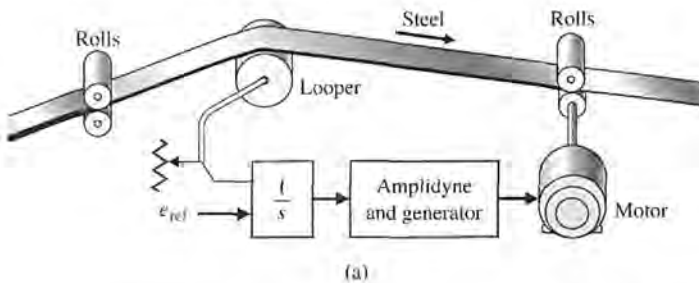
This system is called conditionally stable because it is stable only for a range of the gain  $K$  such that  $k_1 < K < k_2$ . Using the Routh-Hurwitz criteria and the root locus method, determine the range of the gain for which the system is stable. Sketch the root locus for  $0 < K < \infty$ .

- P7.15** Let us again consider the stability and ride of a rider and high performance motorcycle as outlined in Problem P6.13. The dynamics of the motorcycle and rider can be represented by the loop transfer function

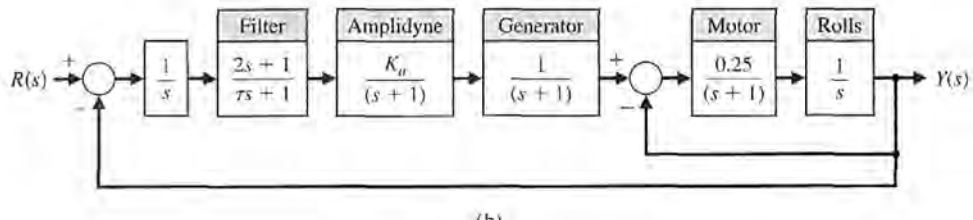
$$G_c(s)G(s) = \frac{K(s^2 + 30s + 625)}{s(s + 20)(s^2 + 20s + 200)(s^2 + 60s + 3400)}.$$

Sketch the root locus for the system. Determine the  $\zeta$  of the dominant roots when  $K = 3 \times 10^4$ .

- P7.16** Control systems for maintaining constant tension on strip steel in a hot strip finishing mill are called "loopers." A typical system is shown in Figure P7.16. The looper is an arm 2 to 3 feet long with a roller on the end; it is raised and pressed against the strip by a motor [18]. The typical speed of the strip passing the looper is 2000 ft/min. A voltage proportional to the looper



(a)



(b)

**FIGURE P7.16**  
Steel mill control system.

position is compared with a reference voltage and integrated where it is assumed that a change in looper position is proportional to a change in the steel strip tension. The time constant  $\tau$  of the filter is negligible relative to the other time constants in the system. (a) Sketch the root locus of the control system for  $0 < K_a < \infty$ . (b) Determine the gain  $K_a$  that results in a system whose roots have a damping ratio of  $\zeta = 0.707$  or greater. (c) Determine the effect of  $\tau$  as  $\tau$  increases from a negligible quantity.

**P7.17** Consider again the vibration absorber discussed in Problems 2.2 and 2.10 as a design problem. Using the root locus method, determine the effect of the parameters  $M_2$  and  $k_{12}$ . Determine the specific values of the parameters  $M_2$  and  $k_{12}$  so that the mass  $M_1$  does not vibrate when  $F(t) = a \sin(\omega_0 t)$ . Assume that  $M_1 = 1$ ,  $k_1 = 1$ , and  $b = 1$ . Also assume that  $k_{12} < 1$  and that the term  $k_{12}^2$  may be neglected.

**P7.18** A feedback control system is shown in Figure P7.18. The filter  $G_c(s)$  is often called a compensator, and the design problem involves selecting the parameters  $\alpha$  and  $\beta$ . Using the root locus method, determine the effect of varying the parameters. Select a suitable filter so that the time to settle (to within 2% of the final value) is less than 4 seconds and the damping ratio of the dominant roots is greater than 0.60.

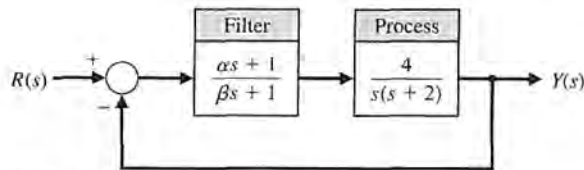


**FIGURE P7.18** Filter design.

**P7.19** In recent years, many automatic control systems for guided vehicles in factories have been installed. One system uses a magnetic tape applied to the floor to guide the vehicle along the desired lane [10, 15]. Using transponder tags on the floor, the automatically guided vehicles can be tasked (for example, to speed up or slow down) at key locations. An example of a guided vehicle in a factory is shown in Figure P7.19(a). We have

$$G(s) = \frac{s^2 + 4s + 100}{s(s+2)(s+6)}$$

and  $K_a$  is the amplifier gain. Sketch a root locus and determine a suitable gain  $K_a$  so that the damping ratio of the complex roots is 0.707.



(a)

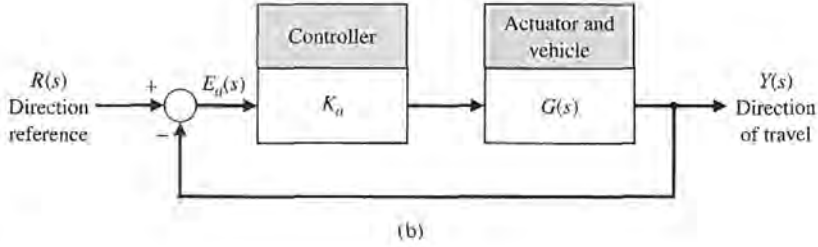


**FIGURE P7.19**  
(a) An automatically guided vehicle. (Photo courtesy of the Jervis B. Webb Company)  
(b) Block diagram.

**P7.20** Determine the root sensitivity for the dominant roots of the design for Problem P7.18 for the gain  $K = 4\alpha/\beta$  and the pole  $s = -2$ .

**P7.21** Determine the root sensitivity of the dominant roots of the power system of Problem P7.7. Evaluate the sensitivity for variations of (a) the poles at  $s = -4$ , and (b) the feedback gain,  $1/R$ .

**P7.22** Determine the root sensitivity of the dominant roots of Problem P7.1(a) when  $K$  is set so that the damping ratio of the unperturbed roots is 0.707. Evaluate and compare the sensitivity as a function of the poles and zeros of  $G_c(s)G(s)$ .

**P7.23** Repeat Problem P7.22 for the loop transfer function  $G_c(s)G(s)$  of Problem P7.1(c).

**P7.24** For systems of relatively high degree, the form of the root locus can often assume an unexpected pattern.

The root loci of four different feedback systems of third order or higher are shown in Figure P7.24. The open-loop poles and zeros of  $KG(s)$  are shown, and the form of the root loci as  $K$  varies from zero to infinity is presented. Verify the diagrams of Figure P7.24 by constructing the root loci.

**P7.25** Solid-state integrated electronic circuits are composed of distributed  $R$  and  $C$  elements. Therefore, feedback electronic circuits in integrated circuit form must be investigated by obtaining the transfer function of the distributed  $RC$  networks. It has been shown that the slope of the attenuation curve of a distributed  $RC$  network is  $10n$  dB/decade, where  $n$  is the order of the  $RC$  filter [13]. This attenuation is in contrast with the normal  $20n$  dB/decade for the lumped parameter circuits. (The concept of the slope of an attenuation curve is considered in Chapter 8. If it is unfamiliar,

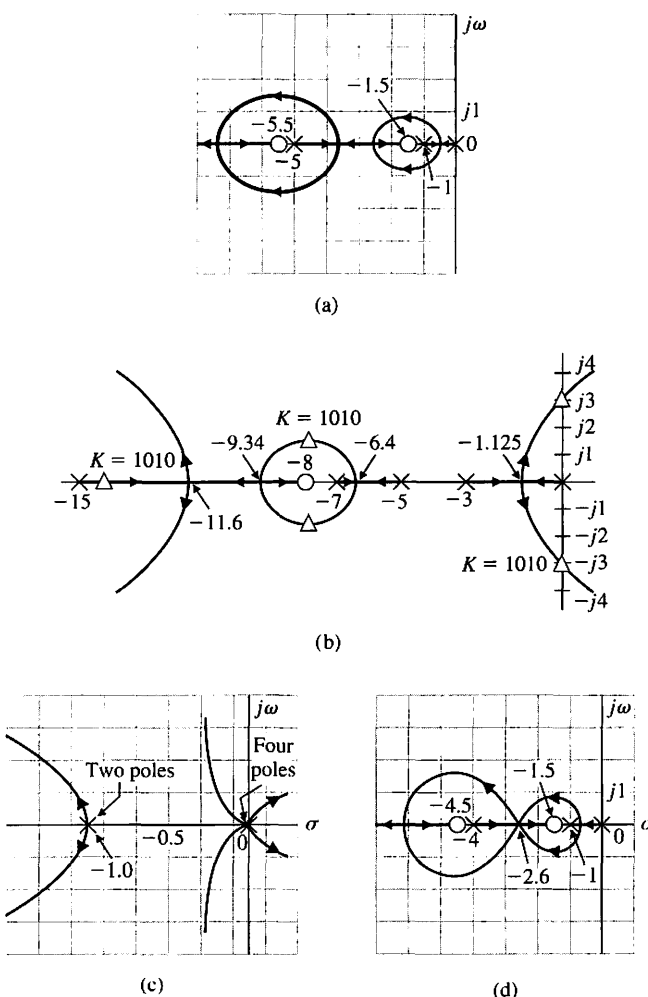


**FIGURE P7.24**  
Root loci of four systems.

reexamine this problem after studying Chapter 8.) An interesting case arises when the distributed  $RC$  network occurs in a series-to-shunt feedback path of a transistor amplifier. Then the loop transfer function may be written as

$$L(s) = G_c(s)G(s) = \frac{K(s - 1)(s + 3)^{1/2}}{(s + 1)(s + 2)^{1/2}}.$$

- (a) Using the root locus method, determine the locus of roots as  $K$  varies from zero to infinity. (b) Calculate the gain at borderline stability and the frequency of oscillation for this gain.

**P7.26** A single-loop negative feedback system has a loop transfer function

$$L(s) = G_c(s)G(s) = \frac{K(s + 2)^2}{s(s^2 + 1)(s + 8)}.$$

- (a) Sketch the root locus for  $0 \leq K \leq \infty$  to indicate the significant features of the locus. (b) Determine the range of the gain  $K$  for which the system is stable. (c) For what value of  $K$  in the range  $K \geq 0$  do purely imaginary roots exist? What are the values of these roots? (d) Would the use of the dominant roots approximation for an estimate of settling time be justified in this case for a large magnitude of gain ( $K > 50$ )?

**P7.27** A unity negative feedback system has a loop transfer function

$$\begin{aligned} L(s) = G_c(s)G(s) &= \frac{K(s^2 + 0.1)}{s(s^2 + 2)} \\ &= \frac{K(s + j0.3162)(s - j0.3162)}{s(s^2 + 1)}. \end{aligned}$$

Sketch the root locus as a function of  $K$ . Carefully calculate where the segments of the locus enter and leave the real axis.

**P7.28** To meet current U.S. emissions standards for automobiles, hydrocarbon (HC) and carbon monoxide (CO) emissions are usually controlled by a catalytic converter in the automobile exhaust. Federal standards for nitrogen oxides ( $NO_x$ ) emissions are met mainly by exhaust-gas recirculation (EGR) techniques. However, as  $NO_x$  emissions standards were tightened from the

current limit of 2.0 grams per mile to 1.0 gram per mile, these techniques alone were no longer sufficient.

Although many schemes are under investigation for meeting the emissions standards for all three emissions, one of the most promising employs a three-way catalyst—for HC, CO, and  $NO_x$  emissions—in conjunction with a closed-loop engine-control system. The approach is to use a closed-loop engine control, as shown in Figure P7.28 [19, 23]. The exhaust-gas sensor gives an indication of a rich or lean exhaust and compares it to a reference. The difference signal is processed by the controller, and the output of the controller modulates the vacuum level in the carburetor to achieve the best air-fuel ratio for proper operation of the catalytic converter. The loop transfer function is represented by

$$L(s) = \frac{Ks^2 + 12s + 20}{s^3 + 10s^2 + 25s}.$$

Calculate the root locus as a function of  $K$ . Carefully calculate where the segments of the locus enter and leave the real axis. Determine the roots when  $K = 2$ . Predict the step response of the system when  $K = 2$ .

**P7.29** A unity feedback control system has a transfer function

$$L(s) = G_c(s)G(s) = \frac{K(s^2 + 10s + 30)}{s^2(s + 10)}.$$

We desire the dominant roots to have a damping ratio equal to 0.707. Find the gain  $K$  when this condition is satisfied. Show that the complex roots are  $s = -3.56 \pm j3.56$  at this gain.

**P7.30** An  $RLC$  network is shown in Figure P7.30. The nominal values (normalized) of the network elements are  $L = C = 1$  and  $R = 2.5$ . Show that the root sensitivity of the two roots of the input impedance  $Z(s)$  to a change in  $R$  is different by a factor of 4.

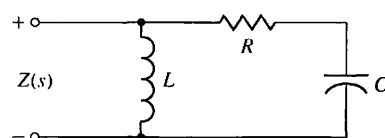


**FIGURE P7.30**  $RLC$  network.

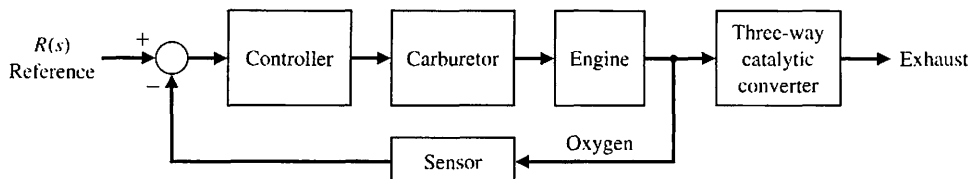


**FIGURE P7.28**  
Auto engine control.

**P7.31** The development of high-speed aircraft and missiles requires information about aerodynamic parameters prevailing at very high speeds. Wind tunnels are used to test these parameters. These wind tunnels are constructed by compressing air to very high pressures and releasing it through a valve to create a wind. Since the air pressure drops as the air escapes, it is necessary to open the valve wider to maintain a constant wind speed. Thus, a control system is needed to adjust the valve to maintain a constant wind speed. The loop transfer function for a unity feedback system is

$$L(s) = G_c(s)G(s) = \frac{K(s + 4)}{s(s + 0.16)(s + p)(s - \bar{p})},$$

where  $p = 7.3 + 9.7831j$ . Sketch the root locus and show the location of the roots for  $K = 326$  and  $K = 1350$ .

**P7.32** A mobile robot suitable for nighttime guard duty is available. This guard never sleeps and can tirelessly patrol large warehouses and outdoor yards. The steering control system for the mobile robot has a unity feedback with the loop transfer function

$$L(s) = G_c(s)G(s) = \frac{K(s + 1)(s + 5)}{s(s + 1.5)(s + 2)}.$$

(a) Find  $K$  for all breakaway and entry points on the real axis. (b) Find  $K$  when the damping ratio of the complex roots is 0.707. (c) Find the minimum value of the damping ratio for the complex roots and the associated gain  $K$ . (d) Find the overshoot and the time to settle (to within 2% of the final value) for a unit step input for the gain,  $K$ , determined in parts (b) and (c).

**P7.33** The Bell-Boeing V-22 Osprey Tiltrotor is both an airplane and a helicopter. Its advantage is the ability to rotate its engines to 90° from a vertical position for takeoffs and landings as shown in Figure P7.33(a), and then to switch the engines to a horizontal position for cruising as an airplane [20]. The altitude control system in the helicopter mode is shown in Figure P7.33(b). (a) Determine the root locus as  $K$  varies and determine the range of  $K$  for a stable system. (b) For  $K = 280$ , find the actual  $y(t)$  for a unit step input  $r(t)$  and the percentage overshoot and settling time (with a 2% criterion). (c) When  $K = 280$  and  $r(t) = 0$ , find  $y(t)$  for a unit step disturbance,  $T_d(s) = 1/s$ . (d) Add a prefilter between  $R(s)$  and the summing node so that

$$G_p(s) = \frac{0.5}{s^2 + 1.5s + 0.5}.$$

and repeat part (b).

**P7.34** The fuel control for an automobile uses a diesel pump that is subject to parameter variations. A unity negative feedback has a loop transfer function

$$G_c(s)G(s) = \frac{K(s + 2)}{(s + 1)(s + 2.5)(s + 4)(s + 10)}.$$

(a) Sketch the root locus as  $K$  varies from 0 to 2000. (b) Find the roots for  $K$  equal to 400, 500, and 600. (c) Predict how the percent overshoot to a step will vary for the gain  $K$ , assuming dominant roots. (d) Find the actual time response for a step input for all three gains and compare the actual overshoot with the predicted overshoot.



(a)

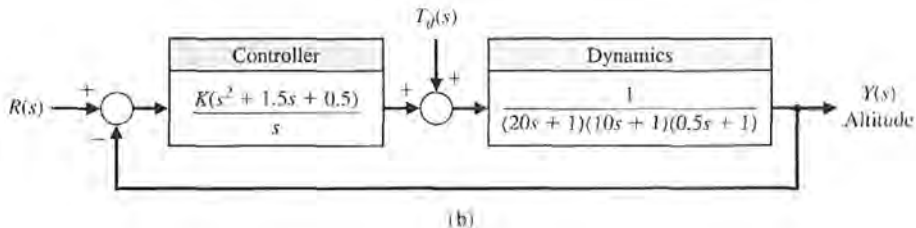


**FIGURE P7.33**  
(a) Osprey Tiltrotor aircraft. (b) Its control system.

- P7.35** A powerful electrohydraulic forklift can be used to lift pallets weighing several tons on top of 35-foot scaffolds at a construction site. The negative unity feedback system has a loop transfer function

$$L(s) = G_c(s)G(s) = \frac{K(s+1)^2}{s(s^2+1)}.$$

(a) Sketch the root locus for  $K > 0$ . (b) Find the gain  $K$  when two complex roots have a  $\zeta$  of 0.707, and calculate all three roots. (c) Find the entry point of the root locus at the real axis. (d) Estimate the expected overshoot to a step input, and compare it with the actual overshoot determined from a computer program.

- P7.36** A microrobot with a high-performance manipulator has been designed for testing very small particles, such as simple living cells [6]. The single-loop unity negative feedback system has a loop transfer function

$$L(s) = G_c(s)G(s) = \frac{K(s+1)(s+2)(s+3)}{s^3(s-1)}.$$

(a) Sketch the root locus for  $K > 0$ . (b) Find the gain and roots when the characteristic equation has two imaginary roots. (c) Determine the characteristic roots when  $K = 20$  and  $K = 100$ . (d) For  $K = 20$ , estimate the percent overshoot to a step input, and compare the estimate to the actual overshoot determined from a computer program.

- P7.37** Identify the parameters  $K$ ,  $a$ , and  $b$  of the system shown in Figure P7.37. The system is subject to a unit step input, and the output response has an overshoot but ultimately attains the final value of 1. When the closed-loop system is subjected to a ramp input, the output response follows the ramp input with a finite steady-state error. When the gain is doubled to  $2K$ , the output response to an impulse input is a pure sinusoid with a period of 0.314 second. Determine  $K$ ,  $a$ , and  $b$ .

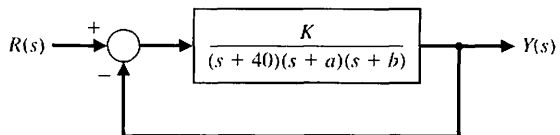


**FIGURE P7.37** Feedback system.

- P7.38** A unity feedback system has the loop transfer function

$$L(s) = G_c(s)G(s) = \frac{K(s+1)}{s(s-3)}.$$

This system is open-loop unstable. (a) Determine the range of  $K$  so that the closed-loop system is stable. (b) Sketch the root locus. (c) Determine the roots for  $K = 10$ . (d) For  $K = 10$ , predict the percent overshoot for a step input using Figure 5.13. (e) Determine the actual overshoot by plotting the response.

- P7.39** High-speed trains for U.S. railroad tracks must traverse twists and turns. In conventional trains, the axles are fixed in steel frames called trucks. The trucks pivot as the train goes into a curve, but the fixed axles stay parallel to each other, even though the front axle tends to go in a different direction from the rear axle [24]. If the train is going fast, it may jump the tracks. One solution uses axles that pivot independently. To counterbalance the strong centrifugal forces in a curve, the train also has a computerized hydraulic system that tilts each car as it rounds a turn. On-board sensors calculate the train's speed and the sharpness of the curve and feed this information to hydraulic pumps under the floor of each car. The pumps tilt the car up to eight degrees, causing it to lean into the curve like a race car on a banked track.

The tilt control system is shown in Figure P7.39. Sketch the root locus, and determine the value of  $K$  when the complex roots have maximum damping. Predict the response of this system to a step input  $R(s)$ .

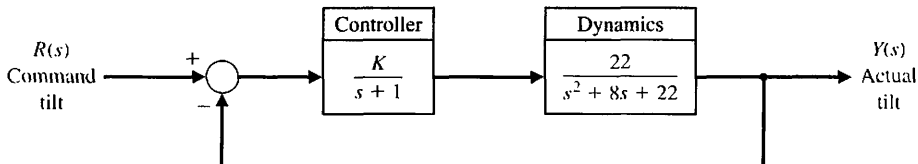
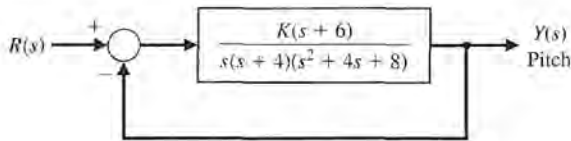
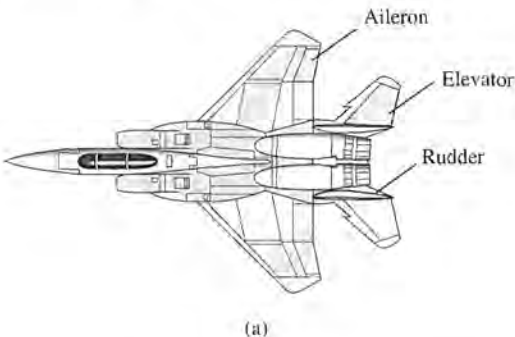


**FIGURE P7.39**  
Tilt control for a high-speed train.

## ADVANCED PROBLEMS

- AP7.1** The top view of a high-performance jet aircraft is shown in Figure AP7.1(a) [20]. Sketch the root locus and determine the gain  $K$  so that the  $\zeta$  of the complex poles near the  $j\omega$ -axis is the maximum achievable.

Evaluate the roots at this  $K$  and predict the response to a step input. Determine the actual response and compare it to the predicted response.



(b)

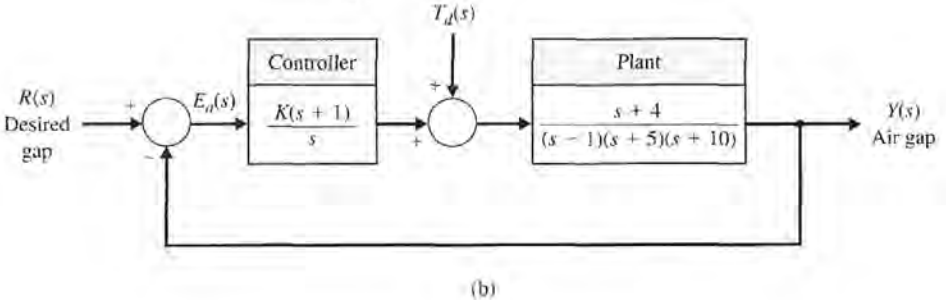
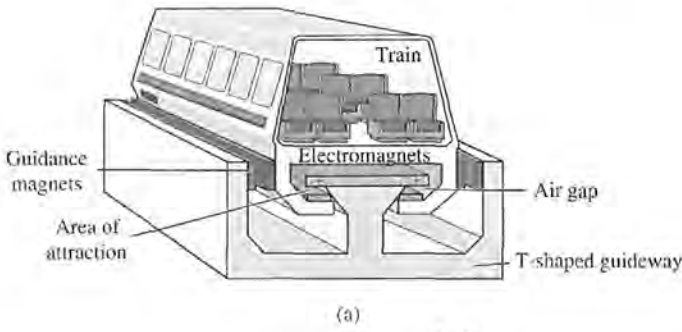
**FIGURE AP7.1**

(a) High-performance aircraft. (b) Pitch control system.

**AP7.2** A magnetically levitated high-speed train “flies” on an air gap above its rail system, as shown in Figure AP7.2(a) [24]. The air gap control system has a unity feedback system with a loop transfer function

$$G_i(s)G(s) = \frac{K(s+1)(s+3)}{s(s-1)(s+4)(s+8)}.$$

The feedback control system is illustrated in Figure AP7.2(b). The goal is to select  $K$  so that the response for a unit step input is reasonably damped and the settling time is less than 3 seconds. Sketch the root locus, and select  $K$  so that all of the complex roots have a  $\zeta$  greater than 0.6. Determine the actual response for the selected  $K$  and the percent overshoot.

**FIGURE AP7.2**

(a) Magnetically levitated high-speed train.  
(b) Feedback control system.

- AP7.3** A compact disc player for portable use requires a good rejection of disturbances and an accurate position of the optical reader sensor. The position control system uses unity feedback and a loop transfer function

$$L(s) = G_c(s)G(s) = \frac{10}{s(s+1)(s+p)}.$$

The parameter  $p$  can be chosen by selecting the appropriate DC motor. Sketch the root locus as a function of  $p$ . Select  $p$  so that the  $\zeta$  of the complex roots of the characteristic equation is approximately  $1/\sqrt{2}$ .

- AP7.4** A remote manipulator control system has unity feedback and a loop transfer function

$$G_c(s)G(s) = \frac{(s+\alpha)}{s^3 + (1+\alpha)s^2 + (\alpha-1)s + 1-\alpha}.$$

We want the steady-state position error for a step input to be less than or equal to 10% of the magnitude of the input. Sketch the root locus as a function of the parameter  $\alpha$ . Determine the range of  $\alpha$  required for the desired steady-state error. Locate the roots for the allowable value of  $\alpha$  to achieve the required steady-state error, and estimate the step response of the system.

- AP7.5** A unity feedback system has a loop transfer function

$$L(s) = G_c(s)G(s) = \frac{K}{s^3 + 10s^2 + 7s - 18}.$$

- Sketch the root locus and determine  $K$  for a stable system with complex roots with  $\zeta$  equal to  $1/\sqrt{2}$ .
- Determine the root sensitivity of the complex roots of part (a).
- Determine the percent change in  $K$  (increase or decrease) so that the roots lie on the  $j\omega$ -axis.

- AP7.6** A unity feedback system has a loop transfer function

$$L(s) = G_c(s)G(s) = \frac{K(s^2 + 3s + 6)}{s^3 + 2s^2 + 3s + 1}.$$

Sketch the root locus for  $K > 0$ , and select a value for  $K$  that will provide a closed step response with settling time less than 1 second.

- AP7.7** A feedback system with positive feedback is shown in Figure AP7.7. The root locus for  $K > 0$  must meet the condition

$$KG(s) = 1/\pm k360^\circ$$

for  $k = 0, 1, 2, \dots$

Sketch the root locus for  $0 < K < \infty$ .

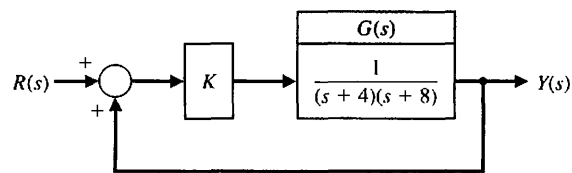


**FIGURE AP7.7** A closed-loop system with positive feedback.

- AP7.8** A position control system for a DC motor is shown in Figure AP7.8. Obtain the root locus for the velocity feedback constant  $K$ , and select  $K$  so that all the roots of the characteristic equation are real (two are equal and real). Estimate the step response of the system for the  $K$  selected. Compare the estimate with the actual response.

- AP7.9** A control system is shown in Figure AP7.9. Sketch the root loci for the following transfer functions  $G_c(s)$ :

- $G_c(s) = K$
- $G_c(s) = K(s+3)$

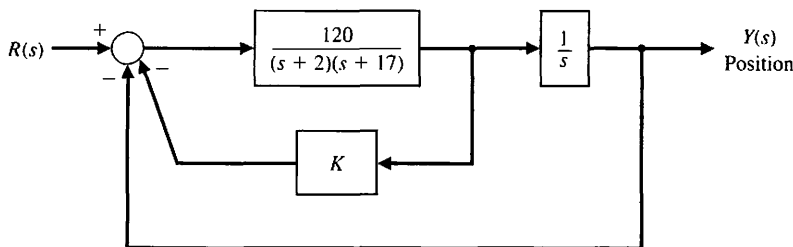


**FIGURE AP7.8**  
A position control system with velocity feedback.

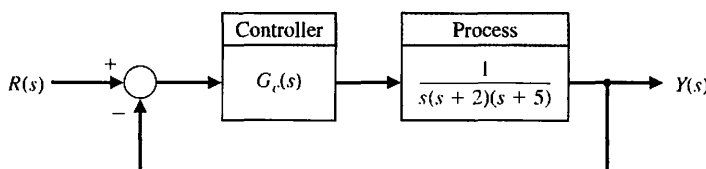


**FIGURE AP7.9**  
A unity feedback control system.

(c)  $G_c(s) = \frac{K(s + 1)}{s + 20}$   
 (d)  $G_c(s) = \frac{K(s + 1)(s + 4)}{s + 10}$

- AP7.10** A feedback system is shown in Figure AP7.10. Sketch the root locus as  $K$  varies when  $K \geq 0$ . Determine a value for  $K$  that will provide a step response with an overshoot less than 5% and a settling time (with a 2% criterion) less than 2.5 seconds.

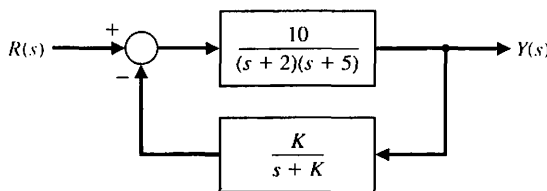


**FIGURE AP7.10** A nonunity feedback control system.

- AP7.11** A control system is shown in Figure AP7.11. Sketch the root locus, and select a gain  $K$  so that the step response of the system has an overshoot of less than 10% and the settling time (with a 2% criterion) is less than 4 seconds.

- AP7.12** A control system with PI control is shown in Figure AP7.12. (a) Let  $K_I/K_P = 0.2$  and determine  $K_P$  so that the complex roots have maximum damping ratio. (b) Predict the step response of the system with  $K_P$  set to the value determined in part (a).

- AP7.13** The feedback system shown in Figure AP7.13 has two unknown parameters  $K_1$  and  $K_2$ . The process transfer function is unstable. Sketch the root locus for  $0 \leq K_1, K_2 < \infty$ . What is the fastest settling time that you would expect of the closed-loop system in response to a unit step input  $R(s) = 1/s$ ? Explain.

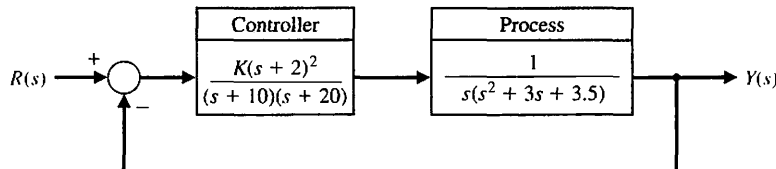


**FIGURE AP7.11**  
A control system  
with parameter  $K$ .

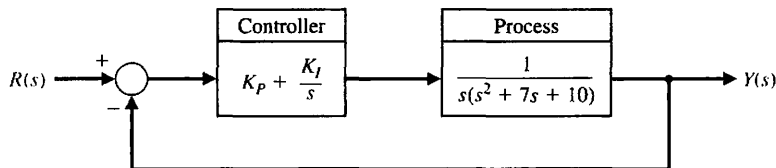
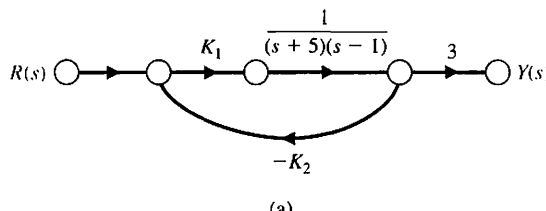
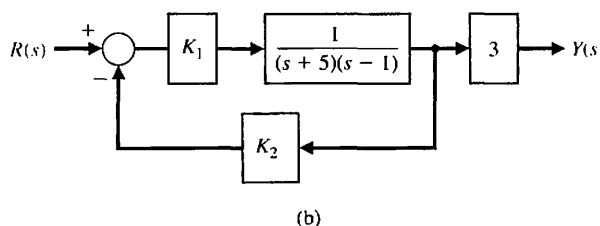


**FIGURE AP7.12**  
A control system  
with a PI controller.



(a)



(b)

**FIGURE AP7.13**  
An unstable plant  
with two  
parameters  $K_1$  and  
 $K_2$ .

**AP7.14** A unity feedback control system shown in Figure AP7.14 has the process

$$G(s) = \frac{10}{s(s+10)(s+7.5)}.$$

Design a PID controller using Ziegler-Nichols methods. Determine the unit step response and the unit disturbance response. What is the maximum percent overshoot and settling time for the unit step input?

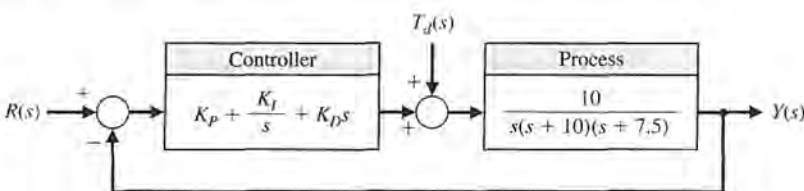


**FIGURE AP7.14**  
Unity feedback loop with PID controller.

## DESIGN PROBLEMS

**CDP7.1** The drive motor and slide system uses the output of a tachometer mounted on the shaft of the motor as shown in Figure CDP4.1 (switch-closed option). The output voltage of the tachometer is  $v_T = K_1\theta$ . Use the velocity feedback with the adjustable gain  $K_1$ . Select the best values for the gain  $K_1$  and the amplifier gain  $K_a$  so that the transient response to a step input has an overshoot less than 5% and a settling time (to within 2% of the final value) less than 300 ms.

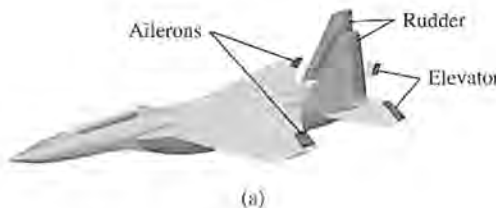
**DP7.1** A high-performance aircraft, shown in Figure DP7.1(a), uses the ailerons, rudder, and elevator to steer through a three-dimensional flight path [20]. The pitch rate control system for a fighter aircraft at 10,000 m and Mach 0.9 can be represented by the system in Figure DP7.1(b), where

$$G(s) = \frac{-18(s+0.015)(s+0.45)}{(s^2 + 1.2s + 12)(s^2 + 0.01s + 0.0025)}.$$

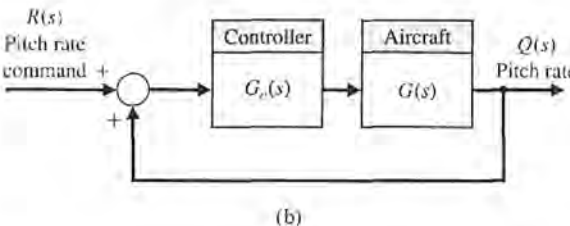
(a) Sketch the root locus when the controller is a gain, so that  $G_c(s) = K$ , and determine  $K$  when  $\zeta$  for the roots with  $\omega_n > 2$  is larger than 0.15 (seek a maximum  $\zeta$ ). (b) Plot the response  $q(t)$  for a step input  $r(t)$  with  $K$  as in (a). (c) A designer suggests an anticipatory controller with  $G_c(s) = K_1 + K_2s = K(s+2)$ . Sketch the root locus for this system as  $K$  varies and determine a  $K$  so that the  $\zeta$  of all the closed-loop roots is  $> 0.8$ . (d) Plot the response  $q(t)$  for a step input  $r(t)$  with  $K$  as in (c).

**DP7.2** A large helicopter uses two tandem rotors rotating in opposite directions, as shown in Figure P7.33(a). The controller adjusts the tilt angle of the main rotor and thus the forward motion as shown in Figure DP7.2. The helicopter dynamics are represented by

$$G(s) = \frac{10}{s^2 + 4.5s + 9},$$



(a)

**FIGURE DP7.1**

(a) High-performance aircraft. (b) Pitch rate control system.

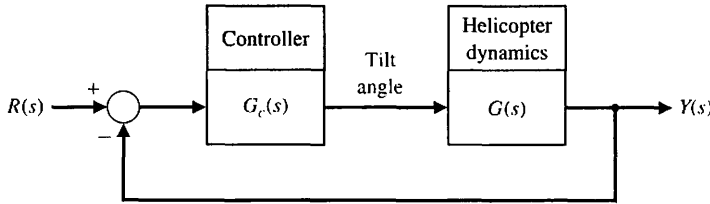


**FIGURE DP7.2**  
Two-rotor helicopter  
velocity control.

and the controller is selected as

$$G_c(s) = K_1 + \frac{K_2}{s} = \frac{K(s+1)}{s}.$$

(a) Sketch the root locus of the system and determine  $K$  when  $\zeta$  of the complex roots is equal to 0.6. (b) Plot the response of the system to a step input  $r(t)$  and find the settling time (with a 2% criterion) and overshoot for the system of part (a). What is the steady-state error for a step input? (c) Repeat parts (a) and (b) when the  $\zeta$  of the complex roots is 0.41. Compare the results with those obtained in parts (a) and (b).

**DP7.3** The vehicle Rover has been designed for maneuvering at 0.25 mph over Martian terrain. Because Mars is 189 million miles from Earth and it would take up to 40 minutes each way to communicate with Earth [22, 27], Rover must act independently and reliably. Resembling a cross between a small flatbed truck and an elevated jeep, Rover is constructed of three articulated sections, each with its own two independent, axle-bearing, one-meter conical wheels. A pair of sampling arms—one for chipping and drilling, the other for manipulating fine objects—extend from its front end like pincers. The control of the arms can

be represented by the system shown in Figure DP7.3. (a) Sketch the root locus for  $K$  and identify the roots for  $K = 4.1$  and 41. (b) Determine the gain  $K$  that results in an overshoot to a step of approximately 1%. (c) Determine the gain that minimizes the settling time (with a 2% criterion) while maintaining an overshoot of less than 1%.

**DP7.4** A welding torch is remotely controlled to achieve high accuracy while operating in changing and hazardous environments [21]. A model of the welding arm position control is shown in Figure DP7.4, with the disturbance representing the environmental changes. (a) With  $T_d(s) = 0$ , select  $K_1$  and  $K$  to provide high-quality performance of the position control system. Select a set of performance criteria, and examine the results of your design. (b) For the system in part (a), let  $R(s) = 0$  and determine the effect of a unit step  $T_d(s) = 1/s$  by obtaining  $y(t)$ .

**DP7.5** A high-performance jet aircraft with an autopilot control system has a unity feedback and control system, as shown in Figure DP7.5. Sketch the root locus and select a gain  $K$  that leads to dominant poles. With this gain  $K$ , predict the step response of the system. Determine the actual response of the system, and compare it to the predicted response.

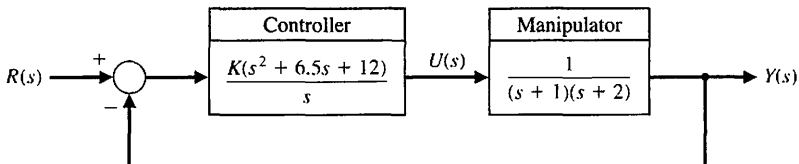


**FIGURE DP7.3**  
Mars vehicle robot  
control system.

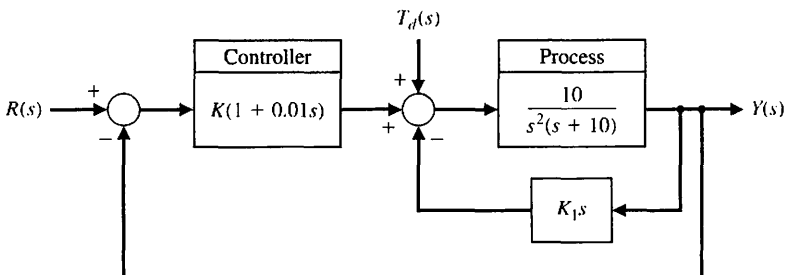


**FIGURE DP7.4**  
Remotely controlled  
welder.

**FIGURE DP7.5**  
High-performance jet aircraft.

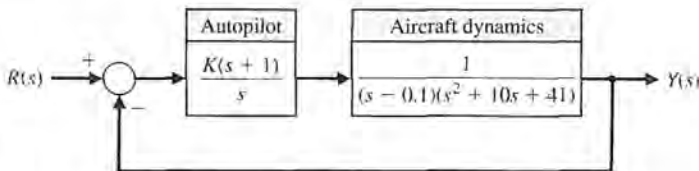
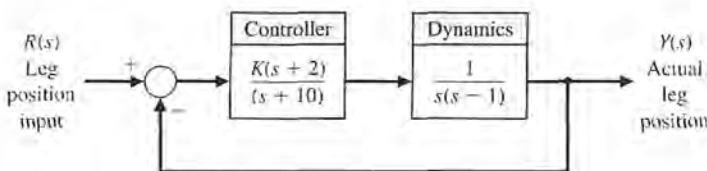


**FIGURE DP7.6**  
Automatic control of walking motion.



**DP7.6** A system to aid and control the walk of a partially disabled person could use automatic control of the walking motion [25]. One model of a system that is open-loop unstable is shown in Figure DP7.6. Using the root locus, select  $K$  for the maximum achievable  $\zeta$  of the complex roots. Predict the step response of the system, and compare it with the actual step response.

**DP7.7** A mobile robot using a vision system as the measurement device is shown in Figure DP7.7(a) [36]. The control system is shown in Figure DP7.7(b) where

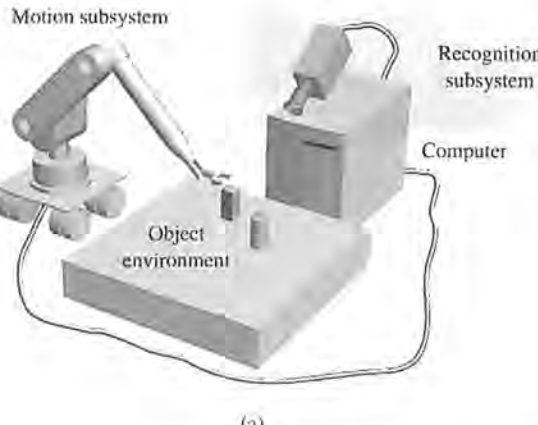
$$G(s) = \frac{1}{(s+1)(0.5s+1)}$$

and  $G_c(s)$  is selected as a PI controller so that the steady-state error for a step input is equal to zero. We then have

$$G_c(s) = K_P + \frac{K_I}{s}$$

Design the PI controller so that (a) the percent overshoot for a step input is  $P.O. \leq 5\%$ ; (b) the settling time (with a 2% criterion) is  $T_s \leq 6$  seconds; (c) the system velocity error constant  $K_v > 0.9$ ; and (d) the peak time,  $T_P$ , for a step input is minimized.

**DP7.8** Most commercial op-amps are designed to be unity-gain stable [26]. That is, they are stable when



(a)

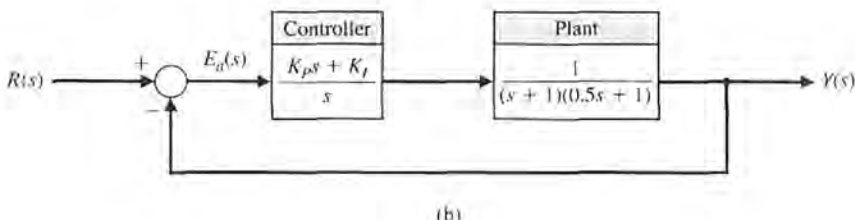
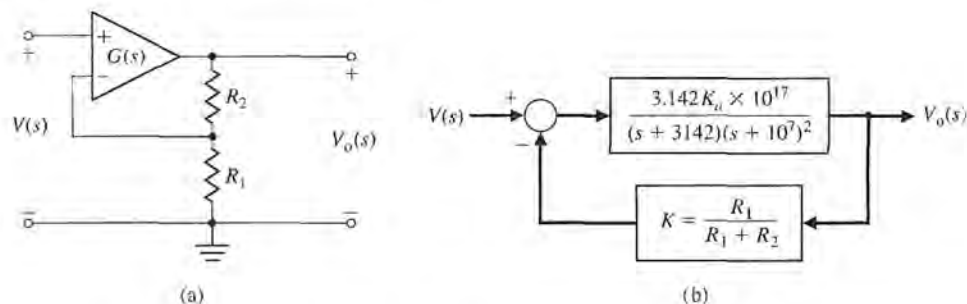


**FIGURE DP7.7**  
(a) A robot and vision system.  
(b) Feedback control system.

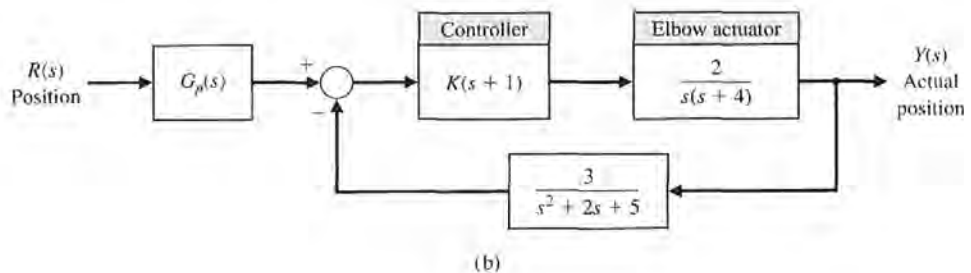
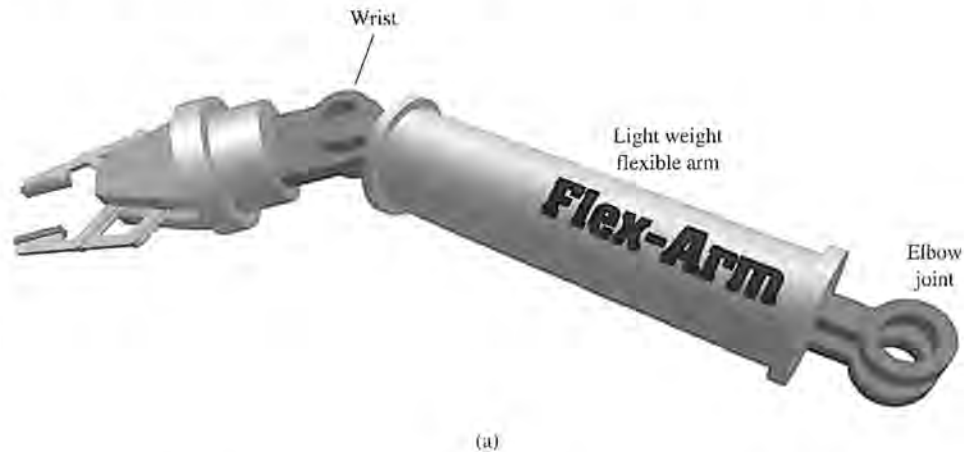


used in a unity-gain configuration. To achieve higher bandwidth, some op-amps relax the requirement to be unity-gain stable. One such amplifier has a DC gain of  $10^5$  and a bandwidth of 10 kHz. The amplifier,  $G(s)$ , is connected in the feedback circuit shown in Figure DP7.8(a). The amplifier is represented by the model shown in Figure DP7.8(b), where  $K_d = 10^5$ . Sketch the root locus of the system for  $K$ . Determine the minimum value of the DC gain of the closed-loop amplifier for stability. Select a DC gain and the resistors  $R_1$  and  $R_2$ .

**DP7.9** A robotic arm actuated at the elbow joint is shown in Figure DP7.9(a), and the control system for the

actuator is shown in Figure DP7.9(b). Plot the root locus for  $K \geq 0$ . Select  $G_p(s)$  so that the steady-state error for a step input is equal to zero. Using the  $G_p(s)$  selected, plot  $y(t)$  for  $K$  equal to 1, 1.5, and 2.85. Record the rise time, settling time (with a 2% criterion), and percent overshoot for the three gains. We wish to limit the overshoot to less than 6% while achieving the shortest rise time possible. Select the best system for  $1 \leq K \leq 2.85$ .

**DP7.10** The four-wheel-steering automobile has several benefits. The system gives the driver a greater degree of control over the automobile. The driver gets a more forgiving vehicle over a wide variety of conditions.



The system enables the driver to make sharp, smooth lane transitions. It also prevents yaw, which is the swaying of the rear end during sudden movements. Furthermore, the four-wheel-steering system gives a car increased maneuverability. This enables the driver to park the car in extremely tight quarters. With additional closed-loop computer operating systems, a car could be prevented from sliding out of control in abnormal icy or wet road conditions.

The system works by moving the rear wheels relative to the front-wheel-steering angle. The control system takes information about the front wheels' steering angle and passes it to the actuator in the back. This actuator then moves the rear wheels appropriately.

When the rear wheels are given a steering angle relative to the front ones, the vehicle can vary its lateral acceleration response according to the loop transfer function

$$G_c(s)G(s) = K \frac{1 + (1 + \lambda)T_1 s + (1 + \lambda)T_2 s^2}{s[1 + (2\zeta/\omega_n)s + (1/\omega_n^2)s^2]},$$

where  $\lambda = 2q/(1 - q)$ , and  $q$  is the ratio of rear wheel angle to front wheel steering angle [14]. We will assume that  $T_1 = T_2 = 1$  second and  $\omega_n = 4$ . Design a unity feedback system, selecting an appropriate set of parameters ( $\lambda, K, \zeta$ ) so that the steering control response is rapid and yet will yield modest overshoot characteristics. In addition,  $q$  must be between 0 and 1.

**DP7.11** A pilot crane control is shown in Figure DP7.11(a). The trolley is moved by an input  $F(t)$  in order to control  $x(t)$  and  $\phi(t)$  [13]. The model of the

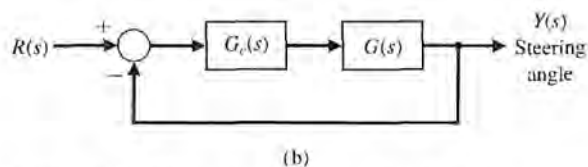
pilot crane control is shown in Figure DP7.11(b). Design a controller that will achieve control of the desired variables when  $G_c(s) = K$ .

**DP7.12** A rover vehicle designed for use on other planets and moons is shown in Figure DP7.12(a) [21]. The block diagram of the steering control is shown in Figure DP7.12(b), where

$$G(s) = \frac{s + 1.5}{(s + 1)(s + 2)(s + 4)(s + 10)}.$$

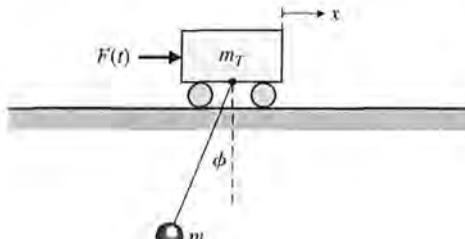


(a)

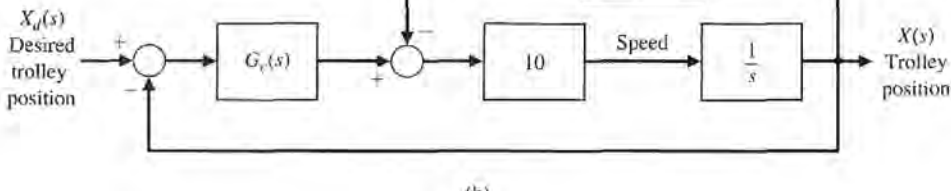


(b)

**FIGURE DP7.12** (a) Planetary rover vehicle. (b) Steering control system.



(a)



(b)

**FIGURE DP7.11**

- (a) Pilot crane control system.
- (b) Block diagram.

(a) When  $G_c(s) = K$ , sketch the root locus as  $K$  varies from 0 to 1000. Find the roots for  $K$  equal to 100, 300, and 600. (b) Predict the overshoot, settling time (with a 2% criterion), and steady-state error for a step input, assuming dominant roots. (c) Determine the actual time response for a step input for the three values of the gain  $K$ , and compare the actual results with the predicted results.

**DP7.13** The automatic control of an airplane is one example that requires multiple-variable feedback methods. In this system, the attitude of an aircraft is controlled by three sets of surfaces: elevators, a rudder, and ailerons, as shown in Figure DP7.13(a). By manipulating these surfaces, a pilot can set the aircraft on a desired flight path [20].

An autopilot, which will be considered here, is an automatic control system that controls the roll angle  $\phi$  by adjusting aileron surfaces. The deflection of the aileron surfaces by an angle  $\theta$  generates a torque due to air pressure on these surfaces. This causes a rolling motion of the aircraft. The aileron surfaces are controlled by a hydraulic actuator with a transfer function  $1/s$ .

The actual roll angle  $\phi$  is measured and compared with the input. The difference between the

desired roll angle  $\phi_d$  and the actual angle  $\phi$  will drive the hydraulic actuator, which in turn adjusts the deflection of the aileron surface.

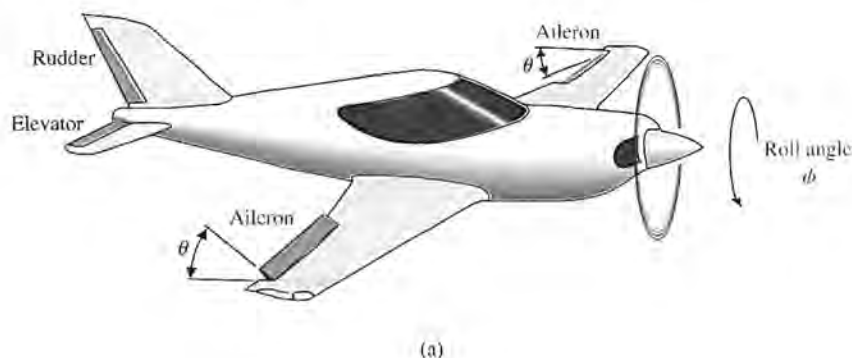
A simplified model where the rolling motion can be considered independent of other motions is assumed, and its block diagram is shown in Figure DP7.13(b). Assume that  $K_1 = 1$  and that the roll rate  $\dot{\phi}$  is fed back using a rate gyro. The step response desired has an overshoot less than 10% and a settling time (with a 2% criterion) less than 9 seconds. Select the parameters  $K_a$  and  $K_2$ .

**DP7.14** Consider the feedback system shown in Figure DP7.14. The process transfer function is marginally stable. The controller is the proportional-derivative (PD) controller

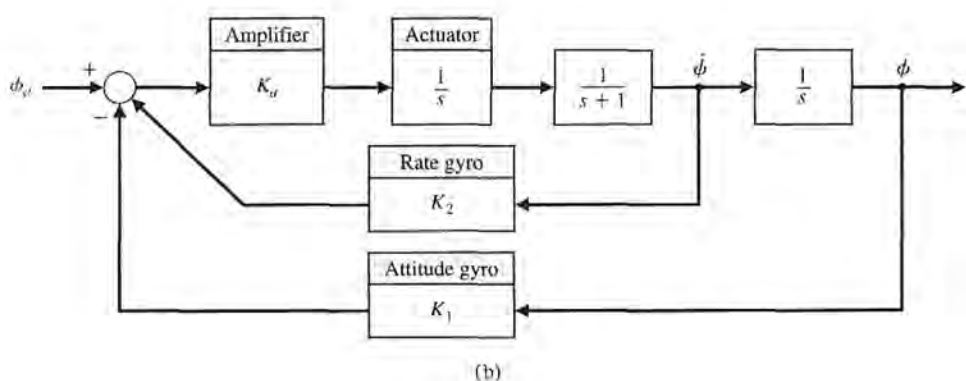
$$G_c(s) = K_P + K_D s.$$

- (a) Determine the characteristic equation of the closed-loop system.
- (b) Let  $\tau = K_P/K_D$ . Write the characteristic equation in the form

$$\Delta(s) = 1 + K_D \frac{n(s)}{d(s)}.$$



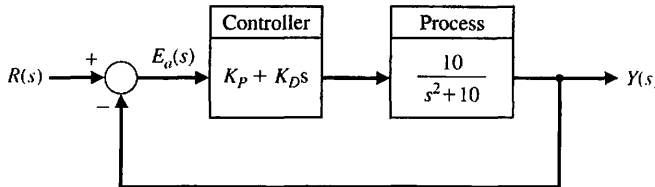
(a)

**FIGURE DP7.13**

(a) An airplane with a set of ailerons.  
(b) The block diagram for controlling the roll rate of the airplane.

- (c) Plot the root locus for  $0 \leq K_D < \infty$  when  $\tau = 6$ .  
 (d) What is the effect on the root locus when  $0 < \tau < \sqrt{10}$ ?

- (e) Design the PD controller to meet the following specifications:  
 (i)  $P.O. < 5\%$   
 (ii)  $T_s < 1$  s

**FIGURE DP7.14**

A marginally stable plant with a PD controller in the loop.



## COMPUTER PROBLEMS

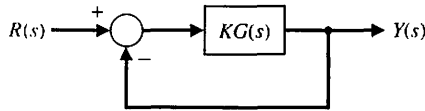
- CP7.1** Using the `rlocus` function, obtain the root locus for the following transfer functions of the system shown in Figure CP7.1 when  $0 < K < \infty$ :

$$(a) G(s) = \frac{30}{s^3 + 14s^2 + 43s + 30},$$

$$(b) G(s) = \frac{s + 20}{s^2 + 4s + 20}$$

$$(c) G(s) = \frac{s^2 + s + 2}{s(s^2 + 6s + 10)}$$

$$(d) G(s) = \frac{s^5 + 4s^4 + 6s^3 + 10s^2 + 6s + 4}{s^6 + 4s^5 + 4s^4 + s^3 + s^2 + 10s + 1}$$

**FIGURE CP7.1** A single-loop feedback system with parameter  $K$ .

- CP7.2** A unity negative feedback system has the loop transfer function

$$KG(s) = K \frac{s^2 - 2s + 2}{s(s^2 + 3s + 2)}.$$

Develop an m-file to plot the root locus and show with the `rlcfnd` function that the maximum value of  $K$  for a stable system is  $K = 0.79$ .

- CP7.3** Compute the partial fraction expansion of

$$Y(s) = \frac{s + 6}{s(s^2 + 5s + 4)}$$

and verify the result using the `residue` function.

- CP7.4** A unity negative feedback system has the loop transfer function

$$G_c(s)G(s) = \frac{(1 + p)s - p}{s^2 + 4s + 10}.$$

Develop an m-file to obtain the root locus as  $p$  varies;  $0 < p < \infty$ . For what values of  $p$  is the closed-loop stable?

- CP7.5** Consider the feedback system shown in Figure CP7.1, where

$$G(s) = \frac{s + 1}{s^2}.$$

For what value of  $K$  is  $\zeta = 0.707$  for the dominant closed-loop poles?

- CP7.6** A large antenna, as shown in Figure CP7.6(a), is used to receive satellite signals and must accurately track the satellite as it moves across the sky. The control system uses an armature-controlled motor and a controller to be selected, as shown in Figure CP7.6(b). The system specifications require a steady-state error for a ramp input  $r(t) = Bt$ , less than or equal to  $0.01B$ , where  $B$  is a constant. We also seek a percent overshoot to a step input of  $P.O. \leq 5\%$  with a settling time (with a 2% criterion) of  $T_s \leq 2$  seconds. (a) Using root locus methods, create an m-file to assist in designing the controller. (b) Plot the resulting unit step response and compute the percent overshoot and the settling time and label the plot accordingly. (c) Determine the effect of the disturbance  $T_d(s) = Q/s$  (where  $Q$  is a constant) on the output  $Y(s)$ .

- CP7.7** Consider the feedback control system in Figure CP7.7. We have three potential controllers for our system:

1.  $G_c(s) = K$  (proportional controller)
2.  $G_c(s) = K/s$  (integral controller)
3.  $G_c(s) = K(1 + 1/s)$  (proportional, integral (PI) controller)

The design specifications are  $T_s \leq 10$  seconds and  $P.O. \leq 10\%$  for a unit step input.

- (a) For the proportional controller, develop an m-file to sketch the root locus for  $0 < K < \infty$ , and

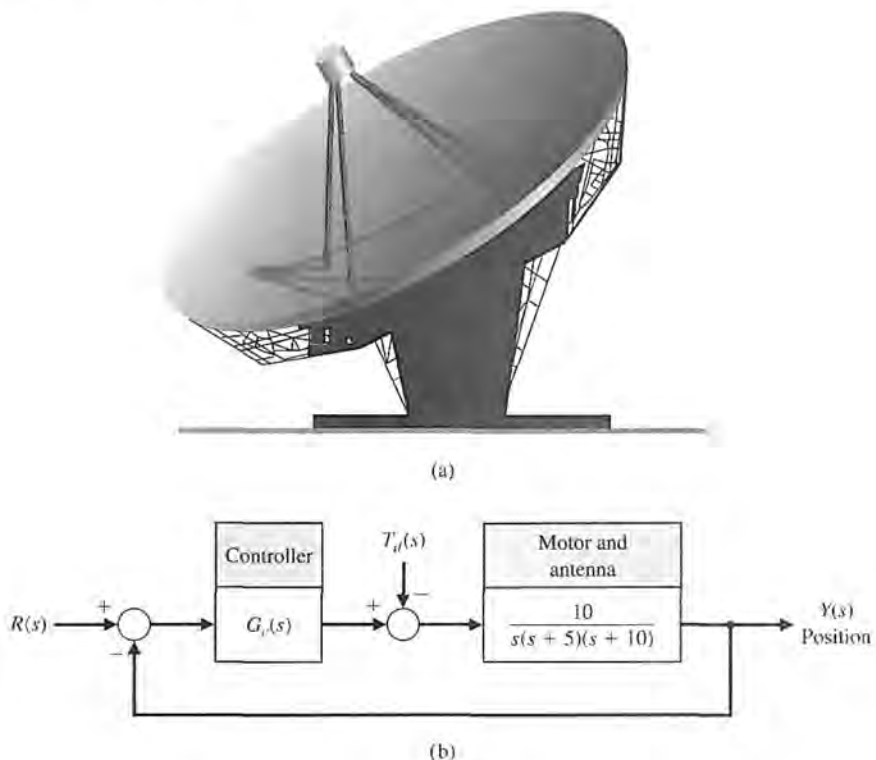
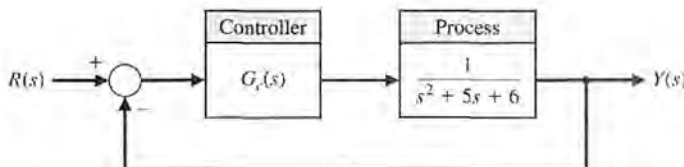


**FIGURE CP7.6**  
Antenna position control.

**FIGURE CP7.7**  
A single-loop feedback control system with controller  $G_c(s)$ .



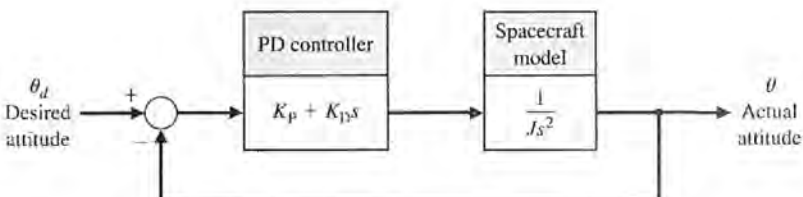
determine the value of  $K$  so that the design specifications are satisfied.

- (b) Repeat part (a) for the integral controller.
- (c) Repeat part (a) for the PI controller.
- (d) Co-plot the unit step responses for the closed-loop systems with each controller designed in parts (a)–(c).

(e) Compare and contrast the three controllers obtained in parts (a)–(c), concentrating on the steady-state errors and transient performance.

**CP7.8** Consider the spacecraft single-axis attitude control system shown in Figure CP7.8. The controller is known as a proportional-derivative (PD) controller. Suppose that we require the ratio of  $K_p/K_D = 5$ . Then, develop

**FIGURE CP7.8**  
A spacecraft attitude control system with a proportional-derivative controller.



an m-file using root locus methods find the values of  $K_D/J$  and  $K_p/J$  so that the settling time  $T_s$  is less than or equal to 4 seconds, and the peak overshoot  $P.O.$  is less than or equal to 10% for a unit step input. Use a 2% criterion in determining the settling time.

**CP7.9** Consider the feedback control system in Figure CP7.9. Develop an m-file to plot the root locus for  $0 < K < \infty$ . Find the value of  $K$  resulting in a damping ratio of the closed-loop poles equal to 0.707.

**CP7.10** Consider the system represented in state variable form

$$\dot{x} = Ax + Bu$$

$$y = Cx + Du,$$

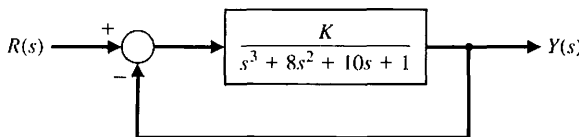
where

$$A = \begin{bmatrix} 0 & 1 & 0 \\ 0 & 0 & 1 \\ -1 & -5 & -2 - k \end{bmatrix}, B = \begin{bmatrix} 1 \\ 0 \\ 4 \end{bmatrix},$$

$$C = [1 \ -9 \ 12], \text{ and } D = [0].$$

(a) Determine the characteristic equation. (b) Using the Routh–Hurwitz criterion, determine the values of  $k$  for which the system is stable. (c) Develop an m-file to plot the root locus and compare the results to those obtained in (b).

**FIGURE CP7.9**  
Unity feedback  
system with  
parameter  $K$ .



## ANSWERS TO SKILLS CHECK

True or False: (1) True; (2) True; (3) False; (4) True;  
(5) True

Multiple Choice: (6) b; (7) c; (8) a; (9) c; (10) a;  
(11) b; (12) c; (13) a; (14) c; (15) b

Word Match (in order, top to bottom): k, f, a, d, i, h,  
c, b, e, g, j

## TERMS AND CONCEPTS

**Angle of departure** The angle at which a locus leaves a complex pole in the  $s$ -plane.

**Angle of the asymptotes** The angle  $\phi_A$  that the asymptote makes with respect to the real axis.

**Asymptote** The path the root locus follows as the parameter becomes very large and approaches infinity. The number of asymptotes is equal to the number of poles minus the number of zeros.

**Asymptote centroid** The center  $\sigma_A$  of the linear asymptotes.

**Breakaway point** The point on the real axis where the locus departs from the real axis of the  $s$ -plane.

**Dominant roots** The roots of the characteristic equation that represent or dominate the closed-loop transient response.

**Locus** A path or trajectory that is traced out as a parameter is changed.

**Logarithmic sensitivity** A measure of the sensitivity of the system performance to specific parameter changes,

given by  $S_K^T(s) = \frac{\partial T(s)/T(s)}{\partial K/K}$ , where  $T(s)$  is the system transfer function and  $K$  is the parameter of interest.

**Manual PID tuning methods** The process of determining the PID controller gains by trial-and-error with minimal analytic analysis.

**Negative gain root locus** The root locus for negative values of the parameter of interest, where  $-\infty < K \leq 0$ .

**Number of separate loci** Equal to the number of poles of the transfer function, assuming that the number of poles is greater than or equal to the number of zeros of the transfer function.

**Parameter design** A method of selecting one or two parameters using the root locus method.

**PID controller** A widely used controller used in industry of the form  $G_c(s) = K_p + \frac{K_I}{s} + K_D s$ , where  $K_p$  is the proportional gain,  $K_I$  is the integral gain, and  $K_D$  is the derivative gain.

**PID tuning** The process of determining the PID controller gains.

**Proportional plus derivative (PD) controller** A two-term controller of the form  $G_c(s) = K_p + K_D s$ , where  $K_p$  is the proportional gain and  $K_D$  is the derivative gain.

**Proportional plus integral (PI) controller** A two-term controller of the form  $G_c(s) = K_p + \frac{K_I}{s}$ , where  $K_p$  is the proportional gain and  $K_I$  is the integral gain.

**Quarter amplitude decay** The amplitude of the closed-loop response is reduced approximately to one-fourth of the maximum value in one oscillatory period.

**Reaction curve** The response obtained by taking the controller off-line and introducing a step input. The underlying process is assumed to be a first-order system with a transport delay.

**Root contours** The family of loci that depict the effect of varying two parameters on the roots of the characteristic equation.

**Root locus** The locus or path of the roots traced out on the  $s$ -plane as a parameter is changed.

**Root locus method** The method for determining the locus of roots of the characteristic equation  $1 + KP(s) = 0$  as  $K$  varies from 0 to infinity.

**Root locus segments on the real axis** The root locus lying in a section of the real axis to the left of an odd number of poles and zeros.

**Root sensitivity** The sensitivity of the roots as a parameter changes from its normal value. The root sensitivity is given by  $S_K = \frac{\partial r}{\partial K/K}$ , the incremental change in the root divided by the proportional change of the parameter.

**Ultimate gain** The PD controller proportional gain,  $K_p$ , on the border of instability when  $K_D = 0$  and  $K_I = 0$ .

**Ultimate period** The period of the sustained oscillations when  $K_p$  is the ultimate gain and  $K_D = 0$  and  $K_I = 0$ .

**Ziegler-Nichols PID tuning method** The process of determining the PID controller gains using one of several analytic methods based on open-loop and closed-loop responses to step inputs.